UNIVERSITAT ROVIRA I VIRGILI

From Gold-Catalyzed Asymmetric or Photoredox-Assisted Cyclizations to Rhodium-Catalyzed C–H Alkynylations

Joan Guillem Mayans Peñarrubia

ADVERTIMENT. L'accés als continguts d'aquesta tesi doctoral i la seva utilització ha de respectar els drets de la persona autora. Pot ser utilitzada per a consulta o estudi personal, així com en activitats o materials d'investigació i docència en els termes establerts a l'art. 32 del Text Refós de la Llei de Propietat Intel·lectual (RDL 1/1996). Per altres utilitzacions es requereix l'autorització prèvia i expressa de la persona autora. En qualsevol cas, en la utilització dels seus continguts caldrà indicar de forma clara el nom i cognoms de la persona autora i el títol de la tesi doctoral. No s'autoritza la seva reproducció o altres formes d'explotació efectuades amb finalitats de lucre ni la seva comunicació pública des d'un lloc aliè al servei TDX. Tampoc s'autoritza la presentació del seu contingut en una finestra o marc aliè a TDX (framing). Aquesta reserva de drets afecta tant als continguts de la tesi com als seus resums i índexs.

ADVERTENCIA. El acceso a los contenidos de esta tesis doctoral y su utilización debe respetar los derechos de la persona autora. Puede ser utilizada para consulta o estudio personal, así como en actividades o materiales de investigación y docencia en los términos establecidos en el art. 32 del Texto Refundido de la Ley de Propiedad Intelectual (RDL 1/1996). Para otros usos se requiere la autorización previa y expresa de la persona autora. En cualquier caso, en la utilización de sus contenidos se deberá indicar de forma clara el nombre y apellidos de la persona autora y el título de la tesis doctoral. No se autoriza su reproducción u otras formas de explotación efectuadas con fines lucrativos ni su comunicación pública desde un sitio ajeno al servicio TDR. Tampoco se autoriza la presentación de su contenido en una ventana o marco ajeno a TDR (framing). Esta reserva de derechos afecta tanto al contenido de la tesis como a sus resúmenes e índices.

WARNING. Access to the contents of this doctoral thesis and its use must respect the rights of the author. It can be used for reference or private study, as well as research and learning activities or materials in the terms established by the 32nd article of the Spanish Consolidated Copyright Act (RDL 1/1996). Express and previous authorization of the author is required for any other uses. In any case, when using its content, full name of the author and title of the thesis must be clearly indicated. Reproduction or other forms of for profit use or public communication from outside TDX service is not allowed. Presentation of its content in a window or frame external to TDX (framing) is not authorized either. These rights affect both the content of the thesis and its abstracts and indexes.

UNIVERSITAT ROVIRA i VIRGILI

From Gold-Catalyzed Asymmetric or Photoredox-Assisted Cyclizations to Rhodium-Catalyzed C–H Alkynylations

Joan Guillem Mayans Peñarrubia

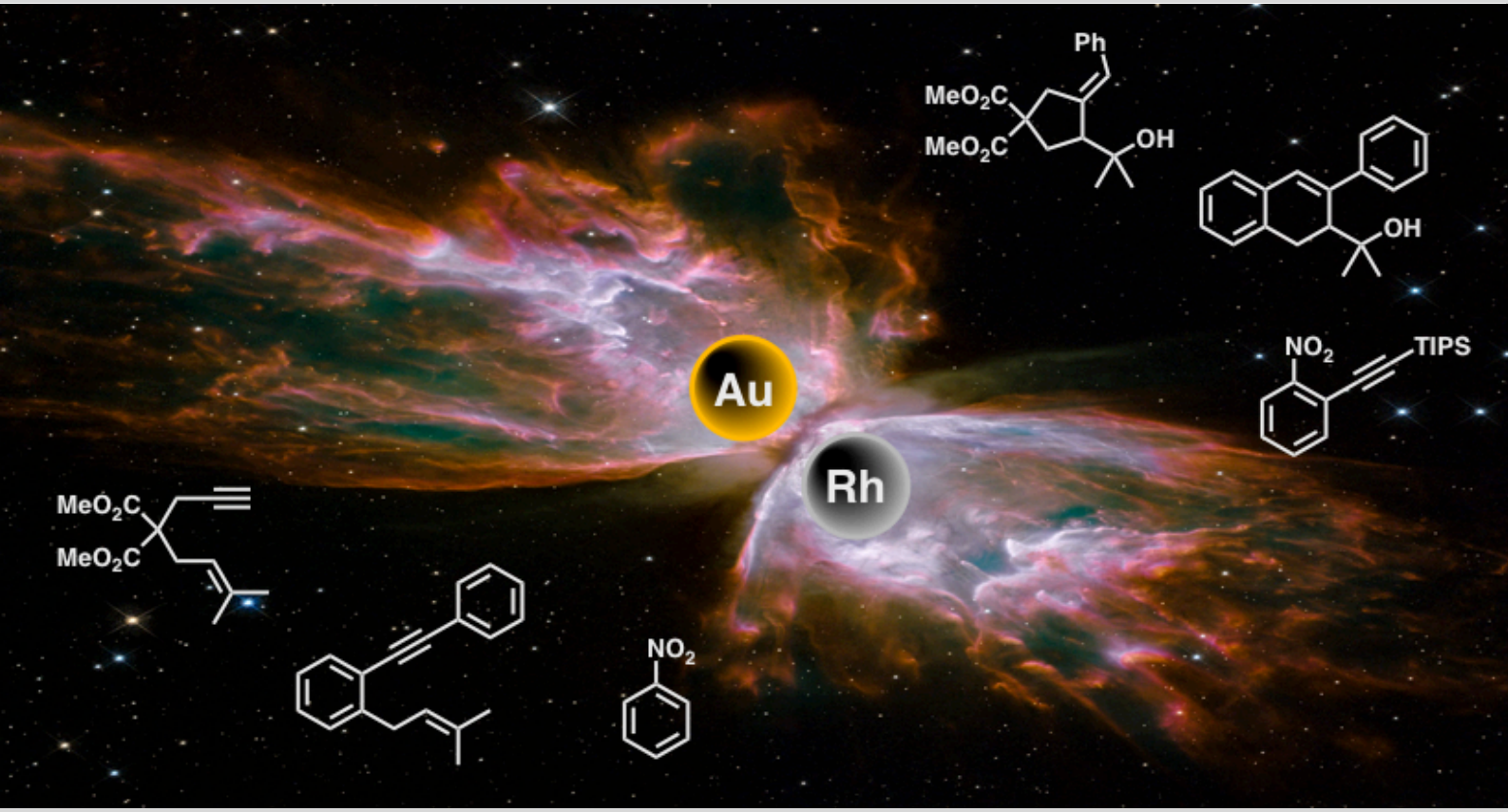

DOCTORAL THESIS
2021

UNIVERSITAT ROVIRA I VIRGILI
From Gold-Catalyzed Asymmetric or Photoredox-Assisted Cyclizations to Rhodium-Catalyzed C–H Alkynylations
Joan Guillem Mayans Peñarrubia

UNIVERSITAT ROVIRA I VIRGILI
From Gold-Catalyzed Asymmetric or Photoredox-Assisted Cyclizations to Rhodium-Catalyzed C–H Alkynylations
Joan Guillem Mayans Peñarrubia

UNIVERSITAT ROVIRA I VIRGILI
From Gold-Catalyzed Asymmetric or Photoredox-Assisted Cyclizations to Rhodium-Catalyzed C–H Alkynylations
Joan Guillem Mayans Peñarrubia

Joan Guillem Mayans Peñarrubia

From Gold-Catalyzed Asymmetric or Photoredox-Assisted Cyclizations to Rhodium-Catalyzed C–H Alkynylations

DOCTORAL THESIS

Supervised by Prof. Antonio M. Echavarren

Institute of Chemical Research of Catalonia (ICIQ)

UNIVERSITAT ROVIRA i VIRGILI

ICIQ Institut Català d'Investigació Química

Tarragona 2021

UNIVERSITAT ROVIRA I VIRGILI
From Gold-Catalyzed Asymmetric or Photoredox-Assisted Cyclizations to Rhodium-Catalyzed C–H Alkynylations
Joan Guillem Mayans Peñarrubia

UNIVERSITAT ROVIRA i VIRGILI

ICIQ
Institut Català d'Investigació Química

I STATE that the present study, entitled "From Gold-Catalyzed Asymmetric or Photoredox-Assisted Cyclizations to Rhodium-Catalyzed C–H Alkynylations", presented by Joan Guillem Mayans Peñarrubia for the award of the degree of Doctor, has been carried out under my supervision at the Institut Català d'Investigació Química (ICIQ).

Tarragona, November 21st, 2021

Doctoral Thesis Supervisor

Prof. Antonio M. Echavarren

UNIVERSITAT ROVIRA I VIRGILI
From Gold-Catalyzed Asymmetric or Photoredox-Assisted Cyclizations to Rhodium-Catalyzed C–H Alkynylations
Joan Guillem Mayans Peñarrubia

A mi familia

UNIVERSITAT ROVIRA I VIRGILI
From Gold-Catalyzed Asymmetric or Photoredox-Assisted Cyclizations to Rhodium-Catalyzed C–H Alkynylations
Joan Guillem Mayans Peñarrubia

"Happiness [is] only real when shared"

Christopher McCandless

UNIVERSITAT ROVIRA I VIRGILI
From Gold-Catalyzed Asymmetric or Photoredox-Assisted Cyclizations to Rhodium-Catalyzed C–H Alkynylations
Joan Guillem Mayans Peñarrubia

Acknowledgements

I would like to start by acknowledging my supervisor Prof. Dr. Antonio M. Echavarren for giving me the opportunity to join his group during these four years. Thank you for trusting in my scientific opinions from the beginning and guiding me gently through this process of self-growth as a scientist and as a person. For giving me the freedom to try my own ideas while keeping the door of your office opened for discussion. Overall, thank you for being a good team leader. I also thank Prof. Dr. Thomas Carell and his group for accepting me during my short-stay and showing me the completely different world of prebiotic chemistry.

A continuació, com no podia ser d'un altra manera, m'agradaria agrair a Sònia Gavaldà per encarregar-se de tota la part administrativa (coses que ni tan sols sé que existeixen) i pels moments que hem compartit. Quan arribe al meu següent destí t'enviaré un WhatsApp confirmant que tot va bé. També agraeixo a la Dr. Imma Escofet l'eficiència i l'esforç a l'hora de coordinar un grup tan gran i mantenir els laboratoris tan bé com estan, però sobretot la seua energia imparable: ¡CLEANING! Gràcies a les dos per fer que tot funcione millor i pel bon ambient que genereu.

I would like to thank Alejandro Bermejo for introducing in my head the idea of coming to ICIQ and offering me the opportunity to experience the wildest adventure of my life. I am also grateful to Alessandra, Iwa, Coco and of course, my insane friend Juanjo for being my home during my first stages in Tarragona.

I thank all the present and former members of the group that helped and supported me during my PhD, in particular the ones I had the pleasure to collaborate with. I feel grateful to Dr. Giuseppe Zuccarello for sharing his passion for chemistry and his always welcomed jokes. To Dr. Fedor Miloserdov for being an inspiration and all the (not always useful) conversations. I acknoledge Dr. Jean-Simon Suppo et Dr. Eric Tan for accepting me in their projects and for the interesting discussions. També t'agraeixo que portares un poc de la terreta cap a Tarragona Dr. Marc Montesinos, i tota l'ajuda que m'has donat en aquestos últims compasos.

My sincere thanks are given to the research support units at ICIQ: Nuclear Magnetic Resonance, High Resolution Mass Spectrometry, X-Ray Diffraction, CELLEX – High Throughput Experimentation, Chemical Reaction Technologies, Chromatography, and Informatics.

Moltes gràcies a tu, Laia Pellejà, per ser com ets i per introduir-me a la divulgació científica, donant-me l'oportunitat de gaudir en situacions en les que no pensava que em trobaria mai. Igualment m'agradaria agrair a Federico Dattila la seua voluntat de clavar-se a tots els fregats per fer d'aquest món un món millor i per discutir amb mi encara que pensarem el mateix.

Gracias a los pingboleros Dr. Xiang Yin, David Nieto, Dr. Leonardo Nannini, Eduardo García y Dr. Franco della Felice por darle una nueva dimensión a la temptation y ayudarme a despejar mi mente de tantas moléculas. También me ha parecido increíble poder compartir mi pasión por la música con Ana, Bafa, Eric, Marcos y el Dandy. Os agradezco el hacer de cada rato que hemos compartido juntos puro GAS y de la imagen de vernos sobre el escenario un recuerdo zooterapéutico inolvidable.

Tarragona no es Tarragona sin montañas y estos años no hubieran sido lo mismo sin la climbing crew: Marino, Rosie, Llorenç, Ludo, Jake&Ana, Jan&Ana, David Bou, Roger Bou, Jeroen, Jessica y Marta. Especial mention para: Ani, que me introdujo al grupo y me llevó de excursión con su furgoneto mientras hablábamos de la vida; Enrique, mi compañero de batallas; Cristina, que em fa sentir com a casa amb la coca de molletes i les abraçades; Patri y su estupenda manera de fluir por la vida y Pablo, por enseñarme el valor del orden y la previsión que no sé si algún día incorporaré y por poder contar contigo. Gracias a todos por acogerme, compartir conmigo esos entrenamientos, jornadas de montaña, viajes y en general todos esos momentos que me han hecho sentir tan bien.

Gracias a los lunchers por ser coprotagonistas de esta historia y los mejores amigos que he podido tener en Tarragona. Dr. Adiran de Aguirre y sus musculosos bíceps, Bruna Sánchez y sus ácidos zumos y el incasable Iron. Ana Arroyo y sus superpoderes, Inma Martín (hola guapa), Otilia Stoica y sus gatitos y Antonia Rinaldi la fortunata. Gracias Mauro Mato por hacerme disfrutar más del laboratorio adivinando melting points, por tu pragmatismo a la hora de ver el mundo y por tu motivación al hacer las cosas.

También he de agradecer a los hogareños del piso patera, mi segundo hogar. Agradezco que Mathou se nos uniera y compartiera su visión del mundo donde ponerse morena es la mayor prioridad. A la Jana amb eixa alegria contagiosa i els camins que ara s'esvaeixen. A Alba Helena Pérez Jimeno con jota por estar siempre ahí para hablar de cualquier cosa y tu efusiva comunicación no verbal. Y por supuesto mis andaluces favoritos. ¡Cómo me habéis ayudado durante este viaje! Cristina, gracias por enseñarme lo que es ser fuerte contra las adversidades y luchar por algo con todo lo que tienes. Por tu valentía a la hora de tomar decisiones y tu capacidad para adivinar lo que pasará a continuación. Y también gracias por nuestras conversaciones de sofá en bata con chocolate 99.99% y todo el apoyo que me has dado. Angelín, tú me has enseñado lo que es cuidar de los demás (personas, animales o recursos) y me has hecho sentir que tenía un hueco real en esta ciudad. Para lo bueno y para lo malo siempre has estado ahí, con tus carcajadas y tus genialidades. Muchas gracias por llenar mi hogar y hacer que oliera a pan. También les agradezco a los nuevos fichajes David y Pablo el buen ambiente que se respira ahora y las partidas al jungle speed y el among us.

Pili, gràcies per iluminar la meua vida amb la teua lleugeresa i el teu riure i per haver compartit amb mi aquesta relació tan especial. Malgrat la distancia, m'has ajudat més que ningú a enfrontar el doctorat tranquilitzant-me i recolzant-me una i altra vegada. Sempre t'agrairé tots els moments, els aprenentatges, l'amor i la sinceritat que em vas donar desde el dia que ens vam trobar fins al dia que em vas deixar marxar.

Por último, me gustaría que las personas que me han visto crecer desde que medía 53 centímetros se sintieran responsables de esta hazaña que es el doctorado. Gracias a mi madre Vicenta Peñarrubia, a mi padre Juan Mayans y a mi hermana Mar Mayans por todo el amor que me han dado y me siguen dando. Gracias por sentar con cariño las bases para que pudiera crecer sano y por confiar tanto en mi. Y me gustaría acabar agradeciéndole al pequeño Pau Sancho todas esas peleas y vuelos sin motor que hemos protagonizado y las mil cosas que nos quedan por hacer.

We thank the Ministerio de Ciencia e Innovación CTQ2016-75960-P (MCI/AEI/FEDER, UE), the European Research Council (Advanced Grant No. 835080), the AGAUR (2017 SGR 1257) and the CERCA Program/Generalitat de Catalunya for financial support.

UNIVERSITAT ROVIRA I VIRGILI
From Gold-Catalyzed Asymmetric or Photoredox-Assisted Cyclizations to Rhodium-Catalyzed C–H Alkynylations
Joan Guillem Mayans Peñarrubia

At the moment of writing this manuscript, the results obtained during my PhD have given rise to the following publications:

Mayans, J. G.; Armengol-Relats, H.; Calleja, P.; Echavarren, A. M. "Gold(I)-Catalysis for the Synthesis of Terpenoids: From Intramolecular Cascades to Intermolecular Cycloadditions" *Isr. J. Chem.* **2018**, *58*, 639–658.

Zuccarello, G.; **Mayans, J. G**.; Escofet, I.; Scharnagel, D.; Kirillova, M. S.; Pérez-Jimeno, A. H.; Calleja, P.; Boothe, J. R.; Echavarren, A. M. "Enantioselective Folding of Enynes by Gold(I) Catalysts with a Remote C_2-Chiral Element" *J. Am. Chem. Soc.* **2019**, *141*, 11858–11863; (highlighted in *Synfacts* **2019**, *15*, 1135).

Mayans, J. G.; Suppo, J.-S.; Echavarren, A. M. "Photoredox-Assisted Gold-Catalyzed Arylative Alkoxycyclization of 1,6-Enynes" *Org. Lett.* **2020**, *22*, 3045–3049.

UNIVERSITAT ROVIRA I VIRGILI
From Gold-Catalyzed Asymmetric or Photoredox-Assisted Cyclizations to Rhodium-Catalyzed C–H Alkynylations
Joan Guillem Mayans Peñarrubia

Table of Contents

Prologue

This manuscript is divided in five main parts including a general introduction, three chapters describing the research results and a final section with the general conclusions. Each chapter contains five sections including a specific introduction in the topic, objectives, results and discussion, conclusion and an experimental section. The references and numbering are organized by chapters.

The **General Introduction** gives an overview on the fundamentals of homogeneous gold(I) catalysis emphasizing the advances relevant to the content of this thesis. For consistency, the chemistry presented in chapter 3 is not introduced in this section. Instead, it will be presented in the introduction of the corresponding chapter

Chapter 1 discloses the first gold(I)-catalyzed enantioselective total synthesis of carexanes I, P and O. The key aspects concerning the gold(I)-promoted step are discussed and the scope of the reaction is investigated. The project was developed in collaboration with Dr. Pilar Calleja, Dr. Giuseppe. Zuccarello, Dr. Imma Escofet and Dr. Dagmar Scharnagel. The discussed results have been published in *J. Am. Chem. Soc.* **2019**, *141*, 11858–11863.

Chapter 2 presents the studies on the photoredox-assisted gold-catalyzed arylative alkoxycyclization of 1,6-enynes. The scope and the mechanism of the reaction are investigated experimentally. The project was developed in collaboration with Dr. Jean-Simon Suppo and the chemistry involved has been published in *Org. Lett.* **2020**, *22*, 3045–3049.

Chapter 3 collects the recent advances in the nitro-directed rhodium(III)-catalyzed C–H alkynylation of arenes. The scope and further derivatization of the resulting alkynylated products are discussed. The mechanism of the transformation is studied encompassing experimental and theoretical approaches. The project was developed in collaboration with Dr. Eric Tan, Dr. Cristina García-Morales and Dr. Marc Montesinos-Magraner.

A **General Conclusion** section is provided at the end of this manuscript summarizing the results obtained during this PhD Thesis.

UNIVERSITAT ROVIRA I VIRGILI
From Gold-Catalyzed Asymmetric or Photoredox-Assisted Cyclizations to Rhodium-Catalyzed C–H Alkynylations
Joan Guillem Mayans Peñarrubia

List of Abbreviations and Acronyms

In this Doctoral Thesis, the abbreviations and acronyms most commonly used in organic and organometallic chemistry have been used following the recommendations from *"Guidelines for authors"* published in *Journal of Organic Chemistry*. Additional abbreviations are listed below:

APCI	Atmospheric pressure chemical ionization
BAr_4^{F-}	Tetrakis[3,5-bis(trifluoromethyl)phenyl]borate
DCE	1,2-Dichloroethane
DMS	Dimethylsulfide
ee	Enantiomeric excess
er	Enantiomeric ratio
ESI	Electrospray Ionization
HFIP	Hexafluoro-2-propanol
HRMS	High Resolution Mass Spectrometry
IMes	1,3-Bis(2,4,6-trimethylphenyl)imidazole-2-ylidene
IPr	1,3-Bis(2,6-diisopropylphenyl)imidazole-2-ylidene
JohnPhos	(2-Biphenyl)di-*tert*-butylphosphine
KIE	Kinetic isotope effect
L	Ligand
NBO	Natural bond orbital
NLMO	Natural localized molecular orbitals
NTf_2	Bis(trifluoromethyl)imidate
OA	Oxidative addition
OTf	Trifluoromethanesulfonate
RE	Reductive elimination
RSM	Recovered starting material
tht	Tetrahydrothiophene
tmbn	Trimethoxybenzonitrile
Ts	*p*-toluenesulfonyl
TIPS	Triisopropylsilyl

Abstract

Over the past two decades, homogenous gold(I) catalysis has become a powerful synthetic tool for the rapid construction of complex molecular structures. The unique carbophilic behavior displayed by gold catalysts has resulted in the development of new transformations that have been widely applied in the total synthesis of biologically active compounds and electronically relevant organic materials. Despite the remarkable performance as Lewis π-acid, the field of asymmetric gold catalysis has witnessed a slower growth mainly due to the linear dicoordination adopted by gold(I), which places the chiral information on the direct opposite site of the reactive center where the outer-sphere nucleophilic attack takes place. In the first chapter of this Doctoral Thesis, we took advantage of a rationally designed chiral gold(I) complex bearing a C_2-symmetric 2,5-disubstituted pyrrolidine next to the reaction center to develop the enantioselective 6-*endo*-dig cyclization of aryl-tethered 1,6-enynes. The reaction was successfully applied in the first enantioselective total synthesis of carexanes I, P and O. The enynes, obtained through a Sonogashira/bromination/prenylation sequence, engaged efficiently in the asymmetric cyclization furnishing the products in good yields and excellent enantiomeric ratios. The natural products were obtained by straightforward derivatization of these bicyclic compounds. Theoretical and experimental studies point towards non-covalent interactions between the substrate and the chiral pocket in the catalyst as the source of enantio-induction during the cyclization.

Likewise, the reluctance of gold to undergo oxidative processes, which is in part related to the relativistic effects, has limited the applicability of this metal in ubiquitous cross-coupling reactions. In this context, the second chapter of the thesis focused in the development of the photoredox-assisted gold(I)/gold(III)-catalyzed arylative alkoxycyclization of 1,6-enynes in the presence of aryldiazonium salts. The reaction tolerated a wide variety of functional groups including halides, remarking the orthogonality of the method with respect to traditional palladium cross-coupling. The resulting exocyclic alkenes were obtained in moderate to good yields with the complementary configuration to the one previously reported in similar gold(I)-catalyzed transformations.

Finally, we developed a method for the selective *ortho*-alkynylation of nitroarenes, where the nitro moiety plays the role of directing group. The approach follows the line of the recent achievements on rhodium(III)-catalyzed C–H alkynylation reported by our group. Under the optimized reaction conditions, a variety of nitro(hetero)arenes could be functionalized including the antihypertensive agent nitrenedipine. The corresponding alkynylated products could be converted in indoles *via* a high-yielding reduction/cyclization sequence or serve as substrates for palladium-catalyzed denitrative cross-coupling reactions. The study of the mechanism using experimental and computational means concluded that the turnover limiting C–H bond cleavage takes place in first place through an electrophilic concerted metalation deprotonation process, followed by alkyne insertion and silver-assisted bromide elimination to close the catalytic cycle.

General Objectives

The main general objective of this Doctoral Thesis was the development of new synthetic strategies for the construction of molecular complexity by employing homogeneous transition metal catalysis. Specifically, our studies focused on the following objectives:

- The development of a new asymmetric gold(I)-catalyzed cyclization and its application to the first total synthesis of different members of the carexane family of natural products.
- The study of the reactivity resulting by merging the gold(I)/gold(III) arylative methodologies with the well-stablished gold(I)-catalyzed cyclization of enynes.
- The exploration of the nitro group as a directing group for the *ortho*-alkynylation of nitro(hetero)arenes.

A more detailed description of the objectives will be presented in the corresponding chapters.

General Introduction

From the Stars to our Laboratories

The immensity of the night sky is flooded with remote shiny stars. The nature of this overwhelming landscape has fascinated humankind for thousands of years, seen from a religious point of view to guide our faith, as a map to guide our expeditions or as an open door to study the universe.

Stars are formed from collapsing clouds of gas and cosmic dust, and its initial chemical composition is mostly based on hydrogen and helium. During its lifetime, stars function as huge nuclear plants fusing hydrogen into helium, a process that releases energy as electromagnetic radiation. Although other fusions take place giving rise to low weight atoms (Li, C, N, O…),[1] hydrogen remains the main fuel of stars. As hydrogen is consumed in nuclear fusion reactions, the stars age towards their final death.[2] For massive stars (more than 8 times heavier than the Sun), one of the last stages in their life can involve the gravitational collapse of its core into a neutron star.[3] When two of these extremely dense astronomical objects orbit each other closely, they spiral inward until they merge giving rise to a more massive neutron star, or a black hole. During this colossal collision, the atomic nuclei present are heavily bombarded with neutrons provoking a fast increase in their size. This process is called the rapid neutron-capture (or *r*-process)[4] and is one of the main sources of gold (as well as other heavy atoms) in the universe. Astrophysical models suggest that the gold produced during these collisions (between 3 and 13 times the mass of Earth) is enough to account for most of the abundance of this element in the universe.[5] All the material expelled in these events spreads into the interstellar medium ready to be incorporated in new forming stars and planetary systems.

In its first stages of accretion (around 4.53 Ga ago), the Earth recollected material from regular clump impacts (mostly gold-containing chondrite-type impactors).[6] Later, around 4.50 Ga ago, a huge impactor called Theia crushed into the young planet, triggering the formation of the Moon.[7] As a result of the constant collisions, the early Earth was completely molten and the dense and highly siderophilic elements (such as Fe, Co, Ni, Ru, Rh, Pd, Re, Os, Ir, Pt, Au…) sank down

1 Hoyle, F. *Mon. Not. R. Astron. Soc.* **1946**, *106*, 343–383.

2 Prialnik, D. (2000). *An Introduction to the Theory of Stellar Structure and Evolution*. ISBN 978-0-521-65937-6.

3 Lattimer, J. M.; Prakash, M. *Science* **2004**, *304*, 536–542.

4 Goriely, S. *Phys. Lett. B* **1998**, *436*, 10–18.

5 (a) Côté, B.; Fryer, C. L.; Belczynski, K.; Korobkin, O.; Chruślińska, M.; Vassh, N.; Mumpower, M. R.; Lippuner, J.; Sprouse, T. M.; Surman, R.; Wollaeger, R. *ApJ.* **2018**, *855*, 99. DOI: 10.3847/1538-4357/aaad67. (b) Perkins, S. *Science AAAS* **2018**. DOI: 10.1126/science.aat6449.

6 Bowring, S. A.; Housh, T. *Science* **1995**, *269*, 1535–1540.

7 Young, E. D., Kohl, I. E.; Warren, P. H.; Rubie, D. C.; Jacobson, S. A.; Morbidelli, A. *Science* **2016**, *351*, 493–496.

into the core of the forming planet.[8] The most accepted hypotheses to rationalize the unexpectedly high abundance of gold (and other siderophilic metals) in today's Earth crust rely on the delivery of these elements from one or more asteroid impacts after planet solidification.[9]

Gold is unevenly distributed on Earth, with an average concentration of 1.5 μg/kg on the crust.[10] As a noble metal, gold does not react easily with other substances. Consequently, this element is often found in nature in its metallic state, most frequently, as fine particles in rocks formed throughout the history of the Earth.[11] Although less frequently, this metal also occurs in different naturally-occurring minerals and alloys.[12] It is known that gold is present in seawaters, albeit in extremely low concentrations.[13] However, the largest sources of the noble metal in our planet are mining deposits, where its concentration exceeds the 10 mg/kg (Figure 1). These reservoirs are present in different parts of the world, such as South Africa, China, Canada, Australia and Russia.

Figure 1. Round Mountain gold mine in Smokey Valley (Nevada).

8 Day, J. M. D.; Brandon, A. D.; Walker, R. J. *Rev. Mineral. Geochem.* **2016**, *81*, 161–238.

9 (a) Brasser, R.; Mojzsis, S. J.; Werner, S. C.; Matsumura, S.; Ida, S. *Earth Planet. Sci. Lett.* **2016**, *455*, 85–93. (b) Genda, H; Brasser, R.; Mojzsis, S. J. *Earth Planet. Sco. Lett.* **2017**, *480*, 25–32.

10 Frimmel, H. E. *Earth Planet. Sci. Lett.* **2008**, *267*, 45–55.

11 La Niece, S. (2009). *Gold*. ISBN 978-0-674-03590-4.

12 Examples of naturally-occurring gold-containing minerals: calaverite, krennerite, petzite and sylvanite (telluride gold/silver minerals), maldonite (Au_2Bi) and aurostibite ($AuSb_2$); alloys: auricupride (Cu_3Au), novodneprite ($AuPb_3$) and weishanite ($(Au,Ag)_3Hg_2$).

13 Falkner, K. K.; Edmond, J. M. *Earth Planetary Sci. Lett.* **1990**, *98*, 208–221.

In artisanal small-scale gold mining, the extraction of gold from its matrix often involves a sequence of mercury amalgamation followed by removal of the mercury by heating.[14] At industrial scale, hydrometallurgical flowsheets such as leaching, solution purification, concentration and metal recovery are implemented for the treatment of larger batches, preceded by an oxidative pretreatment to dissolve gold.[15] Further refinement might be carried out at industrial scale by electrochemical deposition (Wöhlwill process) or by oxidation of the impurities using chlorine (Miller process).[16]

Its unique physical and chemical properties make gold a suitable choice for different applications ranging from jewelry, coinage and ornaments to medicine, dentistry and electronics. According to recent studies,[17] gold is mostly consumed in jewelry and investments (~ 90%). Among the remaining 10%, a tiny fraction is acquired by research groups, kept inside our laboratories.

The Unique Properties of Gold

Undoubtedly, gold is one of the most popular elements in the periodic table. With chemical symbol Au (from Latin *aurum*) and atomic number 79, gold has been present from very early in human history. Due to its intrinsic inertness and its characteristic eye-catching color, gold became a symbol of power and immortality in many ancient cultures (Figure 2).

Figure 2. Examples highlighting the importance of gold in ancient cultures. From left to right: Mask of Tutankhamun; Sripuram temple in India; statue of Pachacuti in Peru.

The unique physical and chemical behavior of gold is in part attributed to the relativistic effects, which are the ensemble of phenomena resulting from the consideration of special

14 Malm, O. *Environ. Res.* **1998**, *77*, 73–78.

15 Marsden, J. O.; House, C. I. (2006). *The Chemistry of Gold Extraction*. ISBN 978-0-87335-240-6.

16 Pletcher, D.; Walsh, F. C. (1982). *Industrial Electrochemistry*. ISBN 978-0-412-30410-1.

17 For a continuously updated website on world gold consumption, visit: https://www.usdebtclock.org/gold-demand-by-country.html

relativity in quantum mechanics.[18] The Schrödinger equation unambiguously predicts the atomic orbital energy levels for hydrogen. However, in heavier atoms in which the inner electrons (*s* and *p*) move close to the speed of light (c), a more general relativistic approach is required.

One basic consequence of the special theory of relativity is that mass increases towards infinity as the speed of a body approaches c, which can be expressed mathematically as:

$$m = \frac{m_0}{\sqrt{1 - (v/c)^2}}$$

where m is the corrected relativistic mass, m_0 is the non-relativistic mass (in the resting state when $v = 0$), and v is velocity. For example, when this equation is applied to 1*s* electrons in gold ($v = 0.58c$), the calculated relativistic mass m is around 1.22 times higher than m_0. This increase of the mass involves a decrease of the Bohr radius, which is defined as the most probable distance between the nucleus and the electron in the hydrogen atom:

$$a_0 = \frac{\hbar^2}{m_e e^2}$$

where a_0 is the Bohr radius, $\hbar$ is the reduced Planck constant, m_e is the mass of the electron and e its charge.[18]

Overall, a physical consequence resulting from the consideration of special relativity in quantum mechanics is a contraction and stabilization of the more penetrating orbitals (*s* and in a lower extent *p*), which entails a higher binding energy of the corresponding *s* and *p* electrons. On the other hand, electrons occupying *d* and *f* orbitals are better shielded by the electrons in the contracted *s* and *p* orbitals and therefore suffer a weaker nuclear attraction. This results in the relative expansion and destabilization of *d* and *f* orbitals and a lower binding energy of the corresponding *d* and *f* electrons.

Although relativistic effects become more relevant as nuclear charge increases and appear in other transition metals, they reach a local maximum in gold,[19] highlighting their critical influence on the physical and chemical properties of this metal (Figure 3).[20]

18 Pyykkö, P.; Desclaux, J.-P. *Acc. Chem. Res.* **1979**, *12*, 276.

19 For an explanation of this local maximum, see: Autschbach, J.; Siekierski, S.; Seth, M.; Schwerdtfeger, P.; Schwarz, W. H. E *J. Comput. Chem.* **2002**, *23*, 804–813.

20 Pyykkö, P. *Chem. Rev.* **1988**, *88*, 563–594.

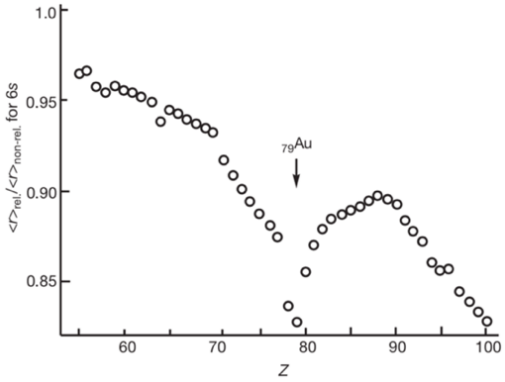

Figure 3. Relativistic contraction of the 6s orbital in atoms from Cs (Z = 55) to Fm (Z = 100).[18]

For instance, the relativistic effects can explain the thermodynamic stability of gold towards oxidation. The energy required to remove the stabilized 6*s* electron and form the gold(I) cation is considerably large (high ionization potential) (Figure 4a). On the other hand, the process of accepting an electron in the stabilized 6*s* orbital is more favored, since its binding energy to the nucleus is higher. This directly translates in high electron affinity and electronegativity values for gold (Figure 4b) offering the possibility to access stable gold(-I) complexes such as CsAu or NMe_4Au.[21]

(a)

Au^+/Au^0	$E^0 = 1.69$ V
Ag^+/Ag^0	$E^0 = 0.80$ V
Pt^{2+}/Pt^0	$E^0 = 1.18$ V
Hg^{2+}/Hg^0	$E^0 = 0.65$ V

(b)

Ti 1.54	V 1.63	Cr 1.66	Mn 1.55	Fe 1.83	Co 1.88	Ni 1.91	Cu 1.90	Zn 1.65
Zr 1.33	Nb 1.6	Mo 2.16	Tc 1.9	Ru 2.2	Rh 2.28	Pd 2.20	Ag 1.93	Cd 1.69
Hf 1.3	Ta 1.5	W 2.36	Re 1.9	Os 2.2	Ir 2.20	Pt 2.28	Au 2.54	Hg 2.00

Figure 4. (a) Reduction potentials for gold and its immediate neighbors.[22] (b) Electronegativity values for the transition metals.

Once the gold(I) species is formed, the subtraction of further electrons from the destabilized 5*d* orbitals becomes relatively easier.[22] This contributes to the stabilization of gold(III) species (more stable than the respective copper(III) and silver(III) analogues) and higher oxidation states.[23]

The characteristic color of gold can be explained through the consideration of relativistic effects.[21] In a non-relativistic study, the energy gap between 5*d* and 6*s* is around 3.6 eV, which lies in the UV spectrum. Introducing relativistic modifications, the new gap between the $5d_{3/2}$ and the stabilized 6*s* is around 2.4 eV, lying now in the visible spectrum (Figure 5a). Thus, gold absorbs violet, blue and a bit of green and reflects the red and yellow (Figure 5b).

21 Jansen, M. *Chem. Soc. Rev.* **2008** 37, 1826–1835.

22 Bratsch, S. G. *J. Phys. Chem. Ref. Data* **1989**, *18*, 1–22.

23 (a) Vasile, M. J.; Richardson, T. J.; Stevie, F. A.; Falconer, W. E. *J. Chem. Soc., Dalton Trans.* **1976**, 351–353. (b) Lin, J.; Zhang, S.; Guan, W.; Yang, G.; Ma, Y. *J. Am. Chem. Soc.* **2018**, *140*, 9545–9550.

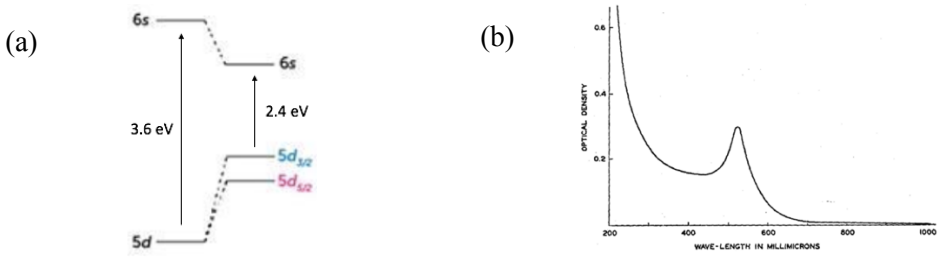

Figure 5. (a) Schematic representation of the energy gap between the frontier orbitals for gold.[21] Left: non-relativistic gap. Right: relativistic gap. (b) Absorption spectrum of colloidal gold.[24]

Relativistic effects are also connected to the chemistry of gold cations in homogeneous catalysis.[25] Hence, the relativistic contraction of the 6*s* orbital results in greatly strengthened Au–L bonds (L = ligand).[26] The smaller energetic gap between the valence orbitals also accounts for an efficient hybridization of the *s*/*d* and *s*/*p* orbitals, which is crucial to explain the preference of gold(I) to form linear two-coordinated complexes.[27]

It has been shown that relativistic considerations are important to understand why aurophilic interactions are comparably as stabilizing as hydrogen bonds (5–10 kcal/mol), a phenomenon that explains the propensity of low-coordinated gold(I) compounds to associate into dimers, clusters or even polymers *via* Au–Au interactions.[28]

Because of its high electronegativity, gold complexes are generally strong Lewis acids. However, in gold(I), the positive charge is highly diluted in a large diffuse cation. As a result, the strongest interactions with Lewis bases arise from efficient orbital overlapping rather than from electrostatic attractions. This soft behavior encompasses both a low oxophilicity and a great affinity for large orbitals such as the π orbitals in a C–C multiple bond. Indeed, years after the pioneering work and Teles[29,30] and Tanaka[31], gold(I) catalysts have been widely applied in the selective electrophilic activation of C–C multiple bonds to generate molecular complexity.[32]

---

24 Turkevich, J.; Garton, G.; Stevenson, P. C. *J. Colloid. Sci.* **1954**, *9*, 26–35.

25 Gorin, D. J.; Toste, F. D. *Nature* **2007**, *446*, 395–403.

26 Desclaux, J. P.; Pyykkö, P. *Chem. Phys. Lett.* **1976**, *39*, 300–303.

27 Gimeno, M. C.; Laguna, A. *Chem. Rev.* **1997**, *97*, 511–522.

28 (a) Scherbaum, F.; Grohmann, A.; Huber, B.; Krüger, C.; Schmidbaur, H. *Angew. Chem. Int. Ed.* **1988**, *27*, 1544–1546. (b) Schmidbaur, H. *Gold Bull*. **2000**, *33*, 3–10.

29 Teles, J. H.; Brode, S.; Chabanas, M. *Angew. Chem. Int. Ed.* **1998**, *37*, 1415–1418.

30 For selected precedents, see: (a) Norman, R. O. C.; Parr, W. J. E.; Thomas, C. B. *J. Chem. Soc., Perkin Trans. 1* **1976**, 1983–1987. (b) Ito, Y.; Sawamura, M.; Hayashi, T. *J. Am. Chem. Soc.* **1986**, *108*, 6405–6406. (c) Fukuda, Y.; Utimoto, K. *J. Org. Chem.* **1991**, *56*, 3729–3731.

31 Mizushima, E.; Sato, K.; Hayashi, T.; Tanaka, M. *Angew. Chem. Int. Ed.* **2002**, *41*, 4563–4565.

32 (a) Hashmi, A. S. K. *Chem. Rev.* **2007**, *107*, 3180–3211. (b) Fürstner, A.; Davies, P. W.; *Angew. Chem. Int. Ed.* **2007**, *46*, 3410–3449. (c) Fürstner, A. *Chem. Soc. Rev.* **2009**, *38*, 3208–3221. (d) Shapiro, N. D.; Toste, F.

Gold(I) complexes, with electronic configuration [Xe] $6s^0\ 4f^{14}\ 5d^{10}$, are diamagnetic, which makes them suitable for NMR studies.[32a] This, together with the concept of isolobality[33] (the fragment $[R_3PAu]^+$ is isolobal to H^+), has contributed significantly to the understanding and development of gold(I)-catalyzed reactions.

Gold(I) Precatalysts

Simple gold salts such as $NaAuCl_4$ or AuCl are active enough to catalyze different chemical transformations.[34] Interestingly, in neutral gold complexes [LAuCl] as well as cationic gold complexes [LAuL']X, the stereoelectronic properties of the ligand(s) strongly influence the nature of the gold catalyst.[35] The possibility to modulate the reactivity of the catalytic center by changing the ligand or the counteranion (X) has led to a substantial expansion of the use of gold homogeneous catalysis.[32,36] However, this highly modular character together with the tendency of gold(I)-catalyzed reactions to yield different isomers makes this chemistry difficult to predict, resulting frequently in the necessity of large catalyst screenings for the development of new reactivity.[37]

As a soft Lewis acid, gold(I) coordinates preferentially to soft Lewis bases such as N-heterocyclic carbenes, phosphines, phosphites, or arsines. Less common nitrogen, oxygen and sulfur-based ligands usually display a more labile character.[38] Due to its low oxophilicity, gold(I) complexes are frequently air and moisture stable. In general, more electron donating ligands

D. *Synlett* **2010**, 675–691. (e) Obradors, C.; Echavarren, A. M. *Acc. Chem. Res.* **2014**, *47*, 902–912. (f) Dorel, R.; Echavarren, A. M. *Chem. Rev.* **2015**, *115*, 9028–9072.

33 (a) Hoffmann, R. *Angew. Chem. Int. Ed.* **1982**, *21*, 711–724. (b) Raubenheimer, H. G.; Schmidbaur, H. *Organometallics* **2011**, *31*, 2507–2522.

34 (a) Karmakar, S.; Kim, A.; Oh, C. H. *Synthesis* **2009**, *2*, 194-198. (b) Brand, J. P.; Chevalley, C.; Waser, J. *Beilstein J. Org. Chem.* **2011**, *7*, 565–569.

35 Gorin, D. J.; Sherry, B. D.; Toste, F. D. *Chem. Rev.* **2008**, *108*, 3351–3378.

36 (a) Partyka, D. V.; Robilotto, T. J.; Zeller, M.; Hunter, A. D.; Gray, T. G. *Organometallics* **2008**, *27*, 28–32. (b) Pérez-Galán, P.; Delpont, N.; Herrero-Gómez, E.; Maseras, F.; Echavarren, A. M. *Chem. Eur. J.* **2010**, *16*, 5324–5332. (c) Hashmi, A. S. K.; Hengst, T.; Lothschütz, C.; Rominger, F. *Adv. Synth. Catal.* **2010**, *352*, 1315–1337. (d) Fortman, G. C.; Nolan, S. P. *Organometallics* **2010**, *29*, 4579–4583.

37 Fürstner, A. *Acc. Chem. Res.* **2014**, *47*, 925–938.

38 (a) Kolb, A.; Bissinger, P.; Schmidbaur, H. *Z. Anorg. Allg. Chem.* **1993**, *619*, 1580–1588. (b) Abdou, H. E.; Mohamed, A. A.; Fackler Jr, J. P. (2009) *Gold Chemistry: Applications and Future Directions in the Life Science* (Chapter 1). ISBN: 978-3-527-32086-8.

render the catalytic center less electrophilic and *vice-versa* (Figure 6a).[35,39] Similarly, more coordinating anions also lead to less electrophilic gold(I) cationic complexes (Figure 6b).[40]

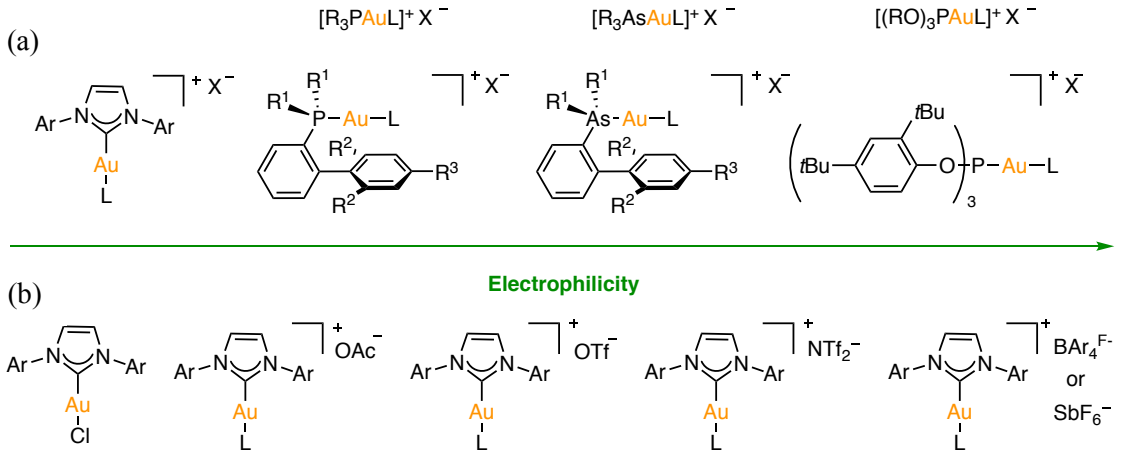

Figure 6. Increase in electrophilicity of gold(I) complexes with the use of: (a) less electron-donating ligands (b) less coordinating counteranions.

More recently, the rational design of ligands to overcome the challenges associated with asymmetric gold(I) catalysis and gold-catalyzed cross-coupling reactions has become an active field of research. These topics will be discussed in more detail in chapters 1 and 2.

The most common precursors for the preparation of gold(I) complexes of type [LAuCl] are gold(III) chlorides such us $NaAuCl_4$ or $HAuCl_4$. Typically, the procedure involves a reduction using excess of dimethylsulfide (DMS) or tetrahydrothiophene (tht), followed by a ligand exchange event with the desired ligand (Scheme 1).[41]

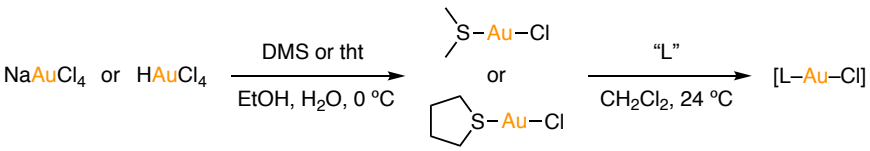

Scheme 1. General synthesis of [LAuCl] precatalysts.

In catalytic cycles, an exchange between a labile ligand and the substrate has to take place. It is known that the mechanism for this ligand exchange process in gold(I) linear complexes is predominantly associative.[42] The alternative dissociative pathway would generate a highly

39 Carreras, J.; Pereira, A.; Zanini, M.; Echavarren, A. M. *Organometallics*, **2018**, *37*, 3588–3597.

40 (a) Zhdanko, A.; Maier, M. E. *ACS Catal.* **2014**, *4*, 2770–2775. (b) Biasiolo, L.; Trinchillo, M.; Belanzoni, P.; Belpassi, L.; Busico, V.; Ciancaleoni, G.; D'Amora, A.; Maccioni, A.; Tarantelli, F.; Zuccaccia, D. *Chem. Eur. J.* **2014**, *20*, 14594–14598. (c) Jia, M.; Bandini, M. *ACS Catal.* **2015**, *5*, 1638–1652. (d) Zuccaccia, D.; Del Zotto, A.; Baratta, W. *Coord. Chem. Rew.* **2019**, *396*, 103–116.

41 Al-Sa'Ady, A. K.; McAuliffe, C. A.; Parish, R. V.; Sandbank, J. A. *Inorg. Synth.* **1985**, 23, 191–194.

42 (a) Dickson, P. N.; Wehrli, A.; Geier, G. *Inorg. Chem.* **1988**, *27*, 2921–2925. (b) Ranieri, B.; Escofet, I.; Echavarren, A. M. *Org. Biomol. Chem.* **2015**, *13*, 7103–7118.

unstable coordinatively unsaturated cationic intermediate, $[LAu]^+$, which is unlikely under mild conditions.[43] Usually, active gold(I) species are generated *in situ* by chloride abstraction from gold chloride complexes upon treatment with a silver salt bearing a weakly coordinating anion.[36] Interestingly, in the absence of substrate or coordinating solvent, less reactive chloride-bridged dinuclear species [L–Au–Cl–Au–L]X are readily formed (Scheme 2).[44] It has been proposed that the formation of this complex could explain, at least partially, the erratic results attributed to the so-called "silver effects".[42b,45] Other possible silver-free protocols include the use of copper or sodium salts as chloride scavengers,[46] or the protonolysis of [L–Au–Me][29,31] and [L–Au–OH][47] complexes with Brønsted acids.

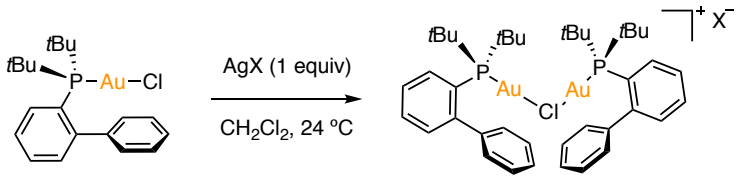

Scheme 2. Synthesis of the cationic chloride bridged gold(I) complex $[((JohnPhos)Au)_2Cl]X$.[44]

An alternative for the generation of active gold(I) species is the use of stable cationic gold(I) precatalysts bearing a labile ligand that readily undergoes exchange with the substrate. Our group pioneered the synthesis of air-stable cationic gold(I) complexes by reacting different [LAuCl] complexes with silver salts in the presence nitriles (Scheme 3).[48] Since then, this concept has been successfully applied in the synthesis of numerous cationic gold(I) complexes.[49]

43 Couce-Ríos, A.; Kovács, G.; Ujaque, G.; Lledós, A. *ACS Catal.* **2015**, *5*, 815–829.

44 (a) Homs, A.; Escofet, I.; Echavarren, A. M. *Org. Lett.* **2013**, *15*, 5782–5785. (b) Zhu, Y.; Day, C. S.; Zhang, L.; Hauser, K. J.; Jones, A. C. *Chem. Eur. J.* **2013**, *19*, 12264–12271.

45 (a) Wang, D.; Cai, R.; Sharma, S.; Jirak, J.; Thummanapelli, S. K.; Akhmedov, N. G.; Zhang, H.; Liu, X.; Petersen, J. L.; Shi, X. *J. Am. Chem. Soc.* **2012**, *134*, 9012–9019. (b) Zhdanko, A.; Maier, M. E. *ACS Catal.* **2015**, *5*, 5994–6004.

46 Guérinot, A.; Fang, W.; Sircoglou, M.; Bour, C.; Bezzenine-Lafollée, S.; Gandon, V. *Angew. Chem. Int. Ed.* **2013**, *52*, 5848–5852.

47 For selected examples see: (a) Gaillard, S.; Slawin, A. M. Z.; Nolan, S. P. *Chem. Commun.* **2010**, *46*, 2742–2744. (b) Gaillard, C.; Bosson, J.; Ramón, R. S.; Nun, P.; Slawin, A. M. Z.; Nolan, S. P. *Chem. Eur. J.* **2010**, *16*, 13729–13740.

48 (a) Nieto-Oberhuber, C.; López, S.; Muñoz, M. P.; Cárdenas, D. J.; Buñuel, E.; Nevado, C.; Echavarren, A. M. *Angew. Chem. Int. Ed.* **2005**, *44*, 6146–6148. (b) Amijs, C. H. M.; López-Carrillo, V.; Raducan, M.; Pérez-Galán, P.; Ferrer, C.; Echavarren, A. M. *J. Org. Chem.* **2008**, *73*, 7721–7730.

49 For selected examples see: (a) Mézailles, N.; Ricard, L.; Gagosz, F. *Org. Lett.* **2005**, *7*, 4133–4136. (b) Duan, H.; Sengupta, S.; Petersen, J. L.; Akhmedov, N. G.; Shi, X. *J. Am. Chem. Soc.* **2009**, *131*, 12100–12102.

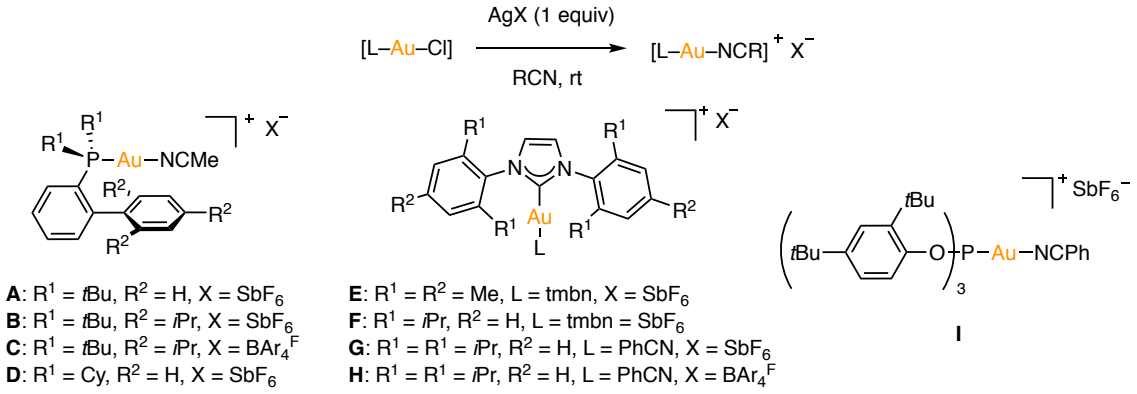

Scheme 3. Synthesis of representative stable gold(I) cationic complexes.

Remarkably, our group achieved the synthesis of the homoleptic complex $[Au(tmbn)_2]SbF_6$ (tmbn = 2,4,6-trimethoxybenzonitrile) that, in the presence of a ligand, easily undergoes ligand exchange furnishing the corresponding versatile cationic $[L–Au–tmbn]SbF_6$ precatalysts.[50]

Homogeneous Gold(I) Catalysis

By the end of last century, homogeneous gold(I) catalysis was not considered a useful tool in organic chemistry. With the exception of a few reports,[51] only two reactions had been explored with regard of their potential for synthesis: the asymmetric aldol reaction developed by the groups of Ito and Togni (Scheme 4a),[30b,52] and the addition of nucleophiles to alkynes, investigated by the groups of Utimoto and Teles (Scheme 4b).[29]

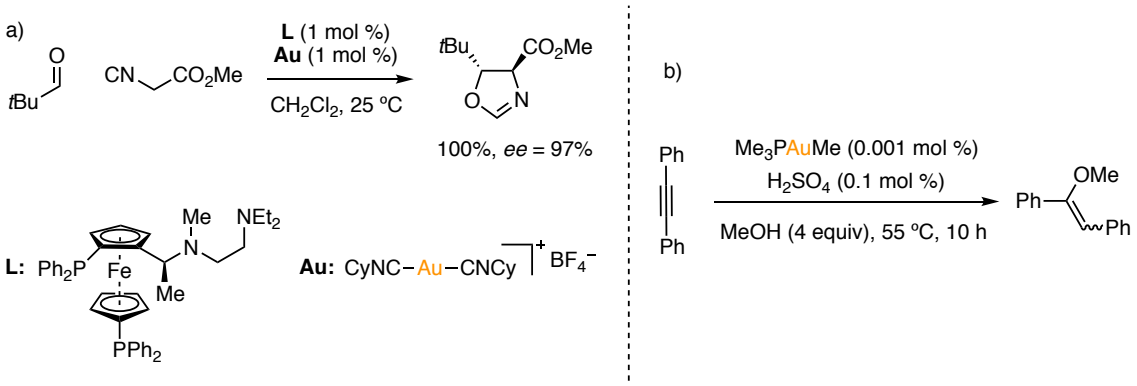

Scheme 4. Selected examples of gold(I)-catalyzed (a) asymmetric aldol reaction between isocyanates and aldehydes,[30b] (b) electrophilic activation of alkynes.[29]

50 Raducan, M; Rodríguez-Escrich, C; Cambeiro, X. C.; Escudero-Adán, E. C.; Pericàs, M. A.; Echavarren, A. M. *Chem. Commun.* **2011**, *47*, 4893–4895.

51 For selected examples see: (a) Schwemberger, W.; Gordon, W. *Chem. Zentralbl.* **1935**, *105*, 514. (b) Gassman, P. G.; Meyer, G. R.; Williams, F. J. *J. Am. Chem. Soc.* **1972**, *94*, 7741–7748. (c) Tamaki, A.; Kochi, J. K. *J. Organometal. Chem.* **1972**, *40*, C81–C84. (d) Meyer, L.-U.; de Meijere, A. *Tetrahedron Lett.* **1976**, *17*, 497–500.

52 Sawamura, M.; Ito, Y. (2000) *Asymmetric Carbon–Carbon Bond–Forming Reactions: Asymmetric Aldol Reactions–Discovery and Development*. ISBN 978-0-471-72150-6.

Over the past two decades, the reactivity of organogold complexes has been studied extensively. Gold(I) catalysts have demonstrated their applicability in the selective intra- or intermolecular functionalization of C–C multiple bonds to form new C–C or C–heteroatom bonds.[32] Typically proposed as intermediates in these and other gold-catalyzed reactions,[53] gold(I) carbenes have engage in a wide range of transformations including cycloadditions,[54] C–H insertion,[55] dimerizations[56] and oxidations,[57] *inter alia.*[58]

There is some controversy surrounding the carbenic or cationic character of these organogold intermediates (Figure 7a).[59] Unfortunately, most of gold(I)-carbene intermediates are too reactive to be isolated.[60] In 2009, Toste and Goddart proposed a fundamental description of the bonding mode in gold carbenes.[61] Accordingly, both the ligand and the carbene fragment donate their paired electrons to gold, forming a 3 center – 4 electron σ-bond. The gold center can, in turn, form two π-bonds by backdonation of its electrons from two filled *d*-orbitals to empty π*-acceptors on the ligand and carbene (Figure 7b). Therefore, these organogold(I) intermediate can be considered anything from metal stabilized carbocations to metal carbenes depending on the stereoelectronic properties of the ligand and the substituents on the carbene.[56]

---

53 For different procedures to generate gold(I) carbenes, see: (a) Shin, S.; *Top. Curr. Chem.* **2015**, *357*, 22–62. DOI: 10.1007/128_2014_589. (b) Harris, R. J.; Widenhoefer, R. A. *Chem. Soc. Rev.* **2016**, *45*, 4533–4551. (c) Mato, M.; García-Morales, C.; Echavarren, A. M. *ChemCatChem* **2019**, *11*, 53–72.

54 (a) Qian, D.; Zhang, J. *Chem. Soc. Rev.* **2015**, *44*, 677–698. (b) Yin, X.; Mato, M.; Echavarren, A. M. *Angew. Chem. Int. Ed.* **2017**, *56*, 14591–14595.

55 (a) De Haro, T.; Nevado, C.; *Synthesis* **2011**, *16*, 2530–2539. (b) Yu, Z.; Ma, B.; Chen, M.; Wu, H.-H.; Liu, L.; Zhang, J. *J. Am. Chem. Soc.* **2014**, *136*, 6904–6907. (c)Yin, X.; Zuccarello, G.; García-Morales, C.; Echavarren, A. M. *Chem. Eur. J.* **2019**, *25*, 9485–9490.

56 García-Morales, C.; Pei, X.-L.; Sarria-Toro, J. M.; Echavarren, A. M. *Angew. Chem. Int. Ed.* **2019**, *58*, 3957–3961.

57 For selected example, see: (a) Harris, R. J.; Widenhoefer, R. A. *Angew. Chem. Int. Ed.* **2014**, *53*, 9369–9371. (b) Wang, J.; Cao, X.; Lv, S.; Zhang, C.; Xu, S.; Shi, M.; Zhang, J. *Nat. Commun.* **2017**, *8*, 14625.

58 For miscellaneous reactions of gold(I) carbenes, see: (a) Mudd, R. J.; Young, P. C.; Jordan-Hore, J. A.; Rosair, G. M.; Lee, A.-L. *J. Org. Chem.* **2012**, *77*, 7633–7639. (b) Zeineddine, A.; Rekhroukh, F.; Carrizo, E. D. S.; Mallet-Ladeira, S.; Miqueu, K.; Amgoune, A.; Bourissou, D. *Angew. Chem. Int. Ed.* **2018**, *57*, 1306–1310.

59 (a) Echavarren, A. M. *Nat. Chem.* **2009**, *1*, 431–433. (b) Wang, Y.; Muratore, M. E.; Echavarren, A. M. *Chem. Eur. J.* **2015**, *21*, 7332–7339.

60 For selected examples in the observation of key species, see: (a) Hashmi, A. S. K. *Angew. Chem. Int. Ed.* **2010**, *49*, 5232–5241. (b) Liu, L.-P.; Hammond, G. B. *Chem. Soc. Rev.* **2012**, *41*, 3129–3139.

61 Benitez, D.; Shapiro, N. D.; Tkatchouk, E.; Wang, Y.; Goddard, W. A.; Toste, F. D. *Nat. Chem.* **2009**, *1*, 482–486.

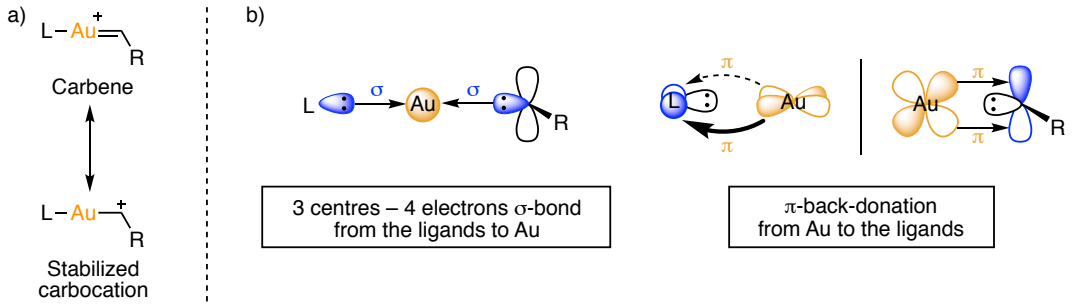

Figure 7. a) Extreme resonance forms and b) bonding components in organogold(I) intermediates.

Among the above-mentioned reactivity, in the vast majority of gold(I)-catalyzed transformations the metal acts as carbophilic Lewis acid promoting the hydrofunctionalization of C–C multiple bonds under remarkably mild conditions. Especially relevant for this thesis is the activation of alkynes towards nucleophilic attack, a well-known reaction the mechanism of which was studied in detail by the group of Maier.[62] A simplified version of the process is depicted in Scheme 5 and all the steps are discussed below.

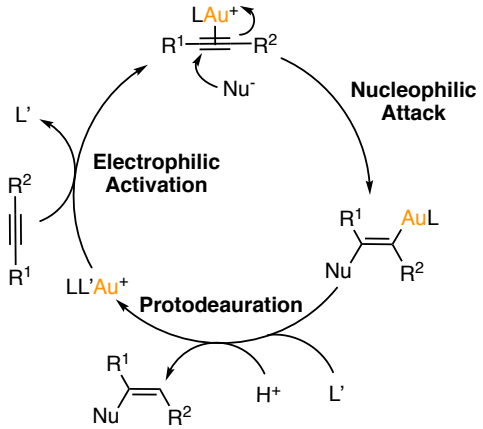

Scheme 5. General mechanism for the gold(I)-catalyzed hydrofunctionalization of alkynes.

Electrophilic Activation of Alkynes

The first complex bearing ethylene as a ligand dates back to 1831.[63] After careful analysis, professor Zeise concluded that a crystalline yellow compound formed in the reaction of $K_2[PtCl_4]$ in boiling ethanol enclosed ethylene derivatives. Although controversial at the time, ulterior studies proved that the mentioned compound contained ethylene itself coming from the formal dehydration of ethanol.[64] This compound (known today as Zeise's salt, $K[PtCl_3(C_2H_4)]\cdot H_2O$) is considered not only the first isolated complex bearing a C–C insaturation as a ligand, but also the first reported organometallic compound.[65]

62 Zhdanko, A.; Maier, M. E. *Chem. Eur. J.* **2014**, *20*, 1918–1930.

63 Zeise, W. C. *Ann. Phys. Chem.* **1831**, *97*, 497–541.

64 Wentrup, C. *Angew.Chem. Int. Ed.* **2020**, *59*, 8332–8342.

65 Hunt, L. B. *Platinum Metals Rev.* **1984**, *28*, 76–83.

Although organogold(I) complexes were known from the beginning of last century,[66] their inherent instability, due to the propensity of gold(I) to disproportionate,[32a] hampered their synthesis and isolation. This is illustrated by the fact that the first gold–alkene complex was reported in 1964,[67] 133 years later than Zeise's salt. More recently, the use of stabilizing ligands has allowed the isolation and characterization of π-complexes with alkynes,[68] as well as with alkenes,[39,69] 1,3-dienes,[70] allenes[71] and arenes.[72]

The bond in gold(I)–alkyne complexes can be rationalized by the Dewar-Chatt-Duncanson model.[73] There are two principal bonding components: the σ-donation from the ligand (π orbital) to gold (hybridized 6*s*-5d_{z^2} orbital) and the $\pi_{\parallel}$-back-donation from gold (5d_{xz} orbital) to the ligand (π^* orbital). Moreover, two minor interactions also take place: the $\pi_{\perp}$-donation from the ligand (π orbital) to gold (5d_{yz} orbital) and the δ-back-donation from gold (5d_{xy} orbital) to the ligand (π^* orbital) (Figure 8).[74] It is important to note that all the M–L interactions weaken the C–C triple bond since electrons from the π-bonding orbital in the ligand are being pulled towards the metal and, simultaneously, π*-antibonding orbitals are receiving electron density. This is translated into an increased reactivity of the coordinated alkyne with respect to the uncoordinated one.

66 Mathews, J. A.; Watters, L. L. *J. Am. Chem. Soc.* **1900**, *22*, 108–111.

67 Chalk, A. J.; *J. Am. Chem. Soc.* **1964**, *86*, 4733–4734.

68 (a) Flügge, S.; Anoop, A.; Goddard, R.; Thiel, W.; Fürstner, A. *Chem. Eur. J.* **2009**, *15*, 8558–8565. (b) Hooper, T. N.; Green, M.; Russell, C. A. *Chem. Commun.* **2010**, *46*, 2313–2315. (c) Brown, T. J.; Widenhoefer, R. A. *J. Organomet. Chem.* **2011**, *696*, 1216–1220. (d) Ferrer, S.; Echavarren, A. M. *Organometallics* **2018**, *37*, 781–786.

69 For selected examples see: (a) Brown, T. J.; Dickens, M. G.; Widenhoefer, R. A. *J. Am. Chem. Soc.* **2009**, *131*, 6350–6351. (b) Brooner, R. E. M.; Widenhoefer, R. A. *Organometallics* **2012**, *31*, 768–771. (c) Brooner, R. E. M.; Brown, T. J.; Widenhoefer, R. A. *Chem. Eur. J.* **2013**, *19*, 8276–8284.

70 (a) Sanguramath, R. A.; Hooper, T. N.; Butts, C. P.; Green, M.; McGrady, J. E.; Russell, C. A. *Angew. Chem. Int. Ed.* **2011**, *50*, 7592– 7595. (b) Brooner, R. E. M.; Widenhoefer, R. A. *Organometallics* **2011**, *30*, 3182–3193. (c) Krossing, I. *Angew. Chem. Int. Ed.* **2011**, *50*, 11576–11578.

71 (a) Brown, T. J.; Sugie, A.; Dickens, M. G.; Widenhoefer, R. A. *Organometallics* **2010**, *29*, 4207–4209. (b) Brown, T. J.; Sugie, A.; Leed, M. G. D.; Widenhoefer, R. A. *Chem. Eur. J.* **2012**, *18*, 6959–6971. (c) Johnson, A.; Laguna, A.; Gimeno, M. C. *J. Am. Chem. Soc.* **2014**, *136*, 12812–12815.

72 (a) Xu, F.-B.; Li, Q.-S.; Wu, L.-Z.; Leng, X.-B.; Li, Z.-C.; Zeng, X.-S.; Chow, Y. L.; Zhang, Z.-Z, *Organometallics* **2003**, 22, 633–640; (b) Herrero-Gómez, E.; Nieto-Oberhuber, C.; López, S.; Benet-Buchholz, J.; Echavarren, A. M. *Angew. Chem. Int. Ed* **2006**, *45*, 5455–5459.

73 (a) Dewar, M. J. S. *Bull. Soc. Chim. Fr.* **1951**, C71. (b) Dewar, M. J. S. *Bull. Soc. Chim. Fr.* **1951**, C79. (c) Chatt, J.; Duncanson, L. A. *J. Chem. Soc.* **1953**, 2939–2947.

74 Nechaev, M. S.; Rayón, V. M.; Frenking, G. *J. Phys. Chem A* **2004**, *108*, 3134–3142.

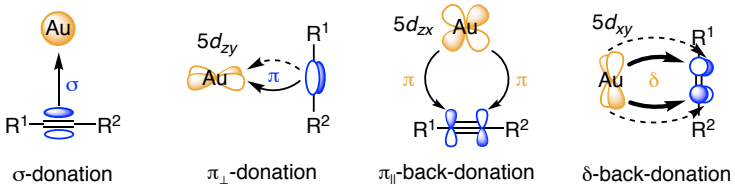

Figure 8. Bonding components in gold-alkyne interactions.

The computational study of $[Au(C_2H_x)]^+$ (X = 4 for ethene and X = 2 for ethyne) as a model complexes for electrophilically activated alkenes/alkynes revealed that the 5*d* electrons of gold(I) are low in energy for an important $\pi_{\parallel}$-back-bonding to the π^* anti-bonding orbitals, suggesting that the main contribution to the M–L bond is the σ-donation.[74,75] More recently, it has been shown that $\pi_{\parallel}$-back-donation in [L–Au–(alkyne)] systems is highly dependent on the structural features of the complex as well as the nature of the ancillary ligand (L), contributing as much as σ-donation in some cases.[76] The contribution of the $\pi_{\perp}$-donation is lower and the δ-back-donation is negligible.[74]

Overall, although dependent on the complex structure and the nature of the ligand, the gold(I)–alkene/alkyne bond is most commonly polarized leaving an electron-rich gold center and an electron-deficient and weakened C–C multiple bond.

Despite the observed selective activation of the alkyne moiety, gold(I) complexes do not coordinate preferentially to alkynes over alkenes. Instead, this selectivity arises from the higher reactivity of the gold(I)-activated alkynes towards nucleophilic attack, which has been attributed to their exceptionally low-in-energy LUMO (lowest unoccupied molecular orbital).[77]

Nucleophilic Attack

η^2-Alkyne gold(I) complexes readily react with nucleophiles often following Markovnikov selectivity.[78] Although some exceptions have been reported,[79] the nucleophilic attack follows an outer-sphere mechanism[80] giving rise to *trans*-alkenyl intermediates (Scheme 5, page 39). Regarding the nature of the nucleophile, different carbon and heteroatom-based compounds such

75 (a) Ziegler, T.; Rauk, A. *Inorg. Chem.* **1979**, *18*, 1558–1565. (b) Hertwig, R. H.; Koch, W.; Schröder, D.; Schwarz, H.; Hrusak, J.; Schwerdtfeger, P. *J. Phys. Chem.* **1996**, *100*, 12253–12260.

76 (a) Salvi, N.; Belpassi, L.; Tarantelli, F. *Chem. Eur. J.* **2010**, *16*, 7231–7240. (b) Bistoni, G.; Belanzoni, P.; Belpassi, L.; Tarantelli, F. *J. Phys. Chem A* **2016**, *120*, 5239–5247.

77 García-Mota, M.; Cabello, N.; Maseras, F.; Echavarren, A. M.; Pérez-Ramírez, J.; López, N. *ChemPhysChem* **2008**, *9*, 1624–1629.

78 For an interesting discussion on the regioselectivity in gold(I)-catalyzed hydroamination of alkenes, see: Couce-Rios, A.; Lledós, A.; Fernández, I.; Ujaque, G. *ACS Catal.* **2019**, *9*, 848–858.

79 Joost, M.; Gualco, P.; Mallet-Ladeira, S.; Amgoune, A.; Bourissou, D. *Angew. Chem. Int. Ed.* **2013**, *52*, 7160–7163.

80 Zhdanko, A.; Maier, M. E. *Angew. Chem. Int. Ed.* **2014**, *53*, 7760–7764.

as alkenes, arenes, heteroarenes, malonates, disulfones, water, alcohols, aldehydes, ketones, acids, amines, imines, sulfoxides, *N*-oxides, thiols and "F⁻" sources have been successfully used in either intra- or intermolecular gold(I)-catalyzed transformations.[32f]

Interestingly, *trans*-alkenyl gold(I) intermediates show a high aurophilic character and readily form *gem*-diaurated species (Scheme 6).[81] These proposed off-cycle intermediates have been characterized in the course of different reactions.[62,82]

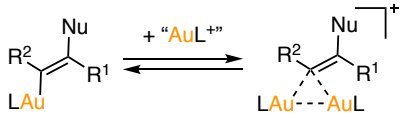

Scheme 6. Formation of *gem*-digold species from *trans*-alkenyl gold(I) intermediates.

Protodeauration

In this step, the *trans*-alkenyl intermediate undergoes a formal gold–proton exchange delivering the final organic product and regenerating the catalytically active species to close the cycle (Scheme 7). The role of proton source can be played by the solvent, water, the nucleophile in excess, or other Brønsted acids present in the reaction mixture.

Although this step was proposed to be fast,[83] the group of Shi was able to isolate and characterize gold(I)–intermediate complexes resistant to protodeauration (Scheme 7).[84]

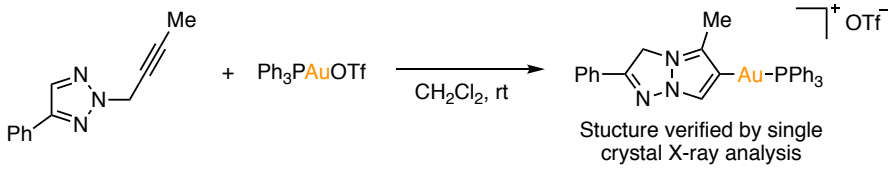

Scheme 7. Synthesis of a stable gold(I)–intermediate complex.

Computational investigations showed that this reaction is indeed under thermodynamic control. A linear correlation was found between the activation barriers and the strength of the C–

81 Weber, D.; Tarselli, M. A.; Gagné, M. R. *Angew. Chem. Int. Ed.* **2009**, *48*, 5733–5736. (b) Weber, D.; Gagné, M. R. *Chem. Sci.* **2013**, *4*, 335−338.

82 (a) Seidel, G.; Lehmann, C. W.; Fürstner, A. *Angew. Chem. Int. Ed.* **2010**, *49*, 8466–8470. (b) Weber, D. University of North Carolina at Chapel Hill. PhD Thesis **2012.** (c) Lu, M.; Su, Y.; Zhao, P.; Ye, X.; Cai, Y.; Shi, X.; Masson, E.; Li, F.; Campbell, J. L.; Chen, H. *Chem. Eur. J.* **2018**, *24*, 2144–2150. (d) Anania, M.; Jašiková, L.; Zelenka, J.; Shcherbachenko, E.; Jašik, J.; Roithova, J. *Chem. Sci.* **2020**, *11*, 980–988.

83 Hashmi, A.S.K. *Gold Bull.* **2004**, *37*, 51–65.

84 Chen, Y.; Wang, D.; Petersen, J. L.; Akhmedov, N. G.; Shi, X. *Chem. Commun.* **2010**, *46*, 6147−6149.

Au bonds, which depends on the stereoelectronic properties of both the alkenyl moiety and the ancillary ligand.[85]

Even though protodeauration remains as the final step in most gold(I) catalytic cycles, alkenyl-gold(I) intermediates can be intercepted with electrophiles different than proton.[86]

Gold(I)-Catalyzed Cyclization of Enynes

The cyclization of enynes is a versatile methodology to construct carbo- and heterocycles of various sizes. These reactions involve the intramolecular nucleophilic attack of an alkene to a gold(I) activated alkyne forming a new C–C bond. The synthetic relevance of this transformation arises from the diversity of structures that can be accessed by tuning the substrates, the stereoelectronic properties of the gold(I) complexes and other reaction conditions.[87] An illustrative example is depicted in Scheme 8, where the cycloisomerization of 1,6-enyne **I** can give rise to 3, 4, 5, 6 and 7-membered ring products.

Enyne **I** can undergo 5-*exo*-dig cyclization generating cyclopropyl gold(I) carbene **II**.[88] In the absence of nucleophiles, this proposed intermediate can rearrange forming 1,3-diene **IV** via a single-cleavage skeletal rearrangement. In this process, a formal 1,3-migration of the terminal carbon of the alkene towards the terminal carbon of the alkyne takes place. Alternatively, intermediate **II** can evolve to generate new rearranged carbene **V** by the formal insertion of the terminal alkene carbon into the alkyne. A sequence of α-proton elimination/protodeauration gives rise to 1,3-diene **VI**, the product of a double-cleavage rearrangement. Similarly, enyne **I** can

85 (a) BabaAhmadi, R.; Ghanbari, P.; Rajabi, N. A.; Hashmi, A.S.K.; Yates, B. F.; Ariafard, A. *Organometallics* **2015**, *34*, 3186–3195. (b) Gaggioli, C. A.; Ciancaleoni, G.; Zuccaccia, D.; Bistoni, G.; Belpassi, L.; Tarantelli, F.; Belanzoni, P. *Organometallics*, **2016**, *35*, 2275–2285.

86 For selected examples, see: (a) Zhang, L. *J. Am. Chem. Soc.* **2005**, *127*, 16804–16805. (b) Miles, D. H.; Veguillas, M.; Toste, F. D. *Chem. Sci.* **2013**, *4*, 3427–3431. (b) Guo, R.; Li, K.-N.; Liu, B.; Zhu, H.-J.; Fan, Y.-M.; Gong, L.-Z. *Chem. Commun.* **2014**, *50*, 5451–5454.

87 For reviews on transition metal-catalyzed enyne cyclization, see: (a) Aubert, C.; Buisine, O.; Malacria, M. *Chem. Rev.* **2002**, *102*, 813–834. (b) Lloyd-Jones, G. C. *Org. Biomol. Chem.* **2003**, *1*, 215–236. (c) Diver, S. T.; Giessert, A. J. *Chem. Rev.* **2004**, *104*, 1317–1382. (d) Echavarren, A. M.; Nevado, C. *Chem. Rev.* **2004**, *33*, 431–436. (e) Escribano-Cuesta, A.; Pérez-Galán, P.; Herrero-Gómez, E.; Sekine, M.; Braga, A. A. C.; Maseras, F.; Echavarren, A. M. *Org. Biomol. Chem.* **2012**, *10*, 6105–6111.

88 (a) Oi, S.; Tsukamoto, I.; Miyano, S.; Inoue, T. *Organometallics* **2001**, *20*, 3704–3709. (b) Nieto-Oberhuber, C.; Muñoz, M. P.; Buñuel, E.; Nevado, C.; Cárdenas, D. J.; Echavarren, A. M. *Angew. Chem. Int. Ed.* **2004**, *43*, 2402–2406. (c) Nieto-Oberhuber, C.; López, S.; Jiménez-Núñez, E.; Echavarren, A. M. *Chem. Eur. J.* **2006**, *12*, 5916–5923. (d) Ferrer, C.; Raducan, M.; Nevado, C.; Claverie, C. K.; Echavarren, A. M. *Tetrahedron* **2007**, *63*, 6306–6316. (e) Obradors, C.; Echavarren, A. M. *Acc. Chem. Res.* **2014**, *47*, 902–912.

undergo 6-*endo*-dig cyclization.[88,89] The resulting cyclopropyl gold(I) carbene **VII** can yield **VIII** upon α-proton elimination and subsequent protodeauration.[90] Intermediate **VII** can also rearrange into bicyclic product **IX**, which readily evolves into highly strained bicyclo[3.2.0]heptenes **X** and **X'**.[91] Interestingly, the ring opening of **IX** gives rise to gold(I) complex **XI**, precursor of single-cleavage 1,3-dienes **IV**.[92,87d] Finally, cleavage of the fusing bond in **VII** delivers cycloheptadiene **XIII** *via* alkenyl-gold(I) intermediate **XII**.[88d] The ring opening rearrangement was also reported for intermediate **II** (Scheme 8).[89]

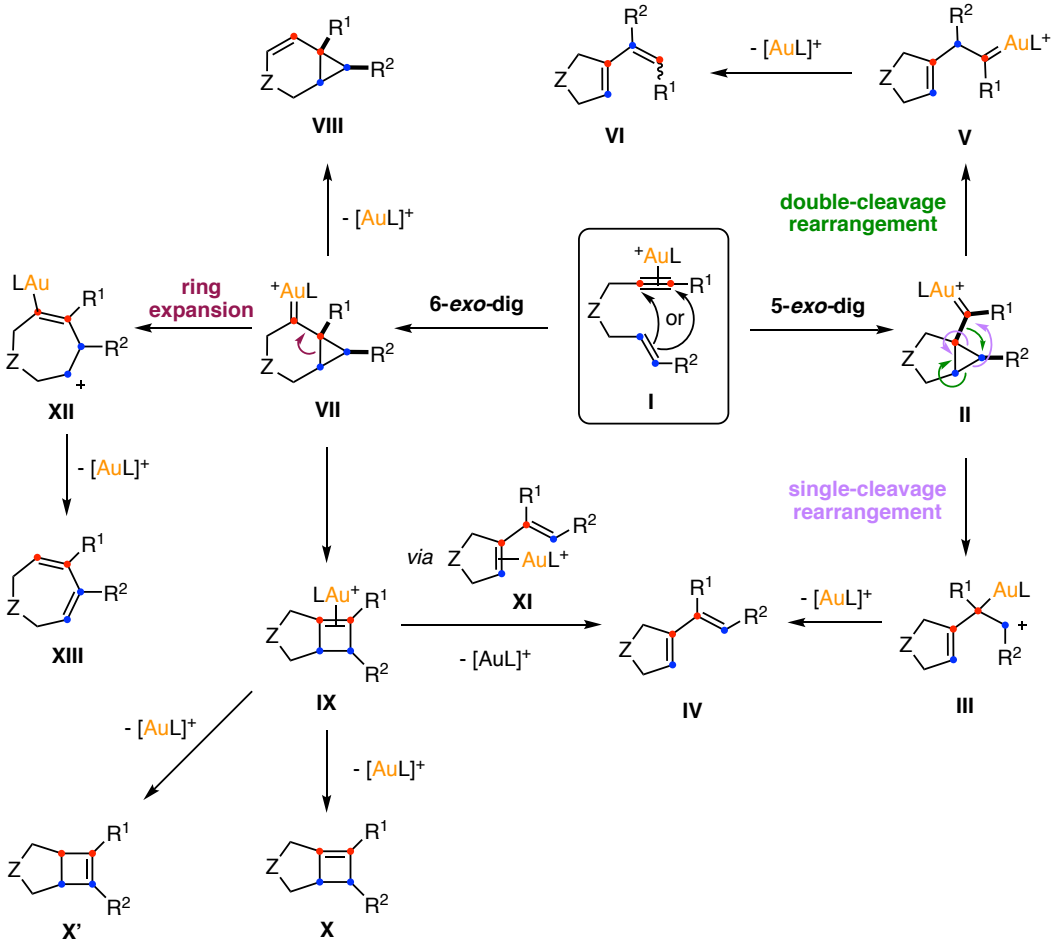

Scheme 8. General pathways for the cycloisomerization of 1,6-enyne **I**.

89 Cabello, N.; Jiménez-Núñez, E.; Buñuel, E.; Cárdenas, D. J.; Echavarren, A. M. *Eur. J. Org. Chem.* **2007**, 4217–4223.

90 Shibata, T.; Kobayashi, Y.; Meakawa, S.; Toshida, S.; Takagi, K. *Tetrahedron* **2005**, *61*, 9018–9024.

91 (a) Lee, Y. T.; Kank, Y. K.; Chung, Y. K. *J. Org. Chem.* **2009,** *74*, 7922–7934. (b) Brooner, R. E. M.; Brown, T. J.; Widenhoefer, R. A. *Angew. Chem. Int. Ed.* **2013**, *52*, 6259–6261.

92 (a) Marion, F.; Coulomb, J.; Courillon, C.; Fensterbank, L.; Malacria, M. *Org. Lett.* **2004**, *6*, 1509–1511. (b) Bajracharya, G. B.; Nakamura, I.; Yamamoto, Y. *J. Org. Chem.* **2005**, *70*, 892–897.

Comparable mechanistic scenarios are observed for 1,5-enynes[93] and 1,7-enynes.[94] Larger cyclic scaffolds can be accessed *via* in the cyclization of higher 1,*n*-enynes (where $7 \leq n \leq 16$).[95]

Cyclopropyl gold(I) carbene intermediates (such us **II** or **VII**) generated in enyne cyclizations can be trapped intra- or intermolecularly by nucleophiles.[96] When hard nucleophiles are used (water, alcohols, amines, electron-rich aryls, etc), the attack leads to the regio- and stereospecific ring-opening of the cyclopropane (Scheme 9).[97]

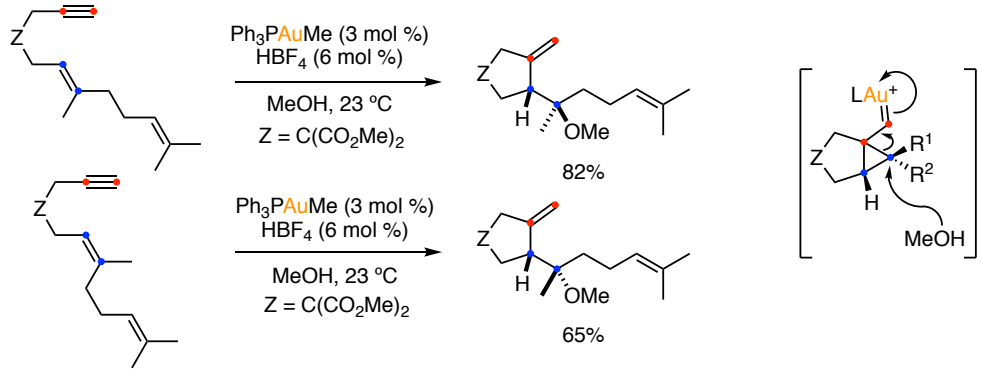

Scheme 9. Markovnikov stereospecific attack of methanol to 1,6-enynes.

In the case of 7-substituted-1,6-enynes with an aromatic ring as tether, the gold(I)-catalyzed hydroxy-/alkoxycyclization proceeds predominantly through a 6-*endo*-dig pathway instead of the 5-*exo*-dig pathway usually observed for 1,6-enynes with trisubstituted alkenes.[98] Interestingly, the cyclopropyl gold(I) carbene formed through the 5-*exo* pathway evolves preferentially by intramolecular Friedel–Crafts-type reaction, while the analogous 6-*endo* intermediate was exclusively trapped by the external nucleophile (Scheme 10).

93 (a) Zhang, L.; Kozmin, S. *J. Am. Chem. Soc.* **2004**, *126*, 11806–11807. (b) Sun, J.; Conley, M.; Zhang, L.; Kozmin, S. *J. Am. Chem. Soc.* **2006**, *128*, 9705–9710. (c) López- Carrillo, V.; Huguet, N.; Mosquera, Á.; Echavarren, A. M. *Chem. Eur. J.* **2011**, *17*, 10972–10978.

94 Cabello, N.; Rodríguez, C.; Echavarren, A. M. *Synlett* **2007**, 1753–1758.

95 (a) Comer, E.; Rohan, E.; Deng, L.; Porco, J. A., Jr. *Org. Lett.* **2007**, *9*, 2123–2126. (b) Obradors, C.; Leboeuf, D.; Aydin, J.; Echavarren, A. M. *Org. Lett.* **2013**, *15*, 1576–1579.

96 For the scope of nucleophiles used in gold(I)-catalyzed enyne cyclizations see reference 36f and references cited therein.

97 (a) Amjis, C. H. M.; López-Carrillo, V.; Raducan, M.; Pérez-Galán, P.; Ferrer, C.; Echavarren, A. M. *J. Org. Chem.* **2008**, *73*, 7721–7730. (b) Dorel, R.; Echavarren, A. M. *J. Org. Chem.* **2015**, *80*, 7321–7332.

98 Sanjuán, A. M.; Martínez, A.; García-García, P.; Fernández-Rodríguez, M. A.; Sanz, R. *Beilstein J. Org. Chem.* **2013**, *9*, 2242–2249.

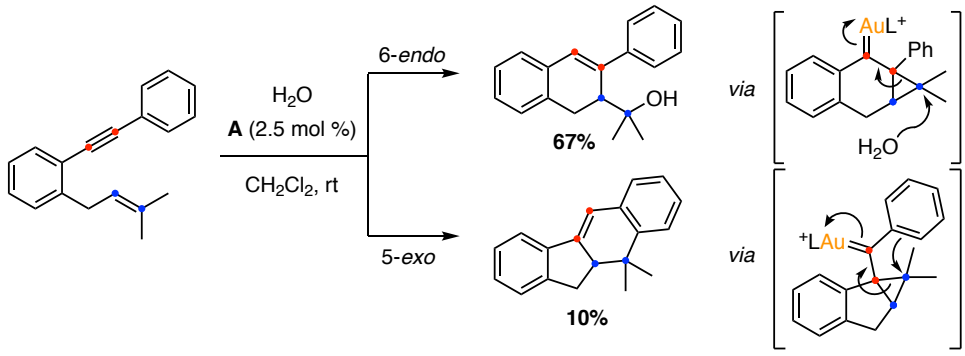

Scheme 10. Gold(I)-catalyzed hydroxycyclization of 1-(prenyl)-2-(phenylethynyl)benzene.

Contrary to hard nucleophiles, soft nucleophiles do not attack the cyclopropane moiety but rather the carbene carbon.[56,58] This reactivity has been exploited in the nucleophilic trapping of gold(I) carbene intermediates of type **II** and **VII** (Scheme 8, page 45) and other carbenes generated from them.[99] Most commonly, akenes,[99,100] aldehydes/ketones[101] and oxygen-donor nucleophiles (*i.e.* sulfoxides,[102] *N*-oxides[103]) have been the reagents of choice for both intra- and intermolecular carbene trapping (Scheme 11).[32f]

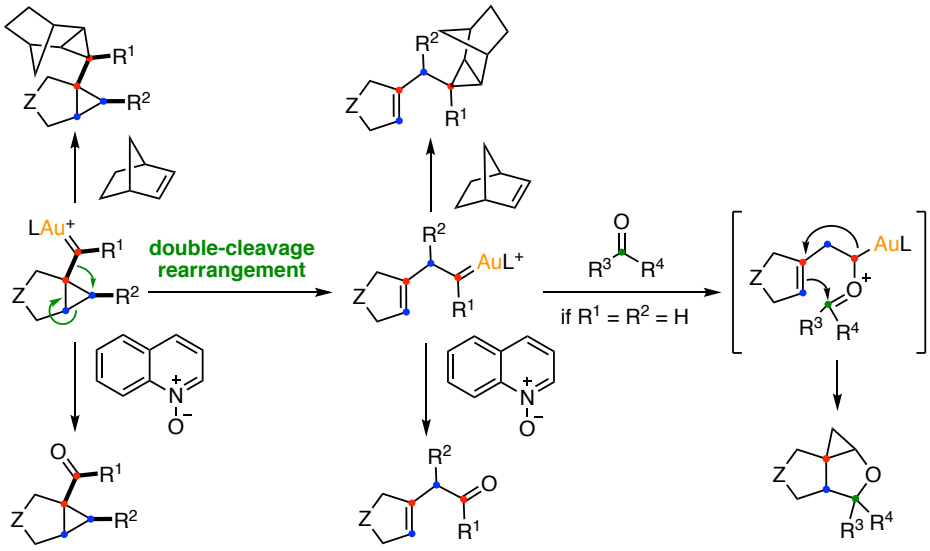

Scheme 11. Gold(I) carbene cyclopropanations and oxidation.

99 López, S.; Herrero-Gómez, E.; Pérez-Galán, P.; Nieto-Oberhuber, C.; Echavarren, A. M. *Angew. Chem. Int. Ed.* **2006**, *45*, 6029–6032.

100 (a) Nieto-Oberhuber, C.; López, S.; Muñoz, M. P.; Jiménez-Núñez, E.; Buñuel, E.; Cárdenas, D. J.; Echavarren, A. M. *Chem. Eur. J.* **2006**, *12*, 1694–1702. (b) Kim, S. M.; Park, J. H.; Choi, S. Y.; Chung, Y. K. *Angew. Chem. Int. Ed.* **2007**, *46*, 6172–6175. (c) Pérez-Galán, P.; Herrero-Gómez, E.; Hog, D. T.; Martin, N. J. A.; Maseras, F.; Echavarren, A. M. *Chem. Sci.* **2011**, *2*, 141–149.

101 Schelweis, M.; Dempwolff, A. L.; Rominger, F.; Helmchen, G. *Angew. Chem. Int. Ed.* **2007**, *46*, 5598–5601.

102 Witham, C. A.; Mauleón, P.; Shapiro, N. D.; Sherry, B. D.; Toste, F. D. *J. Am. Chem. Soc.* **2007**, *129*, 5838–5839.

103 Qian, D.; Zhang, J. *Chem. Commun.* **2011**, *47*, 11152–11154. Qian, D.; Hu, H.; Liu, F.; Tang, B.; Ye, W.; Wang, Y.; Zhang, J. *Angew. Chem. Int. Ed.* **2014**, *53*, 13751–13755.

Gold(I)-catalyzed enyne cyclizations have been extensively applied in the total synthesis of natural products as well as in the synthesis of relevant organic materials. This topic will be covered in chapter 1.

Gold in elemental organometallic reactions

The unique behavior of gold(I) in the catalytic activation of C–C multiple bonds has earned a place in the toolbox of synthetic chemists. Beyond this reactivity, organogold species can also undergo elemental organometallic transformations such as oxidative addition, reductive elimination, transmetalation, C–H auration, migratory insertion and β-hydride elimination.[104]

Oxidative Addition

The high redox potential of the couple gold(III)/gold(I) (E^0 Au(III)/Au(I) = 1.41 V)[22] renders the oxidative addition of commonly used electrophiles, aryl (pseudo)halides, a challenging process.[105] Moreover, the mechanisms described for the oxidative addition to analogous two-coordinate Pd(0) complexes are less favored for gold, since they would involve either the generation of highly unstable mono-coordinated $[LAu]^+$ species[42b] or the energy demanding distortion of the linear geometry (Scheme 12).[106]

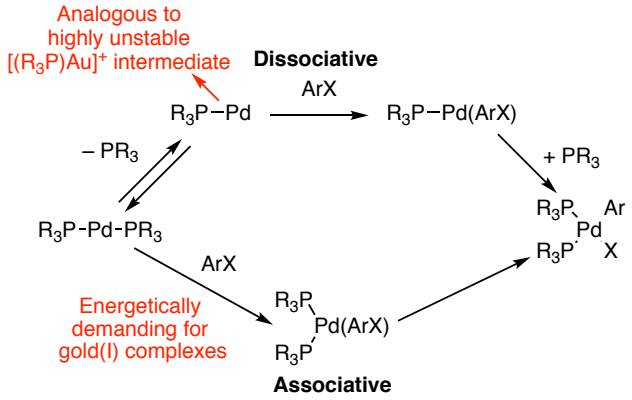

Scheme 12. Alternative mechanisms for the oxidative addition of ArX to $Pd(PR_3)_2$.[104a]

Two different strategies have been used to enable the direct intermolecular oxidative addition to gold(I) complexes. The first relies on the use of bidentate ligands with small bite

104 (a) Joost, M.; Amgoune, A.; Bourissou, D. *Angew. Chem. Int. Ed.* **2015**, *54*, 15022–15045. (b) Mertens, R. T.; Awuah, S. G. (2019) *Catalysis by Metal Complexes and Nanomaterials: Fundamentals and Applications.* Chapter 2: *Gold Catalysis: Fundamentals and Recent Developments.* ISBN 978-0-841-23437-6. DOI: 10.1021/bk-2019-1317.ch002

105 Livendahl, M.; Goehry, C.; Maseras, F.; Echavarren, A. M. *Chem. Commun.* **2014**, *50*, 1533–1536.

106 Carvajal, M. A.; Novoa, J. J.; Álvarez, S. *J. Am. Chem. Soc.* **2004**, *126*, 1465 – 1477.

angles that force the geometry of the resulting gold complexes to be angular and not linear.[107] The second focuses in the stabilization of the hypothetical $[LAu]^+$ intermediates[108] by using either strongly electron-donating NHC carbene ligands[109] or the formation of thigh ion pairs with suitable counteranions.[110] Alternatively, merging gold with photocatalysis has enabled the oxidative addition of electrophilic aryldiazonium salts (ArN_2X).[111] This topic will be discussed in more detail in chapter 2.

Reductive Elimination

The formation of biaryls through the reductive elimination of diarylgold(III) complex was reported three decades ago.[112] This thermodynamically favored process takes place at room temperature yielding the corresponding gold(I) complexes and biaryls in excellent yields. The mechanism of the reductive elimination from mono- and dinuclear gold(III) complexes was studied by Toste and coworkers.[113] Here, they disclosed that the reaction was feasible at -52 ºC and relatively fast at -23 ºC, including this process among the fastest observed C–C bond-forming reductive couplings of any transition metal. The authors also observed an increase of the reaction rate in the presence of an excess of phosphine. Kinetic studies showed that cationic $[(PPh_3)_2Au(Ar)_2]Cl$, generated upon associative ligand exchange from $[(PPh_3)AuCl(Ar)_2]$, underwent reductive elimination 100 times faster than the neutral complex (Scheme 13).

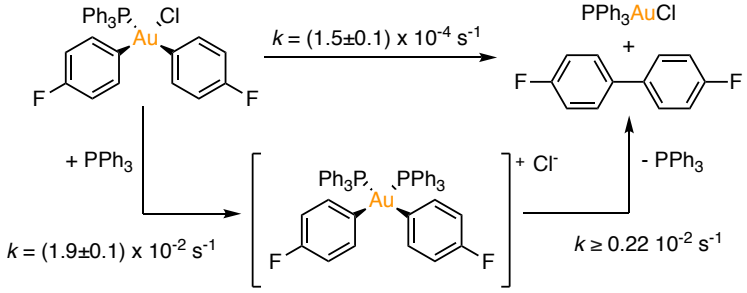

Scheme 13. Plausible mechanism for the reductive elimination on diarylgold(III) complexes.

107 (a) Joost, M.; Zeineddine, A.; Estévez, L.; Mallet-Ladeira, S.; Miqueu, K.; Amgoune, A.; Bourissou, D. *J. Am. Chem. Soc.* **2014**, *136*, 14654–14657. (b) Zeineddine, A.; Estevez, L.; Mallet-Ladeira, S.; Miqueu, K.; Amgoune, A.; Bourissou, D. *Nat. Commun.* **2017**, *8*, 565.

108 To date, there is no structural evidence for the existence of this coordinatively unsaturated gold(I) complex in solution.

109 Wu, C.-Y.; Horibe, T.; Jacobsen, C. B.; Toste, F. D. *Nature* **2015**, *517*, 449–454.

110 Joost, M.; Gualco, P.; Coppel, Y.; Miqueu, K.; Kefalidis, C. E.; Maron, L.; Amgoune, A.; Bourissou, D. *Angew. Chem. Int. Ed.* **2014**, *53*, 747–751.

111 (a) Sahoo, B.; Hopkinson, M. N.; Florius, F. *J. Am. Chem. Soc.* **2013**, *135*, 5505-5508. (b) Shu, X.-Z.; Zhang, M.; He, Y.; Frei, H.; Toste, D. *J. Am. Chem. Soc.* **2014**, *136*, 5844-5847.

112 (a) Vicente, J.; Bermudez, M. D.; Escribano, J.; Carrillo, M. P.; Jones, P. G. *J. Chem. Soc., Dalton Trans.* **1990**, 3083–3089. (b) Vicente, J.; Dolores Bermudez, M.; Escribano, J. *Organometallics* **1991**, *10*, 3380–3384.

113 Wolf, W. J.; Winston, M. S.; Toste, F. D. *Nat. Chem.* **2013**, *6*, 159–164.

Generally, aryl–CF_3 reductive elimination is a slow energy demanding process due to the strong bonding between the metal and the CF_3 ligand. In the case of cationic gold(III) complexes the transformation occurs within seconds at room temperature.[114]

These examples highlight the high propensity of gold(III) complexes to undergo reductive elimination, a tendency that has been exploited in the development of C–heteroatom bond-formation reactions.[115]

Transmetalation to Gold

The high electrophilicity of gold complexes makes them suitable for transmetalation with a wide variety of nucleophiles, including organometallic species (Li, Mg, Ti, Fe, Ni, Zn, Zr, Pd, Pt…)[116] and p-block elements-based partners (B, Si, Ge, and Sn). Especial attention has been devoted to arylboronic acids that easily undergo transmetalation with gold(I)[117] and gold(III)[118] centers to generate the corresponding arylgold complexes (Scheme 14).[119]

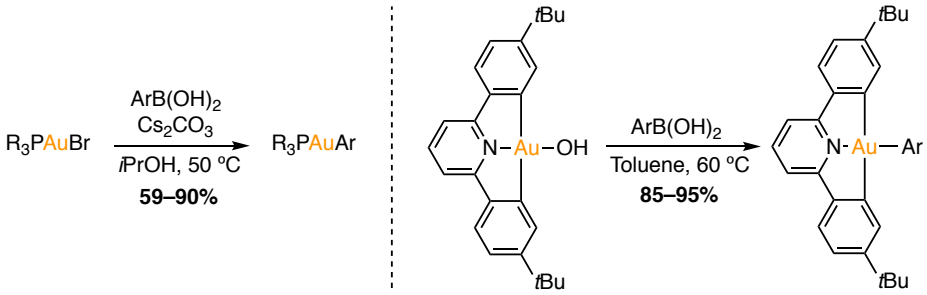

Scheme 14. Transmetalation of boron with gold(I) and gold(III) centers.

114 Winston, M. S.; Wolf, W. J.; Toste, F. D. *J. Am. Chem. Soc.* **2014**, *136*, 7777–7782.

115 (a) Kawai, H.; Wolf, W. J.; DiPasquale, A. G.; Winston, M. S.; Toste, F. D. *J. Am. Chem. Soc.* **2016**, *138*, 587–593. (b) Currie, L.; Rocchigiani, L.; Hughes, D. L.; Bochmann, M. *Dalton Trans.* **2018**, *47*, 6333–6343. (c) Kin, J. H.; Mertens, R. T.; Agarwas, A.; Parkin, S.; Berger, G.; Awuah, S. G. *Dalton Trans.* **2019**, *48*, 6273–6382.

116 For a selected example, see: (a) Contel, M.; Stol, M.; Casado, M. A.; van Klink, G. P. M.; Ellis, D. D.; Spek, A. L.; van Koten, G. *Organometallics* **2002**, *21*, 4556–4559. (b) Shi, Y.; Peterson, S. M.; Haberaecker, W. W.; Blum, S.A. *J. Am. Chem. Soc.* **2008**, *130*, 2168–2169. (c) Hirner, J. J.; Shi, Y.; Blum, S. A. *Acc. Chem. Res.* **2011**, *44*, 603–613. (d) Cornell, T. P.; Shi, Y.; Blum, S. A. *Organometallics* **2012**, *31*, 5990–5993. (e) delPozo, J.; Carrasco, D.; Pérez-Temprano, M. H.; García-Melchor, M.; Álvarez, R.; Casares, J. A.; Espinet, P. *Angew. Chem. Int. Ed.* **2013**, *52*, 2189–2193.

117 Patryka, D. V.; Zeller, M.; Hunter, A. D.; Gray, T. G. *Angew. Chem. Int. Ed.* **2006**, *118*, 8368–8371.

118 Rosca, D.-A.; Smith, D. A.; Bochmann, M. *Chem. Commun.* **2012**, *48*, 7247–7249.

119 For selected examples of gold-catalyzed cross-coupling reactions with boron-derivatives as partners, see: (a) Cai, R.; Lu, M.; Aguilera, E. Y., Xi, Y.; Akhmedov, N. G.; Petersen, J. L.; Chen, H.; Shi, X. *Angew. Chem. Int. Ed.* **2015**, *54*, 8772–8776. (b) Cornilleau, T.; Hermange, P.; Fouquet, E. *Chem. Commun.* **2012**, *52*, 10040–10043. (c) Hofer, M.; Genoux, A.; Kumar, R.; Nevado, C. *Angew. Chem. Int. Ed.* **2017**, *56*, 1021–1025.

The transmetalation from silanes,[120] stannanes[121] and germanes,[122] to gold centers has been applied in the development of gold-catalyzed cross-coupling reactions.[123]

C–H Auration

The direct C–H activation of arenes has become a useful strategy to generate arylgold complexes.[124] Interestingly, different mechanistic scenarios have been proposed depending on the oxidation state of gold. With gold(III), the C–H auration is proposed to occur *via* electrophilic aromatic substitution, which favors the functionalization of electron-rich arenes.[125] On the other hand, electron-poor aromatic rings are preferentially activated by gold(I) complexes. In this case the reaction follows a concerted metallation-deprotonations pathway.[126] A remarkable application of this orthogonal reactivity is the oxidative cross-coupling of electron-rich and electron-poor arenes reported by Larrosa and coworkers.[127] In this work, the auration of the electron-poor arene with $(PPh_3)AuCl$ in the presence of Ag_2O and a base is first achieved. After removal of the silver- and potassium-salt side products, oxidation of the gold(I) intermediate with phenyliodonium tosylate afforded the corresponding gold(III) complex. Selective auration on the electron-rich arene followed by reductive elimination would furnished the cross coupled product (Scheme 15).

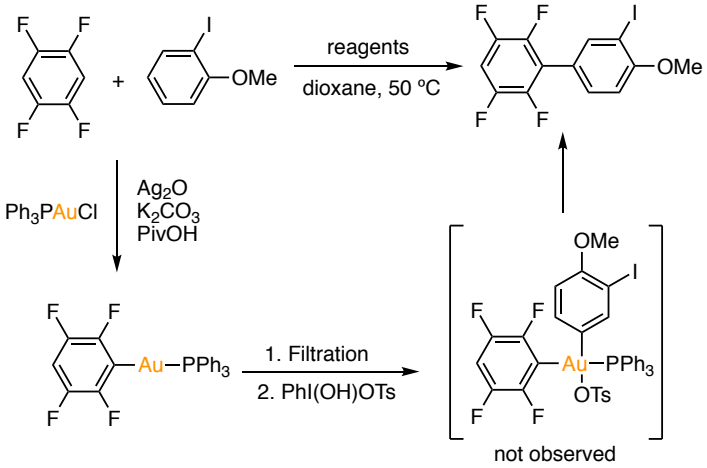

Scheme 15. Gold-catalyzed cross-coupling of electron-rich and electron-poor arenes.

120 (a) Ball, L. T.; Lloyd-Jones, G. C.; Russell, C. A. *Science* **2012**, *337*, 1644–1648. (b) Corrie, T. J. A.; Ball, L. T.; Russell, C. A.; Lloyd-Jones, G. C. *J. Am. Chem. Soc.* **2017**, *139*, 245–254. Chakrabarty, I.; Akram, M. O.; Biswas, S.; Patil, N. T. *Chem. Commun.* **2018**, *54*, 7223–7226.

121 Akram, M. O.; Shinde, P. S.; Chintawar, C. C.; Patil, N. T. *Org. Biomol. Chem*, **2018**, *16*, 2865–2869.

122 Fricke, C.; Dahiya, A.; Reid, W. B.; Schoenebeck, F. *ACS Catal.* **2019**, *9*, 9231–9236.

123 Nijamudheen, A.; Datta, A. *Chem. Eur. J.* **2020**, *26*, 1442–1487.

124 (a) Li, Z.; Brouwer, C.; He, C. *Chem. Rev.* **2008**, *108*, 3239–3265. (b) De Haro, T.; Nevado, C. *Synthesis* **2011**, *2011*, 2530–2539. (c) Xie, J.; Pan, C.; Abdukader, A.; Zhu, C. *Chem. Soc. Rev.* **2014**, *43*, 5245–5256.

125 Hofer, M.; Nevado, C. *Tetrahedron* **2013**, *69,* 5751–5757.

126 Lu, P.; Boorman, T. C.; Slawin, A. M. Z.; Larrosa, I. *J. Am. Chem. Soc.* **2010**, *132*, 5580–5581.

127 Cambeiro, X. C.; Boorman, T. C.; Lu, P.; Larrosa, I. *Angew. Chem. Int. Ed.* **2013**, *52*, 1781–1784.

β-Hydride elimination/migratory insertion

Examples of β-hydride elimination on gold centers are scarce.[128,129] Likewise, gold hydride complexes are not typically reactive through migratory insertion.[104a,130] A computational study by the groups of Köppel and Hashmi highlighted the high energetic barriers associated with these two reactions.[131] The lack of empty 5*d*-orbitals in gold(I) renders impossible the presence of agostic interactions, which hinders the β-hydride elimination. On the other hand, tricoordinate L-gold(I)-olefin-hydride complexes are relatively unstable and tend to decompose at high temperatures. Experimental work showed that thermal degradation of the complexes takes place before migratory insertion, supporting the computational studies.

Nonetheless, the group of Bourissou found that these reactions readily occur in well-stablished gold(III) cationic systems and succeeded in studying the mechanism both experimentally and theoretically (Scheme 16).[129b, 130f]

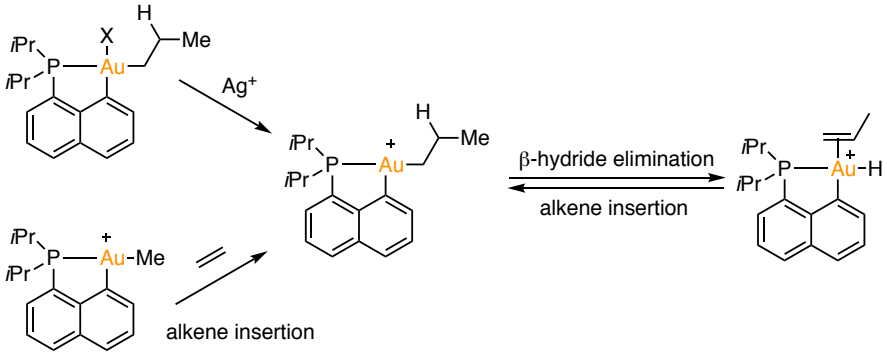

Scheme 16. Alkene insertion and β-hydride elimination in gold (III) complexes.

128 Castiñeira-Reis, M.; Silva-López, C.; Kraka, E.; Cremer, D.; Nieto-Faza, O.; *Inorg. Chem.* **2016**, *55*, 8636–8645.

129 For selected examples of β-hydride elimination in alkylgold(III) complexes, see: (a) Mankad, N. P; Toste, F. D. *Chem. Sci.* **2012**, *3*, 72–76. (b) Rekhroukh, F.; Estévez, L.; Mallet-Ladeira, S.; Miqueu, K.; Amgoune, A.; Bourissou, D. *J. Am. Chem. Soc.* **2016**, *138*, 11920–11929. (c) Kumar, R.; Krieger, J.-P.; Gómez-Bengoa, E.; Fox, T.; Linden, A.; Nevado, C. *Angew. Chem. Int. Ed.* **2017**, *52*, 12862–12865.

130 For selected examples on migratory insertion reactions in gold centers, see: (a) Akana, J. A.; Bhattacharyya, K. X.; Müller, P.; Sadighi, J. P. *J. Am. Chem. Soc.* **2007**, *129*, 7736–7737. (b) Tsui, E. Y.; Müller, P.; Sadighi, J. P. *Angew. Chem. Int. Ed.* **2008**, *47*, 8937–8940. (c) Joost, M.; Gualco, P.; Mallet-Ladeira, S.; Amgoune, A.; Bourissou, D. *Angew. Chem. Int. Ed.* **2013**, *52*, 7160–7163. (d) Joost, M.; Estevez, L.; MalletLadeira, S.; Miqueu, K.; Amgoune, A.; Bourissou, D. *J. Am. Chem. Soc.* **2014**, *136*, 10373–10382. (e) Rekhroukh, F.; Brousses, R.; Amgoune, A.; Bourissou, D. *Angew. Chem., Int. Ed.* **2015**, *54*, 1266–1269. (f) Rekhroukh, F.; Estevez, L.; Bijani, C.; Miqueu, K.; Amgoune, A.; Bourissou, D. *Organometallics* **2016**, *35*, 995–1001.

131 Klatt, G.; Xu, R.; Pernpointner, M.; Molinari, L.; Hung, T. Q.; Rominger, F.; Hasmi, A. S. K.; Köppel, H. *Chem. Eur. J.* **2013**, *19*, 3954–3961.

Chapter I:

Gold(I)-Catalyzed Enantioselective Total Synthesis of Carexanes

In collaboration with Dr. Pilar Calleja, Dr. Giuseppe Zuccarello, Dr. Imma Escofet and Dr. Dagmar Scharnagel

Introduction

Gold Catalysis in Total Synthesis

Gold catalysis constitutes a powerful tool for the electrophilic activation of C–C multiple bonds under mild reaction conditions. The strategic choice of the nucleophile can lead to the formation of a wide diversity of new C–C and C–heteroatom bonds. When the nucleophilic attack takes place intramolecularly, complex polycyclic skeletons can be generated from relatively simple substrates. The notable chemo- and regioselectivity of these processes, combined with high functional group compatibility, have led to the development of new creative retrosynthetic disconnections for target molecules. The application of gold catalysis in the synthesis of natural products, organic materials and molecules with pharmaceutical interest has grown during the last decade along with the discovery of novel methodologies and catalysts.[1]

One of the first implementations of a gold-catalyzed cascade reaction in total synthesis was reported by Hashmi and coworkers in 2003. Here, the authors employed a method previously described by the same group to convert furans into phenols[2] in the synthesis of sesquiterpenoid jungianol.[3] According to mechanistic studies carried out independently by our group,[4] the reaction begins with the nucleophilic attack of the furan ring onto the activated triple bond, generating cyclopropyl gold carbene **1**. This intermediate rearranges into carbene **2** that is trapped intramolecularly by the nucleophilic attack of the carbonyl. Upon deauration, oxepine **3** is formed and its aryl oxide tautomer **4** undergoes regioselective epoxide opening giving rise to phenol **5**. The natural product was obtained in two steps from **5** and its stereochemistry could be clarified (Scheme 1).

1 For detailed reviews on the application of gold catalysis in total synthesis, see: (a) Rudolph, M.; Hashmi, A. S. K. *Chem. Soc. Rev.* **2008**, *37*, 1766–1775. (b) Rudolph, M.; Hashmi, A. S. K. *Chem. Soc. Rev.* **2012**, *41*, 2448–2462. (c) Zhang, Y.; Luo, T.; Yang, Z. *Nat. Prod. Rep.* **2014**, *31*, 489–503. (d) Pflästerer, D.; Hashmi, A. S. K. *Chem. Soc. Rev.* **2016**, *45*, 1331–1367. (e) Sugimoto, K.; Matsuya, Y. *Tetrahedron Lett.* **2017**, *58*, 4420–4426. (f) Mayans, J. G.; Armengol-Relats, H.; Calleja, P.; Echavarren, A. M. *Isr. J. Chem.* **2018**, *58*, 639–658. (g) Gu, Y.; Tan, C.; Gong, J.; Yang, Z. *Synlett* **2018**, *29*, 1552–1571.

2 Hashmi, A. S. K.; Frost, T. M.; Bats, J. W. *J. Am. Chem. Soc.* **2000**, *122*, 11553–11554.

3 Hashmi, A. S. K.; Ding, L.; Bats, J. W.; Fischer, P.; Frey, W. *Chem. Eur. J.* **2003**, *9*, 4339–4345.

4 (a) Martín-Matute, B.; Cárdenas, D. J.; Echavarren, A. M. *Angew. Chem. Int. Ed.* **2001**, *40*, 4754–4757. (b) Martín-Matute, B.; Nevado, C.; Cárdenas, D. J.; Echavarren, A. M. *J. Am. Chem. Soc.* **2003**, *125*, 5757–5766.

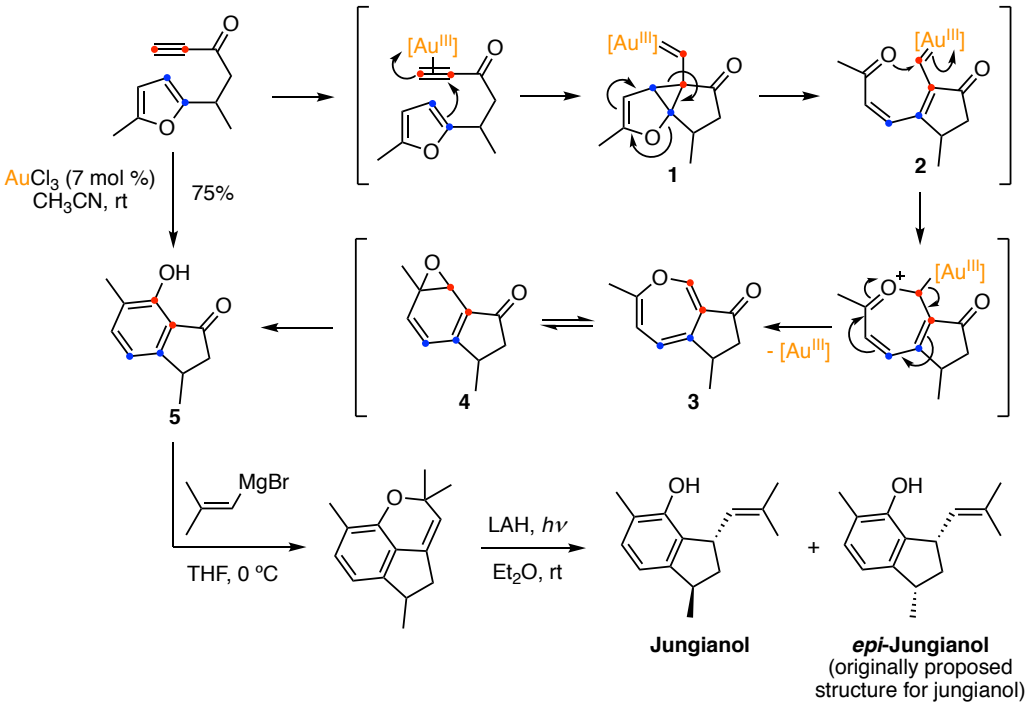

Scheme 1. Gold-catalyzed synthesis of jungianol.

Ventricosene,[5] antrocin,[6] gomerone C,[7] and more recently harziane,[8] are other examples of terpenoids that have been synthetized using gold catalysis in the key step. The synthesis of ventricosene was approached by a gold-catalyzed ring-expanding cycloisomerization of 1,6-enyne **6**. The sesquiterpenoid antrocin was first isolated from *Antrodia camphorata*, a valuable medicinal fungus indigenous in Taiwan. A gold-catalyzed tandem reaction of 1,7-diyne **7** gave access to the tricyclic core of the natural product. Gomerone C, isolated from the red algae *Laurencia majuscula* and named after the island where it was first found (La Gomera), was assembled *via* a gold-catalyzed conia-ene reaction. Lastly, the cyclobutane motif present in harziane was introduced by another gold-catalyzed ring-expanding cycloisomerization of 1,5-enyne **8** (Scheme 2).[9]

5 Sethofer, S. G.; Staben, S. T.; Hung, O. Y.; Toste, F. D. *Org. Lett.* **2008**, *10*, 4315–4318.

6 Shi, H.; Fang, L.; Tan, C.; Shi, L.; Zhang, W.; Li, C.-C.; Luo, T.; Yang, Z. *J. Am. Chem. Soc.* **2011**, *133*, 14944–14947.

7 Huwyler, N; Carreira, E. M. *Angew. Chem. Int. Ed.* **2012**, *51*, 13066–13069.

8 Hönig, M.; Carreira, E. M. *Angew. Chem. Int. Ed.* **2020**, *59*, 1192–1196.

9 Zheng, H.; Felix, R. J.; Gagné, M. R. *Org. Lett.* **2014**, *16*, 2272–2275.

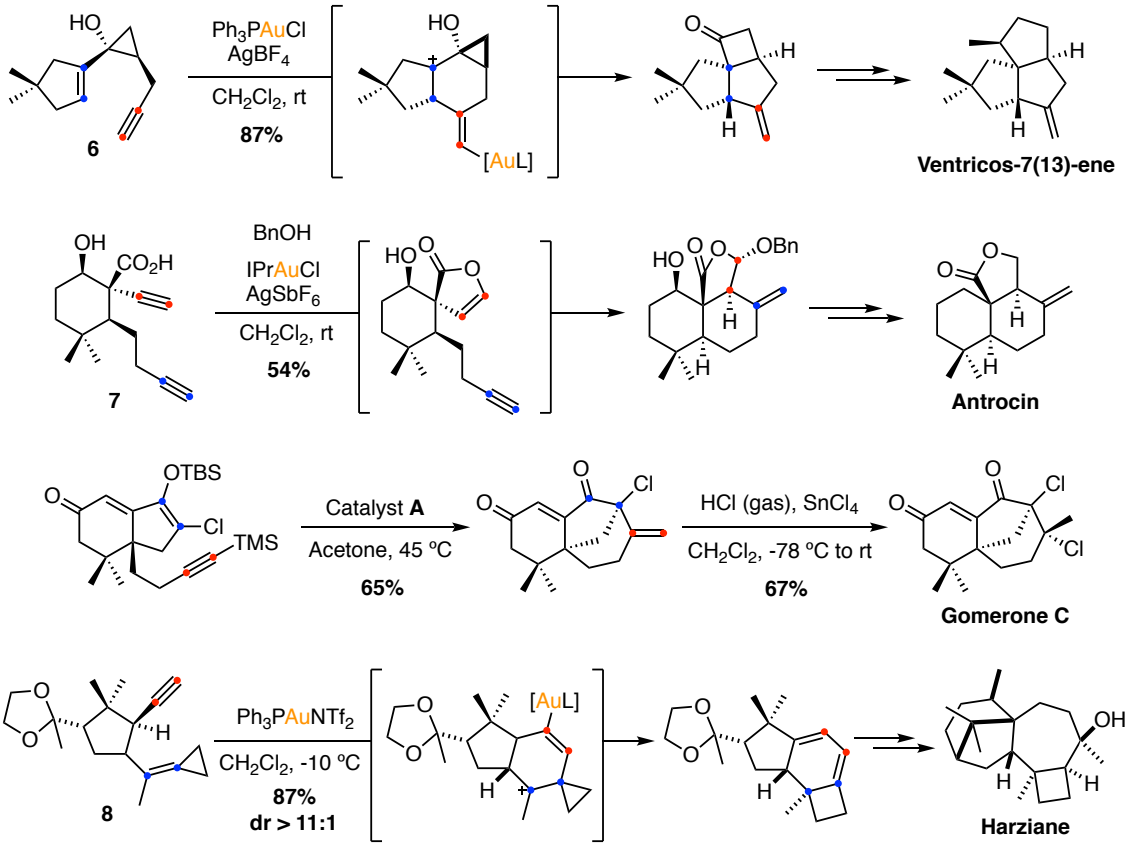

Scheme 2. Terpenoids synthesized *via* gold catalysis

Our group has contributed actively to the field by accomplishing the total synthesis of several bioactive terpenoids (Figure 1).[1f] An illustrative example is the synthesis of (–)-englerin A and its derivatives,[10] in which the oxatricyclic core was accessed through a formal [2+2+2] alkyne/alkene/carbonyl gold(I)-catalyzed cycloaddition reaction.[11] The same methodology was applied in the total synthesis of structurally related (–)-englerin B,[10a] (+)-orientalol F[12] and (±)-pubinernoid.[12] Also notable is the use of a tandem enyne cyclization/1,5-alkoxy migration/cyclopropanation for the construction of the tricyclic scaffold of (–)-4α,7α-aromadendranediol, (–)-4β,7α-aromadendranediol and (–)-epiglobulol.[13]

10 (a) Molawi, K.; Delpont, N.; Echavarren, A. M. *Angew. Chem. Int. Ed.* **2010**, *49*, 3517–3519. (b) López-Suérez, L.; Riesgo, L.; Bravo, F.; Ransom, T. T.; Beutler, J. A.; Echavarren, A. M. *ChemMedChem* **2016**, *11*, 1003–1007. (c) Wu, Z.; Suppo, J.-S.; Tumova, S.; Strope, J.; Bravo, F.; Moy, M.; Weinstein, E. S.; Peer, C. J.; Figg, W. D.; Chain, W. J.; Echavarren, A. M.; Beech, D. J.; Beutler, J. A. *ACS Med. Chem. Lett.* **2020**, *11*, 1711–1716.

11 Jiménez-Núñez, E.; Claverie, C. K.; Nieto-Oberhuber, C.; Echavarren, A. M. *Angew. Chem. Int. Ed.* **2006**, *45*, 5452–5455.

12 Jiménez-Núñez, E.; Molawi, K.; Echavarren, A. M. *Chem. Commun.* **2009**, *47*, 7327–7329.

13 Carreras, J.; Livendahl, M.; McGonigal, P. R.; Echavarren, A. M. *Angew. Chem. Int. Ed.* **2014**, *53*, 4893–4899.

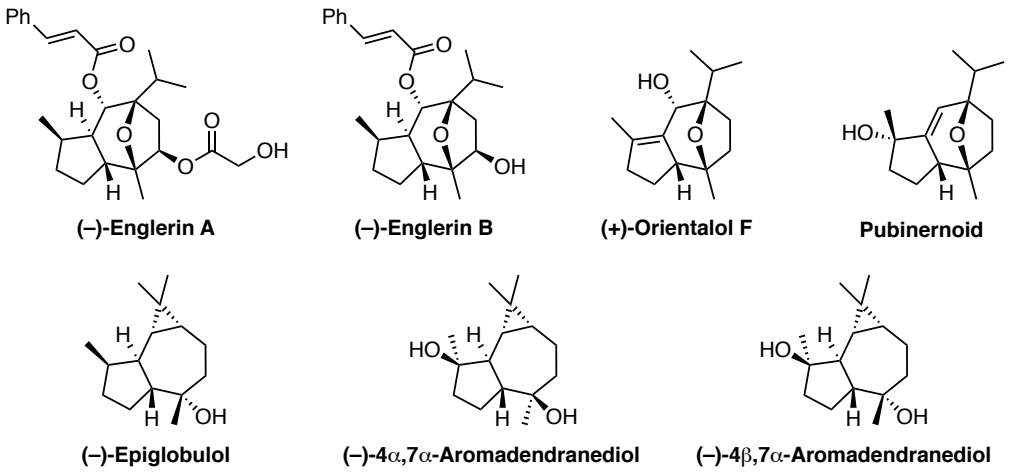

Figure 1. Examples of bioactive sesquiterpenoids synthesized by our group *via* gold catalysis.

It is worth highlighting two more recent synthesis of terpenoids carried out in our group. Rumphellaone A and its derivative (+)-hushinone were first synthetized *via* [2+2] cycloaddition of 1,10-enyne **9**.[14] Later, along with the development of the enantioselective intermolecular gold(I)-catalyzed [2+2] reaction between alkynes and alkenes, an intermolecular version of the synthesis was accomplished (Scheme 3a).[15] On the other hand, the skeleton of repraesentin F was built through a carefully designed gold(I)-catalyzed cycloisomerization/Prins type tandem transformation on 1,6-enyne **10** (Scheme 3b).[16]

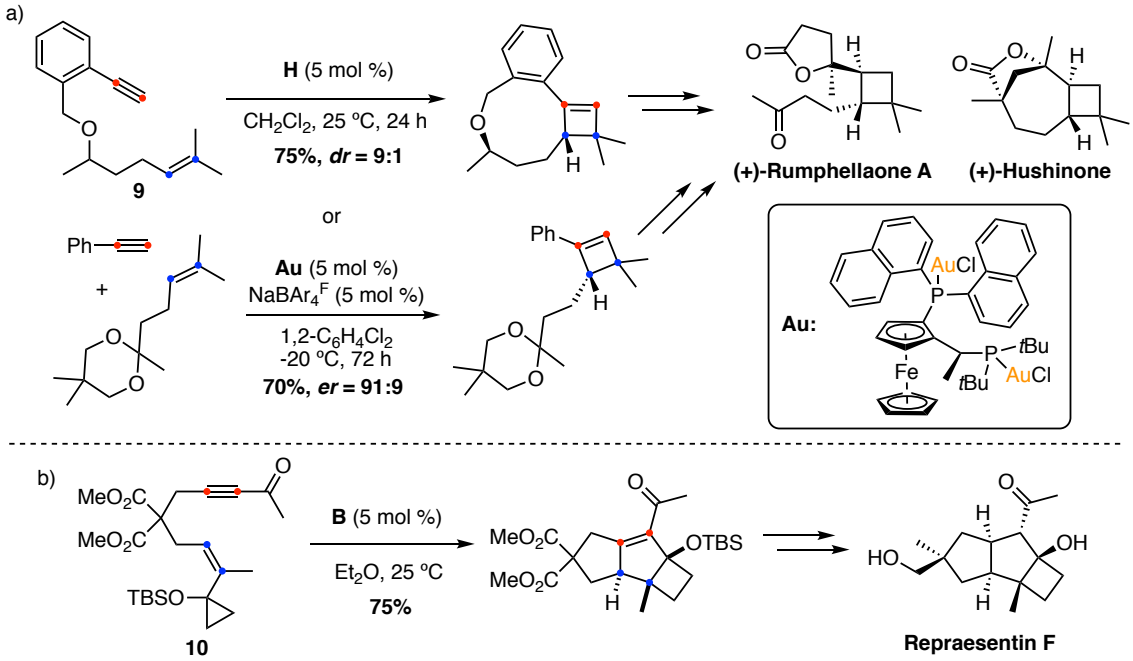

Scheme 3. Gold-catalyzed synthesis of (a) rumphellaone A and hushinone; (b) repraesentin.

14 Ranieri, B.; Obradors, C.; Mato, M.; Echavarren, A. M. *Org. Lett.* **2016**, *18*, 1614–1617.

15 García-Morales, C.; Ranieri, B.; Escofet, I.; López-Suárez, L.; Obradors, C.; Echavarren, A. M. *J. Am. Chem. Soc.* **2017**, *139*, 13628–13631.

16 Ferrer, S.; Echavarren, A. M. *Org. Lett.* **2018**, *20*, 5784–5788.

The application of gold catalysis in total synthesis is not limited to the preparation of terpene derivatives. The synthesis of many polyketides, alkaloids and synthetic drugs has been accomplished using gold catalysis in the key step.[1c] A remarkable example is the first synthesis of polyketide indoxamycin B reported by the group of Carreira.[17] In this case, gold was first used to catalyze a Suacy–Marbet rearrangement yielding allene **11**. After chemo- and diastereoselective reduction of the unsaturated ketone, the formation of the fused tetrahydrofuran ring was enabled by a gold(I)-catalyzed hydroxylation of allene **12** (Scheme 4).

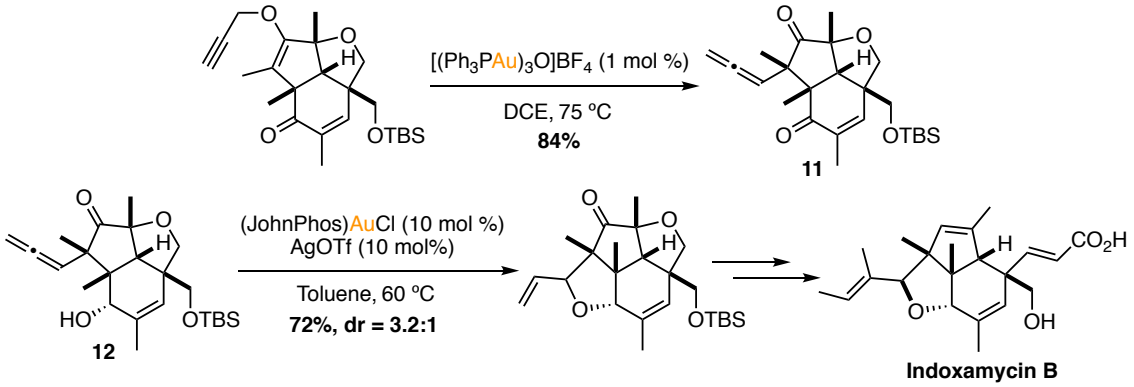

Scheme 4. Gold(I)-catalyzed transformations in the total synthesis of indoxamycin B.

A more recent example is the synthesis of the grandilodine and lapidilectine alkaloid families reported by our group, in which two key steps were catalyzed by gold.[18] First, the 8-membered ring was constructed through a highly regioselective gold-catalyzed cyclization. Later in the synthesis, a gold photocatalyst developed by Barriault and co-workers was used to promote a reductive radical cyclization (Scheme 5).[19]

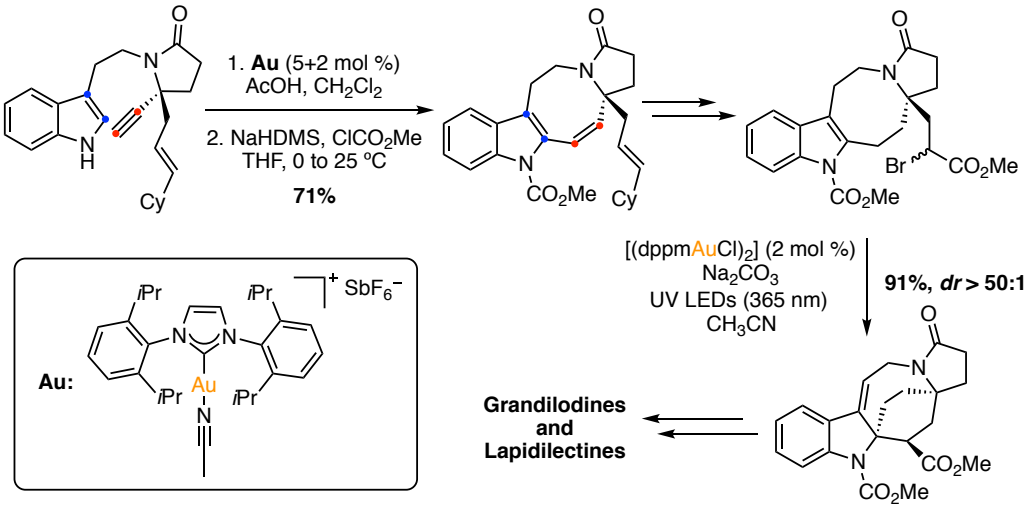

Scheme 5. Total synthesis of the grandilodine and lapidilectine families.

17 Jeker, O. F.; Carreira, E. M. *Angew. Chem. Int. Ed.* **2012**, *51*, 3474–3477.

18 Miloserdov, F. M.; Kirillova, N. S.; Muratore, M. E.; Echavarren, A. M. *J. Am. Chem. Soc.* **2018**, *140*, 5393–5400.

19 Revol, G.; McCallum, T.; Morin, M.; Gagosz, F.; Barriault, L. *Angew. Chem., Int. Ed.* **2013**, *52*, 13342−13345

Steroids are an important type of biomolecules. In animals and fungi, their biosynthesis involves the polyolefin cyclization of oxidosqualene, a process catalyzed by an enzyme called lanosterol cyclase, one of the oxidosqualene cyclase (OSC) (Scheme 6a).[20] In plants, the enzyme cycloartenol synthase promotes the cyclization of oxidosqualene to cycloartenol, whereas in bacteria the enzyme squalene-hopene cyclase gives rise to hopene from squalene. The capability of gold to promote similar kind of transformations in the presence of polyenynes has been well-stablished.[21] This polycyclization proceeds with excellent chemo-, regio- and diastereoselectivity *via* a concerted mechanism,[22] giving raise to steroid-like products (Scheme 6b). An asymmetric version of this reaction was developed by the group of Toste obtaining polycyclic compounds with excellent enantiomeric excesses.[23]

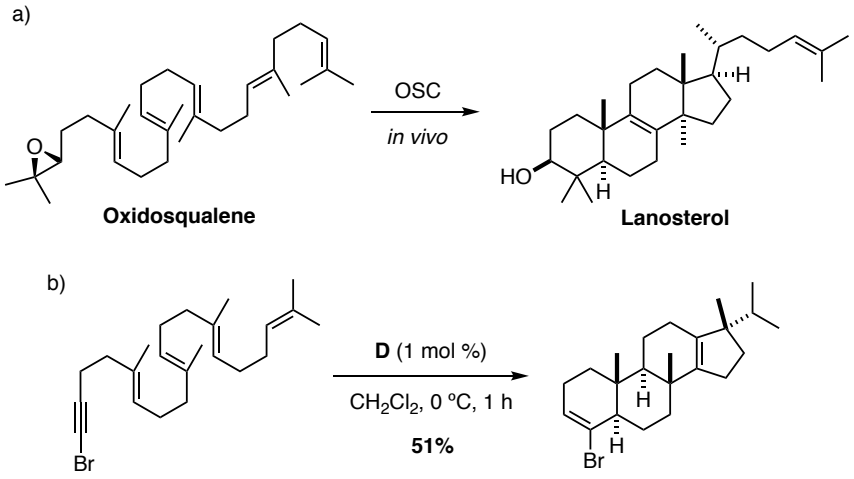

Scheme 6. (a) *In vivo* synthesis of lanosterol *via* polyene cyclization. (b) Gold-catalyzed polyene cyclization.[21i]

Finally, gold catalysis has also been implemented in the synthesis of relevant organic materials. An emblematic example is the synthesis of hydroacenes, stable and soluble precursors of the fully conjugated acenes.[24] The approach relies on the gold(I)-catalyzed 6-*endo*-dig cyclization of 1,7-enynes of type **13** followed by a Friedel-Crafts reaction and methanol

20 (a) Yoder, R. A.; Johnston, J. N. *Chem. Rev.* **2005**, *105*, 4730–4756. (b) Tantillo, D. J. *Chem. Soc. Rev.* **2010**, *39*, 2847–2854.

21 (a) Böhringer, S.; Gagosz, F. *Adv. Synth. Catal.* **2008**, *350*, 2617–2630; (b) Buzas, A.; Istrate, F.; Le Goff, X. F.; Odabachian, Y.; Gagosz, F. *J. Organomet. Chem.* **2009**, *694*, 515–519; (c) Toullec, P. Y.; Blarre, T.; Michelet, V. *Org. Lett.* **2009**, *11*, 2888–2891; (d) Lee, Y.; Lim, C.; Kim S.; Shin, S. *Bull. Korean Chem. Soc.* **2010**, *31*, 670–677; (e) Pradal, A.; Chen, Q.; dit Bel, P. F.; Toullec, P. Y.; Michelet, V. *Synlett*, **2012**, 74–79. (f) Cai, P.-J.; Wang, Y.; Liun C.-H.; Yu, Z.-X. *Org. Lett.* **2014**, *16*, 5898–5901; (g) Danda, A.; Kumar, K.; Waldmann, H. *Chem. Commun.* **2015**, *51*, 7536–7539; (h) Wildermuth, R.; Speck, K.; Magauer, T. *Synthesis*, **2016**, 1814–1824. (i) Rong, Z.; Echavarren, A. M. *Org. Biomol. Chem.* **2017**, *15*, 2163–2167.

22 Fürstner, A.; Morency, L. *Angew. Chem. Int. Ed.* **2008,** *15*, 2163–2167.

23 Sethofer, S. G.; Mayer, T.; Toste, F. D. *J. Am. Chem. Soc.* **2010**, *132*, 8276–8277.

24 Athans, A. J.; Briggs, J. B.; Jia, W.; Miller, G. P. *J. Mater. Chem.* **2007**, *17*, 2636–2641.

elimination (Scheme 7). This route has given access to a broad family of branched and linear acenes with highly interesting electronic properties.[25]

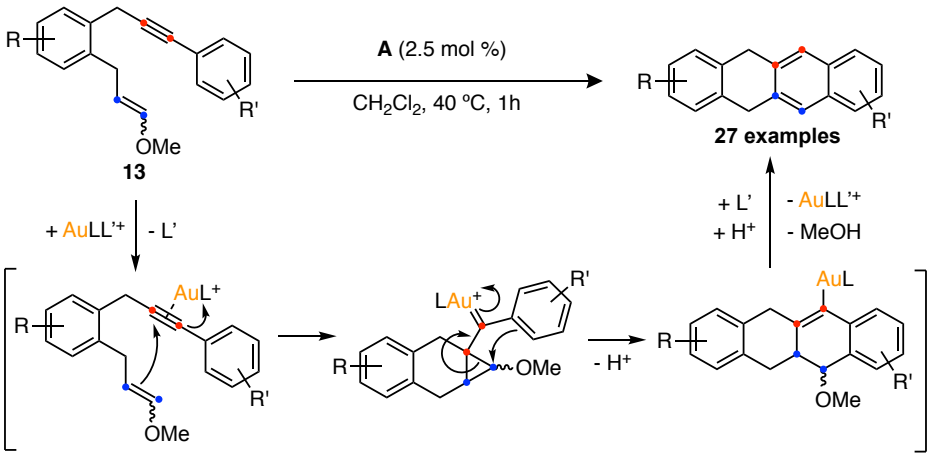

Scheme 7. Gold(I)-catalyzed synthesis of hydroacenes.

Asymmetric Gold Catalysis

The majority of natural products present well-defined stereocenters. As a consequence, asymmetric transformations are highly important in the context of total synthesis. Among all the gold(I)-promoted reactions mentioned above, there are only two examples of enantioselective catalysis. Far from being a coincidence, this illustrates the challenge associated with the development of new gold(I)-catalyzed asymmetric reactions.

In general, transition metal-catalyzed enantioselective transformations rely on the use of chiral ligands. In the case of gold(I), the linear geometry adopted by the complexes locates the substrate on the opposite side from the chiral ligand limiting the efficiency of the enantio-induction during the outer-sphere nucleophilic attack (Figure 2, next page).

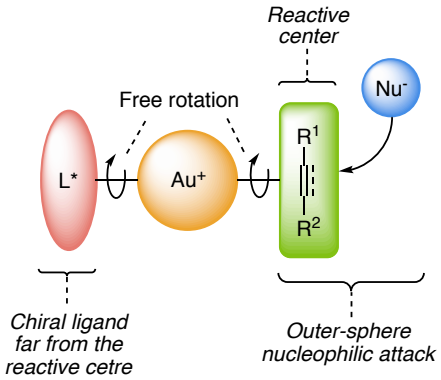

Figure 2. Limitations associated with enantioselective gold(I) catalysis.

25 (a) Dorel, R.; McGonigal, P. R.; Echavarren, A. M. *Angew. Chem. Int. Ed.* **2016**, *128*, 11286–11289. (b) Zuzak, R.; Dorel, R.; Krawiec, M.; Such, B.; Kolmer, M.; Szymonski, M.; Echavarren, A. M. *ACS Nano* **2017**, *11*, 9321–9329. (c) Zuzak, R.; Dorel, R.; Kolmer, M.; Szymonski, M.; Godlewski, S.; Echavarren, A. M. *Angew. Chem. Int. Ed.* **2018**, *57*, 10500–10505.

The design of specific catalytic systems that allow to circumvent this intrinsic limitation is a non-trivial task that has led to a relatively slow growth in the field of asymmetric gold(I) catalysis.[26] Indeed, prior to 2005, there was only one example of an enantioselective gold(I)-catalyzed transformation, reported by Ito and Hayashi in 1986 (see Introduction, Scheme 4a). In early 2005, our group reported the first enantioselective gold(I)-catalyzed alkoxycyclization of enynes using an axially chiral bis(phosphine)digold(I) chloride as precatalyst.[27] Although the enantioselectivities were highly substrate-dependent, the cyclization of enyne **14** occurred with an excellent 94% *ee*, a value that exceeded the best results obtained in Pt^{II}-catalyzed alkoxycyclization of enynes at the time (Scheme 8).[28] This effort towards rendering a well-known gold(I)-catalyzed reaction enantioselective demonstrated the potential of the concept and served as a precedent for the development of new chiral catalytic systems.

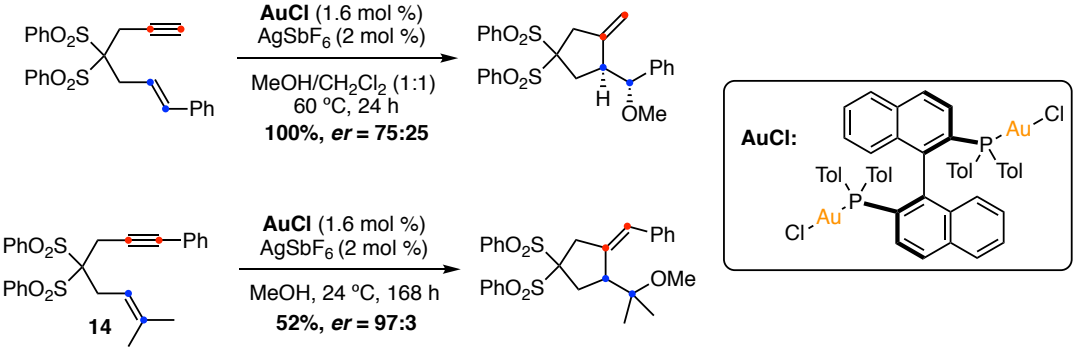

Scheme 8. Selected examples of enantioselective gold(I)-catalyzed alkoxycyclization of enynes.

Since then, several gold(I)-catalyzed asymmetric annulations and hydrofunctionalization have been reported. The main solutions have been based on the use of axially chiral digold complexes[29] or monodentate phosphoramidite ligands (Figure 3).[30]

26 (a) Widenhoefer, R. A. *Chem. Eur. J.* **2008**, *14*, 5382–5391. (b) Pradal, A.; Toullec, P. Y.; Michelet, V. *Synthesis* **2011**, 10, 1501–1514. (c) Wang, Y.-M.; Lackner, A. D.; Toste, F. D. *Acc. Chem. Res.* **2014**, *47*, 889−901. (d) Zi, W.; Toste, F. D. *Chem. Soc. Rev*. **2016**, *45*, 4567−4589. (e) Li, Y.; Li, W.; Zhang, J. *Chem. Eur. J.* **2017**, *23*, 467−512.

27 Muñoz, M. P.; Adrio, J.; Carretero, J. C.; Echavarren, A. M. *Organometallics* **2005**, *24*, 1293–1300.

28 Charruault, L.; Michelet, V.; Taras, R.; Gladialli, S.; Genêt, J.- P. *Chem. Commun.* **2004**, 850-851.

29 For selected examples, see: (a) Zhang, Z.; Widenhoefer, R. A. *Angew. Chem. Int. Ed.* **2007**, *46*, 283–285. (b) Zi, W.; Wu, H.; Toste F. D. *J. Am. Chem. Soc*. **2015**, *137*, 3225–3228.

30 For selected examples, see: (a) Alonso, I.; Trillo, B.; López, F.; Montserrat, S.; Ujaque, G.; Castedo, L.; Lledós, A.; Mascareñas, J. L. *J. Am. Chem. Soc.* **2009**, *131*, 13020–13030. (b) Wang, Y.; Zhang, P.; Qian, D.; Zhang, J. *Angew. Chem. Int. Ed.* **2015**, *54*, 14849–14852.

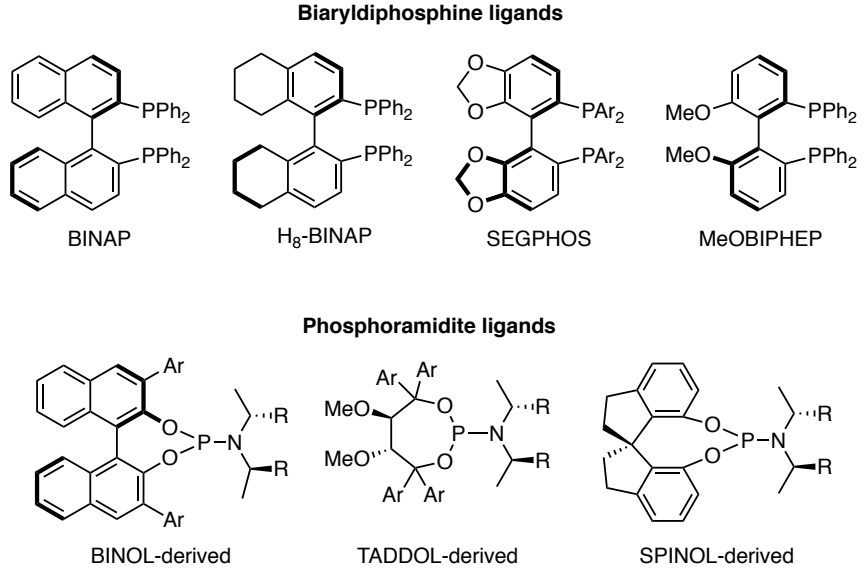

Figure 3. Chiral ligands commonly used in enantioselective gold(I) catalysis.

Other less frequently used strategies rely on the use of chiral counteranions,[31] diaminocarbenes,[32] helically chiral ligands[33] or bifunctional monophosphines that provide substrate fixation and preorientation *via* non-covalent interactions.[34]

31 (a) Hamilton, G. L.; Kang, E. J.; Mba, M.; Toste, F. D. *Science*, **2007**, *317*, 496–499. (b) Inamdar, S. M.; Konala, A.; Patil, N. T. *Chem. Commun.* **2014**, *50*, 15124–15135. (c) Zhang, Z.; Smal, V.; Retailleau, P.; Voituriez, A.; Frison, G.; Marinetti, A.; Guinchard, X. *J. Am. Chem. Soc.* **2020**, 142, 3797–3808.

32 (a) Niemeyer, Z. L.; Pindi, S.; Khrakovsky, D. A.; Kuzniewski, C. N.; Hong, C. M.; Joyce, L. A.; Sigman, M. S.; Toste, F. D. *J. Am. Chem. Soc.* **2017**, *139*, 12943–12946. (b) Wang, Y. M.; Kuzniewski, C. N.; Rauniyar, V.; Hoong, C.; Toste, F. D. *J. Am. Chem. Soc.* **2011**, *133*, 12972–12975. (c) Bartolomé, C.; García-Cuadrado, D.; Ramiro, Z.; Espinet, P. *Inorg. Chem.* **2010**, *49*, 9758–9764.

33 (a) Aillard, P.; Voituriez, A.; Dova, D.; Cauteruccio, S.; Licandro, E.; Marinetti, A. *Chem. Eur. J.* **2014**, *20*, 12373–12376. (b) Yavari, K.; Aillard, P.; Zhang, Y.; Nuter, F.; Retailleau, P.; Voituriez, A.; Marinetti, A. *Angew. Chem. Int. Ed.* **2014**, *53*, 861–865. (c) Aillard, P.; Retailleau, P.; Voituriez, A.; Marinetti, A. *Chem. Eur. J.* **2015**, *21*, 11989–11993.

34 For selected examples, see: (a) Zhang, Z. M.; Chen, P.; Li, W.; Niu, Y.; Zhao, X. L.; Zhang, J. *Angew. Chem. Int. Ed.* **2014**, *53*, 4350–4354. (b) Hu, H.; Wang, Y.; Qian, D.; Zhang, Z. M.; Liu, L.; Zhang, J. *Org. Chem. Front.* **2016**, *3*, 759–763. (c) Wang, Z.; Nicolini, C.; Hervieu, C.; Wong, Y. F.; Zanoni, G.; Zhang, L. *J. Am. Chem. Soc.* **2017**, *139*, 16064–16067. (d) Cheng, X.; Wang, Z.; Quintanilla, C. D.; Zhang, L. *J. Am. Chem. Soc.* **2019**, *141*, 3787–3791.

The Carexanes Family of Natural Products

The carexanes are secondary metabolites isolated from the roots and leaves of the Mediterranean plant *Carex distachya* (Figure 4).[35]

Figure 4. *Carex distachya.*

They consist of a family of bicyclic and tetracyclic prenylstilbenoid derivatives that enhance the growth of *Carex distachya* and serve as phytotoxin for other plant species (Figure 5).[36] The structure and relative configuration of the natural products could be first elucidated using elemental analysis, mass spectroscopy and NMR analysis. In a later article, X-ray diffraction analysis of carexane D led to a reassignment of the relative configuration of C16 with respect to C7 and C8.[35d] Here, the corrected structure was provided for all the members of the family except for carexanes H, I and L, which were not mentioned.

Further studies on the biological activity showed that carexanes, as well as their derivative distachyasin, display antioxidant capabilities analogous to other plant flavonoids.[37] A recent report highlighted that this antioxidant capacity could play an important role in preventing gastric cancer.[38]

35 (a) D'Abrosca, B.; Fiorentino, A.; Golino, A.; Monaco, P.; Oriano, P.; Pacifico, S. *Tetrahedron Lett.* **2005**, *46*, 5269–5272. (b) Fiorentino, A.; D'Abrosca, B.; Izzo, A.; Pacifico, S.; Monaco, P. *Tetrahedron* **2006**, *62*, 3259–3265. (c) Fiorentino, A.; D'Abrosca, B.; Pacifico, S.; Natale, A.; Monaco, P. *Phytochemistry* **2006**, *67*, 971–977. (d) F iorentino, A.; D'Abrosca, B.; Pacifico, S.; Iacovino, R.; Izzo, A.; Uzzo, P.; Russo, A.; Di Blasio, B.; Monaco, P. *Tetrahedron* **2008**, *64*, 7782–7786.

36 Fiorentino, A.; D'Abrosca, B.; Pacifico, S.; Izzo, A.; Letizia, M.; Esposito, A.; Monaco, P. *Biochem. Syst. Ecol.* **2008**, *36*, 691–698.

37 Fiorentino, A.; D'Abrosca, B.; Pacifico, S.; Iacovino, R.; Mastellone, C.; Di Blasio, B.; Monaco, P. *Bioorg. Med. Chem. Lett.* **2006**, *16*, 6096–6101.

38 Buommino, E.; D'Abrosca, B.; Donnarumma, G.; Parisi, A.; Scognamiglio, M.; Fiorentino, A.; De Luca, A. *Microbial Pathogenesis* **2017**, *108*, 71–77.

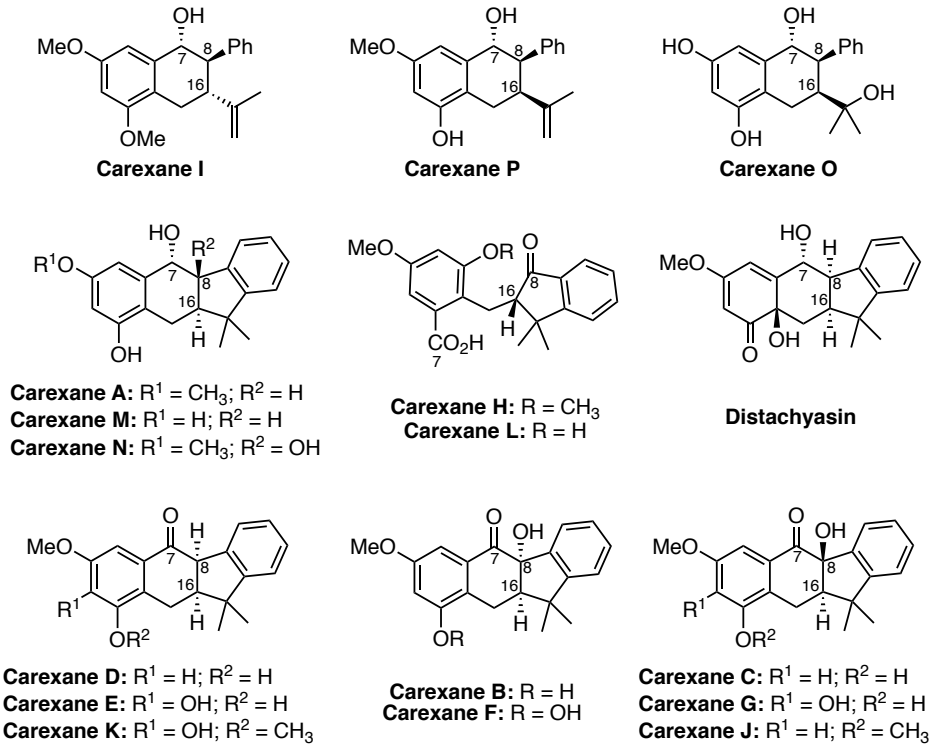

Figure 5. Carexane family of natural products (as reported).

The proposed biosynthesis involves the cyclization of an oxidized prenylstilbenoid of type **15** to generate intermediate **16**. The evolution of this cationic species *via* Friedel-Crafts cyclization would lead to the formation of the tetracyclic carexanes (Scheme 9, red arrow). Alternatively, direct deprotonation of **16** would give access to the bicyclic members of the family (Scheme 9, blue arrow).[35b-c]

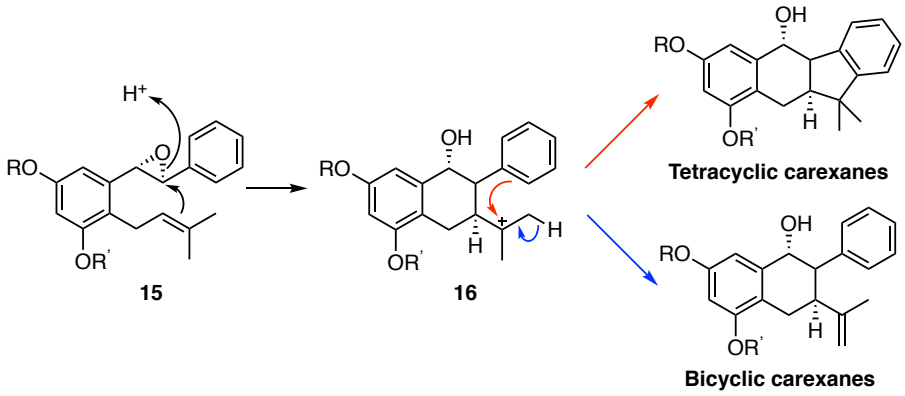

Scheme 9. Biosynthetic proposal for the carexanes.

Objectives

Following our previous reports on the application of gold(I) catalysis to the total synthesis of biologically relevant compounds, we aimed to develop the first enantioselective synthesis of the bicyclic members of the carexane family.

The task was divided in two different parts:

- The enantioselective synthesis of the natural products

To achieve this goal, a new enantioselective gold(I)-catalyzed 6-*endo-dig* hydroxycyclization of 1,6-enynes was developed to give access to the chiral bicyclic scaffold of carexanes I, P and O (Scheme 10). Further derivatization led to the preparation of the natural products which, in turn, allowed to determine whether the relative configuration of C16 with respect to C7 and C8 on carexane I should also be changed as in the case of the other members of the family.

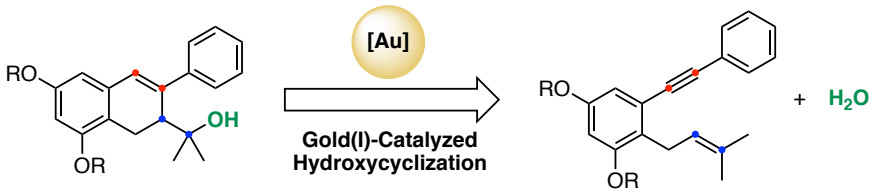

Scheme 10. Assembly of the bicyclic scaffold of carexanes *via* gold(I) catalysis.

- The study of the asymmetric gold(I)-catalyzed cyclization

With the optimal conditions in hand, the scope and the mode of action of the catalyst of the reaction were investigated.

Results and Discussion

Retrosynthetic Strategy

In our initial retrosynthetic approach, we envisioned that diol **19a** would be an advance common intermediate in the synthesis of the three bicyclic carexanes. It could be obtained through a regio- and diastereoselective hydroboration-oxidation of dihydronaphthalene **18a**, the product resulting from the enantioselective gold(I)-catalyzed 6-*endo-dig* hydroxycyclization of 1,6-enyne **17a**. Finally, the enyne could be easily accessed through a sequence of alkynylation/prenylation of a 1,3-dimethoxybenzene derivative (Scheme 11).

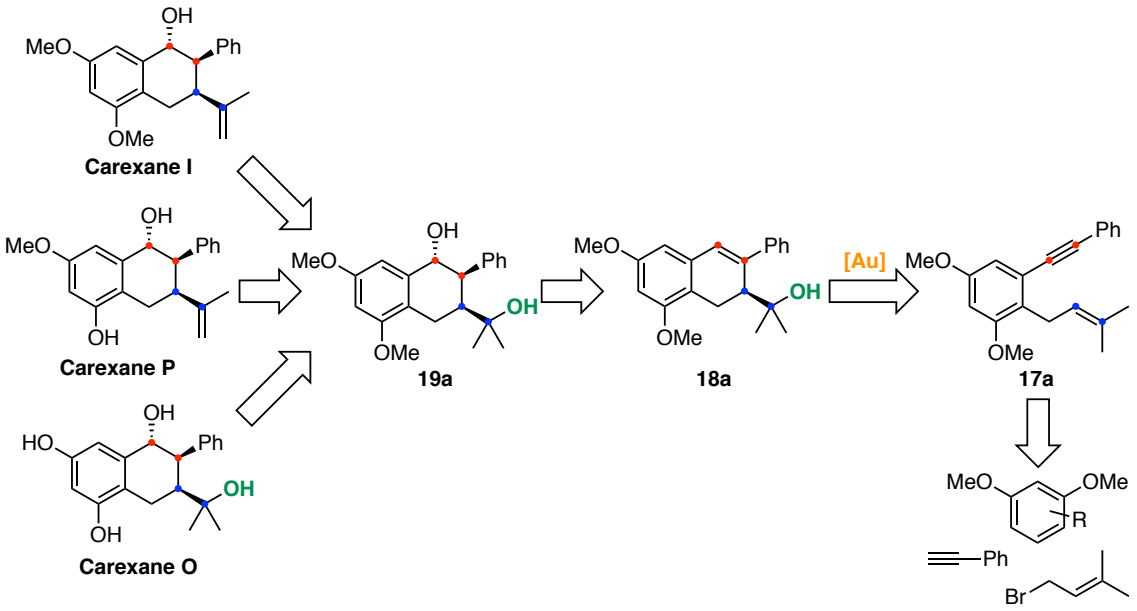

Scheme 11. Retrosynthetic analysis to access bicyclic carexanes I, P and O.

*Synthesis of 1,6-Enyne **17a***

The most efficient strategy to synthetize enyne **17a** started with the alkynylation of 3,5-dimethoxybromobenzene with phenyl acetylene under slightly modified Sonogashira conditions.[39] The resulting internal alkyne **20a** was then subjected to bromination with NBS affording **21a** in 91% yield. Finally, bromine-lithium exchange followed by nucleophilic substitution on prenyl bromide delivered the desired enyne in 65% yield (Scheme 12). This robust synthesis could be performed at large scale (40 mmol) with no significant decrease in the reaction yields (~50% over three steps).

39 Nwokogu, G. C.; *Tetrahedron Lett.* **1984**, *25*, 3263–3266.

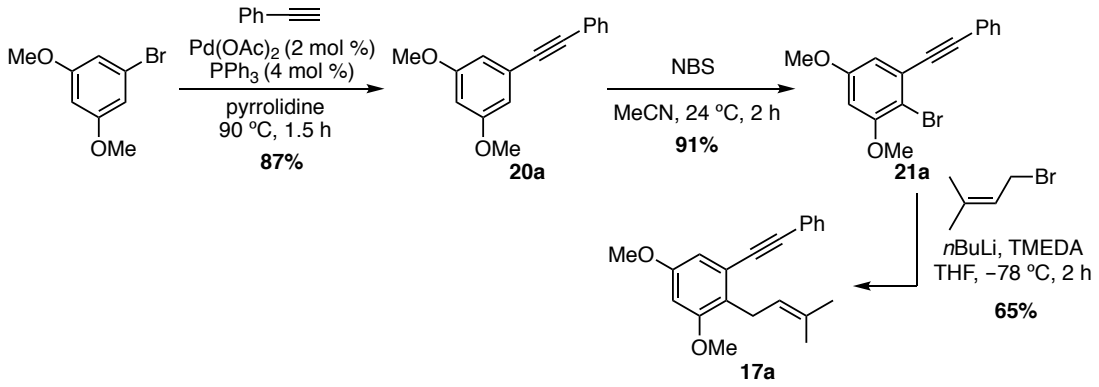

Scheme 12. Synthesis of 1,6-enyne **17a**.

*Studies on the Gold(I)-Catalyzed Hydroxycyclization of **17a***

As mentioned in the Introduction (Scheme 10), the racemic version of this reaction had already been studied by the group of Sanz back in 2013.[40] They found that (JohnPhos)(NCMe)AuSbF$_6$ (catalyst **A**) gave the best results in terms of yield and selectivity. The reaction tolerated different aryl and alkyl groups on the alkyne and proved to be diastereoselective when two stereocenters were formed. In agreement with these results, our initial catalyst screening to convert enyne **17a** into dihydronaphthalene **18a**, highlighted gold catalyst **A** as the best catalytic system, forming the desired product in 69% yield and tetracyclic product **22a** in 21% as the major side-product (Scheme 13).[41]

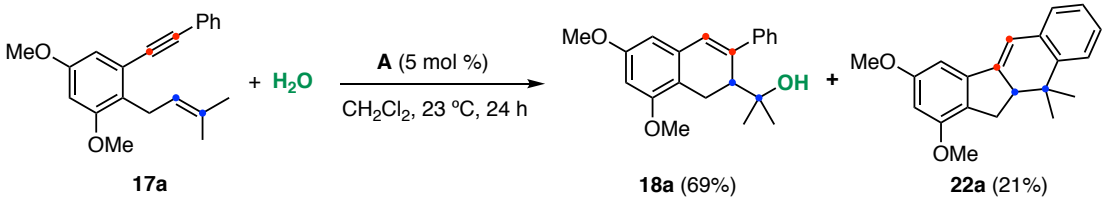

Scheme 13. Gold(I)-catalyzed hydroxycyclization of enyne **17a**.

We reasoned that activated enyne **23a** could evolve both *via* 5-*exo*-*dig* or 6-*endo*-*dig* cyclization, generating cyclopropylgold(I) carbenes **24a** and **25a** respectively. While intermediate **24a** is prone to evolve through Friedel-Crafts alkylation to give **22a**, **25a** shows reluctance to undergo this intramolecular cyclization and it is preferentially trapped by water affording **18a** (Scheme 14). The yield and the 6-*endo*/5-*exo* selectivity (3.3:1) are in the range of the other reported examples.[40]

40 Sanjuán, A. M.; Martínez, A.; García-García, P.; Fernández-Rodríguez, M. A.; Sanz, R. *Beilstein J. Org. Chem.* **2013**, *9*, 2242–2249.

41 Calleja, P. ICIQ PhD Thesis **2017**, unpublished results.

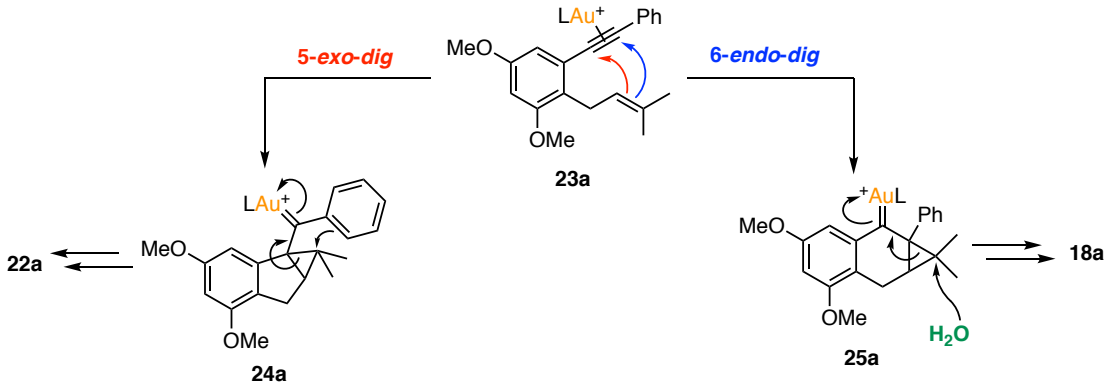

Scheme 14. Proposed mechanism for the formation of **18a** and **22a**.

Next, we focused on the development of the enantioselective version of this reaction. Our initial efforts were carried out in the Cellex-ICIQ high throughput experimentation unit (HTE). Reactions were run at 10 μmol scale in CH_2Cl_2 preforming the gold precatalyst in-situ by mixing the chiral ligands with [(Me_2S)AuCl]. After 22 h, enantiomeric excesses were measured directly form the diluted reaction crudes. We screened more than 80 chiral catalytic systems, dwelling on phosphoramidite ligands as well as chiral biphosphines. Although most of the systems gave the product with enantiomeric ratios lower than 57:43,[42] JosiPhos ligands stood out as the most promising option,[15] affording **18a** in 80:20 *er*. Unfortunately, further attempts to improve this result using different (JosiPhos)Au_2Cl_2 as precatalysts were unsuccessful.[42]

At this stage, a family of chiral gold(I) complexes based on the JohnPhos scaffold bearing a C_2-symmetric pyrrolidine was being developed in the group. We were excited to see that, prior to any optimization, when catalyst (*R*,*R*)-**J** was used in the hydroxycyclization, product **18a** was obtained in yield 55% yield and 95:5 *er* (Scheme 15).

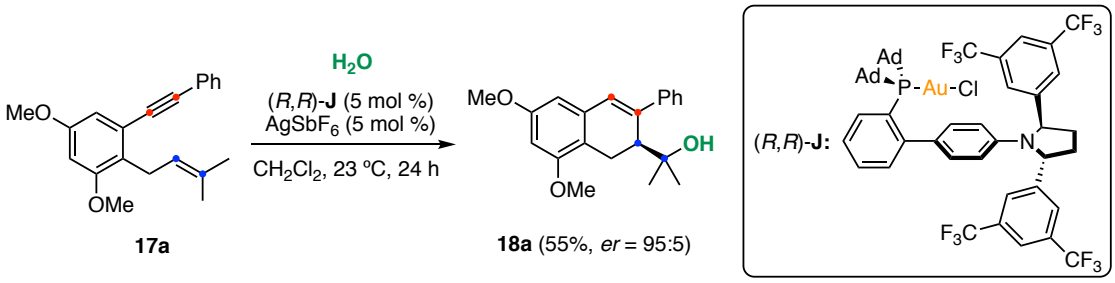

Scheme 15. Enantioselective hydroxycyclization of **18a** catalyzed by (*R*,*R*)-**J**. First attempt.

Encouraged by this result, other precatalysts of the family were also tested (Table 1). Replacing the aryl groups on the pyrrolidine by phenyl [(*S*,*S*)-**K**], perfluorophenyl [(*R*,*R*)-**L**], (3,5-diphenyl)phenyl [(*R*,*R*)-**M**] or cyclohexyl [(*R*,*R*)-**N**] resulted in slightly lower yields and less

42 See Supporting Information of this article for more information.

efficient enantio-inductions (Table1, entries 1-4). In contrast, complex [(*R*,*R*)-**O**] bearing *tert*-butyl groups instead of adamantyl at the phosphine gave comparable results (Table 1, entry 5).

Table 1. Screening of chiral gold(I) complexes.

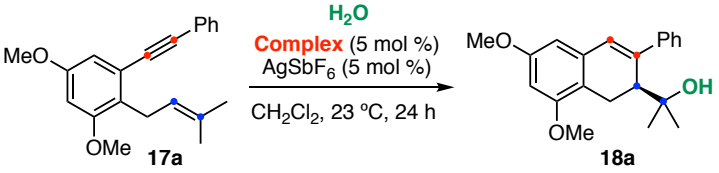

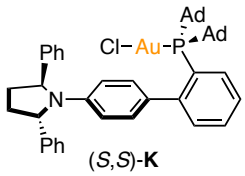

Entry	Complex	Yield 18a (%)[a]	*er*
1	(*S*,*S*)-**K**	52	20:80
2	(*R*,*R*)-**L**	48	77:23
3	(*R*,*R*)-**M**	52	91:9
4	(*R*,*R*)-**N**	53	89:11
5	(*R*,*R*)-**O**	53	94:6

[a] Isolated yields.

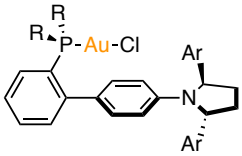

(*R*,*R*)-**L** : R = Ad; Ar = C_6F_5
(*R*,*R*)-**M** : R = Ad; Ar = 3,5-$(Ph)_2C_6H_3$
(*R*,*R*)-**N** : R = Ad; Ar = Cy
(*R*,*R*)-**O** : R = *t*Bu; Ar = 3,5-$(CF_3)_2C_6H_3$

The optimization of the reaction parameters was performed using (*R*,*R*)-**J** as precatalyst (Table 2). Interestingly, variation of the solvent (Table 2, entries 1-5) or the temperature (Table 2, entries 6-9) did not affect the levels of enantio-induction. These results point towards the formation of a relatively rigid catalyst-enyne adduct during the reaction (regardless of the temperature and the solvent), where the attack of one face of the alkene is more favored than the other.

Table 2. Screening of solvents and temperatures.

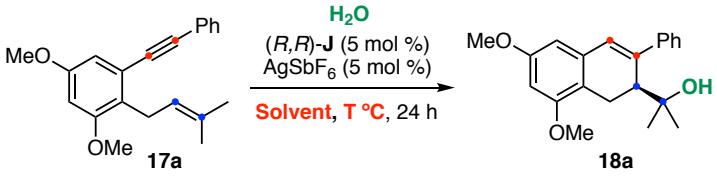

Entry	Solvent	*T* (°C)	Yield (%)[a]	*er*
1	$PhCF_3$	23	58	98:2
2	toluene	23	10	97:3
3	1,2-dichloroethane	23	55	97:3
4	THF	23	45	96:4
5	chlorobenzene	23	50	96:4
6	$PhCF_3$	0	33	98:2
7	$PhCF_3$	–20	30	98:2
8	$PhCF_3$	35	60	96:4
9	$PhCF_3$	50	65	95:5

[a] Isolated yields.

Further optimization experiments showed that it was possible lower the catalyst loading until 1 mol % and highlighted $AgSbF_6$ as the most efficient chloride scavenger.[42] Importantly, recrystallization in hot hexane allowed the isolation of the enantiopure products (the other enantiomer could not be detected in the UPC^2).

With the best conditions in hand, the reaction scope was then explored. Enynes bearing electron-donating or electron-withdrawing groups on either of the aryl rings performed well in the hydroxy- or alkoxycyclization, delivering products **18b-g** in moderate to good yields (43 to 69%) and excellent enantiomeric ratios (94:6 to 97:3).[43]

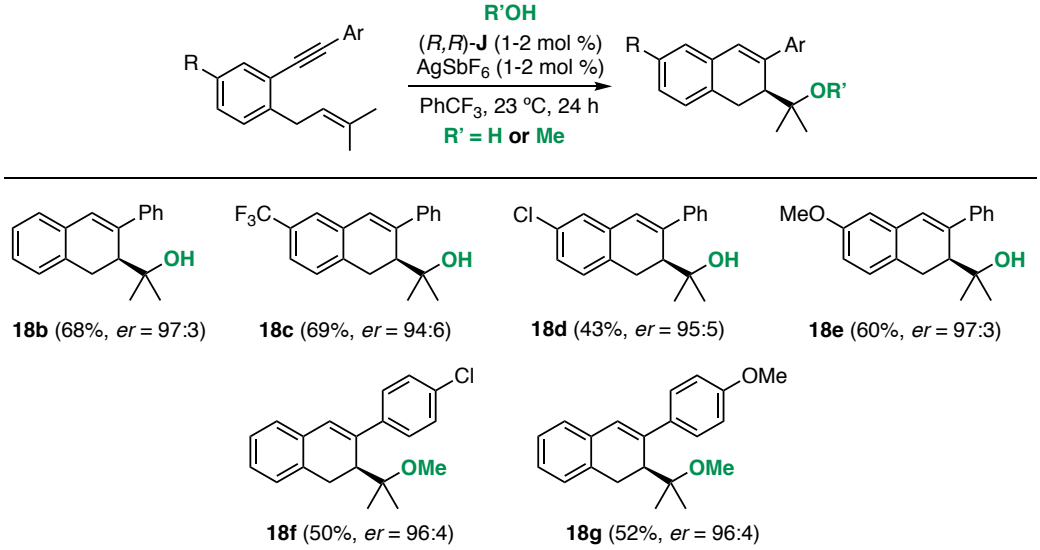

Scheme 16. Scope of the enantioselective gold(I)-catalyzed cyclization: aryl modifications.

Regarding the nature of the nucleophile, different alcohols could be used generating the corresponding ethers **18f-18i** in good yields (50 to 75%) and excellent enantiomeric ratios (95:5 to 96:4). The use of acetic acid as nucleophile led to the formation of **18j** in 41% yield and 90:10 *er*. The significant drop in both yield and enantioselectivity might be explained due to the partial protonation of the pyrrolidine ring and consequent change of the stereoelectronic properties of the complex. Remarkably, fluorinated compound **18k** was obtained in 40% yield and 96:4 *er* when HF·pyridine complex was used as nucleophile (Scheme 17). Other commonly used nucleophiles such as electronrich-(hetero)arenes (indole, trimethoxybenzene, etc…) were not compatible with the reaction.

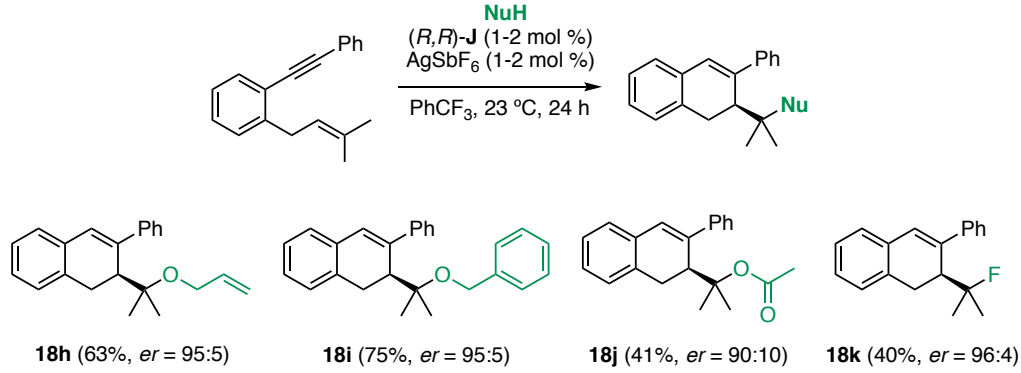

Scheme 17. Scope of the enantioselective gold(I)-catalyzed cyclization: nucleophiles.

43 All enynes (**17b-h**) were prepared following reported procedures (see Experimental Section for more details).

To determine the configuration of the chiral center formed during the reaction, diol **19a**, prepared *via* hydroboration/oxidation of compound **18a** from the least hindered face, was converted into highly crystalline ferrocene carboxylate **26** (Scheme 18).[44] The absolute configuration of **26** was unambiguously assigned as (*S*) by X-ray crystallography.

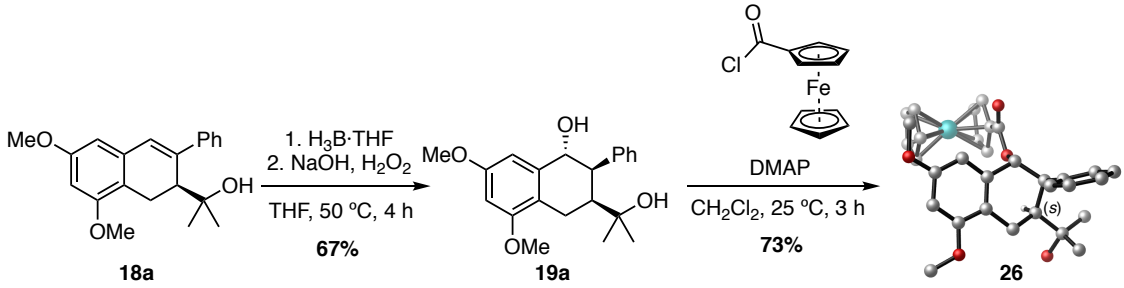

Scheme 18. Synthesis of ferrocene carboxylate **26**.

The configuration of the remaining examples was correlated that of **18a** by circular dichroism (Figure 6).

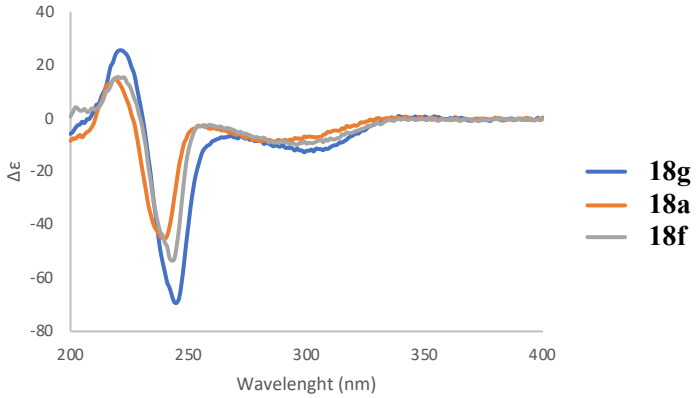

Figure 6. Superimposed CD-spectra of compounds **18a**, **18f** and **18g**.

Catalyst Mode of Action

In parallel to the aforementioned work, Dr. Giuseppe Zuccarello and Dr. Dagmar Scharnagel found that catalyst (*R,R*)-**J** was able to promote the enantioselective cyclization of 1,6-enynes of type **27**[45] and **29**[46] in moderate to excellent yields with high levels of enantio-induction (Scheme 19).[47] Surprisingly, the corresponding cyclized products were obtained with the opposite absolute configuration at the stereocenter.

44 Holstein, P. M.; Holstein, J. J.; Escudero-Adán, E. C.; Baudoin, O.; Echavarren, A. M. *Tetrahedron: Asymmetry* **2017**, *28*, 1321–1329.

45 Nieto-Oberhuber, C.; López, S.; Echavarren, A. M. *J. Am. Chem. Soc.* **2005**, *127*, 6178–6179.

46 (a) Fürstner, A.; Szillat, H.; Stelzer, F. *J. Am. Chem. Soc.* **2000**, *122*, 6785–6786. (b) Fürstner, A.; Stelzer, F.; Szillat, H. *J. Am. Chem. Soc.* **2001**, *123*, 11863–11869.

47 Zuccarello, G. ICIQ PhD Thesis **2020**.

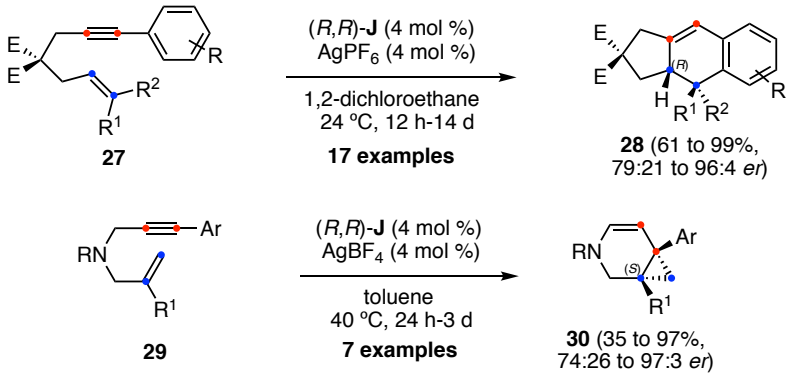

Scheme 19. Enantioselective cyclization of enynes **27** and **29**.

The stereodetermining step in all three cyclizations is the formation of the cyclopropyl gold carbene intermediate upon intramolecular attack of the alkene onto the activated alkyne. We therefore rationalized that, while in enynes **27** and **29** the nucleophilic attack was taking place from the *Si* prochiral face of the alkene, for enynes of type **17** the *Re* face was more favored. This divergency must arise from a different disposition of the enynes inside the chiral cavity of the gold complex. Our hypothesis to explain these different arrangements rely on the presence of non-covalent interactions between the catalyst and the enynes. In the case of 1,6-enynes **27** and **29,** the catalyst would interact with terminal the aryl group (the stereocontrolling element), whereas for enynes **17** this role would be played by the aryl group at the tether (Scheme 20).

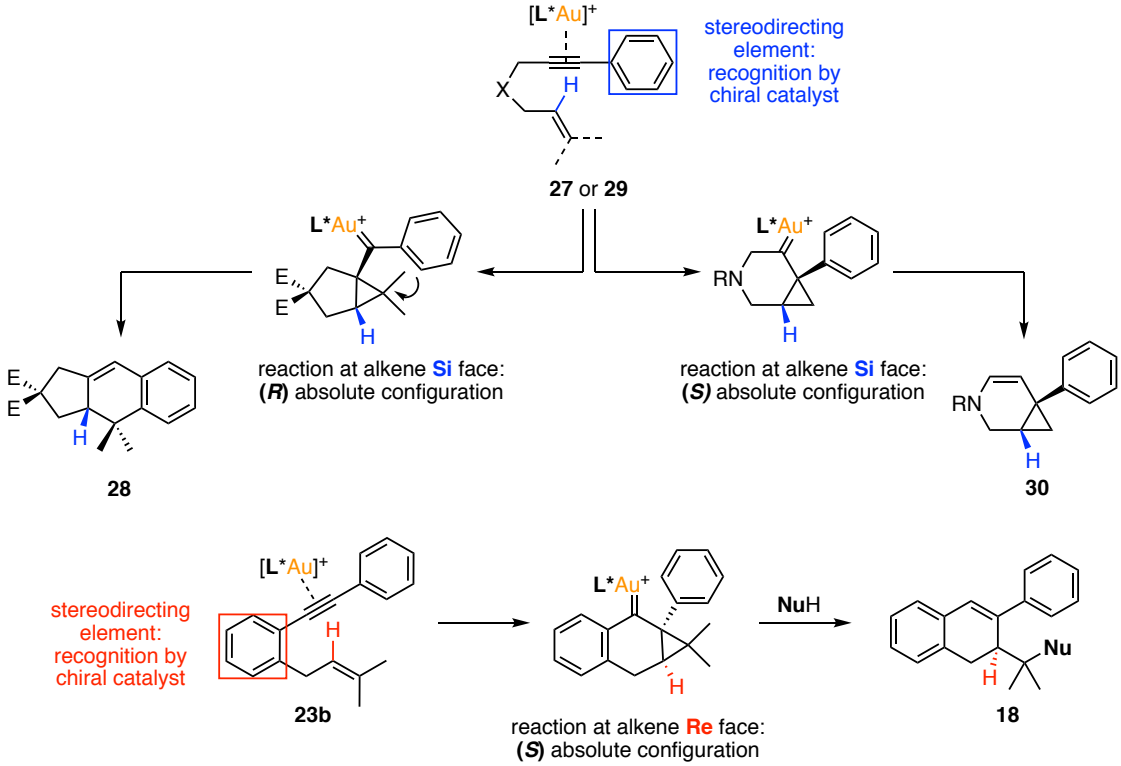

Scheme 20. Working hypothesis for the different stereochemical outcomes observed in the cyclization of enynes **27**, **29** and **17**.

To verify our hypothesis, different control experiments were performed. Thus, the hydroxycyclization of enyne **31** (without the hypothetic stereodirecting aryl) resulted in the quantitative formation of **32** as a racemic mixture, confirming the crucial role of the arene in the enantio-induction.[42,47] In addition, dienyne **33** bearing a double bond instead of the aryl moiety, furnished cycloadduct **34** with a modest 67:33 *er*, presumably due to weaker interactions between the substrate and the catalyst.[42,47] As expected, 1,6-enyne **17h**[43] bearing a cyclohexenyl instead of the phenyl at the alkyne gave dihydronapthalene **18l** in comparable yield and enantioselectivity obtained for **18b** (Scheme 21). Circular dichroism correlation allowed the assignment of the (*S*) absolute configuration in dihydronaphthalene **18l**.

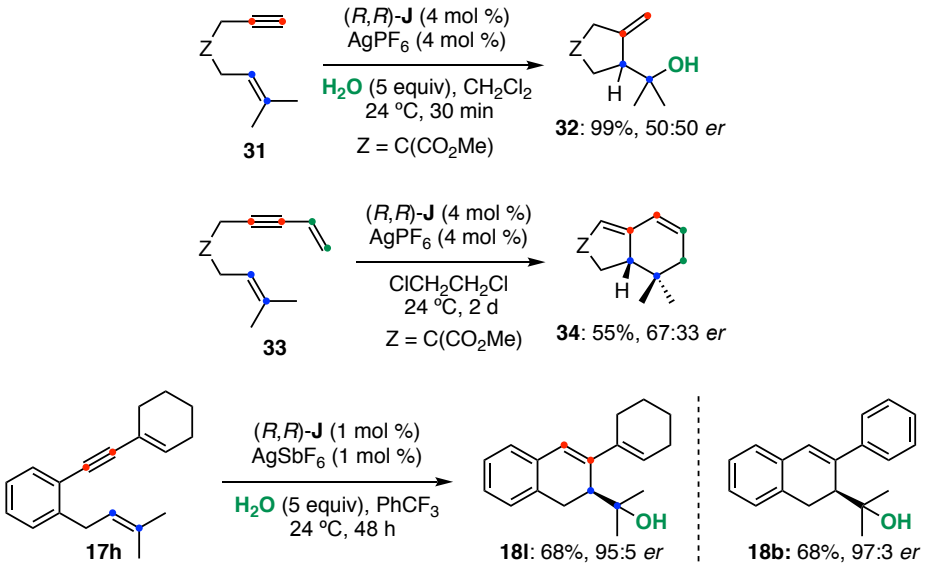

Scheme 21. Cyclization of enynes **31**, **33** and **17h**.

In line with our hypothesis and the experimental results, DFT calculations performed by Dr. Imma Escofet using (*R,R*)-**O** as catalyst confirmed that enynes **27** bind preferentially to gold in the opposite orientation as enynes **17** do due to a series of π–π and OMe-aryl attractive non-covalent interactions between the stereocontrolling elements on the enynes and the aryl groups connected to the pyrrolidine ring of the catalyst (Figure 7). Once the enyne is installed in the chiral cavity, steric interactions favor the selective attack of one of the prochiral faces of the alkene over the other, resulting in high enantioselectivities.[48]

48 The complete energy diagrams including all the calculated transition states can be found in the end of the experimental section of this chapter.

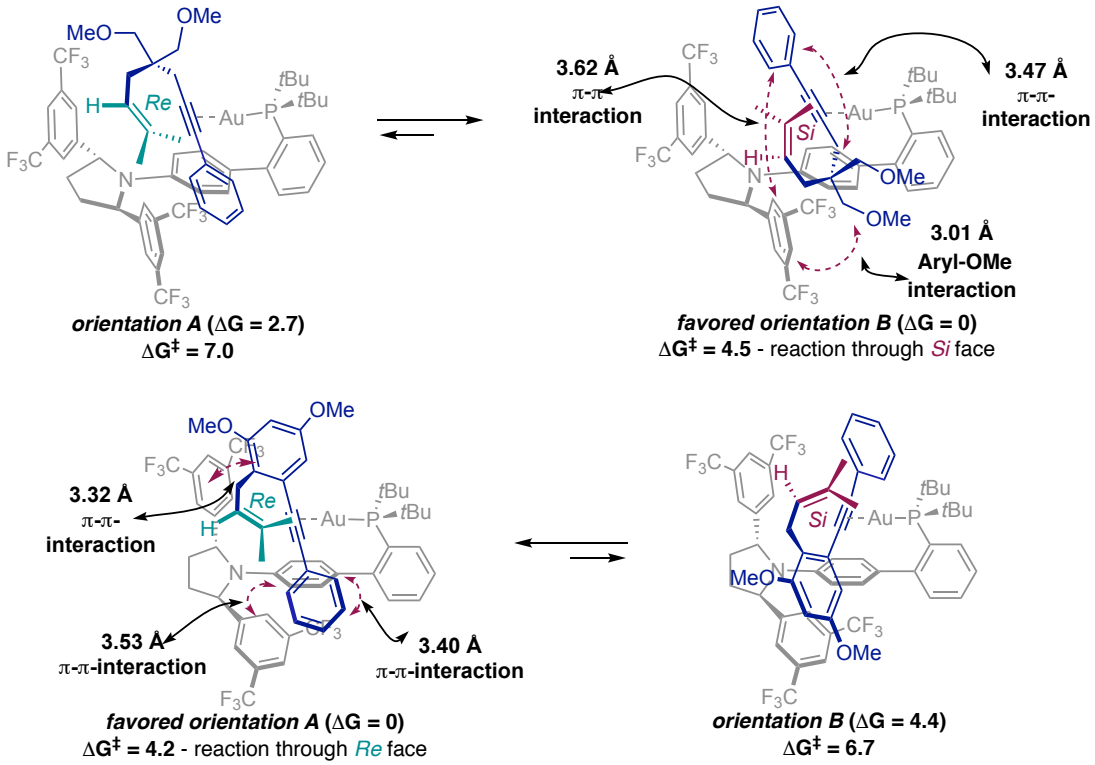

Figure 7. Representation of the two more relevant binding orientation for enynes a) **27** and b) **17** inside the chiral cavity of gold complex (*R,R*)-**O**. Energy values are given in kcal·mol^{-1}.

To gain more insight about the nature of these non-covalent interactions and how they affect the levels of enantio-inductions, a Hammett study was performed.[49] Hence, we observed a linear correlation between log(*er*) and the corresponding Hammett parameters in the formation of products **28** and **18** (Figure 8). The negative values observed for the slopes in both reactions suggest that the non-covalent interactions become stronger with electron-rich aromatic groups.

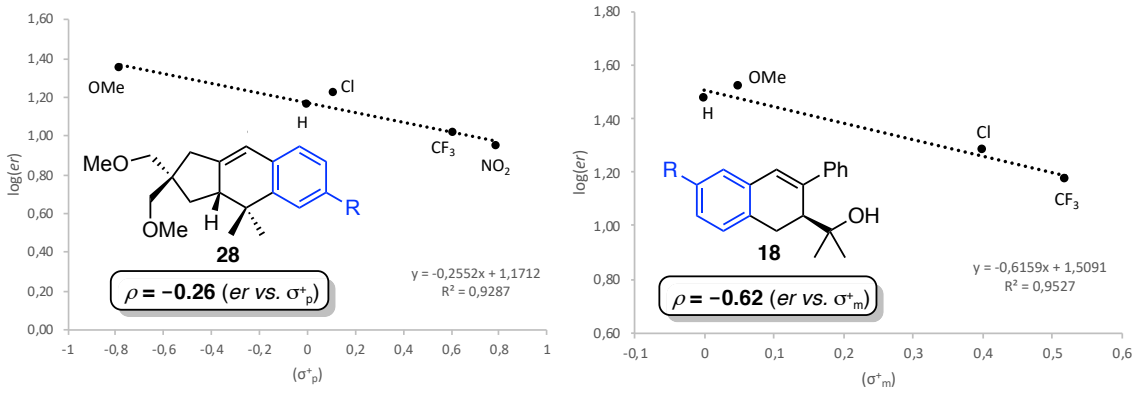

Figure 8. Hammett study for the formation of cyclized products **28** and **18**.

Overall, substrate recognition by the chiral catalyst induces one specific binding orientation stabilized by non-covalent interactions that leads to a particular enantioselective folding and

49 Hammett, L. P. *J. Am. Chem. Soc.* **1937**, *59*, 96–103.

consequently, to the observed absolute configuration.[50] The complete energy diagrams including all the calculated transition states can be found in the Experimental Section of this chapter.

Final Steps in the Synthesis of carexanes I, P and O

It is worth to mention that different strategies were attempted to access the tetracyclic scaffold of the rest of the carexane family from compounds **18a** and **22a**. However, neither the acid-catalyzed intramolecular Friedel-Crafts of **18a** nor the epoxidation/rearrangement of **22a** afforded the desired 6,6,5,6-tetracyclic structure (Scheme 22).[41]

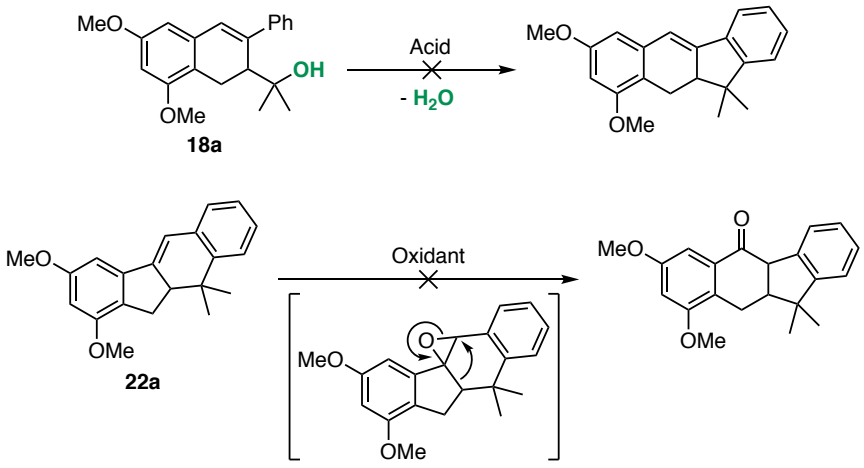

Scheme 22. Efforts to construct the 6,6,5,6-tetracyclic core present in most carexanes.

As depicted in Scheme 11, diol **19a** could serve as an advanced common intermediate for the synthesis of the three natural products. For instance, the selective dehydration of the tertiary alcohol would lead to carexane I. Unfortunately, the benzylic alcohol proved to be more prone to undergo elimination and all the attempts to perform this reaction led to decomposition or the formation of stilbene **18a.** Alternatively, TIPS protection of the secondary alcohol in **19a** produced silyl ether **35** in 87% yield. In this case, the elimination of the tertiary alcohol could be accomplished by treatment with the Burgess reagent.[51] Deprotection of the silyl group in **36** with TBAF delivered carexane I in 92% yield over the two steps (Scheme 23).

50 (a) Neel, A. J.; Hilton, M. J.; Sigman, M. S.; Toste, F. D. *Nature* **2017**, *543*, 637−646. (b) Toste, F. D.; Sigman, M. S.; Miller, S. J. *Acc. Chem. Res.* **2017**, *50*, 609−615.

51 (a) Atkins, G. M.; Burgess, E. M. *J. Am. Chem. Soc.* **1986**, *90*, 4744–4745. (b) Khapli, S.; Dey, S.; Mal, D. *J. Indian Inst. Sci.* **2001**, *81*, 461–476.

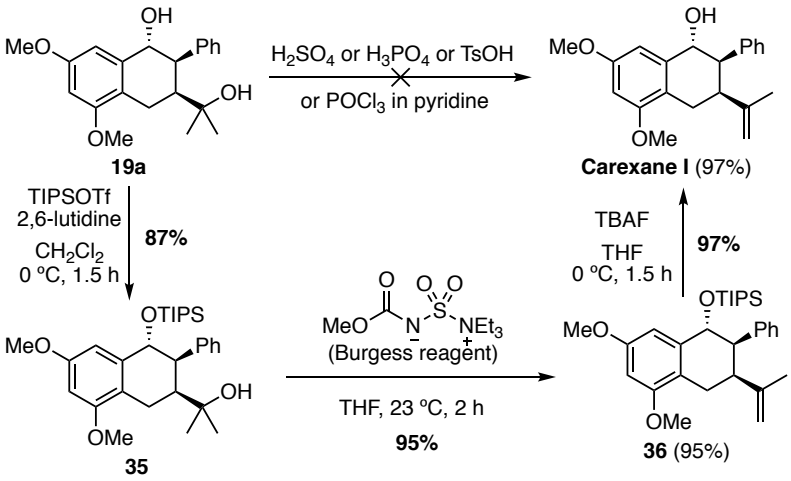

Scheme 23. Synthesis of carexane I from diol **19a**.

Carexane P was prepared in two steps from alkene **36** (Scheme 24). The deprotection of the methyl ether using sodium ethanothiolate furnished an inseparable mixture (2.9:1) of phenol **37a** and **37b** in 70% yield. Subsequent treatment with TBAF led to the isolation of the natural product in 70% yield (calculated considering only the amount of **37a** in the reaction).

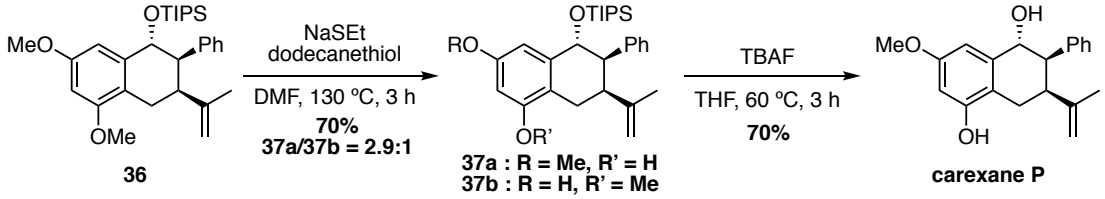

Scheme 24. Synthesis of carexane P from alkene **36**.

Finally, we envisioned that the double methyl ether deprotection on diol **19a** would give rise to carexane O (Table 3). However, the most commonly used methodologies for aryl-methyl ether deprotection failed to deliver the desired product (Table 3, entries 1-5). In fact, although no side products were characterized in these reactions, TLC analysis showed that most of the remaining material was less polar than the starting diol. This suggested that the conditions used were not compatible with the presence of the easily dehydratable benzylic alcohol. Therefore, we examined a methodology used by the group of Hoye in the total synthesis of (–)-cylindrocyclophane, in which four aryl-methyl ethers were deprotected in the presence of two benzylic alcohols.[52] We were delighted to see that reacting **19a** with a large excess of MeMgI in neat conditions yielded the natural product in 39% yield (Table 3, entry 6).

52 Hoye, T. R.; Humpal, P. E.; Moon, B. *J. Am. Chem. Soc.* **2000**, *122*, 4982–5983.

Table 3. Efforts towards the synthesis of carexane O from diol **19a**.

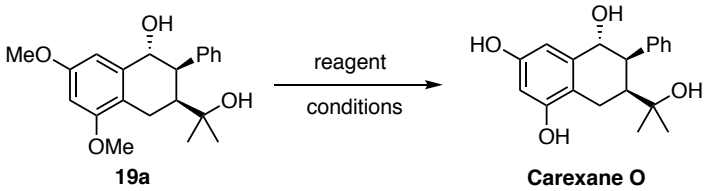

19a **Carexane O**

Entry	Reagent	Conditions	Yield (%)
1	TMSI, NH_3	CH_2Cl_2, 0 ºC	decomposition
2	$AlCl_3$, NaI	neat, 70 ºC	decomposition
3	BBr_3	CH_2Cl_2, 24 ºC	decomposition
4	BCl_3	CH_2Cl_2, 24 ºC	no reaction
5	NaSEt/dodecanethiol	DMF, reflux	decomposition
6	MeMgI	vacuum, neat, 150 ºC	39[a]

[a] Isolated yield.

Since the reaction suffered from reproducibility issues, we decided to design a new synthetic route based on a similar sequence but starting with different protecting group on the phenol moieties. We rationalized that benzyl groups would be suitable since they were compatible with all the reaction conditions along the route and would be easily removed by hydrogenation.

Thus, we commenced the synthesis preparing enyne **17i** from of 3,5-dimethoxybromobenzene following the same alkynylation/bromination/prenylation strategy used in the synthesis of **17a** (47% yield over three steps). The gold(I)-catalyzed hydroxycyclization worked efficiently affording bicyclic product **18m** in 68% yield and 98:2 *er*. After recrystallization in hot hexane, enantiomerically pure **18m** was submitted to hydroboration/oxidation conditions to generate diol **19b** in 62% yield. As in the previous case, the hydroboration took place from the less hindered face of the alkene delivering the desired *trans/cis* configuration between C7, C8 and C16. Carexane O was obtained upon quantitative hydrogenolysis of the benzyl ethers on **19b** using palladium on carbon (Scheme 25).

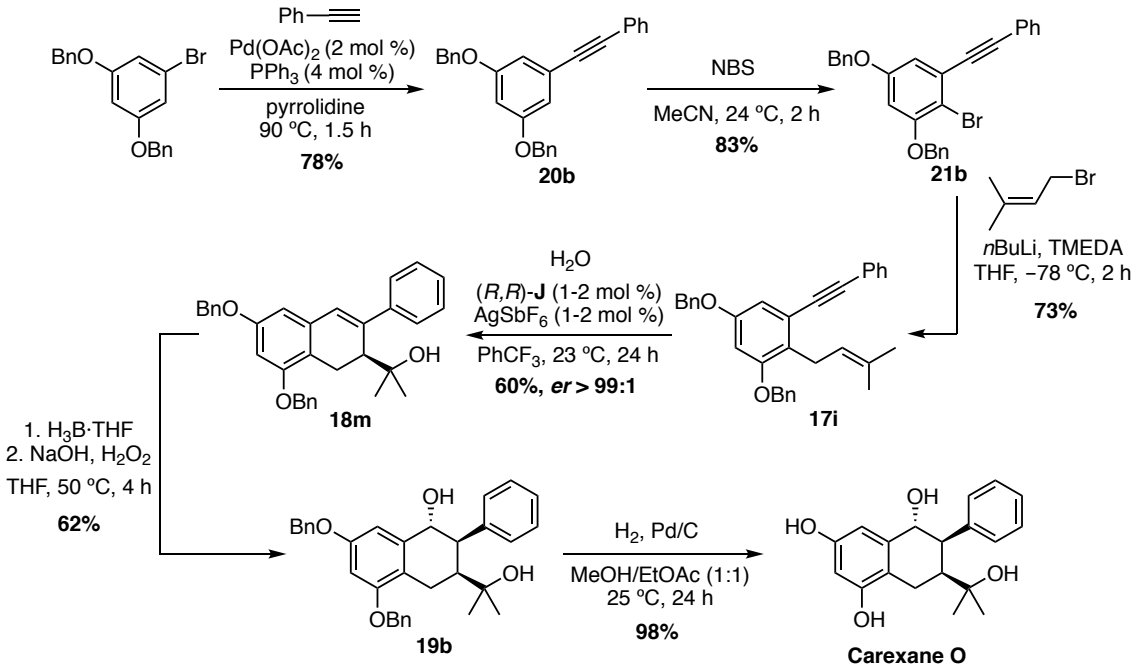

Scheme 25. New approach for the total synthesis of carexane O.

The three naturals products were obtained in an enantiomerically pure form, confirming that no epimerization or partial racemization occurred at any stage of the synthesis after the gold(I)-catalyzed cyclization. The structures as well as the relative and absolute configurations were further confirmed by single-crystal X-ray crystallography (Figure 9).

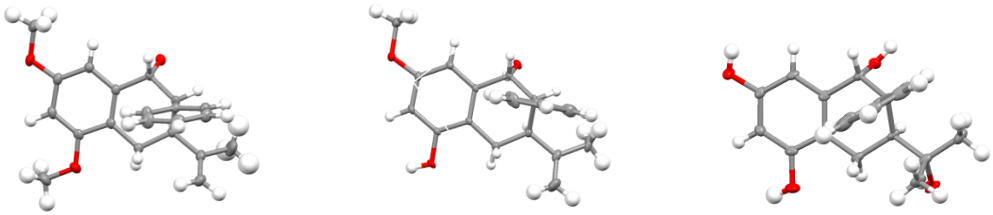

Figure 9. Crystalline structure of carexanes I, P and O.

Comparison between the Isolated and the Synthetic Natural Products

As stated in the introduction, the absolute configuration of the carexanes at the C16 was first misassigned[35a-c] and then corrected.[35d] In this last publication, the group reported the corrected structures of all the members of the family except for carexane H, I and L that were not mentioned. Additionally, in a later report,[38] carexane I appeared with the "non-corrected" (*R*) configuration. To unambiguously determine the relative configuration at C16 with respect to C8 and C7, we compared our characterization data with the signals reported literature (Table 4).[35c]

Table 4. Comparison of NMR shifts between the natural and the synthetic samples of carexane I[35c]

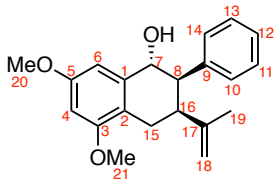

carexane I

Position	^{1}H NMR natural sample (CD_3Cl, 300 MHz)	^{1}H NMR synthetic sample (CD_3Cl, 300 MHz)	^{13}C NMR natural sample (CD_3OD, 75 MHz)	^{13}C NMR synthetic sample (CD_3OD, 101 MHz)
1	-	-	140.0	140.0
2	-	-	120.2	120.2
3	-	-	159.1	159.2
4	6.45 (*d*, 2.4 Hz)	6.45 (*d*, 2.4 Hz)	98.0	98.8
5	-	-	160.5	160.6
6	6.61 (*d*, 2.4 Hz)	6.61 (*d*, 2.4 Hz)	106.5	106.5
7	4.88 (*d*, 2.7 Hz)	4.88 (*d*, 2.6 Hz)	73.2	73.2
8	3.42 (*t*, 3.0 Hz)	3.42 (*t*, 3.1 Hz)	51.4	51.4
9	-	-	140.6	140.6
10	6.86 (*m*)	6.90 – 6.83 (*m*)	129.9	129.9
11	7.14 (*m*)	7.18 – 7.12 (*m*)	128.6	128.6
12	7.14 (*m*)	7.18 – 7.12 (*m*)	127.4	127.4
13	7.14 (*m*)	7.18 – 7.12 (*m*)	128.6	128.6
14	6.86 (*m*)	6.90 – 6.83 (*m*)	129.9	129.9
15	2.78 (*dd*, 17.7, 4.8 Hz), 2.29 (*dd*, 17.7, 12.3 Hz)	2.70 (*dd*, 17.3, 4.5 Hz), 2.22 (*dd*, 17.3, 12.0 Hz)	24.1	24.1
16	2.91 (*dt*, 11.7, 3.0 Hz)	2.95 (*dt*, 12.1, 3.9 Hz)	40.5	40.8
17	-	-	147.9	147.9
18	4.81 (*s*), 4.47 (*s*)	4.81 (*s*), 4.47 (*s*)	111.7	111.7
19	1.79 (*s*)	1.79 (*s*)	22.8	22.8
20	3.81 (*s*)	3.84 (*s*)	55.8	55.9
21	3.80 (*s*)	3.82 (*s*)	55.7	55.8

The agreement of both series of data confirms that the relative configuration of C7/C8/C16 in carexane I should be corrected from *trans*/*trans* to *trans*/*cis* as in the case of the other members of the family. An analogous comparation of the NMR spectra from the isolated and synthetic samples was carried out for carexanes P and O (Tables 5 and 6 respectively).

Table 5. Comparison of NMR shifts between the natural and the synthetic sample of carexane P[35d]

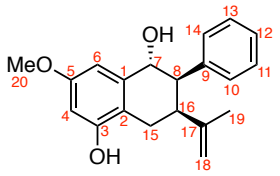

carexane P

Position	^{1}H NMR natural sample (CD_3OD, 300 MHz)	^{1}H NMR synthetic sample (CD_3OD, 500 MHz)	^{13}C NMR natural sample (CD_3OD, 75 MHz)	^{13}C NMR synthetic sample (CD_3OD, 126 MHz)
1	-	-	140.0	140.2
2	-	-	120.2	118.7
3	-	-	156.1	156.6
4	6.37 (*d*, 2.7 Hz)	6.39 (*d*, 2.5 Hz)	98.0	102.0
5	-	-	160.5	160.2
6	6.55 (*d*, 2.7 Hz)	6.56 (*d*, 2.5 Hz)	106.5	106.7
7	4.73 (*d*, 2.7 Hz)	4.74 (*d*, 2.1 Hz)	73.2	73.3
8	3.53 (*m*)	3.37 (*dd*, 3.7, 2.8 Hz)	51.4	51.4
9	-	-	140.6	140.6
10	6.85 (*m*)	6.85 (*m*)	129.9	129.9
11	7.11 (*m*)	7.10 (*m*)	128.6	128.6
12	7.11 (*m*)	7.10 (*m*)	127.4	127.3
13	7.11 (m)	7.10 (*m*)	128.6	128.6
14	6.85 (*m*)	6.85 (*m*)	129.9	129.9
15	2.68 (*dd*, 17.4, 4.5 Hz), 2.22 (*dd*, 17.4, 12.2 Hz)	2.70 (*dd*, 17.0, 4.6 Hz), 2.26 (*dd*, 17.0, 12.4 Hz)	24.1	24.2
16	2.96 (*dt*, 12.2, 4.5 Hz)	2.98 (*dt*, 12.4, 4.2 Hz)	40.5	40.8
17	-	-	147.9	147.9
18	4.57 (*s*), 4.44 (*s*)	4.78 (s), 4.45 (*s*)	111.7	111.7
19	1.80 (*s*)	1.80 (*s*)	22.8	22.9
20	3.77 (*s*)	3.77 (*s*)	55.7	55.6

Table 6. Comparison of NMR shifts between the natural and the synthetic sample of carexane O[35d]

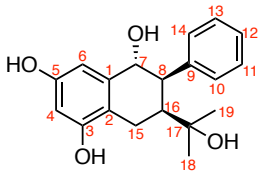

carexane O

Position	^{1}H NMR natural sample (CD_3OD, 300 MHz)	^{1}H NMR synthetic sample (CD_3OD, 500 MHz)	^{13}C NMR natural sample (CD_3OD, 75 MHz)	^{13}C NMR synthetic sample (CD_3OD, 126 MHz)
1	-	-	138.0	139.6
2	-	-	117.5	117.8
3	-	-	157.2	157.2
4	6.31 (*d*, 0.9 Hz)	6.33 (*d*, 2.4 Hz)	109.7	109.5
5	-	-	157.2	156.8
6	6.31 (*d*, 0.9 Hz)	6.32 (*d*, 2.4 Hz)	109.7	102.9
7	4.38 (*d*, 1.8 Hz)	4.39 (*d*, 1.8 Hz)	74.9	75.1
8	3.46 (*br s*)	3.48 (*dd*, 3.4, 1.9 Hz)	49.5	44.4
9	-	-	141.9	142.5
10	6.99 (*m*)	7.01 (*m*)	130.0	130.8
11	7.13 (*m*)	7.15 (*m*)	128.8	129.2
12	7.13 (*m*)	7.15 (*m*)	127.5	127.5
13	7.13 (*m*)	7.15 (*m*)	128.8	129.2
14	6.99 (*m*)	7.01 (*m*)	130.0	130.8
15	2.98 (*dd*, 14.5, 5.8 Hz), 2.38 (*m*)	3.01 (*dd*, 16.5, 4.4 Hz), 2.43 (*dd*, 16.5, 13.0 Hz)	23.4	21.7
16	2.47 (*m*)	2.50 (*ddd*, 13.0, 4.4, 3.4 Hz)	48.1	49.7
17	-	-	74.0	73.9
18	1.14 (*s*)	1.14 (*s*)	27.9	28.2
19	0.92 (*s*)	0.93 (*s*)	27.0	27.6

The small discrepancies found between the two spectra might arise from to the different concentrations of the sample in MeOD. Nonetheless, the similarity between the coupling constants of H7 and H16 suggests that both samples display the same relative configuration.

Finally, to verify if the absolute configurations of carexanes I, P and O were the same as the one assigned to carexane D by single-crystal X-ray crystallography (*R,R,S*), we proceeded to compare the specific rotations of the isolated and synthetic samples. Unfortunately, despite using similar conditions for the measurements, the values obtained for all three synthetic samples were in discrepancy with the ones previously reported, which prevented us from drawing any definitive conclusion (Table 7).

Table 7. Comparison between the specific rotations of the isolated and synthetic carexanes

Natural Product	Literature α_D (deg.cm^2.g$^-$)	Measured α_D (deg.cm^2.g$^-$)
Carexane I	+15.6[35c]	+33.3
Carexane P	-26.7[35d]	+13.0
Carexane O	+10.0[35d]	-40.1

Conclusions

We have developed the enantioselective gold(I)-catalyzed 6-*endo-dig* cyclization of aryl-tethered 1,6-enynes using complex (*R,R*)-**J**, a chiral extended version of catalyst **A** featuring a C_2-symmetric 2,5-disubstiuted pyrrolidine. The proposed cyclopropylgold(I) intermediate can be trapped with different nucleophiles producing dihydronaphthalenes in good yields (40 to 75%) and remarkable enantiomeric ratios (90:10 to 98:2) (Scheme 26). Experimental and theoretical work strongly suggest that non-covalent interactions between the substrate and the ligand are essential for the efficient enantio-induction.

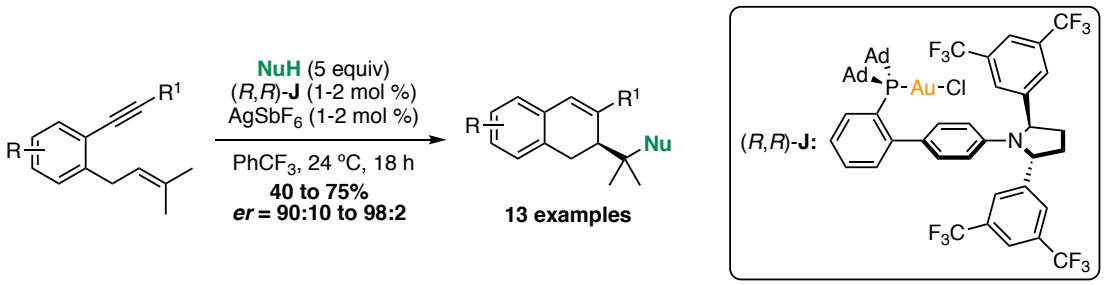

Scheme 26. Enantioselective gold(I) cyclization of aryl-tethered 1,6-enynes.

This reactivity has been successfully applied in first enantioselective total synthesis of carexane I (8 steps, 15% overall yield), carexane P (9 steps, 6% overall yield) and carexane O (6 steps, 17% overall yield) (Scheme 27). The relative configuration of carexane I has been reassigned.

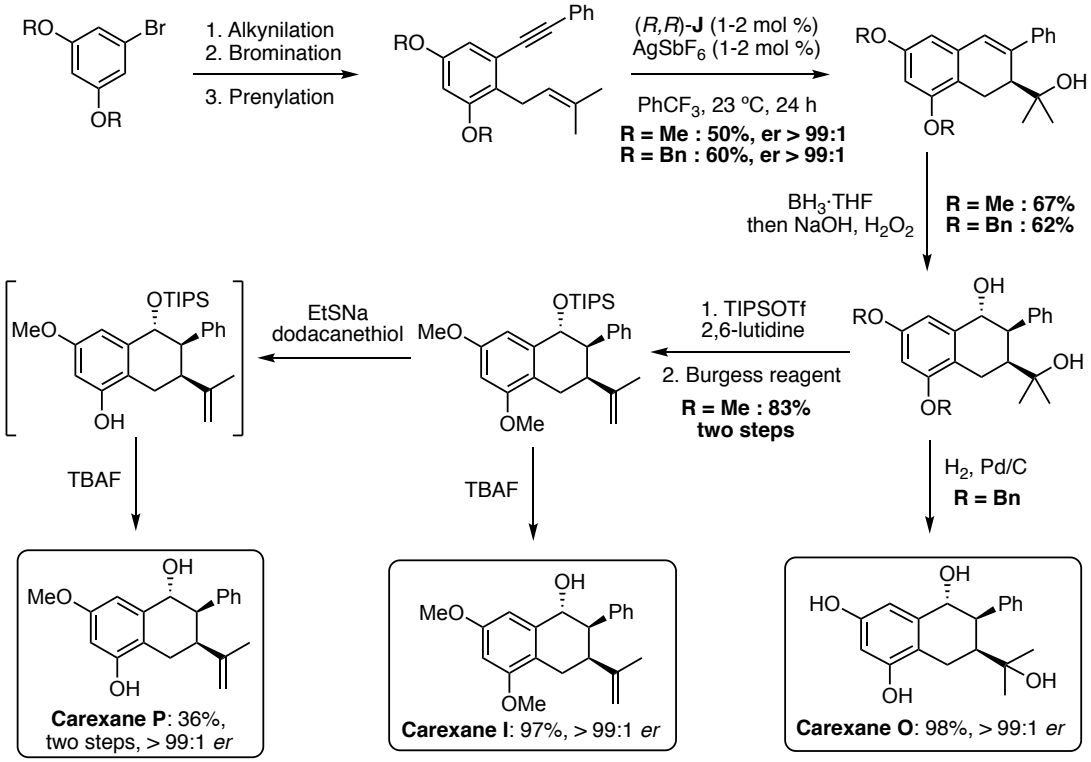

Scheme 27. Enantioselective total synthesis of carexanes I, P and O.

Experimental Part

General Information

Unless otherwise stated, all the reactions were performed under an inert atmosphere of argon. All solvents and other chemicals were used as received. All the reactions were run in dry solvents (passed through an activated alumina column on a PureSolv™ solvent purification system). Reactions were followed using a GC-MS apparatus, by TLC (thin layer chromatography) or by NMR analysis. Analytical thin layer chromatography was carried out using TLC aluminum sheets coated with 0.2 mm of silica gel (Merck 60 F_{254}) using UV light as the visualizing agent and an acidic solution of vanillin in ethanol or basic solution of $KMnO_4$ in water as stain. Chromatographic purifications were carried out using flash grade silica gel (PanReac Silica Gel 60, 40-63 μm) or automated flash column chromatographer CombiFlash Companion. Preparative thin layer chromatography was performed on TLC plates (Analtec Silica Gel GF UV254, 20×20 cm, 1000 μm). Melting points were determined using a Mettler Toledo MP70 melting point apparatus. NMR spectra were recorded at 298 K on BrukerAvance Ultrashield NMR spectrometers (300 MHz, 400 MHz, 500 MHz and 500 MHz with CryoProbe). Chemical shifts (δ) are reported in parts per million (ppm) and referenced to residual solvent (For ^{1}H NMR: $CDCl_3$ at 7.26 ppm, CD_2Cl_2 at 5.31 ppm, C_6D_6 at 7.16 ppm, CD_3OD at 3.31 ppm, for $^{13}C\{^1H\}$ NMR: $CDCl_3$ at 77.16 ppm, CD_2Cl_2 at 54.00 ppm, C_6D_6 at 128.06 ppm, CD_3OD at 49.00 ppm). The following abbreviations were used to explain multiplicities: s = singlet, d = doublet, t = triplet, q = quartet, p = pentet, m = multiplet, br s = broad singlet. Coupling constants (*J*) are reported in Hertz (Hz). Infrared spectra were recorded neat on a Bruker ALPHA FTIR-ATR TR0 spectrometer. The peaks are reported as absorption maxima (n, cm^{-1}). Mass spectra were recorded on MicroTOF Focus or Maxis Impact spectrometers (both from Bruker Daltonics). Specific optical rotation measurements were carried out on a Jasco P-1030 model polarimeter equipped with a PMT detector using the sodium line at 589 nm, and 1 mL (10 mm pathlength) or 2 mL (100 mm pathlength) cells. Chiral HPLC analyses were performed on an Agilent Technologies 1200 series, a Waters ACQUITY UPC^2 System with diode array detector and by Chiral Technologies Europe analytical service. X-ray diffraction data were collected at 100 K on a Rigaku MicroMax-007HF, Mo *Kα* rotating anode, equipped with a Pilatus 200 K detector or on a Bruker APEX DUO, Mo *Kα* Microfocus source E025 IuS anode, equipped with an APEX DUO detector using omega scans. Circular dichroism spectra measurements were carried out on an Applied Photophysics Chirascan Circular Dichroism spectrometer equipped with a photo-multiplier detector, dual polarizing prism design monochromator, photo-elastic modulator (PEM) and 150W Xenon light source.

Synthetic procedures and analytical data for the preparation of enynes with substituents on the aryl-tether (1b-e)

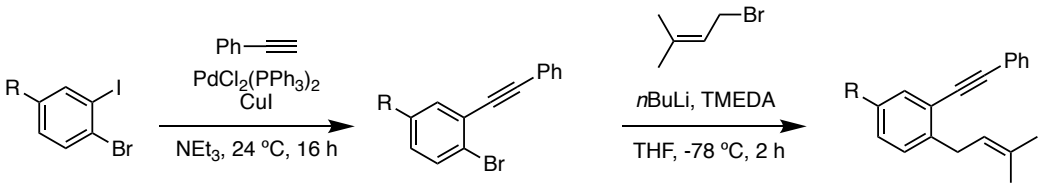

General procedure A: Sonogashira coupling

To a solution of $Pd(PPh_3)_2Cl_2$ (2.5 mol %), copper(I) iodide (5 mol %) and the corresponding aryl iodide (1.0 equiv) in dry NEt_3 (0.25 M) was added ethynylbenzene (1.0 equiv) dropwise at 24 ºC under argon. The reaction was stirred for the given time at the same temperature and quenched with sat. NH_4Cl solution after full conversion of the starting material. The mixture was extracted with CH_2Cl_2 (3x) and the combined organic phases were washed with brine, dried over Na_2SO_4, filtered and concentrated. The crude was purified by flash column chromatography to afford the Sonogashira products.

1-Bromo-2-(phenylethynyl)benzene

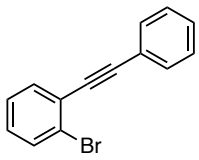

1-Bromo-2-(phenylethynyl)benzene was synthesized following general procedure **A** using 1-bromo-2-iodobenzene (7 g, 24.7 mmol) whereby the reaction was stirred for 14 h. Purification by column chromatography (cyclohexane) afforded the title compound (5.91 g, 23.0 mmol, 93%) as a colorless oil.

The spectral data were fully consistent with those previously reported.[53]

1-Bromo-2-(phenylethynyl)-4-(trifluoromethyl)benzene

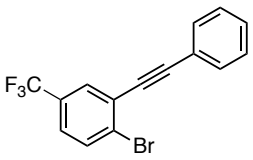

1-Bromo-2-(phenylethynyl)-4-(trifluoromethyl)benzene was synthesized following general procedure **A** from 1-bromo-2-iodo-4-(trifluoromethyl)benzene (3.5 g, 10.0 mmol) whereby the reaction was stirred for 6 h. Purification by column chromatography (cyclohexane) afforded the title compound (2.70 g, 8.4 mmol, 84%) as a white solid.

The spectral data were fully consistent with those previously reported.[54]

53 Liang, B.; Dai, M.; Chen, J.; Yang, Z. *J. Org. Chem.* **2005**, *70*, 391–393.

54 Watanabe, T.; Abe, H.; Mutoh, Y.; Saito, S.; *Chem. Eur. J.* **2018**, *24*, 11545–11549.

1-Bromo-4-chloro-2-(phenylethynyl)benzene

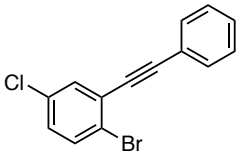

1-Bromo-4-chloro-2-(phenylethynyl)benzene was synthesized following general procedure **A** from 1-bromo-4-chloro-2-iodobenzene (1.0 g, 3.15 mmol) whereby the reaction was stirred for 15 min. Purification by column chromatography (cyclohexane) afforded the title compound (770 mg, 2.64 mmol, 84%) as a white solid.

The compound is known in literature,[55] but spectral data were not fully reported previously.

M.p. = 56 – 58 ºC (pentane). **^{1}H NMR** (500 MHz, $CDCl_3$) δ 7.60 – 7.56 (m, 2H), 7.54 (d, *J* = 2.5 Hz, 1H), 7.53 (d, *J* = 8.6 Hz, 1H), 7.40 – 7.36 (m, 3H), 7.16 (dd, *J* = 8.6, 2.6 Hz, 1H). **^{13}C NMR** (126 MHz, $CDCl_3$) δ 133.6, 133.2, 132.9, 131.9, 129.6, 129.2, 128.6, 127.1, 123.7, 122.6, 95.3, 87.0. **HRMS** (APCI+) calculated for $[C_{14}H_9BrCl]^+$ 290.9571 *m/z*; found $[M + H]^+$ 290.9569 *m/z*.

1-Bromo-4-methoxy-2-(phenylethynyl)benzene

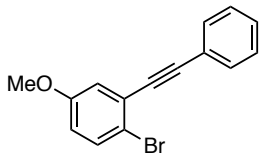

1-Bromo-4-methoxy-2-(phenylethynyl)benzene was synthesized following general procedure **A** from 1-bromo-2-iodo-4-methoxybenzene (1.0 g, 3.20 mmol) whereby the reaction was stirred for 15 min. Purification by column chromatography (pentane) afforded the title compound (832 mg, 2.90 mmol, 91%) as a colorless oil.

The spectral data were fully consistent with those previously reported.[54]

General procedure B: prenylation reaction

A solution of the corresponding alkyne (1.0 equiv) in dry THF (0.2 M) was treated with *n*BuLi (1.5 equiv) at –78 ºC under argon atmosphere and the resulting mixture was stirred for 5 min. TMEDA (1.5 equiv) was added and the mixture was stirred for additional 10 min before adding 1-bromo-3-methylbut-2-ene (1.0 equiv) dropwise. The resulting solution was allowed to reach 24 ºC, quenched with sat. NH_4Cl and extracted with Et_2O. The combined organic phases were washed with brine, dried over Na_2SO_4 and concentrated. The crude product was purified by flash column chromatography to afford the corresponding 1,6-enynes.

1-(3-Methylbut-2-en-1-yl)-2-(phenylethynyl)benzene (17b)

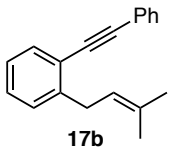

17b

1b was synthesized following general procedure **B** from 1-bromo-2-(phenylethynyl)benzene (2.3 g, 8.9 mmol) whereby the reaction was stirred for 1 h. Purification by column chromatography (cyclohexane) afforded title compound (1.78 g, 7.21 mmol, 81%) as a colorless oil.

The spectral data were fully consistent with those previously reported.[40]

55 Shaikh, A. C.; Ranade, D. S.; Rajamohanan, P. R.; Kulkarni, P. P.; Patil, N. T. *Angew. Chem. Int. Ed.* **2017**, *56*, 757–761.

1-(3-Methylbut-2-en-1-yl)-2-(phenylethynyl)-4-(trifluoromethyl)benzene (17c)

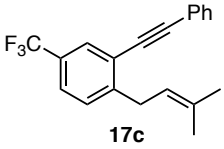

17c

17c was synthesized following general procedure **B** from 1-bromo-2-(phenylethynyl)-4-(trifluoromethyl)benzene (300 mg, 0.92 mmol) whereby the reaction was stirred for 2 h. Purification by column chromatography (cyclohexane) afforded title compound (194 mg, 0.62 mmol, 67%) as a colorless oil.

^{1}H NMR (400 MHz, $CDCl_3$) δ 7.79 (d, *J* = 2.0 Hz, 1H), 7.60 – 7.54 (m, 2H), 7.51 (dd, *J* = 8.1, 1.4 Hz, 1H), 7.42 – 7.33 (m, 4H), 5.42 – 5.36 (m, 1H), 3.66 (d, *J* = 7.3 Hz, 2H), 1.81 –1.78 (m, 3H), 1.77 (s, 3H). **^{13}C NMR** (101 MHz, $CDCl_3$) δ 147.7, 134.1, 131.7, 129.1 (q, *J* = 3.9 Hz), 129.0, 128.8, 128.6, 128.5 (q, *J* = 32.4 Hz), 125.0 (q, *J* = 3.7 Hz), 124.1 (q, *J* = 272.7 Hz), 123.5, 123.1, 121.4, 94.8, 87.0, 33.2, 25.9, 18.1. **^{19}F{^{1}H} NMR** (376 MHz, $CDCl_3$) δ –62.6. **HRMS** (APCI+) calculated for $[C_{20}H_{18}F_3]^+$ 315.1355 *m/z*; found $[M + H]^+$ 315.1354 *m/z*.

4-Chloro-1-(3-methylbut-2-en-1-yl)-2-(phenylethynyl)benzene (17d)

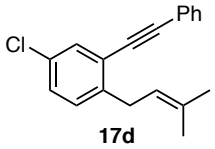

17d

17d was synthesized following general procedure **B** from 1-bromo-4-chloro-2-(phenylethynyl)benzene (100 mg, 0.343 mmol) whereby the reaction was stirred for 1 h. Purification by column chromatography (cyclohexane) afforded title compound (62.3 mg, 0.22 mmol, 65%) colorless oil.

^{1}H NMR (500 MHz, $CDCl_3$) δ 7.56 – 7.52 (m, 2H), 7.49 (d, *J* = 2.3 Hz, 1H), 7.39 – 7.35 (m, 3H), 7.23 (dd, *J* = 8.3, 2.3 Hz, 1H), 7.15 (dd, *J* = 8.3, 0.4 Hz, 1H), 5.37 – 5.31 (m, 1H), 3.55 (d, *J* = 7.3 Hz, 2H), 1.77 – 1.75 (m, 3H), 1.73 (s, 3H). **^{13}C NMR** (126 MHz, $CDCl_3$) δ 142.3, 133.6, 131.8, 131.7, 131.4, 129.8, 128.70, 128.67, 128.6, 124.3, 123.2, 122.0, 94.4, 87.2, 32.6, 25.9, 18.1. **HRMS** (APCI+) calculated for $[C_{19}H_{18}Cl]^+$ 281.1092 *m/z*; found $[M + H]^+$ 281.1092 *m/z*.

4-Methoxy-1-(3-methylbut-2-en-1-yl)-2-(phenylethynyl)benzene (17e)

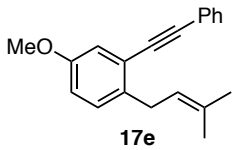

17e

17e was synthesized following general procedure **B** from 1-bromo-4-methoxy-2-(phenylethynyl)benzene (140 mg, 0.49 mmol) whereby the reaction was stirred for 1 h. Purification by preparative TLC (pentane/CH_2Cl_2 95:5) afforded title compound (90 mg, 0.33 mmol, 68%) as a light yellow oil.

^{1}H NMR (500 MHz, $CDCl_3$δ 7.58 – 7.53 (m, 2H), 7.39 – 7.34 (m, 3H), 7.14 (d, *J* = 8.6 Hz, 1H), 7.07 (d, *J* = 2.8 Hz, 1H), 6.86 (dd, *J* = 8.5, 2.8 Hz, 1H), 5.38 (tdt, *J* = 7.3, 2.8, 1.4 Hz, 1H), 3.82 (s, 3H), 3.56 (d, *J* = 7.3 Hz, 2H), 1.77 (dd, *J* = 2.8, 1.4 Hz, 6H). **^{13}C NMR** (126 MHz, $CDCl_3$) δ 157.5, 136.3, 132.6, 131.7, 129.6, 128.5, 128.4, 123.6, 123.3, 123.0, 116.6, 115.5, 93.1, 88.5, 55.5, 32.3, 25.9, 18.1. **HRMS** (ESI+) calculated for $[C_{20}H_{21}O]^+$ 277.1587 *m/z*; found $[M + H]^+$ 277.1573 *m/z*.

Synthetic procedures and analytical data for the preparation of enynes with substituents on the terminal aryl (17f-g)

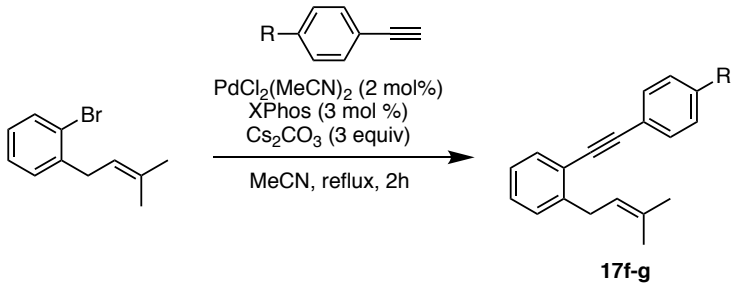

17f-g

General procedure C: Sonogashira coupling

A mixture of 1-bromo-2-(3-methylbut-2-en-1-yl)benzene[56] (1.0 equiv), $PdCl_2(MeCN)_2$ (2 mol %,), XPhos (3 mol %) and Cs_2CO_3 (3.0 equiv), in anhydrous MeCN (1 mL) was stirred under a nitrogen atmosphere at 24 ºC for 25 min.[57] Then, alkyne (1.5 equiv) was added and the mixture was stirred at 85 ºC for the indicated time. The reaction was quenched by addition of water and EtOAc and the aqueous phase was extracted with EtOAc (3x). The combined organic phases were dried over anhydrous Na_2SO_4, filtered and concentrated. The crude was purified by flash column chromatography to afford the corresponding 1,6-enynes.

1-((4-Chlorophenyl)ethynyl)-2-(3-methylbut-2-en-1-yl)benzene (17f)

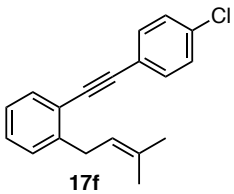

17f

17f was synthesized following general procedure **C** from 1-chloro-4-ethynylbenzene (91 mg, 0.666 mmol) whereby the reaction was stirred for 2 h. The crude was purified by flash column chromatography (cyclohexane/pentane 1:1) to afford the title compound (73 mg, 0.259 mmol, 59%) as a yellow oil.

^{1}H NMR (400 MHz, CD_2Cl_2) δ 7.52 – 7.45 (m, 3H), 7.38 – 7.33 (m, 2H), 7.32 – 7.23 (m, 2H), 7.22 – 7.16 (m, 1H), 5.40 – 5.34 (m, 1H), 3.59 (d, *J* = 7.3 Hz, 2H), 1.75 (s, 6H). **^{13}C NMR** (101 MHz, CD_2Cl_2) δ 144.5, 134.7, 133.5, 133.3, 132.7, 129.4, 129.3, 129.2, 126.4, 122.9, 122.69, 122.68, 92.5, 89.8, 33.6, 26.0, 18.3. **HRMS** (APCI+) calculated for $[C_{19}H_{18}Cl]^+$ 281.1092 *m/z*; found $[M + H]^+$ 281.1095 *m/z*.

1-((4-Methoxyphenyl)ethynyl)-2-(3-methylbut-2-en-1-yl)benzene (17g)

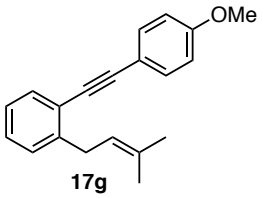

17g

17g was synthesized following general procedure **C** from 1-ethynyl-4-methoxybenzene (86 μL, 0.666 mmol, 1.5 equiv) whereby the reaction was stirred for 2 h. The crude was purified by flash column chromatography (cyclohexane/CH_2Cl_2 20:1 then 10:1) to afford the title compound (78 mg, 0.282 mmol, 64%) as a yellow oil.

56 Xu, L.; Liu, Z.; Dong, W.; Song, J.; Miao, M.; Xu, J.; Ren, H. *Org. Biomol. Chem.* **2015**, *13*, 6333–6337.

57 The procedure was adapted from a reported procedure: see ref. 40.

The spectral data were fully consistent with those previously reported.[40]

Synthetic procedures and analytical data for the preparation of enynes 17a and 17i

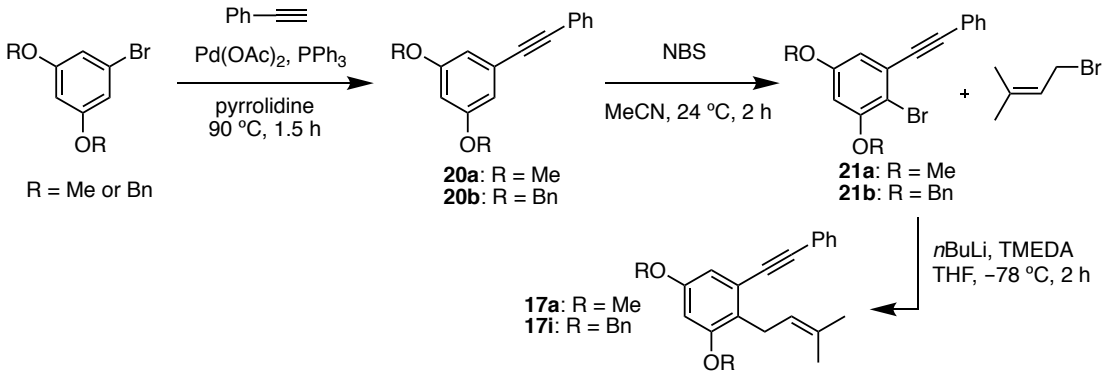

General procedure D: Sonogashira coupling

To a stirred solution of the corresponding aryl bromide (1.0 equiv) and ethynylbenzene (1.5 equiv) in pyrrolidine (0.5 M) were added PPh_3 (4 mol %) and $Pd(OAc)_2$ (2 mol %) under an argon atmosphere. After stirring at 90 ºC for the mentioned time, the mixture was quenched with sat. NH_4Cl (30 mL) and extracted with CH_2Cl_2. The organic extract was dried over Na_2SO_4 and the solvent was removed in vacuo. The crude was purified by flash column chromatography to afford the corresponding alkynes.

1,3-Dimethoxy-5-(phenylethynyl)benzene (20a)

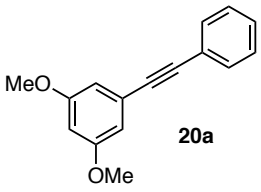

20a was synthesized following general procedure **D** from 1-bromo-3,5-dimethoxybenzene (1.0 g, 4.61 mmol) whereby the reaction was stirred for 90 min. Purification by column chromatography (pentane/Et_2O 98:2) afforded the title compound (956 mg, 4.01 mmol, 87%) as a yellow oil.

The spectral data were fully consistent with those previously reported.[58]

1,3-Dibenzyloxy-5-(phenylethynyl)benzene (20b)

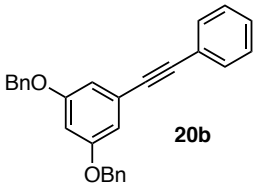

20b was synthesized following general procedure **D** from 3,5-dibenzyloxybromobenzene (6.3 g, 17.1 mmol) whereby the reaction was stirred for 90 min. Purification by column chromatography (pentane/Et_2O 98:2) followed by recrystallization from hot *n*-hexane afforded the title compound (5.21 g, 13.3 mmol, 78%) as a white crystalline solid.

M.p. = 80 – 82 ºC (pentane). **^{1}H NMR** (500 MHz, $CDCl_3$) δ 7.59 – 7.52 (m, 2H), 7.48 – 7.32 (m, 13H), 6.83 (d, J = 2.3 Hz, 2H), 6.65 (t, J = 2.3 Hz, 1H), 5.07 (s, 4H). **^{13}C NMR** (126 MHz, $CDCl_3$)

58 Truong, T., Daugulis, O. *Org. Lett.* **2011**, *13*, 4172–4175.

δ 159.9, 136.8, 131.8, 128.8, 128.5, 128.2, 127.7, 124.8, 123.2, 110.8, 103.6, 100.1, 89.5, 89.2, 70.3. **HRMS** (ESI+) calculated for $[C_{28}H_{22}NaO_2]^+$ 413.1512 *m/z*; found $[M + Na]^+$ 413.1514 *m/z*.

General procedure E: bromination reaction

Under an air atmosphere, the aryl alkyne (1.0 equiv) was dissolved in acetonitrile (0.075 M) and the solution was cooled to 0 ºC. A solution of NBS (1.05 equiv, 0.5 M in acetonitrile) was added dropwise and the reaction was stirred for the given time at the same temperature. The solvent was evaporated and the crude was purified by flash column chromatography. The yellow solid obtained was recrystallized from hot *n*-hexane to afford the corresponding bromides.

2-Bromo-1,5-dimethoxy-3-(phenylethynyl)benzene (21a)

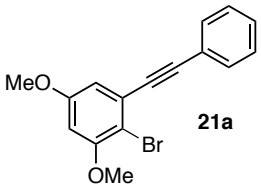

21a

21a was synthesized following general procedure **E** from 1,3-dimethoxy-5-(phenylethynyl)benzene (1.7 g, 7.13 mmol) whereby the reaction was stirred for 2 h. Purification by column chromatography (pentane/Et_2O 98:2) followed by recrystallization from hot *n*-hexane afforded the title compound (2.06 g, 6.49 mmol, 91%) as a white crystalline solid.

M.p. = 80 – 82 ºC (pentane). **^{1}H NMR** (300 MHz, $CDCl_3$) δ 7.63 – 7.55 (m, 2H), 7.39 – 7.32 (m, 3H), 6.73 (d, *J* = 2.7 Hz, 1H), 6.48 (d, *J* = 2.7 Hz, 1H), 3.89 (s, 3H), 3.83 (s, 3H). **^{13}C NMR** (75 MHz, $CDCl_3$) δ 159.5, 157.1, 131.9, 128.8, 128.5, 126.7, 123.0, 108.8, 106.7, 100.8, 93.9, 88.5, 56.5, 55.8. **HRMS** (ESI+) calculated for $[C_{16}H_{14}BrO_2]^+$ 317.0172 *m/z*; found $[M + H]^+$ 317.0172 *m/z*.

2-Bromo-1,5-dibenzyloxy-3-(phenylethynyl)benzene (21b)

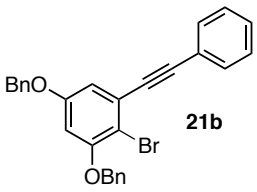

21b

21b was synthesized following general procedure **E** from 1,3-dibenzyloxy-5-(phenylethynyl)benzene (3.5 g, 8.96 mmol) whereby the reaction was stirred for 2 h. Purification by column chromatography (pentane/Et_2O 98:2) followed by recrystallization from hot *n*-hexane afforded the title compound (3.49 g, 7.44 mmol, 83%) as a white crystalline solid.

M.p. = 101 – 103 ºC (pentane). **^{1}H NMR** (500 MHz, $CDCl_3$) δ 7.63 – 7.59 (m, 2H), 7.49 – 7.46 (m, 2H), 7.44 – 7.31 (m, 11H), 6.85 (d, *J* = 2.7 Hz, 1H), 6.61 (d, *J* = 2.7 Hz, 1H), 5.13 (s, 2H), 5.03 (s, 2H). **^{13}C NMR** (126 MHz, $CDCl_3$) δ 158.5, 156.2, 136.4, 136.3, 131.9, 128.81, 128.75, 128.5, 128.4, 128.1, 127.7, 127.2, 126.8, 123.0, 110.4, 107.8, 103.1, 94.0, 88.5, 71.1, 70.6. **HRMS** (ESI+) calculated for $[C_{28}H_{21}BrNaO_2]^+$ 491.0617 *m/z*; found $[M + Na]^+$ 491.0619 *m/z*.

General procedure F: prenylation reaction

A flask was charged with the aryl bromide (1.0 equiv). Three cycles vacuum argon were applied and anhydrous THF (0.05 M) was added. The solution was cooled to –78 °C and *n*BuLi (1.1 equiv) was added dropwise and the reaction mixture was stirred for 3 minutes. TMEDA (1.1

equiv) was then added and stirring was continued for 3 minutes. Finally, 1-bromo-3-methylbut-2-ene (1.25 equiv) was added dropwise and the resulting mixture was stirred for the given time while being allowed to slowly warm to 24 ºC. The suspension was carefully quenched by addition of sat. NH_4Cl and extracted with Et_2O (2x 50 mL). The combined organic phases were washed with brine, dried over Na_2SO_4 and concentrated. The crude was purified by flash column chromatography to afford the corresponding 1,6-enynes.

1,5-Dimethoxy-2-(3-methylbut-2-en-1-yl)-3-(phenylethynyl)benzene (17a)

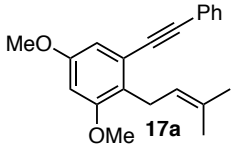

17a

1,6-Enyne **17a** was synthesized following general procedure **F** from 2-bromo-1,5-dimethoxy-3-(phenylethynyl)benzene (7.6 g, 23.9 mmol) whereby the reaction was stirred for 2 h. The crude was purified by flash column chromatography (cyclohexane/CH_2Cl_2, 9:1) and further purified by a second flash column chromatography (pentane/Et_2O 98:2) to afford compound **19** (4.76 g, 15.5 mmol, 65%) as a yellow oil.

^{1}H NMR (400 MHz, $CDCl_3$) δ 7.56 – 7.51 (m, 2H), 7.38 – 7.32 (m, 3H), 6.65 (d, *J* = 2.5 Hz, 1H), 6.46 (d, *J* = 2.5 Hz, 1H), 5.30 – 5.23 (m, 1H), 3.81 (d, *J* = 2.0 Hz, 6H), 3.55 (d, *J* = 7.1 Hz, 2H), 1.80 (d, *J* = 0.7 Hz, 3H), 1.68 (d, *J* = 1.1 Hz, 3H); **^{13}C NMR** (101 MHz, $CDCl_3$) δ 158.49, 158.48, 131.7, 131.4, 128.5, 128.3, 125.8, 123.7, 123.0, 107.5, 100.2, 92.4, 88.9, 55.8, 55.6, 27.3, 26.0, 18.2. **HRMS** (ESI+) calculated for $[C_{21}H_{23}O_2]^+$ 307.1693 *m/z*; found $[M + H]^+$ 307.1680 *m/z*.

1,5-Dibenzyloxy-2-(3-methylbut-2-en-1-yl)-3-(phenylethynyl)benzene (17i)

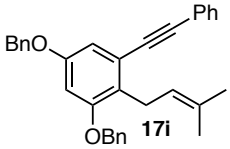

17i

1,6-Enyne **17i** was synthesized following general procedure **F** from 2-bromo-1,5-dibenzyloxy-3-(phenylethynyl)benzene (3.4 g, 7.2 mmol) whereby the reaction was stirred for 2 h. The crude was purified by flash column chromatography (cyclohexane/CH_2Cl_2, 9:1) and further purified by recrystallization from hot *n*hexane to afford title compound **41** (2.43 g, 5.29 mmol, 73%) as a white crystalline solid.

M.p. = 79 – 80 ºC (pentane). **^{1}H NMR** (400 MHz, $CDCl_3$) δ 7.57 – 7.52 (m, 2H), 7.46 – 7.31 (m, 13H), 6.79 (d, *J* = 2.4 Hz, 1H), 6.61 (d, *J* = 2.4 Hz, 1H), 5.36 – 5.29 (m, 1H), 5.05 (d, *J* = 6.9 Hz, 4H), 3.62 (d, *J* = 7.1 Hz, 2H), 1.71 (d, *J* = 0.5 Hz, 3H), 1.68 (d, *J* = 0.9 Hz, 3H). **^{13}C NMR** (101 MHz, $CDCl_3$) δ 157.6, 157.5, 137.1, 137.0, 131.7, 131.4, 128.8, 128.6, 128.5, 128.4, 128.2, 128.0, 127.7, 127.4, 126.3, 123.9, 123.6, 123.0, 108.9, 102.0, 92.6, 88.9, 70.4, 70.3, 27.5, 26.0, 18.2. **HRMS** (ESI+) calculated for $[C_{33}H_{30}NaO_2]^+$ 481.2138 *m/z*; found $[M + Na]^+$ 481.2152 *m/z*.

Synthetic procedures and analytical data for the preparation of 1-(cyclohex-1-en-1-ylethynyl)-2-(3-methylbut-2-en-1-yl)benzene (17h)

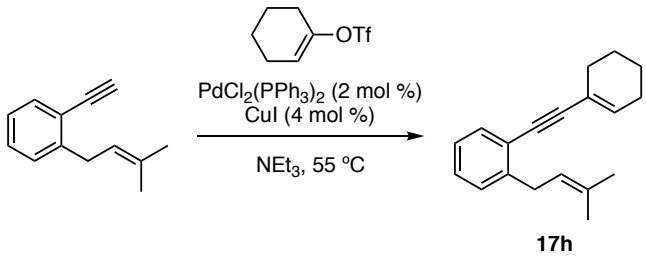

17h

To a solution of cyclohex-1-en-1-yl trifluoromethanesulfonate (125 mg, 0.543 mmol, 1.0 equiv) and 1-ethynyl-2-(3-methylbut-2-en-1-yl)benzene[59] (138 mg, 0.81 mmol, 1.49 equiv) in NEt_3 (2.17 mL) were added [$PdCl_2(PPh_3)_2$] (7.62 mg, 10.9 µmol, 2.0 mol %) and copper(I) iodide (4.14 mg, 0.022 mmol, 4.0 mol %).[60] The resulting mixture was heated under N_2 atmosphere at 55 ºC and the reaction was monitored by TLC. When the reaction was complete, the mixture was allowed to cool to 24 ºC, and the ammonium salt was removed by filtration. The solvent was removed under reduced pressure and the residue was purified by column chromatography (cyclohexane) to afford the title compound (125 mg, 0.499 mmol, 92%) as a yellow liquid.
The spectral data were fully consistent with those previously reported.[40]

Synthetic procedures and analytical data for the products from the scope of the enantioselective gold(I)-catalyzed 6-*endo-dig* cyclization (18a-m)

General procedure G: protocol 1 for the enantioselective 6-endo-dig cyclization

1,6-Enyne (1.0 equiv) and H_2O (5.0 equiv) were dissolved in α,α,α-trifluorotoluene (0.2M). This solution was added to a vial containing gold catalyst (*R*,*R*)-**J** (1 mol %) and $AgSbF_6$ (1 mol %) and the reaction was stirred for 24 h at 25 ºC. The reaction was quenched by addition of 1 drop of NEt_3 and concentrated. The crude was purified by flash column chromatography.

General procedure H: protocol 2 for the enantioselective 6-endo-dig cyclization

1,6-Enyne (1.0 equiv) and the corresponding nucleophile (2.5 equiv) were dissolved in α,α,α-trifluorotoluene (0.05M). This solution was added to a vial containing gold catalyst (*R*,*R*)-**J** (2 mol %) and $AgSbF_6$ (2 mol %) and the reaction was stirred for 24 h at 25 ºC. The reaction was quenched by addition of 1 drop of NEt_3 and concentrated. The crude was purified by flash column chromatography.

59 Wagh, S. B.; Hsu, Y.-C.; Liu, R.-S. *ACS Catal.* **2016**, *6*, 7160–7166.

60 The procedure was adapted from a reported procedure: Yao, T.; Larock, R. C. *J. Org. Chem.* **2003**, *68,* 5936–5942.

As a curiosity, all products featured a highly UV-active *trans*-stilbene moiety that facilitated the reaction monitoring by TLC. Conveniently, when the purifying column was irradiated with the UV lamp, the progression of the product could be easily followed, rendering the isolation as a straightforward process.

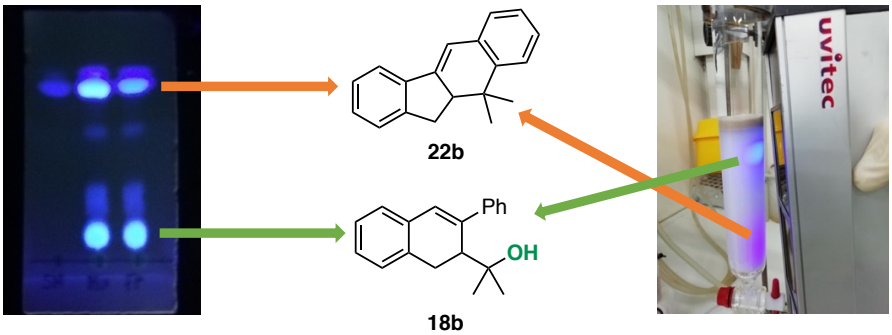

UV-active stilbene derivatives **22b** and **18b** on TLC and column chromatography.

(*S*)-2-(6,8-Dimethoxy-3-phenyl-1,2-dihydronaphthalen-2-yl)propan-2-ol (18a)

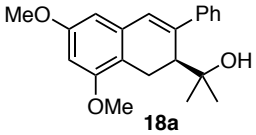

18a

Compound **18a** was synthesized following general procedure **G** from **17a** (205 mg, 0.67 mmol). The crude was purified by flash column chromatography (pentane/CH_2Cl_2 2:1, then pentane/Et_2O 1:1) to afford **18a** (130 mg, 0.40 mmol, 60%) as a white solid in 99:1 *er* (55%, >99:1 *er* after recrystallization). **M.p.** = 102 – 104 ºC (pentane). **^{1}H NMR** (400 MHz, $CDCl_3$) δ 7.57 – 7.52 (m, 2H), 7.41 – 7.35 (m, 2H), 7.31 – 7.25 (m, 1H), 6.79 (s, 1H), 6.37 (q, *J* = 2.4 Hz, 2H), 3.84 (s, 3H), 3.82 (s, 3H), 3.57 (d, *J* = 16.9 Hz, 1H), 3.13 (dd, *J* = 8.3, 1.2 Hz, 1H), 2.77 (dd, *J* = 17.0, 8.2 Hz, 1H), 1.02 (s, 3H), 0.92 (s, 3H). **^{13}C NMR** (101 MHz, $CDCl_3$) δ 159.1, 156.9, 143.3, 141.0, 136.0, 128.8, 128.0, 127.4, 126.7, 115.1, 103.4, 98.1, 75.3, 55.7, 55.5, 45.3, 28.8, 27.9, 22.8. **HRMS** (ESI+) calculated for $[C_{21}H_{24}NaO_3]^+$ 347.1618 *m/z*; found $[M + Na]^+$ 347.1626 *m/z*. α_D^{589} = –253.8 deg.cm^2.g^{-1} ($CHCl_3$, c 1.00, 299 K). **HPLC** Chiralpak IA (250 mm × 4.6 mm, 5 μm) at 25 ºC, flow 1.0 mL/min, isocratic hexane/*i*PrOH 90:10, 280 nm, t_R (major) 8.5; t_R (minor) 15.3.

(*S*)-2-(3-Phenyl-1,2-dihydronaphthalen-2-yl)propan-2-ol (18b)

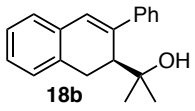

18b

Compound **18b** was synthesized following general procedure **G** from **17b** (30.0 mg, 0.12 mmol). The crude was purified by flash column chromatography (pentane/CH_2Cl_2 4:1, then pentane/Et_2O 1:1) to afford **18b** (21.9 mg, 0.083 mmol, 68%) as a white solid in 97:3 *er*.

M.p. = 138 – 140 ºC (pentane). **^{1}H NMR** (400 MHz, CD_2Cl_2) δ 7.58 – 7.50 (m, 2H), 7.43 – 7.34 (m, 2H), 7.33 – 7.25 (m, 1H), 7.21 – 7.09 (m, 4H), 6.86 (s, 1H), 3.32 – 3.19 (m, 2H), 3.11 (dd, *J* = 7.1, 2.3 Hz, 1H), 1.18 – 1.12 (m, 1H), 0.96 (s, 3H), 0.88 (s, 3H). **^{13}C NMR** (126 MHz, CD_2Cl_2) δ 143.9, 140.9, 136.0, 135.2, 129.1, 128.4, 128.1, 127.8, 127.6, 127.2, 126.9, 126.8, 75.3, 46.0, 31.3, 29.2, 28.1. **HRMS** (ESI+) calculated for $[C_{19}H_{20}NaO]^+$ 287.1406 *m/z*; found $[M + Na]^+$ 287.1394 *m/z*. α_D^{589} = –263.5 deg.cm^2.g^{-1} ($CHCl_3$, c 0.83, 299 K). **UPC^2** Chiralpak IC (150 ×

4.6mm, 3μm) at 35 ºC, flow 3 mL/min, isocratic CO_2/MeOH 95:5, ABRP pressure 1500 psi, 294 nm, t_R (major) 2.8; t_R (minor) 3.1.

(*S*)-2-(3-Phenyl-6-(trifluoromethyl)-1,2-dihydronaphthalen-2-yl)propan-2-ol (18c)

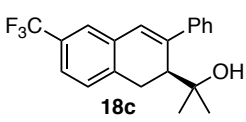

18c

Compound **18c** was synthesized following general procedure **G** from **17c** (30.0 mg, 0.095 mmol). The crude was purified by flash column chromatography (pentane/CH_2Cl_2 4:1, then pentane/Et_2O 1:1) to afford **18c** (21.9 mg, 0.066 mmol, 69%) as a colorless oil in 94:6 *er*.

^{1}H NMR (400 MHz, CD_2Cl_2) δ 7.56 – 7.52 (m, 2H), 7.44 – 7.41 (m, 4H), 7.34 – 7.27 (m, 2H), 6.87 (s, 1H), 3.40 (d, *J* = 16.7 Hz, 1H), 3.26 (ddt, *J* = 16.7, 8.2, 1.7 Hz, 1H), 3.16 (dd, *J* = 8.2, 1.2 Hz, 1H), 1.16 (br s, 1H), 0.95 (s, 3H), 0.88 (s, 3H). **^{13}C NMR** (101 MHz, CD_2Cl_2) δ 143.3, 142.8, 140.4 – 140.3 (m), 135.8, 129.2, 129.1 (q, *J* = 32.1 Hz), 128.2, 127.9, 127.22, 127.17, 125.1 (q, *J* = 272.0 Hz), 124.5 (q, *J* = 4.0 Hz), 123.1 (q, *J* = 3.8 Hz), 75.2, 45.9, 31.2, 29.4, 27.9. **^{19}F{^{1}H} NMR** (376 MHz, CD_2Cl_2) δ –62.8. **HRMS** (APCI+) calculated for $[C_{20}H_{18}F_3]^+$ 315.1355 *m/z*; found $[M - OH]^+$ 315.1355 *m/z*. α_D^{589} = –182.7 deg.cm^2.g^{-1} ($CHCl_3$, c 0.98, 299 K). **HPLC** Chiralpak OJ-H (250 mm × 4.6 mm, 5 μm) at 25 ºC, flow 1.0 mL/min, isocratic hexane/*i*PrOH 90:10, 280 nm, t_R (major) 4.3; t_R (minor) 6.5.

(*S*)-2-(6-Chloro-3-phenyl-1,2-dihydronaphthalen-2-yl)propan-2-ol (18d)

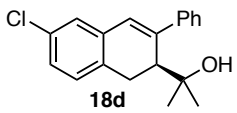

18d

Compound **18d** was synthesized following general procedure **G** from **17d** (50 mg, 0.178 mmol). The crude was purified by flash column chromatography (pentane/CH_2Cl_2 2:1, then pentane/Et_2O 1:1) to afford **18d** (23 mg, 0.077 mmol, 43%) as a white solid in 95:5 *er*.

M.p. = 105 – 108 ºC (pentane). **^{1}H NMR** (400 MHz, $CDCl_3$) δ 7.55 – 7.47 (m, 2H), 7.43 – 7.35 (m, 2H), 7.33 – 7.27 (m, 1H), 7.14 – 7.05 (m, 3H), 6.77 (s, 1H), 3.28 (d, *J* = 15.9 Hz, 1H), 3.25 – 3.09 (m, 2H), 1.00 (s, 3H), 0.90 (s, 3H). **^{13}C NMR** (101 MHz, $CDCl_3$) δ 142.8, 141.9, 136.2, 133.7, 132.0, 128.9, 128.3, 127.8, 127.4, 126.9, 126.8, 126.1, 75.1, 45.7, 30.3, 29.2, 27.7. **HRMS** (ESI+) calculated for $[C_{19}H_{19}ClNaO]^+$ 321.1017 *m/z*; found $[M + Na]^+$ found 321.1011 *m/z*. α_D^{589} = –170.4 deg.cm^2.g^{-1} ($CHCl_3$, c 0.61, 299 K). **HPLC** Chiralpak IA (250 mm × 4.6 mm, 5 μm) at 25 ºC, flow 1.0 mL/min, isocratic hexane/*i*PrOH 90:10, 280 nm, t_R (major) 6.3; t_R (minor) 21.1.

(*S*)-2-(6-Methoxy-3-phenyl-1,2-dihydronaphthalen-2-yl)propan-2-ol (18e)

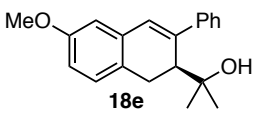

18e

Compound **18e** was synthesized following general procedure **G** from **17e** (50.0 mg g, 0.181 mmol). The crude was purified by flash column chromatography (pentane/CH_2Cl_2 2:1, then pentane/Et_2O 1:1) to afford **18e** (32.1 mg, 0.109 mmol, 60%) as a white solid in 97:3 *er*.

M.p. = 103 – 106 ºC (pentane). **^{1}H NMR** (500 MHz, $CDCl_3$) δ 7.56 – 7.52 (m, 2H), 7.41 – 7.36 (m, 2H), 7.31 – 7.27 (m, 1H), 7.07 (ddd, *J* = 8.0, 1.3, 0.7 Hz, 1H), 6.82 (s, 1H), 6.73 – 6.69 (m, 2H), 3.81 (s, 3H), 3.26 – 3.15 (m, 2H), 3.11 (dd, *J* = 7.3, 1.8 Hz, 1H), 1.01 (s, 3H), 0.92 (s, 3H). **^{13}C NMR** (126 MHz, $CDCl_3$) δ 158.5, 143.2, 140.9, 135.6, 128.8, 128.1, 127.8, 127.5, 127.3, 126.8, 112.7, 112.2, 75.2, 55.4, 45.9, 30.1, 29.1, 27.8. **HRMS** (ESI+) calculated for $[C_{20}H_{22}NaO_2]^+$ 317.1512 *m/z*; found $[M + Na]^+$ found 317.1500 *m/z*. α_D^{589} = –173.0 deg.cm^2.g^{-1} ($CHCl_3$, c 1.03, 299 K). **UPC^2** Chiralpak IA (150 × 4.6mm, 3μm) at 35 ºC, flow 3 mL/min, isocratic CO_2/*i*PrOH 75:25, ABRP pressure 1500 psi, 242 nm, t_R (major) 1.3; t_R (minor) 2.8.

(*S*)-3-(4-Chlorophenyl)-2-(2-methoxypropan-2-yl)-1,2-dihydronaphthalene (18f)

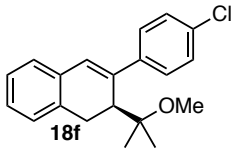

Compound **18f** was synthesized following general procedure **H** from **17f** (120.0 mg, 0.427 mmol). The crude was purified by preparative TLC (pentane/diethyl ether 95:5) to afford **30** (67.0 mg, 0.214 mmol, 50%) as a white solid in 96:4 *er*.

M.p. = 116 – 118 ºC (pentane). **^{1}H NMR** (500 MHz, CD_2Cl_2) δ 7.48 – 7.43 (m, 2H), 7.37 – 7.33 (m, 2H), 7.16 – 7.09 (m, 4H), 6.77 (s, 1H), 3.32 (d, *J* = 16.1 Hz, 1H), 3.19 (d, *J* = 8.6 Hz, 1H), 3.12 (dd, *J* = 16.1, 8.4 Hz, 1H), 3.07 (s, 3H), 0.82 (s, 3H), 0.68 (s, 3H). **^{13}C NMR** (126 MHz, CD_2Cl_2) δ 143.0, 139.9, 136.4, 134.9, 133.0, 129.2, 129.0, 128.6, 128.2, 127.6, 126.8, 126.7, 79.2, 49.1, 42.4, 30.1, 25.02, 22.7. **HRMS** (APCI+) calculated for $[C_{19}H_{18}Cl]^+$ 281.1092 *m/z*; found $[M – CH_3O]^+$ 281.1095 *m/z*. α_D^{589} = –205.0 deg.cm^2.g^{-1} ($CHCl_3$, c 0.50, 299 K). **HPLC** Chiralpak OJ-H (250 mm × 4.6 mm, 5 μm) at 25 ºC, flow 1.0 mL/min, isocratic hexane/*i*PrOH 90:10, 280 nm, t_R (major) 5.5; t_R (minor) 16.6.

(*S*)-3-(4-Methoxyphenyl)-2-(2-methoxypropan-2-yl)-1,2-dihydronaphthalene (18g)

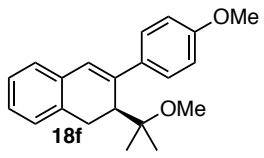

Compound **18g** was synthesized following general procedure **H** from **17g** (51.0 mg, 0.165 mmol). The crude was purified by preparative TLC (pentane/diethyl ether 95:5) to afford **18g** (29.5 mg, 0.096 mmol, 52%) as a white solid in 96:4 *er*.

M.p. = 104 – 106 ºC (pentane). α_D^{589} = –221.7 deg.cm^2.g^{-1} ($CHCl_3$, c 1.19, 299 K). **HPLC** Chiralpak IA (250 × 4.6mm, 5μm), flow 1.0 mL/min, isocratic hexane/*i*PrOH 98:2, 280 nm, t_R (major) 5.9 ; t_R (minor) 7.3. The spectral data of **31** were fully consistent with those previously reported.[40]

(*S*)-2-(2-(Allyloxy)propan-2-yl)-3-phenyl-1,2-dihydronaphthalene (18h)

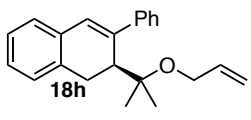

Compound **18h** was synthesized following general procedure **H** from **17b** (30.0 mg, 0.12 mmol). The crude was purified by flash column chromatography (pentane/CH_2Cl_2 4:1, then pentane/Et_2O 9:1) to afford **18h** (23.4 mg, 0.077 mmol, 63%) as a light-yellow solid in 95:5 *er*.

M.p. = 78 – 80 ºC (pentane). **^{1}H NMR** (400 MHz, CD_2Cl_2) δ 7.56 – 7.50 (m, 2H), 7.42 – 7.35 (m, 2H), 7.32 – 7.26 (m, 1H), 7.19 – 7.10 (m, 4H), 6.80 (s, 1H), 5.77 (ddt, *J* = 17.2, 10.4, 5.2 Hz, 1H), 5.16 (dq, *J* = 17.2, 1.8 Hz, 1H), 5.04 (dq, *J* = 10.4, 1.6 Hz, 1H), 3.87 (ddt, *J* = 12.5, 5.3, 1.6 Hz, 1H), 3.80 (ddt, *J* = 12.4, 5.1, 1.6 Hz, 1H), 3.40 (d, *J* = 16.4 Hz, 1H), 3.30 (d, *J* = 8.4 Hz, 1H), 3.17 (dd, *J* = 16.3, 8.4 Hz, 1H), 0.89 (s, 3H), 0.75 (s, 3H). **^{13}C NMR** (126 MHz, CD_2Cl_2) δ 144.4, 141.2, 136.8, 136.4, 135.3, 129.0, 128.91, 128.87, 128.0, 127.6, 127.5, 127.2, 126.7, 115.3, 79.6, 62.8, 42.9, 30.4, 25.7, 23.2. **HRMS** (ESI+) calculated for $[C_{22}H_{24}NaO]^+$ 327.1719 *m/z*; found $[M + Na]^+$ 327.1712 *m/z*. α_D^{589} = –181.4 deg.cm^2.g^{-1} ($CHCl_3$, c 0.66, 299 K). **UPC^2** Chiralpak IC (150 × 4.6mm, 3μm) at 35 ºC, flow 3 mL/min, isocratic CO_2/MeOH 95:5, ABRP pressure 1500 psi, 293 nm, t_R (major) 1.1; t_R (minor) 1.3.

(*S*)-2-(2-(Benzyloxy)propan-2-yl)-3-phenyl-1,2-dihydronaphthalene (18i)

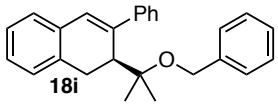

Compound **18i** was synthesized following general procedure **H** from **17b** (30.0 mg, 0.12 mmol). The crude was purified by flash column chromatography (pentane/CH_2Cl_2 4:1, then pentane/Et_2O 9:1) to afford **18i** (32.4 mg, 0.091 mmol, 75%) as a white solid in 95:5 *er*.

M.p. = 79 – 81 ºC (pentane). **^{1}H NMR** (400 MHz, CD_2Cl_2) δ 7.57 – 7.52 (m, 2H), 7.41 – 7.34 (m, 2H), 7.31 – 7.20 (m, 4H), 7.19 – 7.11 (m, 6H), 6.82 (s, 1H), 4.39 (d, *J* = 11.2 Hz, 1H), 4.31 (d, *J* = 11.2 Hz, 1H), 3.45 (d, *J* = 16.5 Hz, 1H), 3.36 (d, *J* = 8.4 Hz, 1H), 3.19 (dd, *J* = 16.3, 8.2 Hz, 1H), 0.95 (s, 3H), 0.84 (s, 3H). **^{13}C NMR** (126 MHz, CD_2Cl_2) δ 144.4, 141.1, 140.4, 136.5, 135.3, 129.0, 128.9, 128.6, 128.0, 127.8, 127.6, 127.50, 127.47, 127.3, 126.7, 79.9, 63.8, 43.3, 30.5, 25.6, 23.2. **HRMS** (ESI+) calculated for $[C_{26}H_{26}NaO]^+$ 377.1876 *m/z*; found $[M + Na]^+$ 377.1869 *m/z*. α_D^{589} = –137.1 deg.cm^2.g^{-1} ($CHCl_3$, c 1.19, 299 K). **UPC^2** Chiralpak IC (150 × 4.6mm, 3μm) at 35 ºC, flow 3 mL/min, isocratic CO_2/MeOH 90:10, ABRP pressure 1500 psi, 293 nm, t_R (major) 1.4; t_R (minor) 1.7.

(*S*)-2-(3-Phenyl-1,2-dihydronaphthalen-2-yl)propan-2-yl acetate (18j)

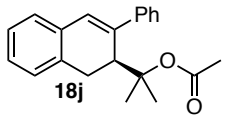

Compound **18j** was synthesized following general procedure **H** from **17b** (30.0 mg, 0.12 mmol). The crude was purified by flash column chromatography (pentane/CH_2Cl_2 4:1, then pentane/Et_2O 2:1) to afford **18j** (15.3 mg, 0.050 mmol, 41%) as a white solid in 90:10 *er*.

M.p. = 93 – 96 ºC (pentane). **^{1}H NMR** (400 MHz, CD_2Cl_2) δ 7.51 – 7.46 (m, 2H), 7.41 – 7.35 (m, 2H), 7.30 – 7.24 (m, 1H), 7.18 – 7.11 (m, 4H), 6.82 (s, 1H), 3.88 (dd, *J* = 8.4, 1.3 Hz, 1H), 3.27 (dd, *J* = 16.7, 8.4 Hz, 1H), 3.11 (dd, *J* = 16.7, 1.2 Hz, 1H), 1.39 (s, 3H), 1.34 (s, 3H), 1.00 (s, 3H). **^{13}C NMR** (126 MHz, CD_2Cl_2) δ 170.8, 143.9, 140.8, 135.5, 135.2, 129.1, 128.9, 128.1, 127.5, 127.4, 127.0, 126.7, 86.0, 41.8, 31.1, 25.2, 25.0, 22.2. **HRMS** (ESI+) calculated for $[C_{21}H_{22}NaO_2]^+$ 329.1512 *m/z*; found $[M + Na]^+$ 329.1514 *m/z*. α_D^{589} = –196.4 deg.cm^2.g^{-1} ($CHCl_3$,

c 0.46, 299 K). **UPC²** Chiralpak IC (150 × 4.6mm, 3μm) at 35 ºC, flow 3 mL/min, isocratic CO_2/MeOH 95:5, ABRP pressure 1500 psi, 290 nm, t_R (major) 1.7; t_R (minor) 1.8.

(*S*)-2-(2-Fluoropropan-2-yl)-3-phenyl-1,2-dihydronaphthalene (18k)

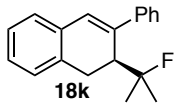

18k

Compound **18k** was synthesized following general procedure **H** from **17b** (20.0 mg, 0.08 mmol) and 5 equiv of HF·pyridine complex. The reaction was carried out in an Eppendorf vial using 3 mol % of gold catalyst and silver salt each. The crude was purified by flash column chromatography (pentane) to afford **18k** (8.44 mg, 0.032 mmol, 40%) as a white solid in 96:4 *er*.

M.p. = 72 – 75 ºC (pentane). **^{1}H NMR** (400 MHz, CD_2Cl_2) δ 7.56 – 7.51 (m, 2H), 7.42 – 7.35 (m, 2H), 7.32 – 7.26 (m, 1H), 7.21 – 7.11 (m, 4H), 6.87 (s, 1H), 3.38 – 3.29 (m, 1H), 3.28 – 3.23 (m, 2H), 1.13 (d, *J* = 21.9 Hz, 3H), 0.94 (d, *J* = 22.9 Hz, 3H). **^{13}C NMR** (126 MHz, CD_2Cl_2) δ 143.3, 139.6 (d, *J* = 6.2 Hz), 135.4, 135.0, 129.0, 128.6, 128.2, 127.8, 127.6, 127.2, 127.0, 126.9, 99.0 (d, *J* = 170.8 Hz), 44.4 (d, *J* = 22.7 Hz), 30.7 (d, *J* = 6.6 Hz), 27.0 (d, *J* = 24.0 Hz), 24.9 (d, *J* = 24.6 Hz). **^{19}F{^{1}H} NMR** (376 MHz, CD_2Cl_2) δ –132.9. **HRMS** (ESI+) calculated for $[C_{19}H_{19}FNa]^+$ 289.1363 *m/z*; found $[M + Na]^+$ 289.1360 *m/z*. α_D^{589} = –164.5 deg.cm^2.g^{-1} ($CHCl_3$, c 0.165, 299 K). **UPC²** Chiralpak IG (150 × 4.6mm, 3μm) at 35 ºC, flow 2 mL/min, isocratic CO_2/MeOH 85:15, ABRP pressure 2000 psi, 292 nm, t_R (major) 1.9; t_R (minor) 4.6.

(*S*)-2-(3-(Cyclohex-1-en-1-yl)-1,2-dihydronaphthalen-2-yl)propan-2-ol (18l)

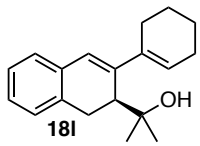

18l

Compound **18l** was synthesized following general procedure **G** from **17h** (40.0 mg, 0.160 mmol). After 48 h, the crude was purified by preparative TLC (pentane) to afford **18l** (29.0 mg, 0.108 mmol, 68%) as a white solid in 95:5 *er*.

M.p. = 68 – 72 ºC (pentane). α_D^{589} = –157.1 deg.cm^2.g^{-1} ($CHCl_3$, c 0.37, 299 K). **HPLC** Chiralpak IA (250 × 4.6mm, 5μm), flow 1.0 mL/min, isocratic hexane/*i*PrOH 90:10, 280 nm, t_R (major) 4.6; t_R (minor) 7.3. The spectral data of **18l** were fully consistent with those previously reported.[40]

(*S*)-2-(6,8-Bis(benzyloxy)-3-phenyl-1,2-dihydronaphthalen-2-yl)propan-2-ol (18m)

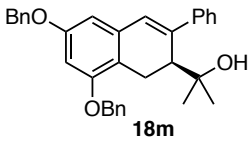

18m

Compound **18m** was synthesized following general procedure **G** from **17i** (1.2 g, 2.62 mmol). The crude was purified by flash column chromatography (pentane/CH_2Cl_2 2:1, then pentane/Et_2O 1:1) to afford **18m** (484 mg, 1.78 mmol, 68%) as a white solid in 98:2 *er* (60%, >99:1 *er* after recrystallization).

M.p. = 112 – 113 ºC (pentane). **^{1}H NMR** (500 MHz, $CDCl_3$) δ 7.55 (d, *J* = 7.6 Hz, 2H), 7.48 – 7.27 (m, 13H), 6.80 (s, 1H), 6.53 (d, *J* = 2.3 Hz, 1H), 6.48 (d, *J* = 2.3 Hz, 1H), 5.09 (s, 2H), 5.05 (s, 2H), 3.67 (d, *J* = 17.0 Hz, 1H), 3.15 (d, *J* = 8.1 Hz, 1H), 2.83 (dd, *J* = 17.0, 8.2 Hz, 1H), 1.21 (s, 1H), 1.03 (s, 3H), 0.93 (s, 3H). **^{13}C NMR** (126 MHz, $CDCl_3$) δ 158.3, 156.0, 143.2, 141.2, 137.5, 137.2, 136.3, 128.8, 128.73, 128.71, 128.1, 128.0, 127.7, 127.5, 127.4, 126.7, 116.0, 105.1,

100.5, 100.1, 75.3, 70.40, 70.38, 45.3, 28.7, 28.0, 23.1. **HRMS** (ESI+) calculated for $[C_{33}H_{32}NaO_3]^+$ 499.2244 *m/z*; found $[M + Na]^+$ found 499.2265 *m/z*. α_D^{589} = –174.5 deg.cm^2.g^{-1} ($CHCl_3$, c 1.00, 299 K). **HPLC** Chiralpak IA (250 mm × 4.6 mm, 5 μm) at 25 ºC, flow 1.0 mL/min, isocratic hexane/*i*PrOH 90:10, 280 nm, t_R (major) 12.3; t_R (minor) 33.0.

Synthetic procedures and analytical data for the products 19a and 26

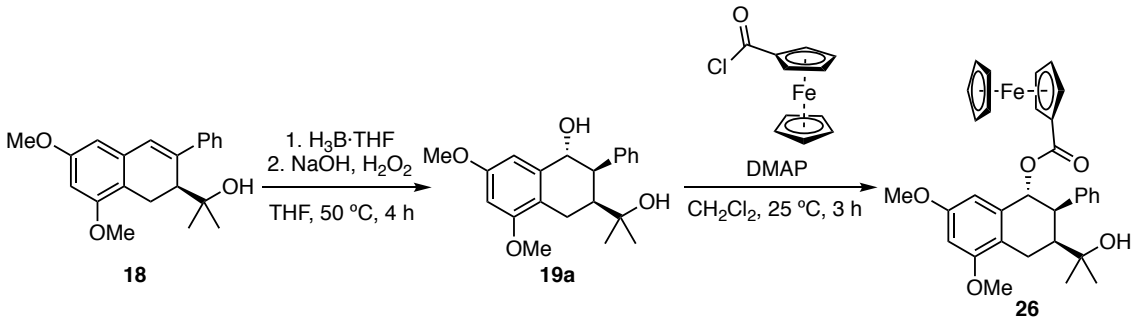

(1*R*,2*R*,3*S*)-3-(2-Hydroxypropan-2-yl)-5,7-dimethoxy-2-phenyl-1,2,3,4-tetrahydro-naphthalen-1-ol (19a)

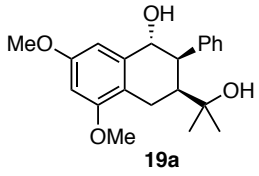

To a solution of **18a** (1.00 g, 3.08 mmol, 1.0 equiv) in dry THF (65 mL), BH_3·THF complex (12.3 mL, 12.3 mmol, 4 equiv, 1M in THF) was added dropwise at 23 ºC. The reaction mixture was warmed to 65 ºC and stirred for 4 h. After consumption of starting material, the reaction was cool down to 0 ºC, NaOH (5 mL; 10%) was added dropwise followed by H_2O_2 solution (5 mL, 50%). The mixture was stirred for 2 h at 23 ºC. The reaction was treated with water and extracted with EtOAc. The combined organic phases were washed with sat. $Na_2S_2O_3$, water, brine and dried over $MgSO_4$. The crude was purified by flash column chromatography (Et_2O) to afford title compound **19a** (708 mg, 2.06 mmol, 67%) as a white solid.

M.p. = 85 – 87 ºC (pentane). **^{1}H NMR** (500 MHz, $CDCl_3$) δ 7.20 – 7.14 (m, 3H), 7.04 – 6.99 (m, 2H), 6.46 (d, *J* = 6.4, 2.4 Hz, 1H), 6.45 (d, *J* = 6.4, 2.4 Hz, 1H) 4.58 (d, *J* = 0.8 Hz, 1H), 3.85 (s, 3H), 3.79 (s, 3H), 3.61 – 3.58 (m, 1H), 3.03 (dd, *J* = 17.8, 5.3 Hz, 1H), 2.59 (dd, *J* = 17.8, 12.8 Hz, 1H), 2.43 (ddd, *J* = 12.8, 5.3, 3.7 Hz, 1H), 2.15 (br s, 1H), 1.23 (s, 3H), 1.18 (s, 3H), 1.15 (br s, 1H). **^{13}C NMR** (126 MHz, $CDCl_3$) δ 159.2, 158.3, 140.3, 138.2, 129.7, 128.8, 127.1, 119.4, 105.2, 98.5, 74.3, 73.3, 55.52, 55.48, 47.6, 42.5, 29.1, 28.2, 20.5. **HRMS** (ESI+) calculated for $[C_{21}H_{26}NaO_4]^+$ 365.1723 *m/z*; found $[M + Na]^+$ = 365.1730 *m/z*. α_D^{589} = –49.8 deg.cm^2.g^{-1} ($CHCl_3$, c 1.00, 299 K).

(1*R*,2*R*,3*S*)-3-(2-Hydroxypropan-2-yl)-5,7-dimethoxy-2-phenyl-1,2,3,4-tetrahydro-naphthalen-1-yl ferrocenoate (26)

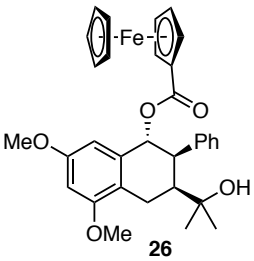

26

Compound **19a** (20 mg, 0.058 mmol, 1.0 equiv) and DMAP (8.56 mg, 0.070 mmol, 1.2 equiv) were weighted into a small vial and a solution of freshly prepared ferrocenoyl chloride[44] (21.77 mg, 0.088 mmol, 1.5 equiv) in CH_2Cl_2 (1 mL) was added dropwise. The resulting deep red solution was stirred at 25 ºC for 3 h. The reaction mixture was quenched by adding a small amount of silica gel and all volatiles were removed under reduced pressure. The crude product was purified by flash column chromatography (pentane/Et_2O 4:1) to afford **26** (23.7 mg, 0.042 mmol, 73%) as a crystalline orange solid in 96:4 *er*.

M.p. = 182 – 184 ºC (Et_2O). **^{1}H NMR** (500 MHz, $CDCl_3$) δ 7.22 – 7.18 (m, 3H), 7.10 – 7.04 (m, 2H), 6.51 (q, *J* = 2.4 Hz, 2H), 5.97 (d, *J* = 1.6 Hz, 1H), 4.81 (dq, *J* = 13.3, 1.9 Hz, 2H), 4.39 (t, *J* = 2.0 Hz, 2H), 4.18 (s, 5H), 3.89 (s, 3H), 3.76 (s, 3H), 3.67 (dd, *J* = 3.8, 1.9 Hz, 1H), 3.13 (dd, *J* = 17.9, 5.4 Hz, 1H), 2.70 (dd, *J* = 17.9, 12.8 Hz, 1H), 2.51 (ddd, *J* = 12.7, 5.4, 3.8 Hz, 1H), 1.25 (s, 3H), 1.19 (s, 3H), 1.06 (br s, 1H). **^{13}C NMR** (126 MHz, $CDCl_3$) δ 171.1, 159.0, 158.1, 139.4, 134.7, 129.9, 129.0, 127.4, 120.5, 105.7, 99.0, 74.6, 73.1, 71.5, 70.49, 70.48, 69.9, 55.53, 55.51, 45.8, 43.5, 29.3, 28.4, 20.7. **HRMS** (ESI+) calculated for $[C_{32}H_{34}NaFeO5_5]^+$ 575.1695 *m/z*; found $[M + Na]^+$ = 575.1700 *m/z*. α_D^{589} = –33,1 deg.cm^2.g^{-1} ($CHCl_3$, c 1.00, 299 K). **HPLC** Chiralpak IA (250 mm × 4.6 mm, 5 μm) at 25 ºC, flow 1.0 mL/min, isocratic hexane/*i*PrOH 90:10, 220 nm, t_R (major) 11.2; t_R (minor) 14.2.

Synthetic procedures and analytical data for the products from the synthesis of carexane I

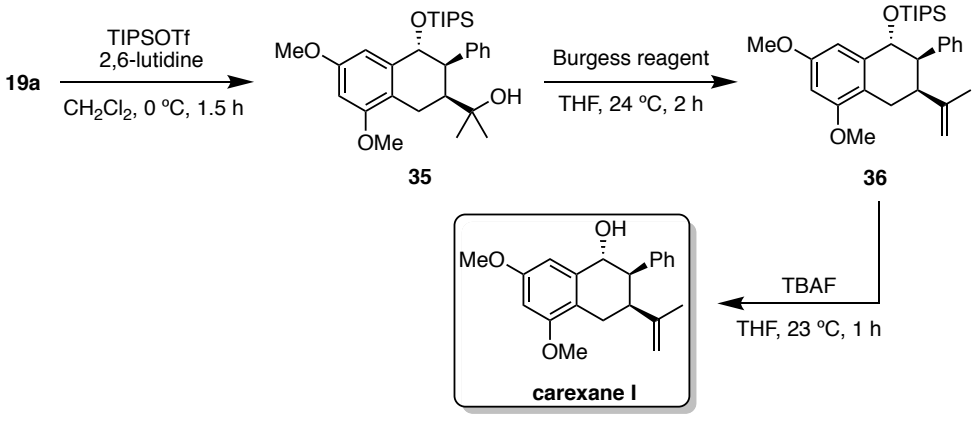

2-((2*S*,3*R*,4*R*)-6,8-Dimethoxy-3-phenyl-4-((triisopropylsilyl)oxy)-1,2,3,4-tetrahydro-naphthalen-2-yl)propan-2-ol (35)

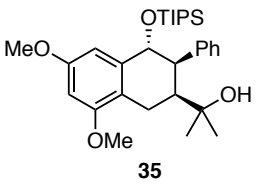

35

To a solution of **19a** (30 mg, 0.088 mmol, 1.0 equiv) in anhydrous CH_2Cl_2 (1.2 mL), 2,6-lutidine (15 µL, 0.132 mmol, 1.5 equiv) and TIPSOTf (25 µL, 0.092 mmol, 1.05 equiv) were added dropwise at 0 ºC. The resulting mixture was stirred for 1.5 h at the same temperature. Upon completion, the reaction was treated with water and extracted with CH_2Cl_2. The combined organic phases were washed with brine and dried over $MgSO_4$. The crude was purified by flash column chromatography (cyclohexane/EtOAc 9:1 to 8:2) to afford title compound **35** (38 mg, 0.077 mmol, 87%) as a white solid.

M.p. = 43 – 46 ºC (pentane). **^{1}H NMR** (500 MHz, $CDCl_3$) δ 7.18 – 7.14 (m, 3H), 6.99 – 6.94 (m, 2H), 6.44 (d, *J* = 2.4 Hz, 1H), 6.40 (d, *J* = 2.4 Hz, 1H), 4.69 (d, *J* = 2.0 Hz, 1H), 3.86 (s, 3H), 3.77 (s, 3H), 3.59 – 3.56 (m, 1H), 3.09 – 3.02 (m, 1H), 2.68 – 2.56 (m, 2H), 1.25 (s, 3H), 1.21 (s, 3H), 1.19 – 1.12 (m, 3H), 1.10 (d, *J* = 7.0 Hz, 9H), 1.07 (d, *J* = 7.0 Hz, 9H), 0.91 (br s, 1H). **^{13}C NMR** (126 MHz, $CDCl_3$) δ 158.5, 158.1, 140.4, 138.6, 129.9, 128.9, 127.0, 119.4, 105.9, 98.0, 74.9, 73.4, 55.4, 55.3, 49.1, 42.1, 29.1, 28.5, 20.7, 18.48, 18.45, 13.0. **HRMS** (ESI+) calculated for $[C_{30}H_{46}NaO_4Si]^+$ 521.3058 *m/z*; found $[M + Na]^+$ 521.3060 *m/z*. α_D^{589} = –42.0 deg.cm^2.g^{-1} ($CHCl_3$, c 1.00, 299 K).

(((1*R*,2*R*,3*S*)-5,7-Dimethoxy-2-phenyl-3-(prop-1-en-2-yl)-1,2,3,4-tetrahydronaphthalen-1-yl)oxy)triisopropylsilane (36)

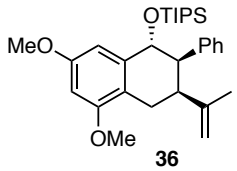

36

The reaction was carried out under argon atmosphere. To a solution of **35** (618 mg, 1.239 mmol, 1.0 equiv) in anhydrous THF (18 mL), burgess reagent (400 mg, 1.679 mmol, 1.36 equiv) was added at 23 ºC. The resulting mixture was stirred for 2 h (TLC monitoring). Then, the reaction was treated with water and extracted with EtOAc. The combined organic phases were washed with water and brine, dried over $MgSO_4$. The crude product was purified by flash column chromatography (cyclohexane/EtOAc 95:5) to afford **36** (565 mg, 1.177 mmol, 95%) as a white solid.

M.p. = 71 – 73 ºC (pentane). **^{1}H NMR** (400 MHz, $CDCl_3$) δ 7.14 – 7.08 (m, 3H), 6.82 – 6.77 (m, 2H), 6.53 (d, *J* = 2.4 Hz, 1H), 6.42 (d, *J* = 2.4 Hz, 1H), 4.96 (d, *J* = 1.7 Hz, 1H), 4.80 (s, 1H), 4.49 (s, 1H), 3.82 (s, 3H), 3.81 (s, 3H), 3.42 – 3.38 (m, 1H), 3.14 (dt, *J* = 13.3, 4.3 Hz, 1H), 2.75 (dd, *J* = 17.3, 4.6 Hz, 1H), 2.23 (dd, *J* = 17.3, 13.0 Hz, 1H), 1.82 (s, 3H), 1.22 – 1.14 (m, 3H), 1.12 (d, *J* = 6.9 Hz, 9H), 1.09 (d, *J* = 7.0 Hz, 9H). **^{13}C NMR** (101 MHz, $CDCl_3$) δ 158.6, 157.9, 146.9, 139.3, 139.2, 129.1, 127.8, 126.4, 119.4, 111.5, 105.5, 98.0, 73.6, 55.44, 55.38, 51.2, 39.1, 22.9, 22.7, 18.51, 18.47, 13.1. **HRMS** (ESI+) calculated for $[C_{30}H_{44}NaO_3Si]^+$ 503.2952 *m/z*; found $[M + Na]^+$ 503.2951 *m/z*. α_D^{589} = –9.1 deg.cm^2.g^{-1} ($CHCl_3$, c 1.00, 299 K).

Carexane I[35c]

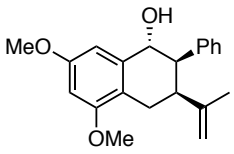

A solution of **36** (17 mg, 0.035 mmol, 1.0 equiv) in anhydrous THF (3 mL) was treated with TBAF (70 µL, 0.0699 mmol, 2.0 equiv, 1M in THF) at 0 ºC under argon. After 1.5 h, the mixture was concentrated upon addition of Florisil® and the crude was purified by flash column chromatography (cyclohexane/EtOAc 9:1 to 7:3) to afford enantiopure **carexane I** (11 mg, 0.034 mmol, 97%) as an off-white solid with *er* > 99:1.

M.p. = 128 – 130 ºC (pentane). **IR** (cm^{-1}) ν 3297, 2932, 1604, 1491, 1457, 1273, 1194, 1147, 1021, 888, 834, 669. **^{1}H NMR** (400 MHz, CD_3OD) δ 7.12 – 7.08 (m, 3H), 6.85 – 6.80 (m, 2H), 6.63 (d, *J* = 2.4 Hz, 1H), 6.49 (d, *J* = 2.4 Hz, 1H), 4.79 – 4.77 (m, 1H), 4.76 (d, *J* = 2.1 Hz, 1H), 4.42 (s, 1H), 3.82 (s, 3H), 3.81 (s, 3H), 3.37 (dd, *J* = 3.7, 1.8 Hz, 1H), 2.95 (dt, *J* = 12.2, 3.9 Hz, 1H), 2.70 (dd, *J* = 17.2, 4.5 Hz, 1H), 2.22 (dd, *J* = 17.3, 12.4 Hz, 1H), 1.80 (s, 3H). **^{13}C NMR** (101 MHz, CD_3OD) δ 160.6, 159.2, 147.9, 140.6, 140.0, 129.9, 128.6, 127.4, 120.2, 111.7, 106.5, 98.8, 73.2, 55.9, 55.8, 51.4, 40.8, 24.1, 22.8. **HRMS** (ESI+) calculated for $[C_{21}H_{24}NaO_3]^+$ 347.1618 *m/z*; found $[M + Na]^+$ 347.1609 *m/z*. α_D^{589} = +33.3 deg.cm^2.g^{-1} (MeOH, c 0.15, 299 K); lit.[35c] α_D = +15.6 deg.cm^2.g^{-1} (MeOH, c 0.15, 298 K). **HPLC** Chiralpak IA (250 mm × 4.6 mm, 5 µm) at 25 ºC, flow 1.0 mL/min, isocratic hexane/*i*PrOH 90:10, 220 nm, t_R (minor) 14.3; t_R (major) 17.3.

Synthetic procedures and analytical data for the products from the synthesis of carexane P

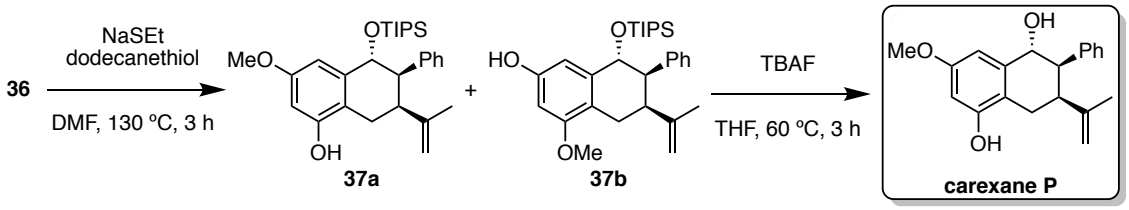

(5*R*,6*R*,7*S*)-3-Methoxy-6-phenyl-7-(prop-1-en-2-yl)-5-((triisopropylsilyl)oxy)-5,6,7,8-tetrahydronaphthalen-1-ol (37a) and (6*S*,7*R*,8*R*)-4-methoxy-7-phenyl-6-(prop-1-en-2-yl)-8-((triisopropylsilyl)oxy)-5,6,7,8-tetrahydronaphthalen-2-ol (37b)

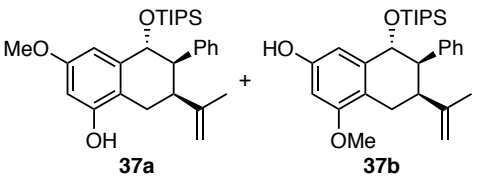

To a solution of **36** (496 mg, 1.03 mmol, 1.0 equiv) in dry DMF (10.3 mL) was added dodecane-1-thiol (0.544 mL, 2.27 mmol, 2.2 equiv) and sodium ethanethiolate (278 mg, 3.30 mmol, 3.2 equiv). The solution was heated at 130 ºC and stirred for 3 h. After cooling to 24 ºC, water was added and the mixture was extracted with EtOAc. The crude was purified by flash column chromatography (pentane/Et_2O 8:2). The regioisomers were obtained as a pale-yellow oil (inseparable mixture, 2.9:1 ratio; 340 mg, 0.722 mmol, 70%).

Major isomer (37a; 52% NMR yield): **^{1}H NMR** (500 MHz, CD_2Cl_2) δ 7.17 – 7.09 (m, 3H), 6.83 – 6.79 (m, 2H), 6.57 (d, *J* = 2.4 Hz, 1H), 6.40 (d, *J* = 2.5 Hz, 1H), 4.97 (br s, 1H), 4.97 (d, *J* = 1.6 Hz, 1H), 4.83 (s, 1H), 4.48 (s, 1H), 3.78 (s, 3H), 3.46 – 3.44 (m, 1H), 3.22 (dt, *J* = 12.8, 4.0 Hz, 1H), 2.65 (dd, *J* = 16.5, 4.7 Hz, 1H), 2.29 (dd, *J* = 16.5, 12.8 Hz, 1H), 1.87 (s, 3H), 1.25 – 1.17(m, 3H), 1.15 – 1.05 (m, 18H). **^{13}C NMR** (126 MHz, CD_2Cl_2) δ 159.2, 154.6, 147.3, 140.4, 139.4, 129.5, 128.3, 127.0, 117.0, 111.5, 107.9, 101.8, 73.9, 55.8, 51.3, 39.4, 23.2, 23.0, 18.71, 18.67, 13.5.

Minor isomer (**37b**; 18% NMR yield): **^{1}H NMR** (500 MHz, CD_2Cl_2) δ 7.17 – 7.09 (m, 3H), 6.83 – 6.79 (m, 2H), 6.46 (d, *J* = 2.3 Hz, 1H), 6.40 (d, *J* = 2.5 Hz, 1H), 4.92 (d, *J* = 1.6 Hz, 1H), 4.88 (br s, 1H), 4.80 (s, 1H), 4.48 (s, 1H), 3.81 (s, 3H), 3.43 – 3.41 (m, 1H), 3.15 (dt, *J* = 13.0, 4.1 Hz, 1H), 2.74 (dd, *J* = 17.2, 4.8 Hz, 1H), 2.23 (dd, *J* = 17.4, 13.0 Hz, 1H), 1.84 (s, 3H), 1.25 – 1.17 (m, 3H), 1.15 – 1.05 (m, 18H). **^{13}C NMR** (126 MHz, CD_2Cl_2) δ 158.7, 155.1, 147.6, 140.0, 139.6, 129.5, 128.2, 126.9, 119.4, 111.4, 108.8, 98.4, 73.8, 56.0, 51.3, 39.4, 23.4, 23.0, 18.7, 18.6, 13.5. **HRMS** (ESI+) calculated for $[C_{29}H_{42}NaO_3Si]^+$ 489.2795 *m/z*; found $[M + Na]^+$ 489.2793 *m/z*.

Carexane P[35d]

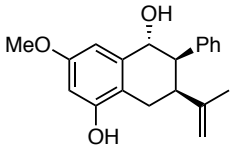

A mixture (2.9:1) of **37a** and **37b** (210 mg, 0.316 mmol, 1.0 equiv) was dissolved in dry THF (6 mL) and TBAF (1.9 mL, 1.90 mmol, 6.0 equiv, 1M in THF) was added at 0 ºC. The solution was heated to 60 ºC and the reaction was stirred at this temperature for 3 h. The reaction was quenched with water, extracted with EtOAc and the crude was purified by flash column chromatography (cyclohexane/EtOAc 3:2) to afford **carexane P** (70.2 mg, 0.22 mmol, 70%) as white amorphous solid with *er* > 99:1. **M.p.** = 162 – 164 ºC (pentane). **IR** (cm^{-1}) ν 3387, 2918, 1620, 1513, 1441, 1256, 1195, 1146, 1058, 1019, 969, 890, 842, 699. **^{1}H NMR** (500 MHz, CD_3OD) δ 7.13 – 7.07 (m, 3H), 6.87 – 6.82 (m, 2H), 6.56 (d, *J* = 2.5 Hz, 1H), 6.39 (d, *J* = 2.5 Hz, 1H), 4.78 (s, 1H), 4.74 (d, *J* = 2.1 Hz, 1H), 4.45 (s, 1H), 3.77 (s, 3H), 3.37 (dd, *J* = 3.7, 2.8 Hz, 1H), 2.98 (dt, *J* = 12.4, 4.2 Hz, 1H), 2.70 (dd, *J* = 17.0, 4.6 Hz, 1H), 2.26 (dd, *J* = 17.0, 12.4 Hz, 1H), 1.80 (s, 3H). **^{13}C NMR** (126 MHz, CD_3OD) δ 160.2, 156.6, 147.9, 140.6, 140.2, 129.9, 128.6, 127.3, 118.7, 111.7, 106.7, 102.0, 73.3, 55.6, 51.4, 40.8, 24.2, 22.9. **HRMS** (ESI+) calculated for $[C_{20}H_{22}NaO_3]^+$ 333.1461 *m/z*; found $[M + Na]^+$ 333.1464 *m/z*. α_D^{589} = +13.0 deg.cm^2.g^{-1} (MeOH, c 0.15, 299 K); lit.[35d] α_D = – 26.7 deg.cm^2.g^{-1} (MeOH, c 0.02, 298 K). **HPLC** Chiralpak IA (250 mm × 4.6 mm, 5 μm) at 25 ºC, flow 1.0 mL/min, isocratic hexane/*i*PrOH 80:20, 220 nm, t_R (major) 13.0; t_R (minor) 19.0.

Synthetic procedures and analytical data for the products from the synthesis of carexane O

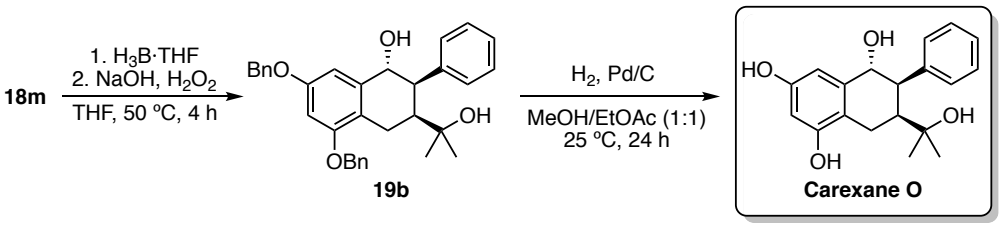

(1*R*,2*R*,3*S*)-5,7-Bis(benzyloxy)-3-(2-hydroxypropan-2-yl)-2-phenyl-1,2,3,4-tetrahydronaphthalen-1-ol (19b)

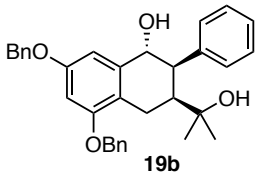

Compound **18m** (700 mg, 1.47 mmol, 1.0 equiv) was dissolved in anhydrous THF (20 mL). $BH_3 \cdot THF$ complex (8.2 mL, 8.20 mmol, 5.6 equiv, 1M in THF) was added dropwise and the solution was stirred for 4 h at 50 ºC. After cooling to 0 ºC, sodium hydroxide (2.94 mL, 7.34 mmol, 5.0 equiv; 2.5M) was added dropwise followed by hydrogen peroxide (1.67 mL, 14.7 mmol, 10.0 equiv; 8.8M). The mixture was stirred for 3 h at 24 ºC and then extracted with Et_2O. The crude was purified by flash column chromatography (pentane/Et_2O 4:1) to afford **19b** (448 mg, 0.91 mmol, 62%) as a white solid.

M.p. = 91 – 93 ºC (pentane). **^{1}H NMR** (500 MHz, $CDCl_3$) δ 7.48 – 7.36 (m, 8H), 7.36 – 7.31 (m, 2H), 7.22 – 7.17 (m, 3H), 7.07 – 7.02 (m, 2H), 6.64 (d, *J* = 2.3 Hz, 1H), 6.59 (d, *J* = 2.3 Hz, 1H), 5.15 (d, *J* = 12.0 Hz, 1H), 5.09 (d, *J* = 12.0 Hz, 1H), 5.04 – 4.98 (m, 2H), 4.61 (d, *J* = 1.2 Hz, 1H), 3.63 (dd, *J* =3.8, 1.9 Hz, 1H), 3.15 (dd, *J* = 17.9, 5.4 Hz, 1H), 2.70 (dd, *J* = 17.9, 12.8 Hz, 1H), 2.47 (ddd, *J* = 12.8, 5.4, 3.7 Hz, 1H), 2.11 (br s, 1H), 1.28 (s, 3H), 1.20 (s, 3H), 1.10 (br s, 1H). **^{13}C NMR** (126 MHz, $CDCl_3$) δ 158.4, 157.4, 140.3, 138.4, 137.1, 137.0, 129.7, 128.9, 128.73, 128.72, 128.2, 128.0, 127.8, 127.3, 127.1, 120.1, 106.8, 100.7, 74.3, 73.2, 70.3, 70.1, 47.5, 42.5, 29.2, 28.3, 20.7. **HRMS** (ESI+) calculated for $[C_{33}H_{34}NaO_4]^+$ 517.2349 *m/z*; found $[M + Na]^+$ 517.2340 *m/z*. α_D^{589} = –39.6 deg.cm^2.g^{-1} ($CDCl_3$, c 1.00, 299 K).

Carexane O[35d]

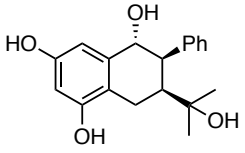

In a microwave vial **19b** (40 mg, 0.418 mmol, 1.0 equiv) and Pd/C 10% (4.7 mg, 4.4 μmol, 1 mol %) were added. The vial was covered with a septum and evacuated during 5 min through a needle. Then the vial was filled with H_2 and a mixture of methanol (2 mL) and EtOAc (2 mL) was added. The system was purged with 5 fast cycles of vacuum and hydrogen. The reaction mixture was stirred under hydrogen atmosphere (1 atm) for 24 h until full conversion. The reaction was filtered through Celite® and the solvent was evaporated under reduced pressure. **Carexane O** (130 mg, 0.080 mmol, 98%) was obtained as a white solid with *er* > 99:1.

M.p. = 189 – 191 ºC (Et_2O). **IR** (cm^{-1}) ν 3371, 2913, 1596, 1452, 1254, 1143, 840, 699. **^{1}H NMR** (500 MHz, CD_3OD) δ 7.18 – 7.13 (m, 3H), 7.03 – 6.99 (m, 2H), 6.33 (d, *J* = 2.4 Hz, 1H), 6.32 (d,

J = 2.4 Hz, 1H), 4.39 (d, *J* = 1.8 Hz, 1H), 3.48 (dd, *J* = 3.4, 1.9 Hz, 1H), 3.01 (dd, *J* = 16.5, 4.4 Hz, 1H), 2.50 (ddd, *J* = 13.0, 4.4, 3.4 Hz, 1H), 2.43 (dd, *J* = 16.5, 13.0 Hz, 1H), 1.14 (s, 3H), 0.93 (s, 3H). **^{13}C NMR** (126 MHz, CD_3OD) δ 157.2, 156.8, 142.5, 139.6, 130.8, 129.2, 127.5, 117.8, 109.5, 102.9, 75.1, 73.9, 49.7, 44.4, 28.2, 27.6, 21.7. **HRMS** (ESI+) calculated for $[C_{19}H_{22}NaO_4]^+$ 337.1410 *m/z*; found $[M + Na]^+$ 337.1411 *m/z*. α_D^{589} = –40,1 deg.cm^2.g^{-1} (MeOH, c 0.31, 299 K); lit.[35d] α_D = +10.0 deg.cm^2.g^{-1} (MeOH, c 0.04, 298 K). **HPLC** Chiralpak IA (250 mm × 4.6 mm, 5 μm) at 25 ºC, flow 1.0 mL/min, isocratic hexane/*i*PrOH 80:20, 220 nm, t_R (minor) 12.3; t_R (major) 15.7.

Calculated Energy Diagrams

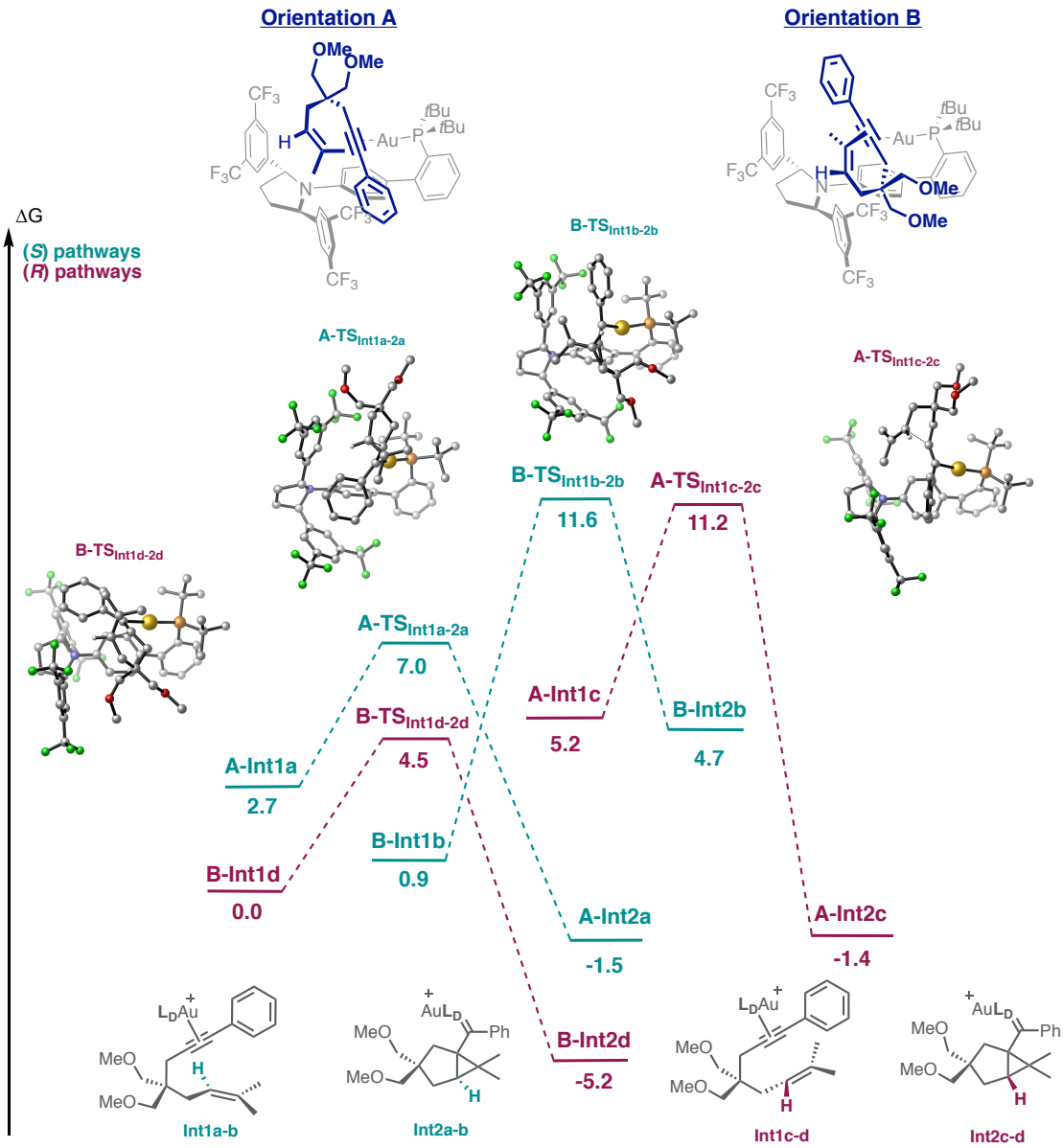

Free energy profiles for the enantioselective 5-*exo*-dig cyclization reaction of 1,6-enyne **27a** with (*R*,*R*)-**O**. (*S*) pathway is depicted in green and (*R*) pathway in purple. The energy values are given in kcal·mol^{-1} and represent the relative free energies. Hydrogen atoms have been omitted for clarity.

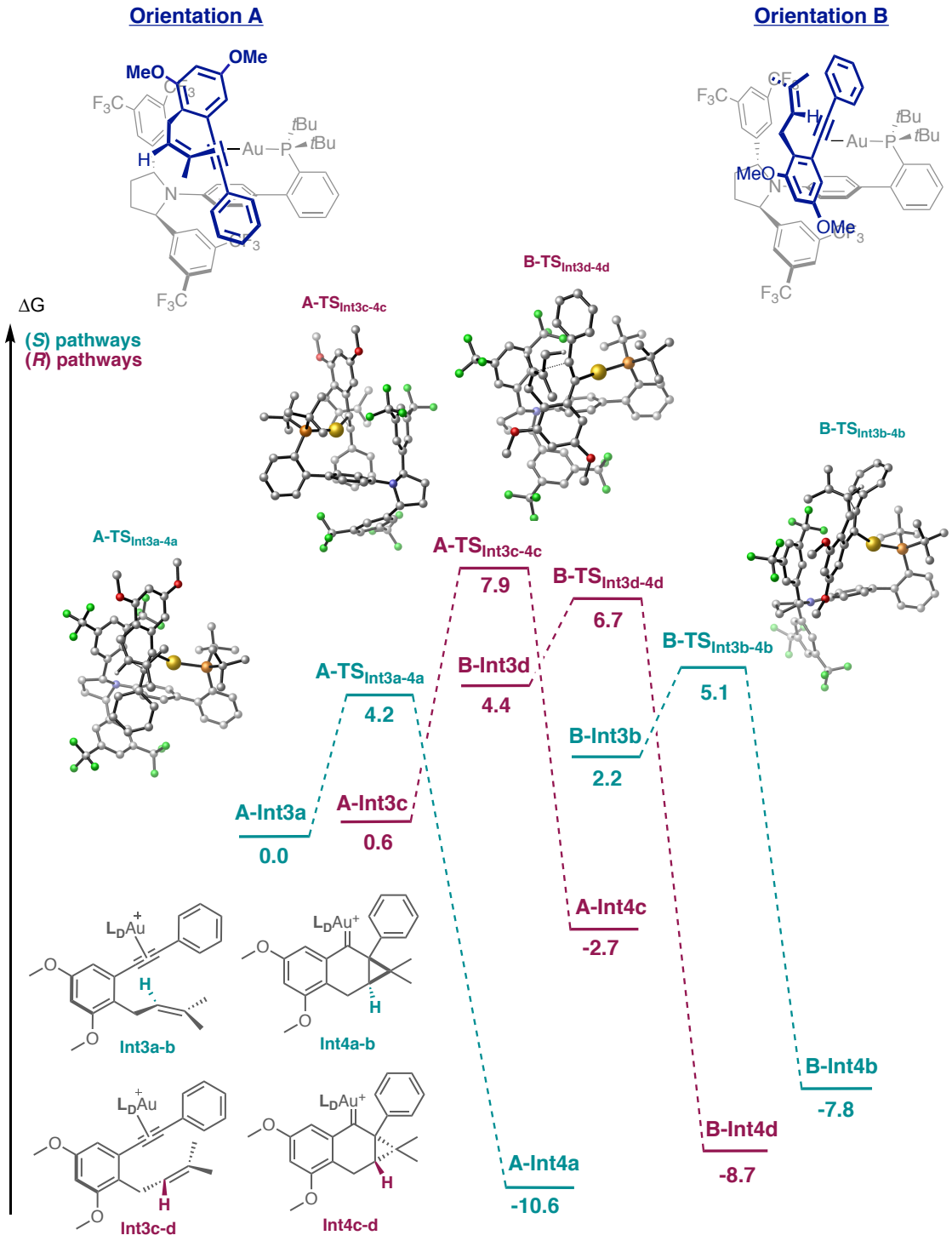

Free energy profiles for the enantioselective 6-*endo*-dig cyclization reaction of 1,6-enyne **17a** with (*R*,*R*)-**O**. (*S*) pathway is depicted in green and (*R*) pathway in purple. The energy values are given in kcal·mol^{-1} and represent the relative free energies. Hydrogen atoms have been omitted for clarity.

Chapter II:

Photoredox-Assisted Gold-Catalyzed Arylative Alkoxycyclization of 1,6-Enynes

In collaboration with Dr. Jean S. Suppo

Introduction

Gold-Catalyzed Cross-Coupling Reactions

Transition metal-catalyzed cross-coupling reactions are a critical component in organic synthesis.[1] The landmark studies of Richard Heck, Ei-icih Negishi and Akira Suzuki, among other authors, on the palladium catalyzed coupling of organometallic nucleophiles with different types of electrophiles laid the foundations for the development of this field and were rewarded with the Nobel Prize in 2010.[2] This breakthrough changed the paradigm of C–C bond construction and therefore, the current view of retrosynthetic analysis. Accordingly, the mechanistic study of these reactions has led to a better understanding of elemental organometallic chemistry and its potential application in organic synthesis.

In general, metal-catalyzed cross-coupling reactions proceed through three fundamental organometallic steps: (1) oxidative addition of an electrophilic carbon-heteroatom bond into the low valent transition metal, (2) transmetalation or displacement of a leaving group by the nucleophilic partner and (3) reductive elimination to form a C–Nu bond (Scheme 1).

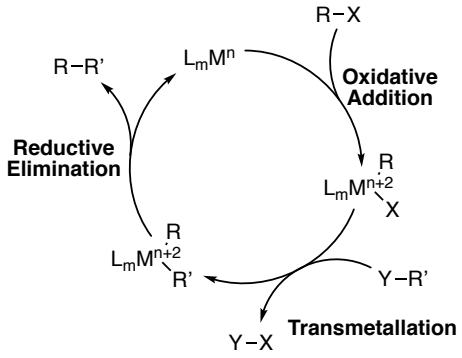

Commonly used partners in cross-coupling reactions:

R = Csp^3, Csp^2 or Csp organic fragments.
X = Halogens (I, Br, Cl) or pseudohalogens (OTs).
R' = Carbon based (Csp^3, Csp^2 and Csp organic fragments) or heteroatom based (N, O, P, S…).
Y = Metals (Sn, Zn, Mg, Ag, Au…), metalloids (B, Si, Ge…) or proton.

Scheme 1. General mechanism for the TM-catalyzed cross-coupling reactions.

The discovery of new cross-coupling reactions engaging different nucleophiles and electrophiles has been an active research area since the field was first stablished. Despite the supremacy of palladium catalysts in this field,[1] other transition metals such as Fe, Ni and Cu have proved to efficiently catalyze this kind of transformations.[3] However, the use of gold in cross-coupling reactions has been limited and gold complexes have been often considered as redox-neutral. As explained in the general introduction, this is mainly due to the relatively high redox potential of the gold(I)/gold(III) couple (E^o = 1.41V), that hinders the direct oxidative addition of aryl (pseudo)halides. The combination of gold(I)/gold(III) catalytic cycles with the singular carbophilic character of gold complexes would substantially broaden the field cross-coupling reactions as well as the scope of homogeneous gold catalysis.

1 Diederich, F.; Stang, P. J. (1999). *Metal-Catalyzed Cross-Coupling Reactions.* ISBN 3-527-29421-X.

2 https://www.nobelprize.org/prizes/chemistry/2010/summary/

3 Jana, R.; Pathak, T. P.; Sigman, M. S. *Chem. Rev.* **2011**, *111*, 1417–11492.

Early studies by the groups of Schmidbaur,[4] Kochi[5] and Puddephatt[6] showed that the oxidative addition of C(sp^3)–I to gold(I) centers readily occurs at -20 ºC. The authors investigated the reaction [(R_3P)AuMe] complexes and MeI to produce ethane. Mechanistically, the reaction starts with the S_N2-type oxidative addition of the alkyl halide to generate gold(III) complex **1** that rapidly engages in a ligand scramble process. Subsequent reductive elimination from organogold(III) species **2** delivers ethane and regenerates the initial gold(I) complex (Scheme 2). Interestingly, the steric hindrance at the phosphine was found to have a great impact on the rate of the reductive elimination. In the case of triphenylphosphine, the evolution of ethane was relatively fast whereas for less bulky trimethylphosphine the reaction took weeks to be completed. This mechanistic picture was supported by the results reported by Wendt and Ahlquist on the reactivity of (NHC)Au(I)–R complexes with MeI and MeOTf.[7]

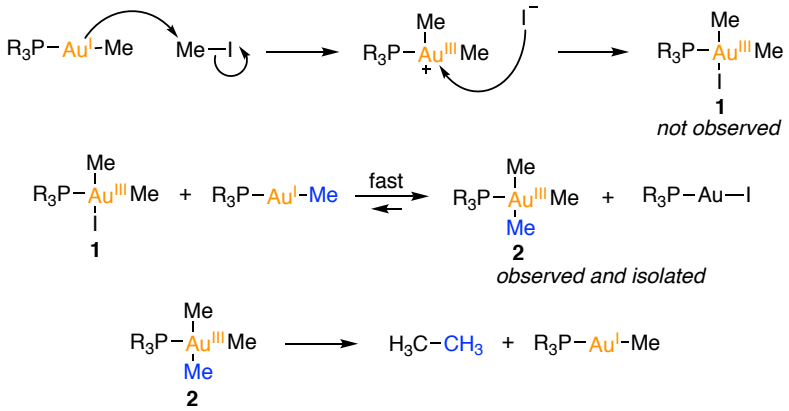

Scheme 2. Reaction mechanism for the formation of ethane from [(R_3P)AuMe] and MeI.

The facile oxidative addition of C(sp^3)–X to gold was exploited by the group of Toste in the gold-catalyzed cross-coupling reaction between arylboronic acids and allyl bromides.[8] The use of a bimetallic gold complex **3** was key to facilitate the challenging C(sp^3)–C(sp^2) reductive elimination. Control experiments indicated that Au–B transmetalation was taking place first, followed by oxidative addition and reductive elimination (Scheme 3).

4 Shiotani, A.; Schmidbaur, H. *J. Organomet. Chem.* **1972**, *37*, C24–C26.

5 (a) Tamaki, A.; Kochi, J. K. *J. Organomet. Chem.* **1972**, *40*, C81–C84. (b) Tamaki, A.; Kochi, J. K. *J. Organomet. Chem.* **1974**, *64*, 411–425.

6 (a) Johnson, A.; Puddephatt, R. *Inorg. Nucl. Chem. Lett.* **1973**, *9*, 1175–1177. (b) Johnson, A.; Puddephatt, R. *J. Organomet. Chem.* **1975**, *85*, 115–121.

7 Johnson, M. T.; van Rensburg, J. M. J.; Axelsson, M.; Ahlquist, M. S. G; Wendt, O. F. *Chem. Sci.* **2011**, *2*, 2373–2377.

8 Levin, M. D.; Toste, F. D. *Angew. Chem. Int. Ed.* **2014**, *53*, 6211–6215.

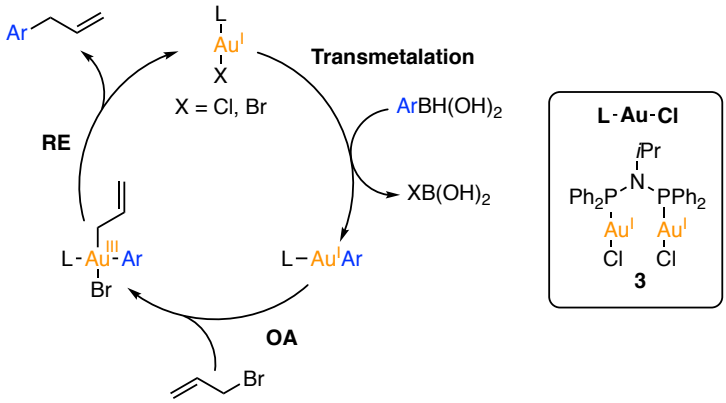

Scheme 3. Gold-catalyzed cross-coupling of arylboronic acids with allyl bromides.

In contrast, the oxidative addition of C(sp^2)–X bonds to mononuclear gold(I) linear complexes is a highly disfavored process.[9,10] As a corollary, the development of gold-catalyzed cross-coupling methodologies to form C(sp^2)–C(sp^2) or C(sp^2)–C(sp) is a challenging process that usually requires the use of very specific systems and conditions.

Use of Sacrificial Oxidants

The most common strategies to circumvent the demanding oxidative addition of C(sp^2)–X bonds to gold(I) centers relies in the use of strong oxidants that enable the oxidation of gold(I) to gold(III).[11] One of the first examples using this approach was reported by the group of Zhang.[12] While attempting the gold(I)-catalyzed tandem propargylic ester rearrangement/electrophilic fluorination using Selectfluor, they were able to isolate the product from the oxidative homo-coupling **5**, which suggested that Selectfluor was promoting the oxidation of gold(I) to gold(III). To further investigate this reactivity, they performed the reaction in the presence of arylboronic acids. In this case the cross-coupling product **4** was formed predominantly together with lower amounts of homocoupled dienone **5** and enone **6** (Scheme 4a). The proposed reaction mechanism starts with the gold(I)-catalyzed rearrangement of the propargylic acetate to form alkenylgold(I) species **7**.[13] Next, oxidation with Selectfluor to the corresponding gold(III) analogue **8** takes place,

9 (a) Livendahl, M.; Goehry, C.; Maseras, F.; Echavarren, A. M. *Chem. Commun.* **2014**, *50*, 1533–1536. (b) Fernández, I.; Wolters, L. P.; Bickelhaupt, F. M. *J. Comp. Chem.* **2014**, *45*, 2140–2145.

10 For a recent example, see: Daley, R. A.; Morrenzin, A. S.; Neufeldt, S. R.; Topczewski, J. J. *J. Am. Chem. Soc.* **2020**, *142*, 13210–13218.

11 For selected reviews, see: (a) Hopkinson, M. N.; Gee, A. D.; Gouverneur, V. *Chem. Eur. J.* **2011**, *17*, 8248–8262. (b) Wegner, H. A.; Auzias, M. *Angew. Chem. Int. Ed.* **2011**, *50*, 8236–8247.

12 (a) Zhang, G.; Peng, Y.; Cui, L.; Zhang, L. *Angew. Chem. Int. Ed.* **2009**, *48*, 3112–3115. (b) Cui, L.; Zhang, G.; Zhang, L. *Bioorg. Med. Chem. Lett.* **2009**, *19*, 38

13 (a) Yu, M.; Li, G.; Wang, S.; Zhang, L. *Adv. Synth. Catal.* **2007**, *349*, 871–875 (b) Marion, N; Carlqvist, P.; Gealageas, R.; de Frémont, P.; Maseras, F.; Nolan, S. P. *Chem. Eur. J.* **2007**, *13*, 6437–6451.

followed by transmetalation and reductive elimination (Scheme 4b).[14] Under similar conditions, the use of propargyl benzoates resulted in the formation of C–O bonds.[15]

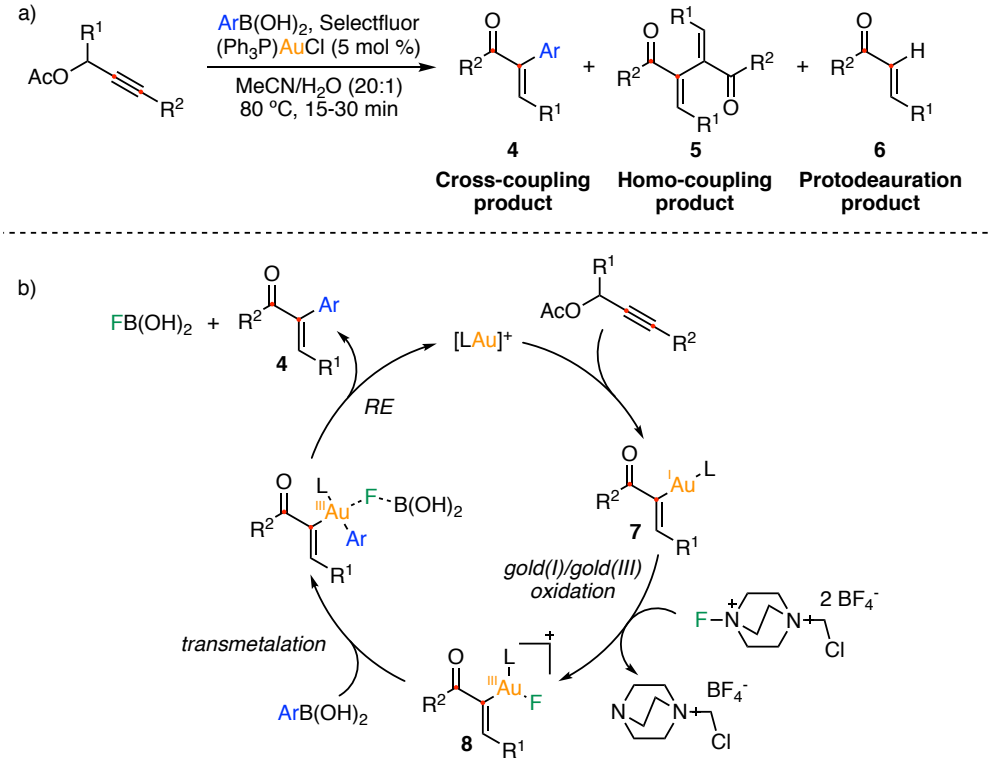

Scheme 4. (a) Gold-catalyzed oxidative cross-coupling of propargyl esters with arylboronic acids; (b) plausible mechanism.

Following this pioneering example, different well-known gold-catalyzed transformations were submitted to oxidative conditions with the aim of unlocking new reactivities. The formation of C(sp^3)–heteroatom bonds was achieved *via* the oxi- and aminoarylation of alkenes, studied by the groups Zhang and Toste (Scheme 5a).[16] Contrary to the previous example, here the catalytic cycle initiates with the oxidation of the gold(I) catalyst. Next, the alkene is activated by the strong electrophilic gold(III) complex and the intramolecular nucleophilic attack takes place. The resulting alkylgold(III) species undergoes transmetalation with the arylboronic ester and upon reductive elimination the C(sp^3)–C(sp^2) bond is formed (Scheme 5b).

14 Nieto-Faza, O.; Silva-López, C. *J. Org. Chem.* **2013**, *78*, 4929–2939.

15 Peng, Y.; Cui, L.; Zhang, G.; Zhang, L. *J. Am. Chem. Soc.* **2009**, *131*, 5062–5063.

16 (a) Zhang, G.; Cui, L.; Wang, Y.; Zhang, L. *J. Am. Chem. Soc.* **2010**, *132*, 1474–1475. (b) Brenzovich, W. E.; Benítez, Jr. D.; Lackner, A. D.; Shunatona, H. P.; Tkatchouk, E.; Goddard III, W. A.; Toste, F. D. *Angew. Chem. Int. Ed.* **2010**, *49*, 5519–5522.

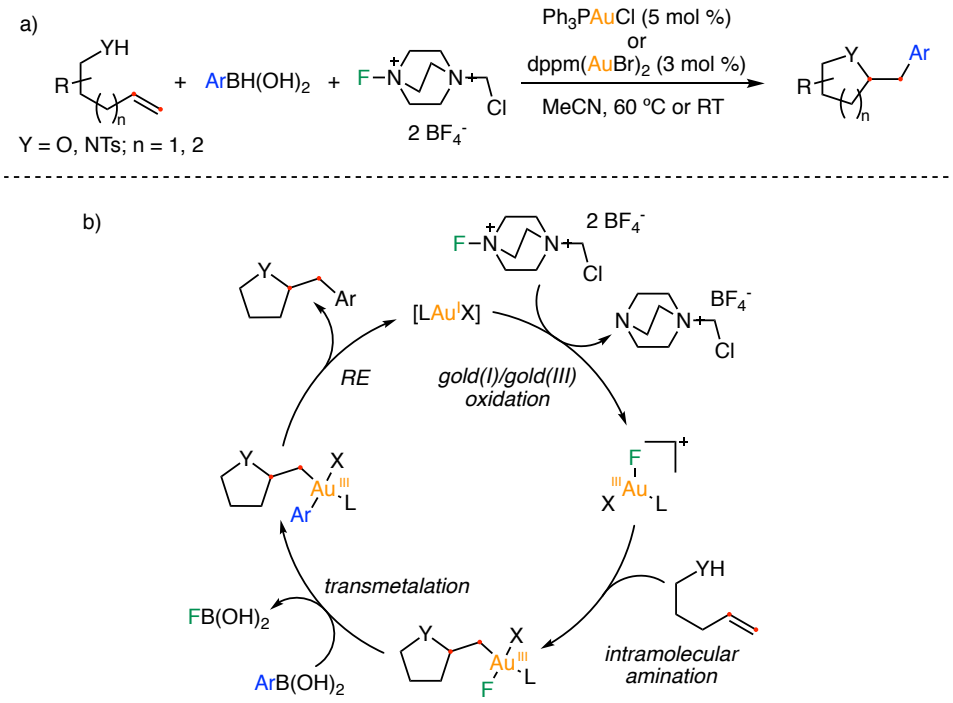

Scheme 5. (a) Gold-catalyzed oxi- and aminoarylation of alkenes in the presence of arylboronic acids; (b) plausible mechanism.

Aryl silanes[17] or simple arenes[18] have also been used as nucleophilic partners in this kind of reactions.

Gold-catalyzed formation of C(sp)–C(sp^2)[19] and C(sp)–C(sp)[20] bonds under oxidative conditions has also been explored. Assisted by a base, terminal alkynes form the corresponding gold(I) acetylide complexes **9**. This species can be oxidized by Selectfluor and subsequently engaged in the transmetalation with arylboronic acids. In the absence of other transmetalating agents, gold(III) acetylide complex **10** can undergo transmetalation with **9** affording bisacetylide **11**. In both scenarios, reductive elimination closes the catalytic cycle releasing the "Sonogashira-type" product and the "Ullmann-type" diyne respectively (Scheme 6).

17 (a) Ball, L. T.; Green, M.; Lloyd-Jones, G. C.; Russel, C. A. *Org. Lett.* **2010**, *12*, 4724–4727, (b) Brenzovich, W. E.; Jr; Brazeau, J.-F.; Toste, F. D. *Org. Lett.* **2010**, *12*, 4728–4731.

18 Zhang, G.; Luo, Y.; Wang, Y.; Zhang, L. *Angew. Chem. Int. Ed.* **2011**, *50*, 4450–4454.

19 Qian, D.; Zhang, J. *Bailstein, J. Org. Chem.* **2011**, *7*, 808–812.

20 Leyva-Pérez, A.; Doménech, A.; Al-Resayes, S. I.; Corma, A. *ACS Catal.* **2012**, *2*, 121–126.

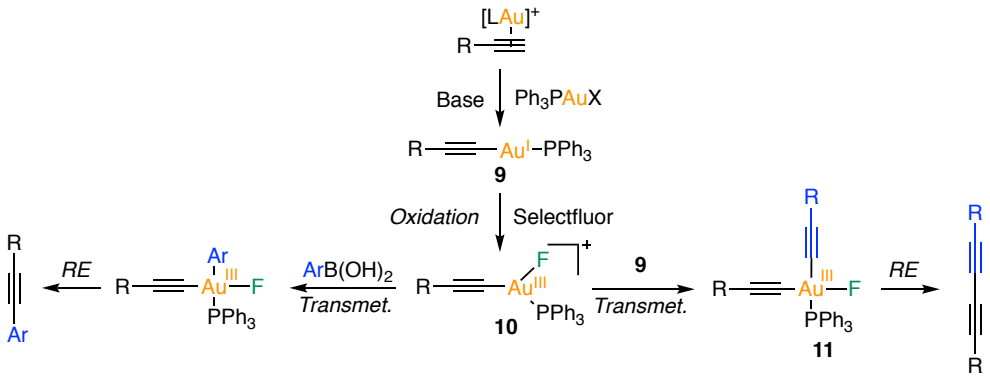

Scheme 6. Gold-catalyzed formation of C(sp)–C(sp^2) and C(sp)–C(sp) bonds under oxidative conditions.

In 2008, Tse and co-workers reported the first example of gold-catalyzed oxidative homocoupling of arenes assisted by hypervalent iodine compounds.[21] Hence, two electron-rich arenes are activated through C–H auration with $HAuCl_4$ under strong acidic conditions. Next, reductive elimination produces the homo-coupling product and AuCl that, in the presence of $PhI(OAc)_2$, gets reoxidized to gold(III) and restarts the cycle (Scheme 7).

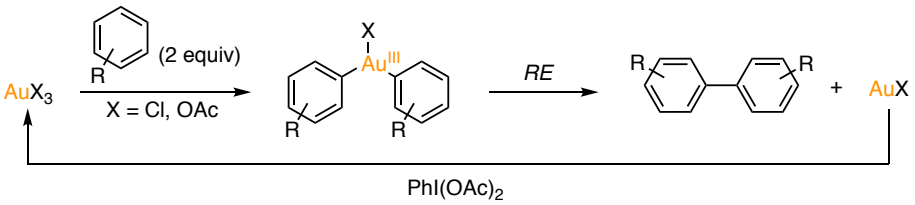

Scheme 7. Mechanism of the $PhI(OAc)_2$-assisted gold-catalyzed homo-coupling of arenes.

After this report, hypervalent iodine derivatives have been used in a wide range of gold-catalyzed oxidative coupling reactions such as difunctionalization of alkenes,[22] biaryls synthesis[23] and alkynylations.[24] Especial attention has been devoted to the gold-catalyzed oxidative alkynylation using 1-([(triisopropylsilyl)ethynyl]-1,2-benziodoxol-3(1H)-one (TIPS-EBX), an iodine compound that acts both as an oxidant and as a coupling partner.[25] In combination with of

21 Kar, A.; Mangu, N.; Kaiser, H. M.; Beller, M.; Tse, M. K. *Chem. Commun.* **2008**, 386–388.

22 Ball, L. T.; Llyod-Jones, G. C.; Russel, C. A. *Chem. Eur. J.* **2012**, *18*, 2931–2937.

23 (a) Ball, L. T.; Llyod-Jones, G. C.; Russel, C. A. *Science* **2012**, *337*, 1644–1648. (b) Hofer, M.; Genoux, A.; Kumar, R.; Nevado, C. *Angew. Chem. Int. Ed.* **2017**, *56*, 1021–1025. (c) Fricke, C.; Dahiya, A.; Reid, W. B.; Schoenebeck, *ACS Catal.* **2019**, *9*, 9231–9236.

24 For selected examples, see: (a) De Haro, T.; Nevado, C. *J. Am. Chem. Soc.* **2010**, *132*, 1512–1513. (b) Peng, H.; Xi, Y.; Ronaghi, N.; Dong, B.; Akhmedov, N. G.; Shi, X. *J. Am. Chem. Soc.* **2014**, *136*, 13174–13177.

25 Zhdnkin, V. V.; Kuehl, C. J.; Krasutski, A. P.; Bolz, J. T.; Simonsen, A. J. *J. Org. Chem.* **1996**, *61*, 6574–6551.

AuCl as catalyst, this system has shown great performances in the alkynylation of various types of C–H bonds (Scheme 8).[26]

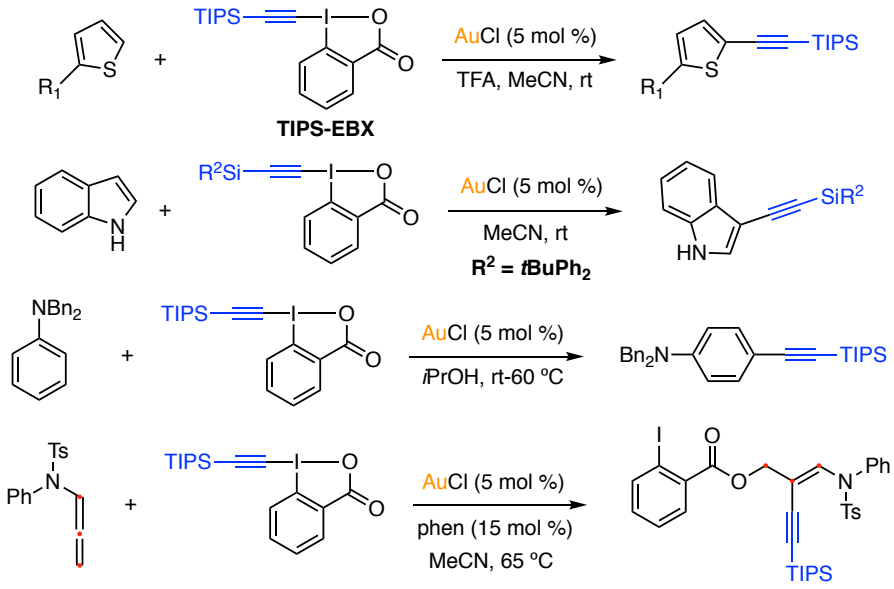

Scheme 8. Gold-catalyzed C–H alkynylation of different substrates using TIPS-EBX.

Despite of the applicability of these oxidative conditions, the scope of this reactivity is limited to the use of oxidation-stable substrates. Furthermore, the generation of stoichiometric amounts of waste (sacrificial oxidant) renders these reactions inefficient in terms of atom economy. These disadvantages have encouraged the scientific community to find other alternatives to develop gold-catalyzed cross-coupling reactions.

Substrate Facilitated Oxidative Additions

The oxidative addition of C(sp^2)–X bonds to gold can be kinetically eased by the preorganized structure of the reactant. An illustrative example is the intramolecular oxidative addition of aryl iodides to gold(I) centers under mild to yield thermally stable cyclometalated gold(III) complexes (Scheme 9).[27]

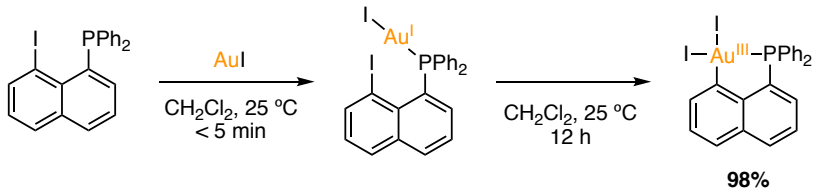

Scheme 9. Synthesis of cyclometalated gold(III) complexes *via* intramolecular OA.

26 (a) Brand, J. P.; Waser, J. *Angew. Chem. Int. Ed.* **2010**, *49*, 7304–7307. (b) Brand, J. P.; Chevalley, C.; Scopelliti, R.; Waser, J. *Chem. Eur. J.* **2012**, *18*, 5655–5666. (c) Brand, J. P.; Waser, J. *Org. Lett.* **2012**, *14*, 744–747. (d) Banerjee, B.; Senthilkumar, B.; Patil, N. T. *Org. Lett.* **2019**, *21*, 180–184.

27 Guenther, J.; Mallet-Ladeira, S.; Estévez, L.; Miqueu, K.; Amgoune, A.; Bourissou, D. *J. Am. Chem. Soc.* **2014**, *136*, 1778–1781.

Although the method was not further applied to gold-promoted cross-coupling reactions, this prove of concept stimulated the design of new structural oriented approaches to enable the intermolecular oxidative addition. In this regard, the oxidative addition of aryl halides to gold enabled by the use of directing groups was studied by Ribas et al. Taking advantage of the chelation effect, the authors developed the gold-catalyzed halide exchange and the C_{aryl}–O and C_{aryl}–N Ullmann-type couplings (Scheme 10).[28] Importantly, a C^N cyclometalated gold(III) complex could be isolated and characterized, validating the intermediacy of gold(III) spieces in this oxidant-free cross-coupling reactions.

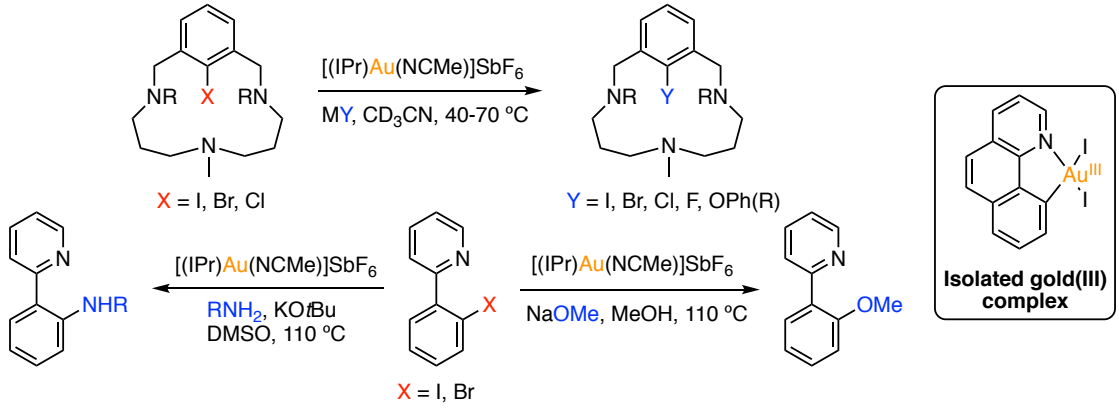

Scheme 10. Application of the directed oxidative additions of C_{aryl}–X bonds to gold(I) centers in cross-coupling reactions.

Ligand Facilitated Oxidative Additions

As mentioned in the general introduction, the use of bidentate ligands with small bite angles forces gold(I) dicoordinated complexes to adopt angular geometries. Upon bending, the ML_2 fragment displays enhanced reactivity and is preorganized to accommodate the square-planar geometry of the ensuing oxidative addition products.[29] As a result, the oxidative addition is both thermodynamically and kinetically favored compared with the classical linear gold(I) complexes. Although most bidentate ligands form Au···Au dinuclear species,[30] Bourissou and co-workers succeeded in studying the oxidative addition[31,32] of aryl iodides using the tricoordinated carborane

28 (a) Serra, J.; Whiteoak, C. J.; Acuña-Perés, F.; Font, M.; Llui, J. M.; Lloret-Fillol, J.; Ribas, X. *J. Am. Chem. Soc.* **2015**, *137*, 13389–13397. (b) Serra, J.; Parella, T.; Ribas, X. *Chem. Sci.* **2017**, *8*, 946–952.

29 Hofmann, P.; Heis, P.; Müller, G. Z. *Naturforsch. B* **1987**, *42*, 395–409.

30 (a) Gimeno, M. C.; Laguna, A. *Chem. Rev.* **1997**, *97*, 511–522. (b) Mohamed, A. A.; Krause Bauer, J. A.; Bruce, A. E.; Bruce, M. R. M. *Acta Crystallogr.* **2003**, *59*, m84–m86. (c) Schmidbaur, H.; Schier, A. *Chem. Soc. Rev.* **2012**, *41*, 370–412.

31 Joost, M.; Zeineddine, A.; Estévez, L.; Mallet-Ladeira, S.; Miqueu, K.; Amgoune, A.; Bourissou, D. *J. Am. Chem. Soc.* **2014**, *136,* 14654–14657.

32 For the application of this catalyst in the oxidative additions of $C(sp^2)$–$C(sp^2)$ strained bonds, see: Joost, M.; Estévez, L.; Miqueu, K.; Amgoune, A.; Bourissou, D. *Angew. Chem. Int. Ed.* **2015**, *54,* 5236–5240.

diphosphine gold(I) chloride complexes reported by Laguna and Jones.[33] They found that upon activation with a silver salt, complex **12** underwent fast oxidative addition of different C_{aryl}–I bonds under remarkably mild conditions (Scheme 11).

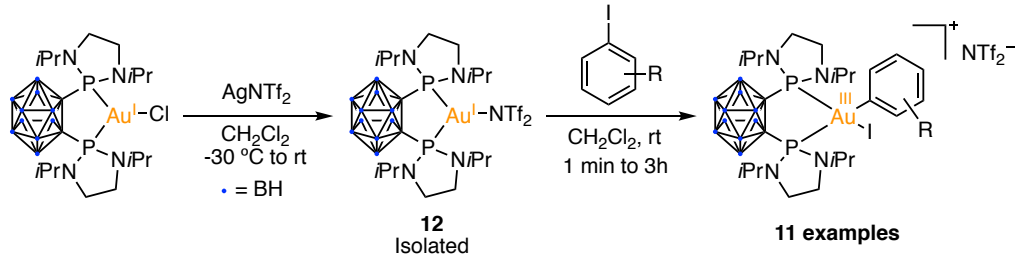

Scheme 11. Oxidative addition of aryl iodides to carborane diphosphine gold(I) complexes.

2,2'-Bipyridines have also shown to be suitable bidentate ligands for the synthesis of gold(I) tricoordinate complexes. In a recent work, Russell et al. disclosed the potential of gold(I) catalyst **13** to undergo oxidative addition of aryl iodides forming isolable gold(III) complexes. As evidenced by mass spectroscopy experiments, **14** could be engaged in transmetalation reactions with organozinc nucleophiles. Upon reductive elimination the biaryl product was obtained in good yields through an overall stepwise Negishi-type crossed-coupling process (Scheme 12).[34] Similar reactivity was found by using organotin partners. Despite the feasibility of all three steps of the catalytic cycle, the efforts to render the whole process catalytic resulted unsuccessful, presumably due to the different reaction temperatures needed for the oxidative addition (50 ºC) and the transmetalation-reductive elimination sequence (below -30 ºC).

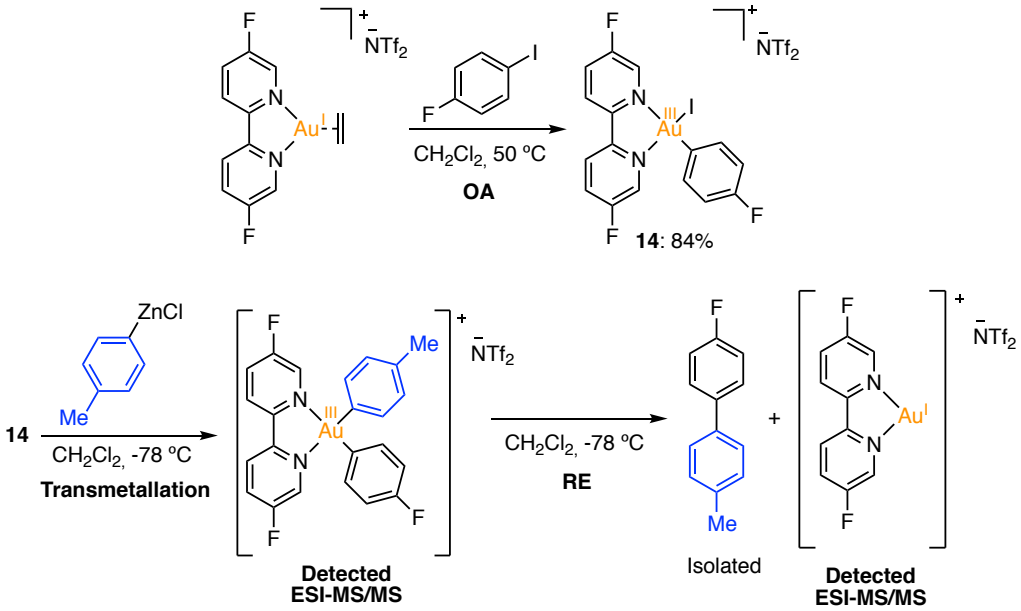

Scheme 12. Gold-catalyzed stepwise Negishi-type cross-coupling.

33 Crespo, O.; Gimeno, M. C.; Laguna, A.; Jones, P. G. *J. Chem. Soc. Dalton Trans.* **1992**, 1601–1605.

34 Harper, M. J.; Arthur, C. J.; Crosby, J.; Emmett, E. J.; Falconer, R. L.; Fensham-Smith, A. J.; Gates, P. J.; Leman, T.; Mcgrady, J. E.; Bower, J. F.; Russell, C. A. *J. Am. Chem. Soc.* **2018**, *140*, 4440–4445.

Recently, the group of Bourissou achieved the gold-catalyzed (hetero)arylation of arenes (Scheme 13).[35] In this case, Me-Dalphos ligands assisted the oxidative addition with the coordination of the hemilabile dimethylamino moiety. In contrast with the higher reactivity displayed by electron-defficient arenes in Pd-catalyzed oxidative addition, the authors found that gold reacted preferentially with electron-rich substrates. The experimental and theoretical study of the mechanism revealed that the difference in behavior between the two metals relies on the nature of the M–Ar bond. For highly electrophilic gold centers the major component of this interaction comes from the donation of electron density from the aryl to the metal while for less electrophilic palladium complexes, back-donation becomes more important and electron-poor substrates are preferred.[35b]

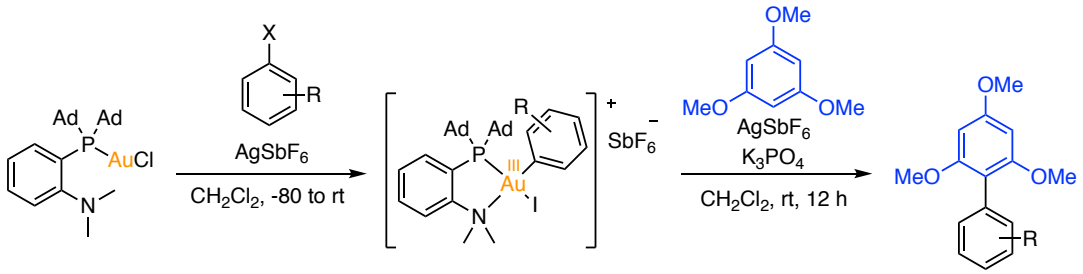

Scheme 13. Arylation of haloarenes enabled by (Me-Dalphos)AuCl complexes.

The tendency of [(Me-Dalphos)AuCl] to undergo rapid oxidative addition of aryl iodides has opened the door to merge gold(I)/gold(III) catalytic cycles with the traditional π-activation gold chemistry. A recent example is the gold-catalyzed difunctionalization of alkenes studied by the groups of Patil,[36] Bourissou[37] and Shi.[38]

Use of Aryldiazonium Salts

The propensity of aryldiazonium salts to eliminate N_2 and produce highly reactive aryl radicals upon 1*e*-reduction, thermal decomposition or base-assisted degradation, has been extensively used in the development of new cross-coupling reactions.[39] In the presence of low-valent transition metals, the aryl radical can act both as a strong 1*e*- oxidant and as a coupling

35 (a) Zeineddine, A.; Estévez, L.; Mallet-Ladeira, S.; Miqueu, K.; Amgoune, A.; Bourissou, D. *Nat. Commun.* **2017**, *8,* 565–572. (b) Rodríguez, J.; Zeineddine, A.; Carrizo, E. D. S; Miqueu, K.; Saffon-Merceron, N.; Amgoune, A.; Bourissou, D. *Chem. Sci.* **2019**, *10*, 7183–7192.

36 Chintawar, C. C.; Yadav, A. K.; Patil, N. T. *Angew. Chem. Int. Ed.* **2020**, *59*, 11808–11813.

37 Rigoulet, M.; du Boullay, O. T.; Amgoune, A.; Bourissou, D. *Angew. Chem. Int. Ed.* **2020**, *59*, 16625–16630.

38 Zhang, S.; Wang, C.; Ye, X.; Shi, X. *Angew. Chem. Int. Ed.* **2020**, *59*, 20470–20474.

39 (a) Roglans, A.; Pla-Quintana, A.; Moreno-Mañas, M. *Chem. Rev.* **2006**, *106*, 4622–4643. (b) Hari, D. P.; König, B. *Angew. Chem. Int. Ed.* **2013**, *52*, 2–12. (c) Mo, F.; Dong, G.; Zhang, Y.; Wang, J. *Org. Biomol. Chem.* **2013**, *11*, 1582–1593. (d) Kaziakov, D.; Wy, G.; von Wangelin, A. J. *Org. Biomol. Chem.* **2018**, *16*, 4942–4953.

partner. Taking advantage of this reactivity, the Glorius group envisioned that the energetically demanding two-electron oxidation of gold(I) to gold(III) could be bypassed to more facile, two single-electron oxidation steps by using photocatalytically generated aryl radicals. To prove this concept, the dual gold-photoredox-catalyzed intramolecular oxy- and aminoarylation of alkenes in the presence of diazonium salts was investigated (Scheme 14a).[40] The mechanism of the reaction was studied by the group of Yu using hybrid DFT calculations.[41] Among the computed pathways, the most favorable initiates with the addition of an aryl radical, generated from the corresponding aryldiazonium salt in the photocatalytic cycle, to the gold(I) catalyst. The resulting gold(II) intermediate **15** is further oxidized by the photocatalyst to afford the corresponding gold(III) complex **16**, that catalyzes the cyclization of the substrate. Finally, $C(sp^2)$–$C(sp^3)$ reductive elimination furnishes the cross-coupling product and closes the catalytic cycle by regenerating the gold(I) complex. Interestingly, the oxidation sequence was found to be almost barrierless and cyclization proved to be the rate-limiting step of the reaction (Scheme 14b).

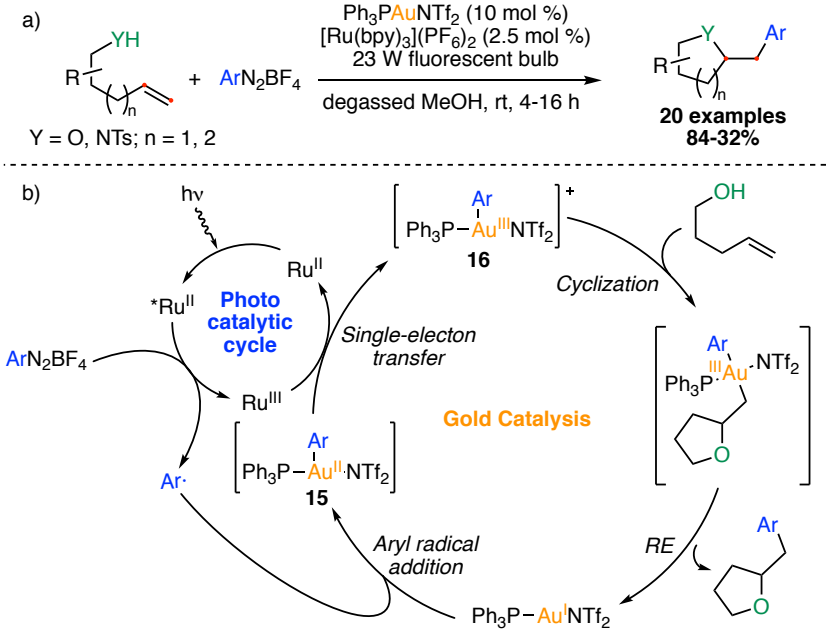

Scheme 14. (a) Dual gold-photoredox-catalyzed intramolecular oxy- and aminoarylation of alkenes in the presence of aryldiazonium salts; (b) plausible mechanism.

Shortly after, Toste and co-workers reported the dual gold-photoredox-catalyzed arylative ring expansion of vinylcyclopropanols and cyclobutanols into the corresponding arylated cyclobutanones and cyclopentanones (Scheme 15).[42] In line with the results described by Glorius,[40] only traces of product were obtained when the reaction was run in the absence of light, photocatalyst or gold catalyst. The different functional groups present in the reactants and the

40 Sahoo, B.; Hopkinson, M. N.; Glorius, F. *J. Am. Chem. Soc.* **2013**, *135*, 5505–5508.

41 Zhang, Q.; Zhang, Z.-Q.; Fu, Y.; Yu, H.-Z. *ACS Catal.* **2016**, *6* ,798–808.

42 Shu, X.-Z.; Zhang, M.; He, Y.; Frei, H.; Toste, F. D. *J. Am. Chem. Soc.* **2014**, *136*, 5844–5847.

product allowed the study of the mechanism by time-resolved FT-IR spectroscopy. As in the previous case, the stepwise oxidation of gold occurred in the first place. Then, the activation of the double bond by the gold(III) catalyst promotes the diastereoselective ring expansion. Reductive elimination closes the catalytic cycle and furnishes the final cyclic ketones.

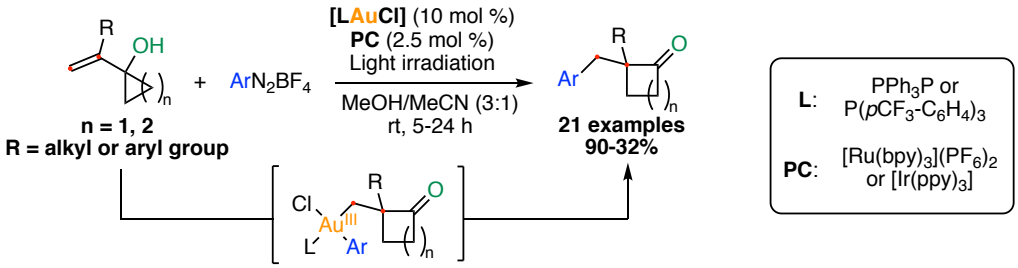

Scheme 15. Dual gold-photoredox-catalyzed arylative ring expansion.

This new catalytic system has allowed the development of several gold-catalyzed arylative transformations[43] such as tandem rearrangement/arylations,[44] nucleophilic addition/arylations,[45] diarylations[46] and cross-coupling reactions.[47]

Although the photoredox-assisted stepwise oxidation of gold(I) to gold(III) has been proposed as a common step in the catalytic cycle of these reactions, some of the above-mentioned transformations readily occur in the absence of light and photocatalyst.[47a,d] These results suggest the presence of a competitive chain propagation mechanism in which the photocatalytic cycle does not play any role, a hypothesis that was further supported by the measurement of quantum yields significantly higher than 1.

Confirming the feasibility of the photocatalyst-free oxidation of gold in the presence of diazonium salts, the group of Shi developed the gold-catalyzed Sandmeyer-type reaction. In this

43 Hopkinson, M. N.; Thahuext-Aca, A.; Glorius, F. *Acc. Chem. Res.* **2016**, *49*, 2261–2272.

44 (a) Patil, D. V.; Yun, H.; Shin, S. *Adv. Synth. Catal.* **2015**, *357*, 2622–2628. (b) Alcaide, B.; Almendros, P.; Busto, E.; Luna, A. *Adv. Synth. Catal.* **2016**, *358*, 1526–1533.

45 (a) Xia, Z.; Khaled, O.; Mouriès-Mansuy, V.; Ollivier, C. Fensterback, L. *J. Org. Chem.* **2016**, *81*, 7182–7190. (b) Qu, C.; Zhang, S.; Du, H.; Zhy, C. *Chem. Commun.* **2016**, *52*, 14400–14403. (c) Bansode, A. H.; Shaikh, S. R.; Gonnade, R. G.; Patil, N. T. *Chem. Commun.* **2017**, *53*, 9081–9084.

46 (a) Alcaide, B.; Almendros, P.; Busto, E.; Lázaro-Milla, C. *J. Org. Chem.* **2017**, *82*, 2177–2186. (b) Alcaide, B.; Almendros, P.; Busto, E.; Herrera, F.; Lázaro-Milla, C.; Luna, A. *Adv. Synth. Catal.* **2017**, *359*, 2640–3653. (c) Wang, Z.-S.; Tan, T.-D.; Wang, C.-M.; Yuan, D.-Q.; Zhang, T.; Zhu, P.; Zhu, C.; Zhou, J.-M.; Ye, L.-W. *Chem. Commun.* **2017**, *53*, 6848–6851.

47 (a) Y. He, H. Wu, F. D. Toste, Chem. Sci. 2015, 6, 1194 – 1198. (b) Thahuext-Aca, A.; Hopkinson, M. N.; Sahoo, B.; Glorius, F. *Chem. Sci.* **2016**, *7*, 89–93. (c) Kim, S.; Rojas-Martín, J.; Toste, F. D. *Chem. Sci.* **2016**, *7*, 85–88. (d) Cornilleau, T.; Hermagne, P.; Fouquet, E. *Chem. Commun.* **2016**, *52*, 10040–10043. (e) Gauchot, V.; Sutherland, D. R.; Lee, A.-L. *Chem. Sci.* **2017**, *8*, 2885–2889. (f) Chakrabarty, I.; Akram, M. O.; Biswas, S.; Patil, N. T. *Chem. Commun.* **2018**, *54*, 7223–7226.

case, the decomposition of the aryldiazonium salt is enabled by the use of a nucleophile that also acts as a coupling partner.[48] The transformation worked efficiently in the absence of photocatalyst and the presence of light did not affect significantly the outcome of the reaction. A variety of new C–Br, C–S and C–P bonds could be formed in good yields and the detection of gold(III) intermediates by ESI-MS evidenced the redox-active character of gold in catalytic cycle (Scheme 16).

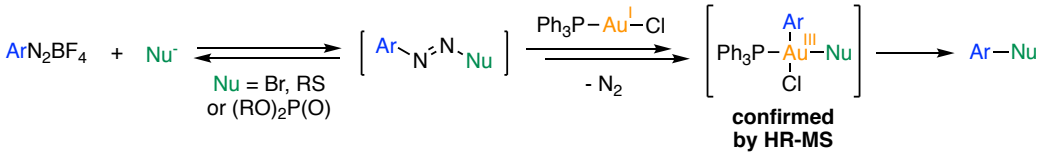

Scheme 16. Gold-catalyzed Sandmeyer-type reaction.

The same group demonstrated the usefulness of the base-mediated decomposition of aryldiazonium salts in a variety of gold-catalyzed cross-coupling reactions previously performed in the presence of a photocatalyst.[49]

In 2018, Patil and co-workers described the gold-catalyzed crossed-coupling of aryldiazonium salts which organostannanes.[50] In this work, the mechanism for the oxidation of gold in the absence of the photoredox cycle is discussed. Thus, after the initial Sn–Au transmetalation, gold(I) complex **17** can undergo a two-electron oxidative process with the diazonium salt to form gold(III) intermediate **18**,[51] that upon a transmetalation/N_2 extrusion sequence affords gold(III) species **19**. Alternatively, the oxidation can take place in a stepwise manner going through gold(II) complex **20**. In this case, a second equivalent of aryldiazonium further oxidizes **20** to generate **21** that, upon transmetalation, forms gold(III) species **19**. In both cases, RE closes the cycle delivering the biaryl products (Scheme 17).

48 Peng, H.; Cai, R.; Xu, C.; Chen, H.; Shi, X. *Chem. Sci.* **2016**, *7*, 6190–6196.

49 Dong, B.; Peng, H.; Motika, S. E.; Shi, X. *Chem. Eur. J.* **2017**, *23*, 11093–11099

50 Akram, M. O.; Shinde, P. S.; Chintawar, C. C.; Patil, N. T. *Org. Biomol. Chem.* **2018**, *16*, 2865–2869.

51 Cai, R.; Lu, M.; Aguilera, E. Y.; Xi, Y.; Akhmedov, N. G.; Petersen, J. L.; Chen, H.; Shi, X. *Angew. Chem. Int. Ed.* **2015**, *54*, 8772–87776

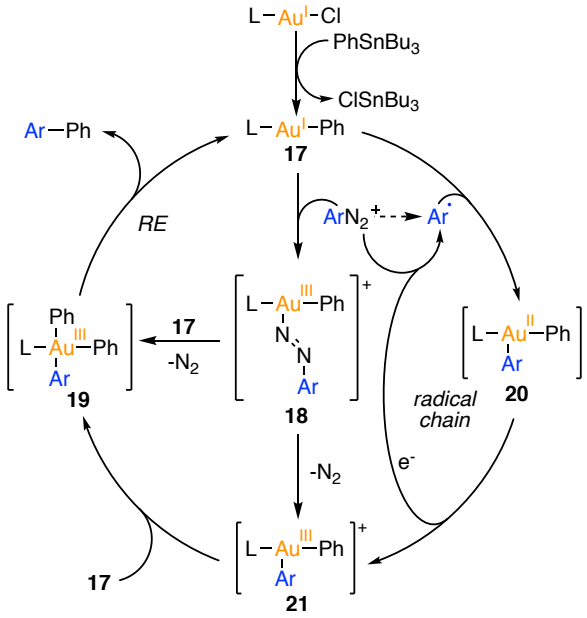

Scheme 17. Proposed mechanism for the gold-catalyzed coupling of arylstannanes with aryldiazonium salts.

In parallel, the group of Hashmi discovered that the oxidation of gold could be achieved in the absence of photocatalyst under the irradiation of UV/visible light. This concept was applied in the gold-catalyzed cross-coupling of arylboronic acids with aryldiazonium salts[52] as well as in the 1,2-difuntionalization of alkynes.[53] Theoretical studies on the latter reaction predicted that the adduct formed upon interaction of the gold complex with the diazonium salt could play the role of photosensitizer.[54]

Miscellaneous Methods

The gold-catalyzed alkynylation of sp^2 and sp carbons has also been reported in the absence of sacrificial oxidants. In 2019, the group of Hashmi reported the coupling of stable alkenylgold(I) complexes[55] with bromoalkynes.[56] This discovery led to the development of the gold-catalyzed cyclization/alkynylation cascade reaction of allenoates like **22** (Scheme 18). Although the order of the events in the catalytic cycle could not be disambiguated (cyclization/OA *vs* OA/cyclization), a mechanism involving the OA of bromoalkynes was proposed and supported by the detection of alkynylgold(III) complexes by ESI-MS experiments.[56]

52 Witzel, S.; Xie, J.; Rudolph, M.; Hashmi, A. S. K. *Adv. Synth. Catal.* **2017**, *359*, 1522–1528.

53 Huang, L.; Rudolph, M.; Rominger, F.; Hashmi, A. S. K. *Angew. Chem. Int. Ed.* **2016**, *55*, 4808–4813.

54 Liu, Y.; Yang, Y.; Zhu, R.; Liu, C.; Zhang, D. *Chem. Euc. J.* **2018**, *24*, 14119–14126.

55 Liu, L.-P.; Xu, B.; Mashuta, M. S.; Hammond, G. B. *J. Am. Chem. Soc.* **2008**, *130*, 17642–17643.

56 Yang, Y.; Schieβs, J.; Zallouz, S.; Göker, V.; Gross, J.; Rudolph, M.; Rominger, F.; Hashmi, A. S. K. *Chem. Eur. J.* **2019**, *25*, 9624–9628.

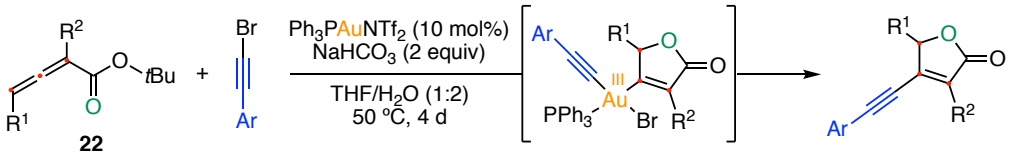

Scheme 18. Gold-catalyzed cyclization/alkynylation cascade reaction of allenoates **22**.

Using a completely different approach, Fensterbank et al. achieved the OA of iodoalkynes to gold(I) centers in the presence of a photocatalyst. The reactivity was applied in the tandem cyclization/alkynylation of *o*-(alkynyl)phenols like **23** to yield benzofurans.[57] A meticulous luminescence study, supported by DFT calculations allowed the proposal of a plausible mechanistic scenario involving an energy transfer event from the blue LED-excited iridium photocatalyst to the vinylgold(I) intermediate **24** generated upon 5-*endo*-dig cyclization of the substrate. The resulting photosensitized gold(I) catalyst **25** and the iodoalkyne readily engage in OA process. Finally, *trans/cis* isomerization followed by reductive elimination furnishes the alkynylated benzofuran products (Scheme 19).

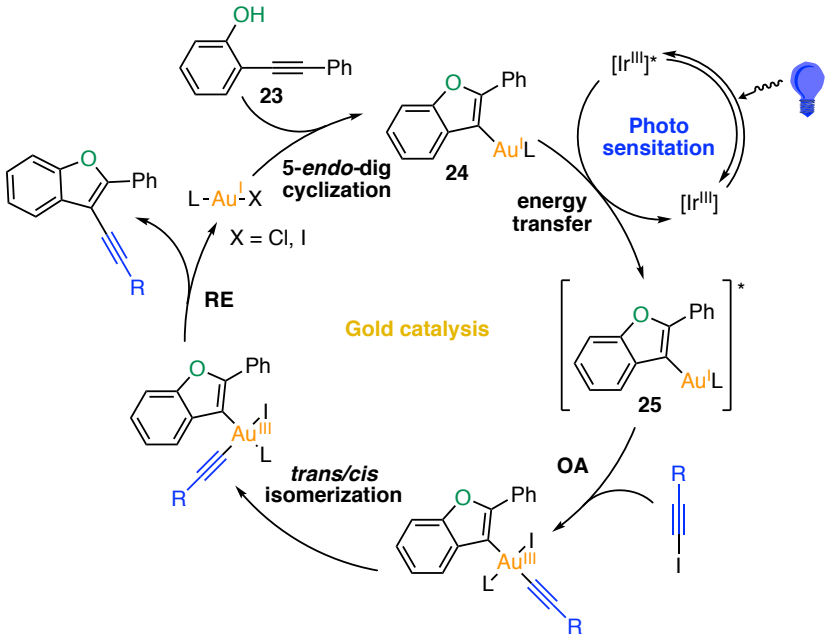

Scheme 19. Plausible mechanism for the gold-catalyzed tandem cyclization/alkynylation of **23**. [Ir] = $Ir[dF(CF_3)ppy]_2(dtbbpy)PF_6$; L = $P(pCF_3\text{-}C_6H_4)_3$.

Recently, electrochemistry has emerged as an efficient alternative to sacrificial oxidants for the oxidation of gold(I) to gold(III). In a pioneering work using this approach, Shi and co-workers developed the gold-catalyzed homo- and cross-coupling of terminal alkynes.[58]

57 Xia, Z.; Corcé, V.; Zhao, F.; Przybylski, C.; Espagne, A.; Jullien, L.; Le Saux, T.; Gimbert, Y.; Dossmann, H.; Mouriès-Mansuy,V.; Ollivier, C.; Fensterbank, L. *Chem. Sci.* **2019**, *11*, 797–805.

58 Ye, X.; Zhao, P.; Zhang, S.; Zhang, Y.; Wang, Q.; Shan, C.; Wojtas, L.; Guo, H.; Chen, H.; Shi, X. *Angew. Chem. Int. Ed.* **2019**, *58*, 17226–17230.

Objectives

The main goal of the work summarized in this chapter was to develop a new reactivity by merging the well-known gold-catalyzed alkoxycyclization of enynes with the arylation methodologies enabled by gold(I)/gold(III) cycles in the presence of diazonium salts (Scheme 20).

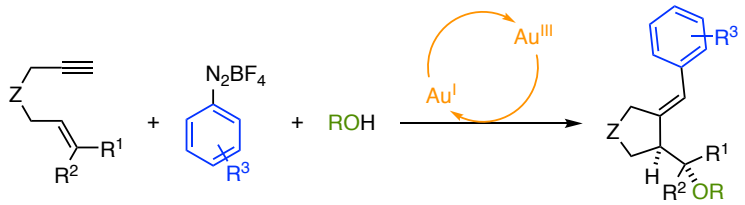

Scheme 20. Gold-Catalyzed arylative cyclization of enynes.

The task was divided into three different parts:

- Find the optimal conditions for the reaction to proceed.
- Evaluate the reaction scope by modifying the different partners involved.
- Perform control experiments to have a better understanding about the reaction mechanism.

Results and Discussion

Optimization

Initially, we decided to apply the dual gold-photoredox catalysis strategy, since this approach had been successfully applied in similar tandem rearrangement/arylation transformations.[40,45] A desk lamp with a 23 W fluorescent bulb was used as a visible-light source and a cryocooler allowed the control of the reaction temperature (Figure 1).

Figure 1. Set-up for the arylative cyclization of enynes.

Enyne **26a** was used as a model substrate for two different reasons. First, the presence of the *gem*-diesther moiety at the tether facilitates the cyclization by bringing the alkene and the alkyne closer in space (Thorpe-Ingold effect).[59] Second, since the cyclization of **26a** is well studied, the identifications of the side products generated during the reaction was relatively easy.

For the first tentative of converting **26a** into the arylated cyclized product **27a** in the presence of phenyldiazonium tetrafluoroborate **30a**, [(Ph_3P)AuCl] was used as gold catalyst and [$Ru(bpm)_3$]Cl_2 as photocatalyst. Running the reaction methanol at 25 ºC led to the formation of the desired product in 21% yield along with 43% of terminal alkene **28a** and 10% of internal alkyne **29a** (Scheme 21). Interestingly, the configuration of the alkene in **27a** is opposite to the one obtained in previously reported gold(I)-catalyzed methoxycyclization of enyne **26a**.[60,61]

59 (a) Beesley, R. M.; Ingold, C. K.; Thorpe, J. F. *J. Chem. Soc., Trans.* **1915**, *107*, 1080–1106. (b) Jung, M. E.; Piizi, G. *Chem. Rev.* **2005**, *105*, 1735–1766.

60 (a) Nieto-Oberhuber, C.; Muñoz, M. P.; Buñuel, E.; Nevado, C.; Cardenas, D. J.; Echavarren, A. M. *Angew. Chem. Int. Ed.* **2004**, *43*, 2402−2406. (b) Nieto-Oberhuber, C.; López, S.; Echavarren, A. M. *J. Am. Chem. Soc.* **2005**, *127*, 6178–6179.

61 The configuration of the alkene was determined by NMR studies (see Experimental Section for more details).

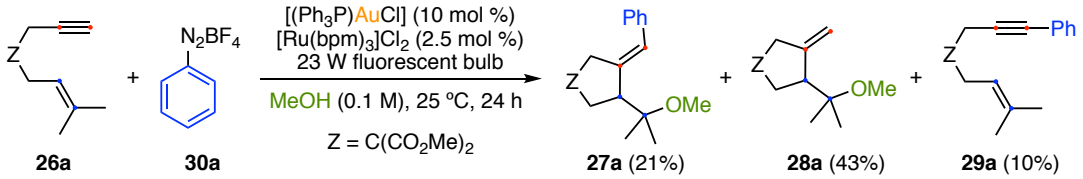

Scheme 21. Dual gold-photoredox-catalyzed arylative cyclization of enyne **26a**; first try. bpm = 2,2'-bipyrimidine.

We rationalized that the formation of products **28a** over **27a** resulted from the competition between protodeauration and reductive elimination from gold(III) intermediate **31a** (Scheme 22). On the other hand, product **29a** could arise from the direct dual gold-photoredox-catalyzed cross-coupling of the terminal alkyne with the aryldiazonium salt.[47b]

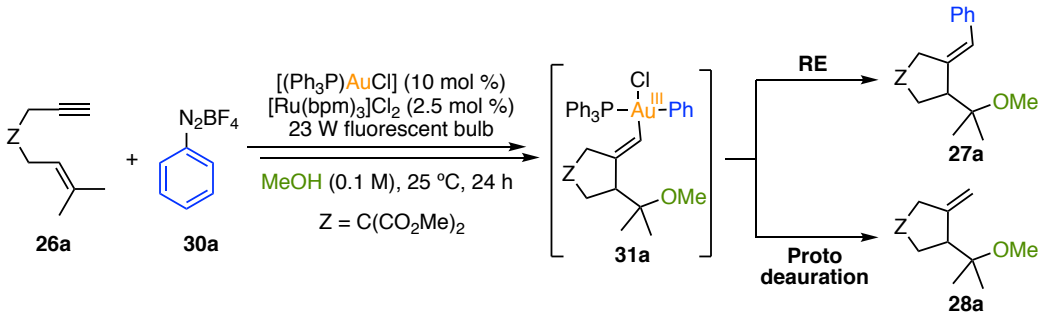

Scheme 22. Plausible formation of products **27a** and **28a**.

Encouraged by this first result we then performed a screening of gold(I) complexes (Table 1). Modifying the electronic properties on the [(Ar_3P)AuCl] complex pointed out that electron-donating phosphine ligands favored the formation of **27a** over **28a** (Table 1, entries 1-7). Following this trend, we then examined the performance of highly electron-donating trialkylphosphine ligands (Table 1, entries 8-10). Better yields and selectivities towards the formation of **27a** were observed in all cases and trimethylphosphinegold(I) chloride stood out as the best catalyst for the transformation. The more electrophilic methylphosphite analogue led to significant lower yields, highlighting the importance of the electronic properties of the catalyst (Table 1, entry 11). The use of other phosphites (Table 1, entry 12), bulkier phosphines (Table 1, entries 13-15) or NHC ligands (Table 1, entry 16) resulted in no formation of the desired product. Further comparison between Entries 1, 2, 13, and 14 revealed that an increase of the steric bulk in the proximity of the phosphorus center hampers the formation of the arylated product.

Table 1. Screening of gold(I) complexes.[a]

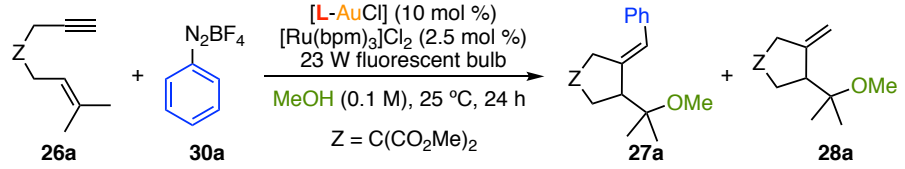

26a 30a 27a 28a

Entry	Ligand (L)	Yield 27a (%)[b]	Yield 28a (%)[b]
1	PPh_3	21	46
2	(oMe-C_6H_4)$_3$P	-	-
3	(pCF$_3$-C_6H_4)$_3$P	18	64
4	(pOMe-C_6H_4)$_3$P	39	33
5[c]	**P**	54	-
6[c]	(pNMe$_2$-C_6H_4)$_3$P	34	47
7[c]	(C_6F_5)$_3$P	-	52
8	PCy_3	54	20
9[c]	PEt_3	68	15
10	PMe_3	70	11
11	$P(OMe)_3$	28	10
12[c]	**Q**	-	6
13[d]	JohnPhos	-	42
14	(1-naphthyl)$_3$P	-	56
15[c]	**R**	-	83
16	IPr	-	8

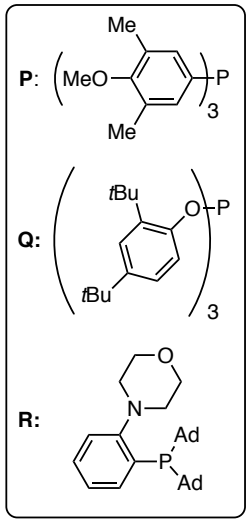

[a] In some cases, Sonogashira product **29a** could be observed by ^{1}H NMR (10 % yield maximum). [b] Yields determined by ^{1}H NMR using 3,5-dimethylpyrazole as internal standard. [c] Reaction conducted at 0.04 M. [d] Reaction conducted at -10 ºC in MeOH/AcOEt (1:1).

The effect of different light sources and photocatalysts was evaluated (Table 2). Constant irradiation at 450 nm, where $[Ru(bpm)_3]^{2+}$ presents a maximum of absorbance,[62] gave slightly worse results (Table 2, entries 1-2). Surprisingly, when the reaction was run in the dark by covering the Schlenk flask with aluminum foil, **27a** was detected in 18% yield (Table 2, entry 3). To verify that no traces of light were catalyzing the reaction, a similar experiment was carried out in a dark laboratory equipped with red lights (Table 2, entry 4). The reproducibility of the reaction outcome supported the feasibility of the transformation in the absence of light and suggested the presence of an alternative mechanism where the photoredox cycle is not involved.

Regarding the nature of the photocatalyst, structurally similar $[Ru(bpz)_3](PF_6)$ performed slightly better (Table 2, entry 5) while less oxidizing $[Ru(bpy)_3]^{2+}$ species afforded the product in lower yields (Table 2, entries 6-7).[62,63] In contrast, no conversion was observed when the more rigid $[Ru(phen)_3]Cl_2$ was used (Table 2, entry 8).

62 http://chemlabs.princeton.edu/macmillan/wp-content/uploads/sites/6/Merck-Photocatalysis-Chart.pdf

63 For a report on the redox potentials of Ru photocatalyst, see: Prier, C. K.; Rankic, D. A.; MacMillan, D. W. C. *Chem. Rev.* **2013**, *113*, 5322−5363.

Table 2. Screening of light sources and photocatalysts.[a]

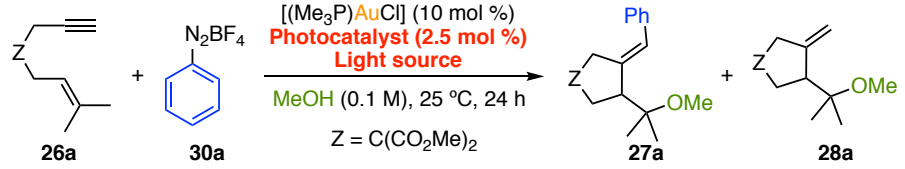

Entry	Photocatalyst	Light source	Yield 27a (%)[a]	Yield 28a (%)[a]
1	$[Ru(bpm)_3]Cl_2$	23 W CLF	70	11
2	$[Ru(bpm)_3]Cl_2$	Blue led (450 nm)	63	14
3	$[Ru(bpm)_3]Cl_2$	Dark	18	21
4	$[Ru(bpm)_3]Cl_2$	Dark lab (red light)	19	13
5	$[Ru(bpz)_3](PF_6)_2$	23 W CLF	72	10
6	$[Ru(bpy)_3]Cl_2 \cdot 6H_2O$	23 W CLF	61	5
7	$[Ru(bpy)_3](PF_6)_2$	23 W CLF	59	14
8	$[Ru(phen)_3]Cl_2$	23 W CLF	-	-

[a] Yields determined by ^{1}H NMR using 3,5-dimethylpyrazole as internal standard.

bpy = 2,2'bipyridine; bpz = 2,2'bipyrazine; bpm = 2,2'bipyrimidine; phen = phenanthroline

Further experiments allowed the adjustment of the optimal reaction conditions (Table 3). Upon screening of different co-solvents (Table 3, entries 1-4), concertations (Table 3, entries 5-6) and temperatures (Table 3, entries 7-8), the best result was obtained while running the reaction in a 0.04 M (1:1) mixture of methanol and acetonitrile at -15 ºC (Table 3, entry 3). Interestingly, no formation of **28a** was observed at temperatures below 0 ºC.

Table 3. Screening of solvents, concentrations and temperatures.

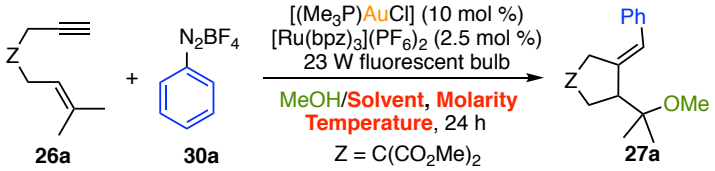

Entry	Solvent	Concentration (M)	T (ºC)	Yield 27a (%)[a]
1	MeOH	0.04	-15	81
2	MeOH/Dioxane (1:1)	0.04	-15	31
3	MeOH/MeCN (1:1)	0.04	-15	90
4	MeOH/AcOEt (1:1)	0.04	-15	61
5	MeOH/MeCN (1:1)	0.10	-15	64
6	MeOH/MeCN (1:1)	0.02	-15	87
7	MeOH/MeCN (1:1)	0.04	0	73
8	MeOH/MeCN (1:1)	0.04	-10	78

[a] Yields determined by ^{1}H NMR using 3,5-dimethylpyrazole as internal standard.

Finally, the possibility of developing a photocatalyst-free version of the reaction was investigated (Table 4). In the absence of additives, product **28a** was formed predominantly and only traces of the arylated product were observed (Table 4, entry 1). However, when the reaction was run at 0 ºC, only traces of the terminal alkene were observed and **27a** was formed in 39% yield (Table 4, entry 2). As in the presence of photocatalyst, below 0 ºC the formation of **28a** was unfavored. This observation suggests that, despite the different reaction conditions, the rate-

limiting step for the formation of **27a** is similar in both cases and the same gold intermediate is involved. Next, we studied the effect of different additives on the reaction. Although acceptable yields were obtained using sodium or potassium carbonate (Entries 3-4), the presence of a base also facilitated the formation of **29a**, presumably by assisting deprotonation of the terminal alkyne, leading to undesired mixtures of products (Table 4, entries 3-8). Likewise, the presence of organic (Table 4, entry 9) or inorganic (Table 4, entries 10-13) reducing agents afforded unproductive mixtures of products. Further attempts to improve the results obtained using sodium and potassium carbonate as additives were unsuccessful (Table 4, entries 14-16).

Table 4. Screening of additives in the absence of photocatalyst

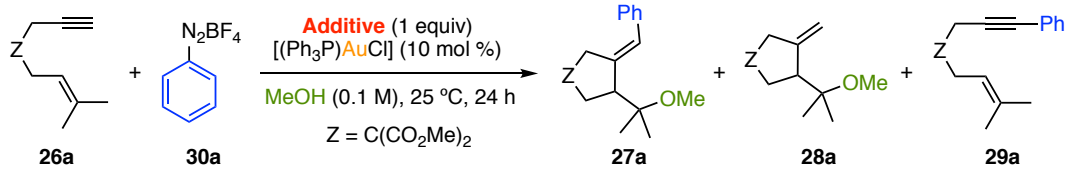

Entry	Additive	Yield 27a (%)[a]	Yield 28a (%)[a]	Yield 29a (%)[a]	RSM[b] (%)[a]
1	-	< 5	70	-	14
2[c]	-	39	< 5	-	26
3	Na_2CO_3	40	-	55	-
4	K_2CO_3	52	8	35	-
5	Cs_2CO_3	-	-	20	76
6	NaOAc	< 5	25	63	5
7	KOAc	< 5	41	47	5
8	KOH	32	39	10	-
9	TTF	45	8	-	21
10	CuCl	29	39	-	-
11	CuCN	13	10	-	69
12	$FeCl_2$	25	48	-	16
13	$CrCl_2$	22	43	-	20
14[c]	Na_2CO_3	21	-	32	30
15[c]	K_2CO_3	25	-	16	38
16[d]	K_2CO_3	55	17	12	-

[a] Yields determined by ^{1}H NMR using 3,5-dimethylpyrazole as internal standard.

[b] Recovered starting material. [c] Reaction conducted at 0 ºC. [d] Reaction conducted in the dark.

Reaction Scope

The scope of the reaction was studied using the optimized conditions in the presence of photocatalyst. Our attention was first focused in the diversity of nucleophiles that could be incorporated (Scheme 23). In a control experiment, similar reactivity was observed using 10 equivalents of nucleophile in acetonitrile instead of a (1:1) mixture. Therefore, the scope of nucleophiles was evaluated using this modification.

Primary and secondary alcohols delivered the corresponding arylated products **27a-c** in good yields. Nevertheless, *tert*-butanol proved to be too sterically hindered to attack and **27d** could not be detected. **27e** could be isolated in 60% yield, without observation of by-products

related to the propargyl alcohol, showing the excellent selectivity of the reaction toward arylative enyne alkoxycyclization. Benzyl alcohol afforded **27f** in 51% yield. Lower reactivity was observed while using allyl alcohol, obtaining **27g** in 35%. This could arise from the consumption of the aryl radicals by a side reactivity with the alkene moiety. The presence of water in the reaction mixture was well-tolerated and alcohol **27h** could be isolated in 67% yield. Unfortunately, using acetic acid or the HF·Et_3N resulted in low reactivity and only traces of **27i** and **27j** were detected. When the reaction was run in the absence of an external nucleophile, lower conversions were achieved and inseparable mixtures of products were obtained. GC-MS analysis confirmed the presence of four isomers of **26a** together with two arylated isomers and **29a**.

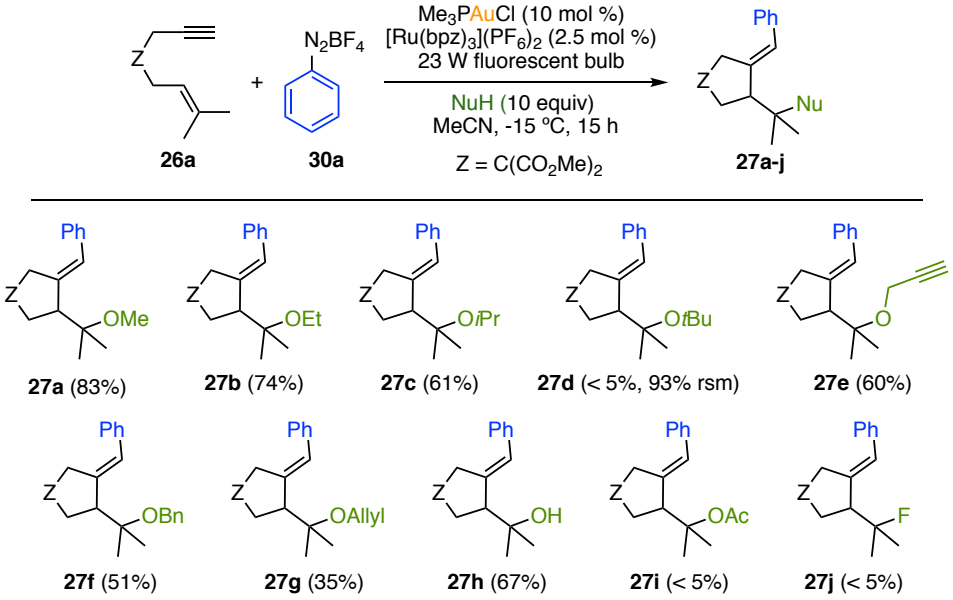

Scheme 23. Scope of nucleophiles in the gold-photoredox-catalyzed arylative cyclization of **26a**. Isolated yields given in parenthesis for **27a-c** and **27e-h**.

Encouraged by our initial results, we then turned our attention to the screening of aryldiazonium salt. As summarized in Scheme 24, differently *para*-substituted aryldiazonium salts could be employed. Thus, diazonium salts with halogen atoms in *para* position, F, Cl, Br and I delivered the corresponding arylated cyclized compounds **27k-n** in 71%, 59%, 63% and 38% yield, respectively. These results highlight the orthogonality of this method with the traditional palladium-catalyzed cross-coupling transformations. Other electron-withdrawing groups such as *p*-CF_3, *p*-CN, *p*-CO_2Et and *p*-NO_2 aryldiazonium salts were also reactive and gave the corresponding products (**27o-r**) in moderate to good yields (50% - 71%). Steric hindrance did not affect negatively the reaction in this position. Indeed, products **27s** and **27t** were isolated in 71% and 67% yields, respectively. Arenediazonium salts bearing electron-donating substituents at the *para* position (Me and OMe), delivered products **27u** and **27v** in 72% and 40% upon treatment with the optimized reaction conditions. Electronic and steric effects were tested in *meta* and *ortho* positions by reacting the corresponding Me, OMe, F and Br substituted diazonium salts. To our

delight, products **27w-ad** were obtained in good yields regardless of the substituents on the diazonium salt, which remarks the high tolerance of functional groups and substitution patterns of the reaction.

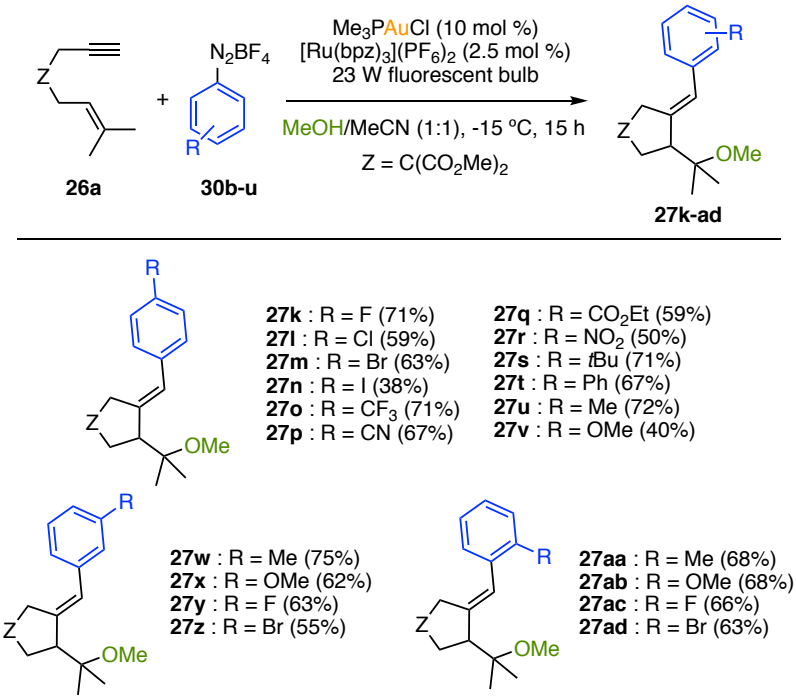

Scheme 24. Scope of aryldiazonium salts in the gold-photoredox-catalyzed arylative cyclization of **26a**. Isolated yields given in parenthesis for **27k-ad**.

We next sought to investigate the reactivity of different alkyl radical precursors under the optimized reaction conditions. To this end, the reaction was performed in the presence of redox-active ester **32**[64] or Katritzky pyridinium **33** (Scheme 25).[65] Unfortunately, no conversion was observed even at higher temperatures and the corresponding alkylated product **27ae** could not be detected.

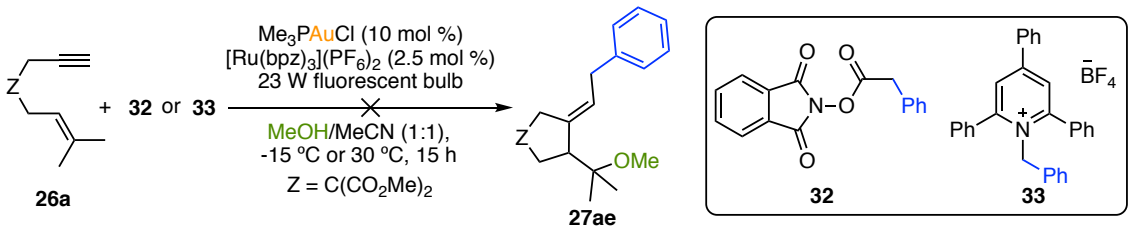

Scheme 25. Attempts on the gold-photoredox-catalyzed alkylative cyclization of **26a**.

64 (a) Toriyama, F.; Cornellà, J.; Wimmer, L.; Chen, T.-G.; Dixon, D. D.; Creech, G.; Baran, P. S. *J. Am. Chem. Soc.* **2016**, *138*, 11132–11135. (b) Niu, P.; Li, J.; Zhang, Y.; Huo, C. *Eur. J. Org. Chem.* **2020**, 5801–5814.

65 (a) Katritzky, A. R.; Thind, S. S. *J. Chem. Soc., Perkin Trans. 1*, **1980**, 1895–1900 (b) Correia, J. T. M.; Fernandes, V. A.; Matsuo, B. T.; Delgado, J. A. C.; de Souza, W. C.; Paixão, M. W. *Chem. Commun.* **2020**, *56*, 503–514.

Alternatively, we hypothesized that the aryl radical generated upon decomposition of diazonium salt **30v**, bearing a *tert*-butyl group in the *ortho* position, could generate a more stable alkyl radical through a hydrogen atom transfer. The addition of this radical to the gold(I) catalyst would enable the stepwise OA and eventually deliver the alkylated product **27af** in the presence of enyne **26a** (Scheme 26). However, **30v** decomposed violently during its isolation.[66]

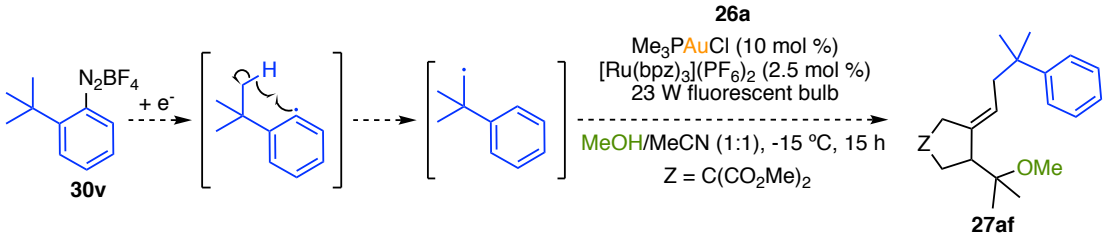

Scheme 26. Attempts on the gold-photoredox-catalyzed alkylative cyclization of **26a**.

The scope of enynes was also evaluated (Scheme 27).[67] Moving from the prenyl chain to the corresponding geranyl afforded product **27ag** in 66% isolated yield as a single diastereomer. Enynes bearing a styrene moiety proved to be active providing **27ah-aj** diastereoselectively in 69%, 75% and 79% yield respectively. Modifications on the tether moiety were also tolerated giving rise to products **27ai-am** in moderate to good yields. Unfortunately, internal alkynes were unreactive even at higher temperatures (**27an**).

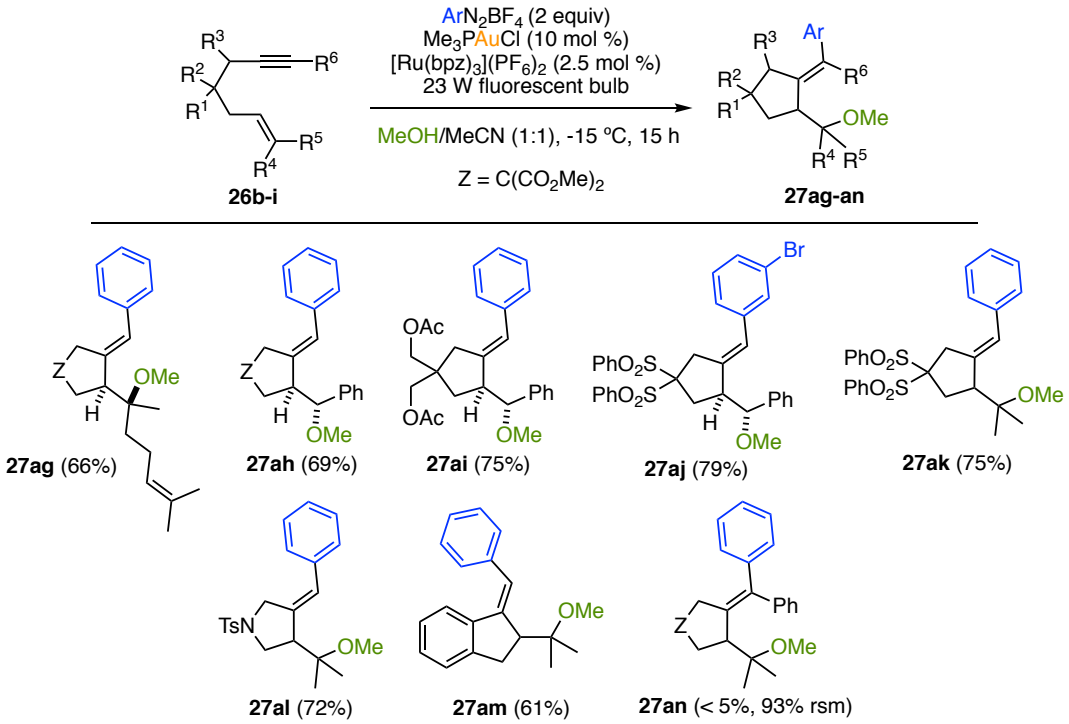

Scheme 27. Gold-photoredox-catalyzed arylative cyclization of enynes **26b-i**.

66 Firth, J. D.; Fairlamb, I. J. S. *Org. Lett.* **2020**, *22*, 7057–7059.

67 All enynes (**26b-k**) were prepared following reported procedures (see Experimental Section for more details).

In an attempt to extend the scope of the transformation to smaller and larger enynes, 1,5-enyne **26j** and 1,7-enyne **26k** were also submitted to the reaction conditions.[67] In this case, no formation of the arylated products **27ao** or **27ap** was observed (Scheme 28).

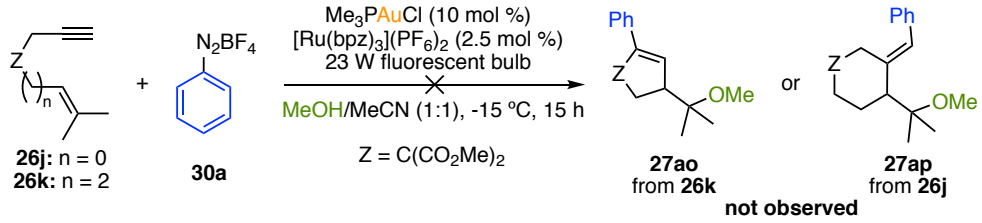

Scheme 28. Unsuccessful gold-photoredox-catalyzed arylative cyclization of **26j** and **26k**.

The development of asymmetric gold(III) transformations is a challenging topic in field homogeneous gold catalysis.[68] This is meanly due to the difficulties associated with synthesis of stable but catalytically active gold(III) complexes.[69] The group of Fouquet investigated the possibility of synthetizing enantioselectivity atropoisomers *via* gold-catalyzed cross-coupling of aryldiazonium salts with boronic acids.[70] Although modest enantioselectivities were obtained (up to 26%), this is the only reported example where chirality has been induced in a gold(I)/gold(III)-promoted reaction. We also explored the possibility of rendering the gold-catalyzed arylative cyclization of enynes enantioselective by using chiral gold(I) complexes **S** and **T**, bearing ligands frequently used in asymmetric gold(I) catalysis. Nonetheless, no formation of product **27a** was observed in any case. These results are in agreement with the results obtained during the catalyst screening, where bulky phosphines and phosphites failed to yield the arylated product (Table 1, Entries 12-15). We rationalized that catalyst **U** featuring a (trialkylphosphine)gold(I) chloride moiety would be a superior chiral catalyst for the transformation. In this case, **27a** could be isolated in 35% yield but chiral HPLC analysis showed that the product was obtained as a racemic mixture (Table 5, catalysts shown in the next page).

Table 5. Screening of chiral gold(I) complexes.[a]

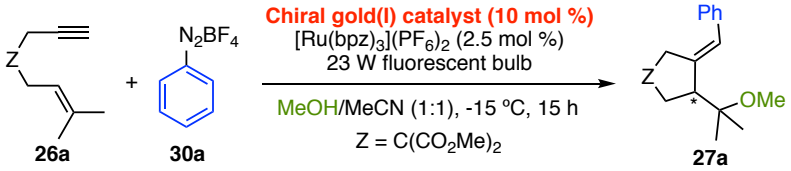

Entry	Gold complex	Yield 27a (%)[a]	*ee* 27a (%)
1	S	-	-
2	T	-	-
3	U	35	<1

[a] Yields determined by ^{1}H NMR using 3,5-dimethylpyrazole as internal standard.

68 For an example of asymmetric gold(III) catalysis, see: Bohan, P. T.; Dean Toste, F. *J. Am. Chem. Soc.* **2017**, *139*, 11016–11019.

69 (a) Rocchigiani, L.; Bochmann, M.; *Chem. Rev.* **2020**, DOI: 10.1021/acs.chemrev.0c00552. (b) Wu, C. Y.; Horibe, T.; Jacobsen, C. B.; Toste, F. D. *Nature* **2015**, *517*, 449–454.

70 Tabey, A.; Berlande, M.; Hermange, P.; Fouquet, E. *Chem. Commun.* **2018**, *54*, 12867–12870.

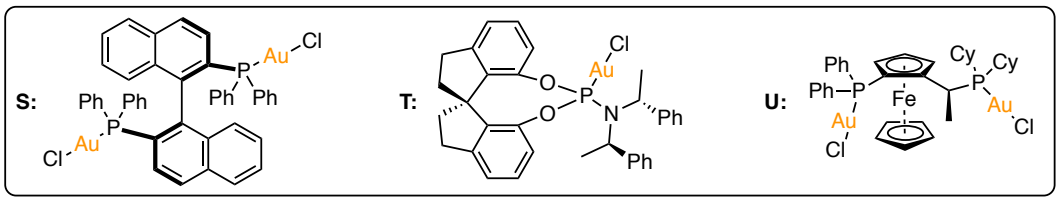

Mechanistic investigations

The mechanism of the gold-catalyzed arylative cyclizations of enynes was studied experimentally. Control experiments showed that, in the absence of gold, no conversion of the starting enyne **26a** takes place. Likewise, only starting material was found in a control reaction in the absence of arenediazonium salt and photocatalyst (Scheme 29a). The fact that (trimethylphosphine)gold(I) chloride was not able to catalyzed the cyclization of **26a** to give **28a** suggests that oxidation of gold(I) to gold(III) takes place in first place, followed by π-activation and reductive elimination. Indeed, the reaction of Me_3PAuCl with diazonium salt **30w** led to the formation of gold(III) complex **34**, reinforcing the idea of a direct interaction between the gold catalyst and the diazo compound (Scheme 29b).[71] The structure of **34** was determined by single crystal X-ray crystallography.

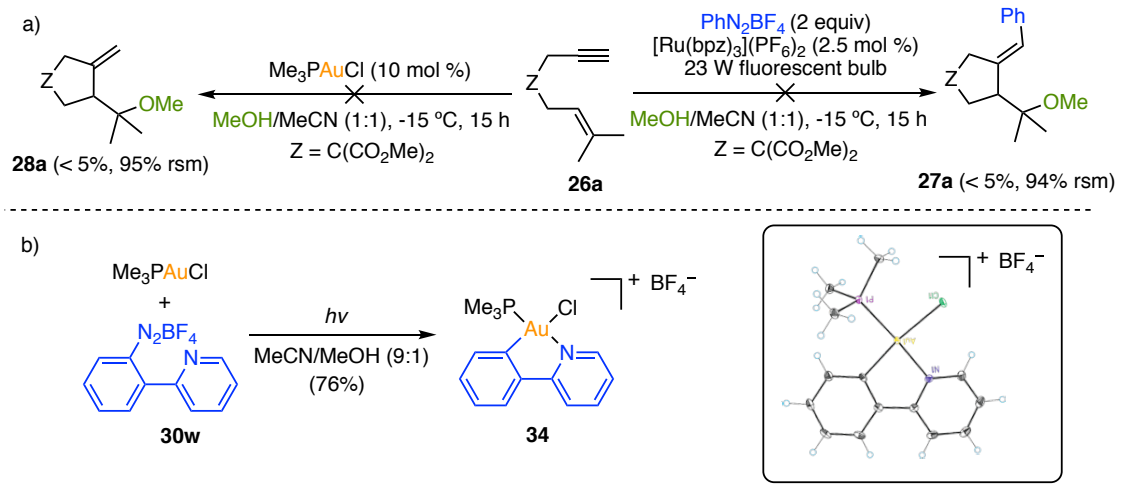

Scheme 29. a) Control experiment in the absence of: diazonium salt and photocatalyst (left); gold catalyst (right). b) Synthesis of gold(III) complex **34**.

As stated in the optimization section, the reaction worked in the absence of light. Running the reaction in the dark under the optimized conditions afforded **27a** in 19% yield and 49% yield if the photocatalyst was also excluded from the set up. This shows that gold catalytic turnover could happen in the absence of the photocatalytic cycle. In this scenario, small amounts of aryl radicals could be first generated upon thermal decomposition or nucleophile-mediated degradation of diazonium salts (dashed arrow). Upon addition to the gold(I) catalyst, the resulting

71 Tlahuext-Aca, A.; Hopkinson, M. N.; Daniliuc, C. G.; Glorius, F. *Chem. Eur. J.* **2016**, *22*, 11587–11592.

gold(II) intermediate **I** further oxidizes to gold(III) complex **II** by reducing the aryldiazonium salt to the corresponding aryl radical through a radical chain mechanism. Subsequent gold(III)-catalyzed 5-*exo*-dig alkoxycyclization of enyne **26** delivers alkenyl gold(III) species **III**[72] that undergoes reductive elimination furnishing the arylated product **27**. Alternatively, the oxidation of gold(I) to gold(III) could take place *via* a two-electron oxidative process with the diazonium salt (Scheme 30).[50,51]

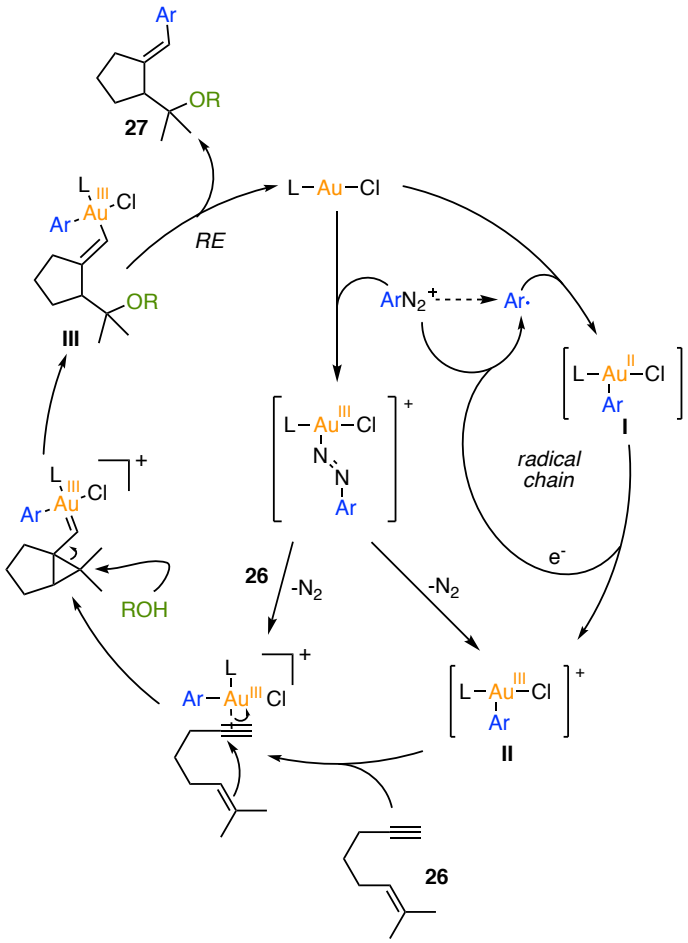

Scheme 30. Proposed mechanism for the gold-catalyzed arylative cyclization of enyne **26** in the absence of photocatalytic cycle. L = Trimethylphosphine.

Although these pathways might still operate in the presence of the photocatalytic cycle, the difference in reactivity between the two scenarios implies a change in the overall mechanistic picture. Based on previous reported studies,[41] we propose that the role of the photocatalytic cycle is to assist the oxidation of gold by promoting the production of aryl radicals in a more favorable manner and facilitating the oxidation of the proposed gold(II) intermediate **I** to gold(III) species **II** (Scheme 31).

72 Reiersølmoen, A. C.; Csókás, D.; Pápai, I.; Fiksdahl, A.; Erdélyi, M. *J. Am. Chem. Soc.* **2019**, *141*, 18221–18229.

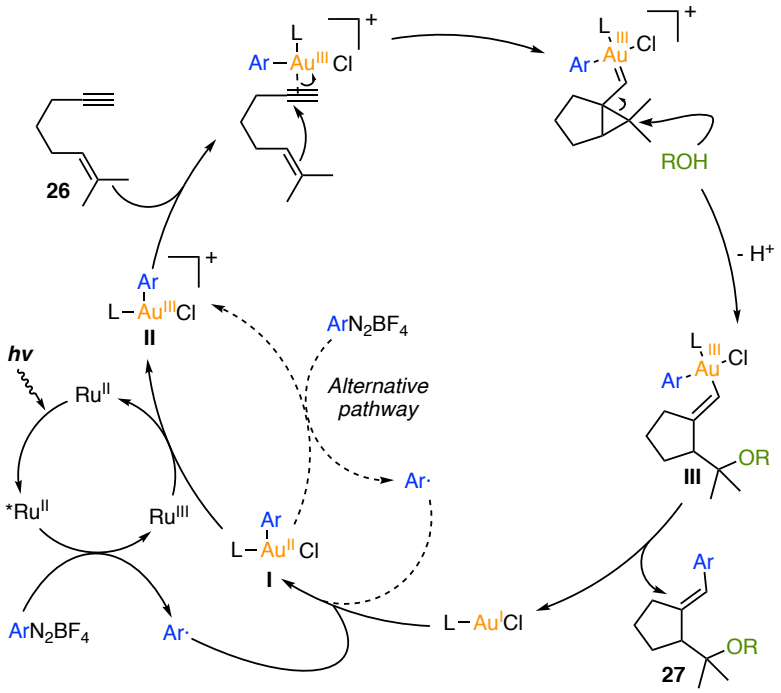

Scheme 31. Proposed mechanism for the gold-catalyzed arylative cyclization of enyne **26** in the presence of photocatalytic cycle. L = Trimethylphosphine.

Finally, we studied the possibility that the system proceeded *via* a Sonogashira type coupling of the alkyne of enynes **26**[47b] followed by a gold-catalyzed enyne alkoxycyclization[60a] and isomerization of the aryl-substituted alkene (Scheme 32a). However, compound **35a** with a *Z*-configured alkene prepared by our reported procedures,[60a] did not undergo *Z* to *E* isomerization to form **27a** under the optimized reaction conditions, discarding the feasibility of this alternative mechanism (Scheme 32b).

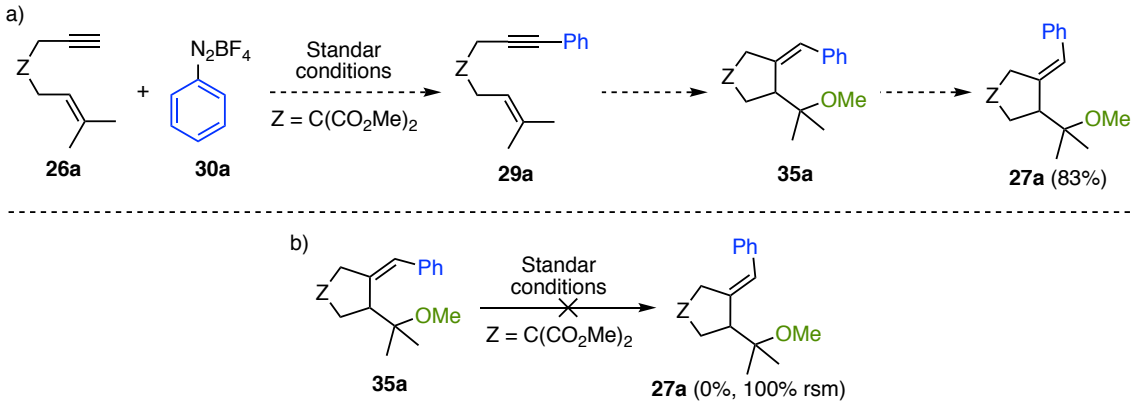

Scheme 32. (a) Alternative mechanism for the gold-catalyzed arylative cyclization of **26a**. (b) Unsuccessful alkene isomerization of **35a**.

Conclusions

We have developed a photoredox-assisted gold-catalyzed arylative alkoxycyclization of 1,6-enynes using aryldiazonium salts in the presence of alcohols as nucleophiles. This three-component reaction leads to the formation of five-membered ring compounds with an *E*-configured exocyclic alkene, complementing the previous reports on gold(I)-catalyzed cyclization of enynes. The reaction shows high functional group tolerance allowing the incorporation of a wide variety of nucleophiles and diazonium salts into different 1,6-enynes. Mechanistic investigations suggest that, in agreement with previous reports, the catalytic cycle starts with the stepwise oxidative formation of the gold(I) catalyst followed by gold(III)-catalyzed 5-*exo*-alkoxycyclization of the enyne and reductive elimination. (Scheme 33).

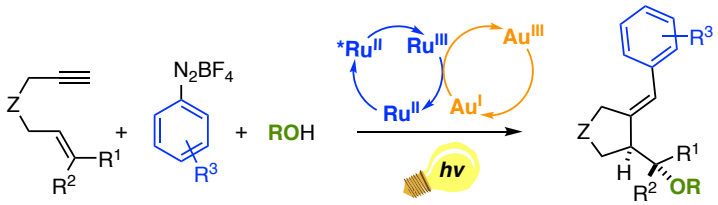

Scheme 33. Photoredox-assisted gold-catalyzed arylative cyclization of 1,6-enynes.

Experimental Part

General Information

Unless otherwise noted, all the reactions were performed under an inert atmosphere of argon. Reagents were obtained commercially and used without further purification. Reactions were run in dry solvents degassed by bubbling argon during 20 minutes before being used. A desk lamp with a 23 W bulb was used as the light source (emission spectra shown in **Figure 2**). Reactions were followed using a GC-MS apparatus, by TLC (thin-layer chromatography) or by NMR analysis. Analytical thin layer chromatography was carried out using TLC aluminum sheets with 0.2 mm of silica gel (Merk GF234) using UV light as the visualizing agent and an acidic solution of vanillin in ethanol or basic solution of $KMnO_4$ in water as stain. Chromatographic purifications were carried out using flash grade silica gel (SDS Chromatogel 60 ACC, 40-60 μm), using a CombiFlash® Rf Teledyne Isco apparatus with RediSep® Rf normal phase silica columns or by preparative thin layer chromatography (Analtec Silica Gel GF UV254, 20×20 cm, 1000 μm). Melting points were determined using a Mettler Toledo MP70 melting point apparatus. GC-MS were NMR spectra were recorded at 298 K on the following spectrometers: Bruker Avance 400 Ultrashield (400 MHz for ^{1}H, and 101 MHz for ^{13}C), and Bruker Avance 500 Ultrashield (500 MHz for ^{1}H, and 126 MHz for ^{13}C). Chemical shifts (δ) are reported in parts per million (ppm) downfield from tetramethylsilane, using the residual protosolvent or tetramethylsilane as reference (for ^{1}H NMR: $CDCl_3$ at 7.26 ppm, CD_2Cl_2 at 5.31 ppm, acetone-d_6 at 2.05 ppm, for ^{13}C NMR: $CDCl_3$ at 77.16 ppm, CD_2Cl_2 at 54.00 ppm, acetone-d_6 at 206.2 and 29.8 ppm). The following abbreviations were used to explain multiplicities: s = singlet, d = doublet, t = triplet, q = quartet, p = pentet, m = multiplet, br s = broad singlet. Coupling constants (*J*) are reported in hertz (Hz). Mass spectra were recorded on MicroTOF Focus or Maxis Impact spectrometers (both from Bruker Daltonics) using ESI+ or APCI + as ionization techniques. X-ray diffraction data were collected at 100 K on a Rigaku MicroMax-007HF, Mo *Kα* rotating anode, equipped with a Pilatus 200 K detector or on a Bruker APEX DUO, Mo *Kα* Microfocus source E025 IuS anode, equipped with an APEX DUO detector using omega scans.

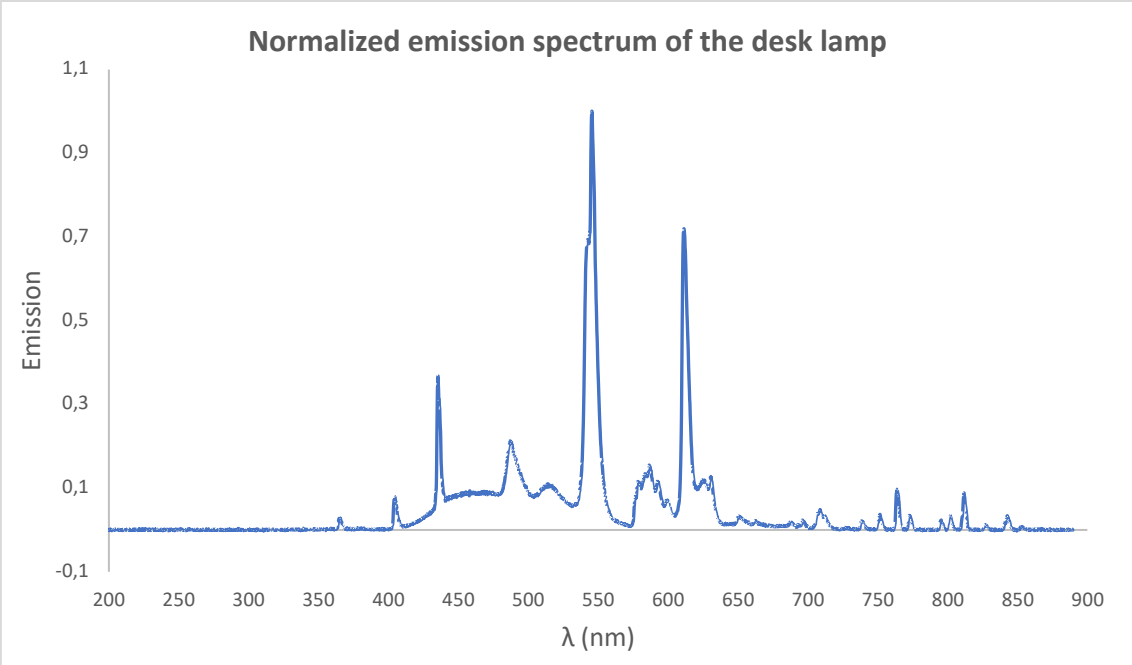

Figure 2. Normalized emission spectrum of the light irradiated during the reactions.

Synthetic procedures and analytical data for the preparation of enynes (26a-k)

Enynes **26a-c** and **26f-k** were synthetized following the reported protocols.[73]

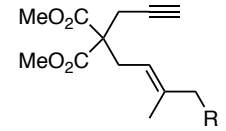

R = H : **26a**[73a]
R = Prenyl : **26b**[73b]

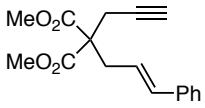

26c[73c]

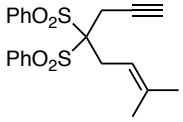

26f[73a]

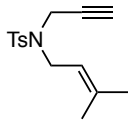

26g[73d]

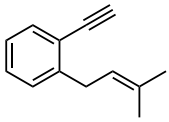

26h[73e]

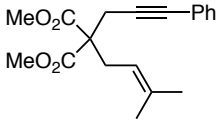

26i[73d]

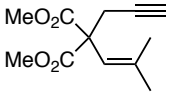

26j[73f]

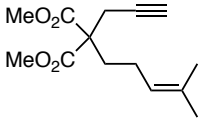

26k[73g]

73 (a) Muñoz, M. P.; Méndez, M.; Nevado, C.; Cárdenas, D.; Echavarren, A. M. *Synthesis* **2003**, *18*, 2898–2902. (b) Tripp, J. C.; Schiesser, C. H.; Curran, D. P. *J. Am. Chem. Soc.* **2005**, *127*, 5518–5527. (c) Zhong, M.-J.; Zhu, H.-T.; Gao, P.; Qiu, Y.-F.; Liang, Y.-M. *RSC Adv.* **2014**, *4*, 8914–8917. (d) Qiu, Y. F.; Zhu, X.-Y.; Li, Y.-X.; He, Y.-T.; Yang, F.; Wang, J.; Hua. H.-L.; Zheng, L.; Wang, L.-C.; Liu, X.-Y.; Liang, Y.-M. *Org. Lett.* **2015**, *17*, 3694–3697. (e) Sanjuán, A. M.; Martínez, A.; García-García, P.; Fernández-Rodríguez, M. A.; Sanz, R. *Beilstein J. Org. Chem.* **2013**, *9*, 2242–2249. (f) Meyer, V. J.; Fu, L.; Marquardt, F.; Niggemann, M. *Adv. Synth. Catal.* **2013**, *355*, 1943–1947. (g) Peil, S.; Guthertz, A.; Biberger, T.; Fürstner, A. *Angew. Chem. Int. Ed.* **2019**, *58*, 8851–8856.

(*E*)-2-Cinnamyl-2-(prop-2-yn-1-yl)propane-1,3-diyl diacetate (26d)[74]

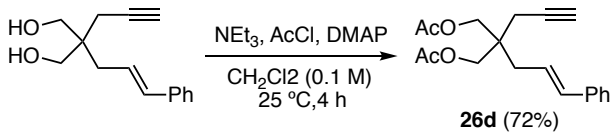

26d (72%)

2-Cinnamyl-2-(prop-2-yn-1-yl)propane-1,3-diol (200 mg, 0.87 mmol), acetyl chloride (129 μL, 1.82 mmol, 2.1 equiv) and DMAP (159 mg, 1.30 mmol, 1.5 equiv) were dissolved in CH_2Cl_2 (9 mL) and NEt_3 (0.36 mL, 2.61 mmol, 3.0 equiv) was added. The mixture was stirred at 24 ºC for 4 h. Water was added to the mixture and the aqueous phase was extracted with CH_2Cl_2 (3x). The combined organic phases were washed with brine, dried over Na_2SO_4, filtered and concentrated. The crude was purified by flash column chromatography (pentane/Et_2O, 20:1) to afford **1e** (197 mg, 0.625 mmol, 72%) as a white solid.

M.p. (pentane): 63-65 ºC. **^{1}H NMR** (500 MHz, $CDCl_3$) δ 7.37 – 7.28 (m, 4H), 7.25 – 7.20 (tt, *J* = 7.1, 1.5 Hz, 1H), 6.48 (d, *J* = 15.7 Hz, 1H), 6.15 (dt, *J* = 15.6, 7.7 Hz, 1H), 4.08 (s, 4H), 2.39 (dd, *J* = 7.7, 1.3 Hz, 2H), 2.32 (d, *J* = 2.7 Hz, 2H), 2.08 (s, 6H), 2.07 (t, *J* = 2.7 Hz, 1H). **^{13}C NMR** (126 MHz, $CDCl_3$) δ 136.8, 136.7, 136.1, 135.0, 131.8, 128.8, 128.7, 128.0, 126.6, 120.9, 89.1, 76.0, 74.6, 33.1, 21.2. **HRMS** (ESI+) calcd for $[C_{19}H_{22}NaO_4]^+$ 337.1410 m/z; found [M + Na]+ 337.1402 m/z.

(*E*)-(1-phenylhept-1-en-6-yne-4,4-diyldisulfonyl)dibenzene (26e)[75]

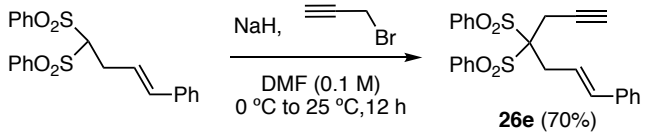

26e (70%)

A solution (E)-(4-phenylbut-3-ene-1,1-diyldisulfonyl)dibenzene (0.5 g, 1.212 mmol) in DMF (4.04 ml) was added to a suspension of sodium hydride (0.053 g, 1.333 mmol, 1.1 equiv) in DMF (8,08 ml) at 0 °C, followed by the addition of propargyl bromide (0.145 ml, 1.333 mmol, 1.1 equiv). The mixture was stirred 13 h at 25 °C. After quenching with H_2O, extractive work-up (Et_2O), and flash chromatography on silica (2:1 hexane-EtOAc as eluent), **1f** (380 mg, 0.843 mmol, 70 % yield) was obtained as a white solid.

M.p. (pentane): 170-172 ºC. **^{1}H NMR** (400 MHz, $CDCl_3$) δ 8.16 – 8.12 (m, 4H), 7.72 (tt, *J* = 7.4, 1.2 Hz, 2H), 7.61 – 7.55 (m, 4H), 7.39 – 7.30 (m, 4H), 7.26 (tt, *J* = 7.2, 1.4 Hz, 1H), 6.58 (d, *J* = 15.7 Hz, 1H), 6.37 (dt, *J* = 15.7, 7.1 Hz, 1H), 3.29 (dd, *J* = 7.1, 1.5 Hz, 2H), 3.22 (d, *J* = 2.8 Hz, 2H), 2.12 (t, *J* = 2.7 Hz, 1H). **^{13}C NMR** (101 MHz, $CDCl_3$) δ 136.8, 136.7, 136.1, 135.0, 131.8,

74 Miller, R.; Carreras, J.; Muratore, M. E.; Gaydou, M.; Camponovo, F.; Echavarren, A. M. *J. Org. Chem.* **2016**, *81*, 1839–1849.

75 Teller, H.; Corbet, M; Mantilli, L.; Gopakumar, G.; Goddard, R.; Thiel, W; Fürster, A. *J. Am. Chem. Soc.* **2012**, *134*, 15331–15342.

128.8, 128.7, 128.0, 126.6, 120.9, 89.1, 76.0, 74.6, 33.1, 21.2. **HRMS** (ESI+) calcd for $[C_{25}H_{22}NaO_4S_2]^+$ 473.0852 m/z; found $[M + Na]^+$ 473.0846 m/z.

Synthetic procedures for the preparation of aryldiazonium salts (30a-w)

Aryldiazonium salts were prepared according to the procedure of Hanson.[76]

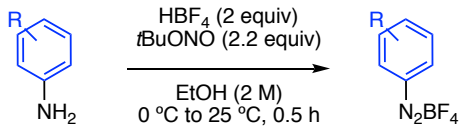

The aniline was dissolved in a mixture of fluoroboric acid (2.0 equiv) and ethanol (2.0 M) at 0 ºC. Then, a solution of *t*-BuONO (2.2 equiv) was slowly added. The mixture was stirred for 30 min at room temperature and the thick precipitate was collected by filtration and washed with Et_2O. The diazonium tetrafluoroborate was then dissolved in minimal amount of acetone and precipitated by the addition of Et_2O, filtered and washed with Et_2O. The product was dried under high vacuum and stored under argon, in the freezer in the dark.

Synthetic procedures and analytical data for the products from the scope of the photoredox-assisted gold-catalyzed arylative cyclization of enynes (27a-am)

*General procedure for the arylative cyclization of enynes**

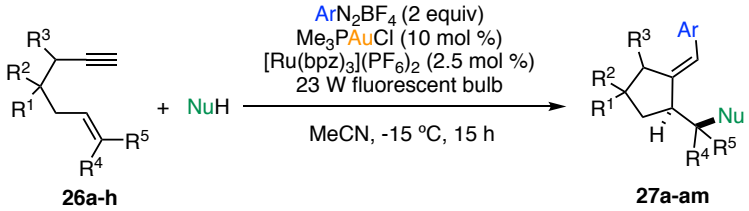

Aryldiazonium tetrafluoroborate (2.0 equiv.), $[Ru(bpz)_3](PF_6)_2$ (2.5 mol%) and Me_3PAuCl (10 mol%) were placed in a vial equipped with a stir bar. To the vial kept in the dark was added the solution of enyne (1 equiv) in degassed MeOH/MeCN (1:1) previously cooled at – 15 ºC (0.04 M). The vial was evacuated and refilled with nitrogen three times. The mixture was placed at -15 ºC and stirred for 15 h under a desk lamp with a 23 W fluorescent light bulb. After the completion of the reaction, saturated $NaHCO_3$ and CH_2Cl_2 were added and the layers separated. The aqueous layer was further extracted twice with CH_2Cl_2, the combined organic layers washed with brine, dried over Na_2SO_4 and concentrated in vacuo. The crude was purified by preparative TLC eluting with pentane/Et_2O to give the desired products.

* For the scope of nucleophiles, the reactions were run in acetonitrile using 10 equiv. of the corresponding nucleophile.

76 Hanson, P.; Jones, J. R.; Taylor, A.B.; Walton, P. H.; Timms, A. W. *J. Chem. Soc. Perkin Trans. 2.* **2002**, 1135–1150.

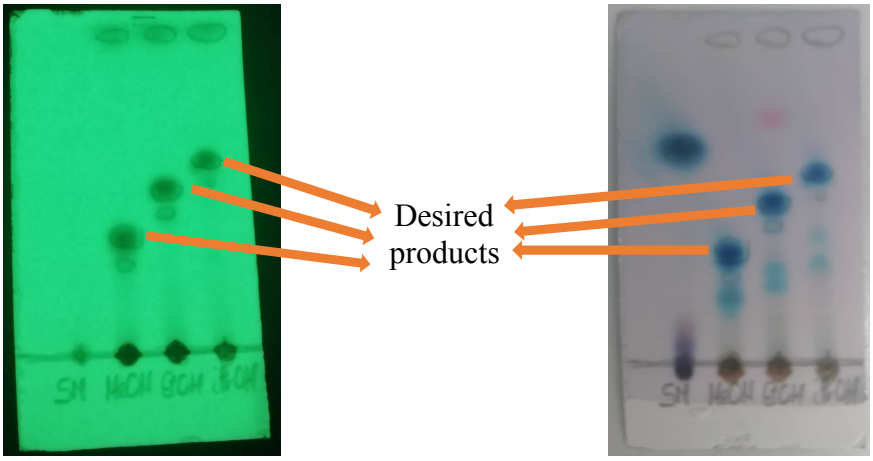

TLC (pentane/diethyl ether, 4:1) after 15 h under UV irradiation (left) and upon vanillin stain (right). Spots from left to right: starting material (**26a**), reaction with MeOH, reaction with EtOH and reaction with *i*PrOH.

Dimethyl (*E*)-3-benzylidene-4-(2-methoxypropan-2-yl)cyclopentane-1,1-dicarboxylate (27a)

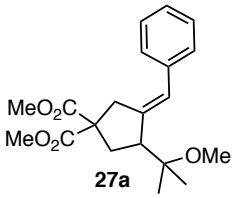

27a

Product **27a** was synthesized following the general procedure using enyne **26a** (50 mg, 0.210 mmol) whereby the reaction was stirred for 15 h. Purification by preparative TLC on silica (pentane:diethyl ether, 7:3) afforded the title compound **27a** (60.3 mg, 0.174 mmol, 83% yield) as a colorless oil.

^{1}H NMR (500 MHz, $CDCl_3$) δ 7.34 – 7.29 (m, 2H), 7.25 – 7.22 (m, 2H), 7.19 (tt, *J* = 7.3, 1.3 Hz, 1H), 6.54 (s, 1H), 3.75 (s, 3H), 3.62 (s, 3H), 3.26 (dt, *J* = 16.0, 1.6 Hz, 1H), 3.23 (s, 3H), 3.10 – 3.01 (m, 2H), 2.57 (ddd, *J* = 13.5, 8.4, 1.9 Hz, 1H), 2.05 (dd, *J* = 13.4, 8.9 Hz, 1H), 1.23 (s, 3H), 1.17 (s, 3H). **^{13}C NMR** (126 MHz, $CDCl_3$) δ 172.2, 172.1, 141.7, 138.3, 128.8, 128.3, 126.5, 126.4, 77.6, 59.6, 52.88, 52.85, 51.4, 49.2, 40.1, 35.1, 23.1, 22.2. **HRMS** (ESI+) calcd for $[C_{20}H_{26}NaO_5]^+$ 369.1672 *m/z*; found $[M + Na]^+$ 369.1680 *m/z*.

Dimethyl (*E*)-3-benzylidene-4-(2-ethoxypropan-2-yl)cyclopentane-1,1-dicarboxy-late (27b)

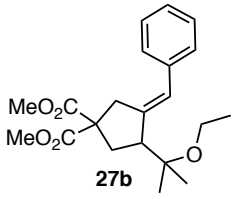

27b

Product **27b** was synthesized following the general procedure using enyne **26a** (50 mg, 0.210 mmol) and 10 equivalents of the ethanol whereby the reaction was stirred for 15 h. Purification by preparative TLC on silica (pentane:diethyl ether, 7:3) afforded the title compound **27b** (56.0 mg, 0.155 mmol, 74% yield) as a colorless oil.

^{1}H NMR (500 MHz, $CDCl_3$) δ 7.34 – 7.29 (m, 2H), 7.25 – 7.22 (m, 2H), 7.19 (tt, *J* = 7.3, 1.3 Hz, 1H), 6.58 (s, 1H), 3.74 (s, 3H), 3.62 (s, 3H), 3.51 – 3.39 (m, 2H), 3.28 (dt, *J* = 16.2, 1.7 Hz, 1H), 3.08 – 3.02 (m, 2H), 2.56 (ddd, *J* = 13.8, 8.4, 2.0 Hz, 1H), 2.04 (dd, *J* = 13.6, 9.3 Hz, 1H), 1.23 (s, 3H), 1.18 (t, *J* = 7.0 Hz, 3H), 1.17 (s, 3H). **^{13}C NMR** (126MHz, $CDCl_3$) δ 172.17, 172.15, 141.8, 138.4, 128.7, 128.3, 126.39, 126.38, 77.3, 59.6, 56.5, 52.88, 52.85, 51.5, 40.2, 35.2, 23.8,

22.6, 16.1. **HRMS** (ESI+) calcd for $[C_{21}H_{28}NaO_5]^+$ 383.1829 *m/z*; found $[M + Na]^+$ 383.1823 *m/z*.

Dimethyl (*E*)-3-benzylidene-4-(2-isopropoxypropan-2-yl)cyclopentane-1,1-dicarbo-xylate (27c)

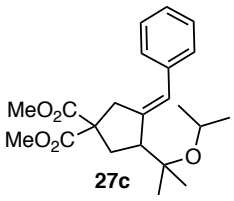

27c

Product **27c** was synthesized following the general procedure using enyne **26a** (50 mg, 0.210 mmol) and 10 equivalents of the isopropanol whereby the reaction was stirred for 15 h. Purification by preparative TLC on silica (pentane:diethyl ether, 4:1) afforded the title compound **27c** (47.9 mg, 0.128 mmol, 61% yield) as a colorless oil.

^{1}H NMR (500 MHz, $CDCl_3$) δ 7.34 – 7.29 (m, 2H), 7.25 – 7.22 (m, 2H), 7.19 (tt, *J* = 7.3, 1.3 Hz, 1H), 6.68 (s, 1H), 3.85 (hept, *J* = 5.9 Hz, 1H), 3.74 (s, 3H), 3.61 (s, 3H), 3.26 (dt, *J* = 15.9, 1.7 Hz, 1H), 3.06 (dt, *J* = 15.9, 2.8 Hz, 1H), 2.90 (tt, *J* = 8.7, 2.2 Hz, 1H), 2.59 (ddd, *J* = 13.4, 8.4, 1.8 Hz, 1H), 2.06 (dd, *J* = 13.4, 9.1 Hz, 1H), 1.21 (s, 3H), 1.18 (s, 3H), 1.13 (dd, *J* = 6.1, 3.2 Hz, 6H). **^{13}C NMR** (126 MHz, $CDCl_3$) δ 172.3, 172.2, 142.1, 138.5, 128.7, 128.3, 126.6, 126.3, 77.9, 63.5, 59.6, 53.9, 52.9, 52.8, 40.1, 35.3, 25.2, 25.1, 24.7, 22.4. **HRMS** (ESI+) calcd for $[C_{22}H_{30}NaO_5]^+$ 397.1985 *m/z*; found $[M + Na]^+$ 397.1982 *m/z*.

Dimethyl (*E*)-3-benzylidene-4-(2-(prop-2-yn-1-yloxy)propan-2-yl)cyclopentane-1,1-dicar-boxylate (27e)

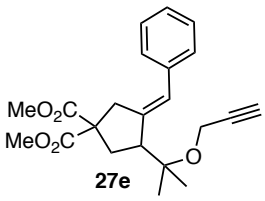

27e

Product **27e** was synthesized following the general procedure using enyne **26a** (50 mg, 0.210 mmol) and 10 equivalents of the propargyl alcohol whereby the reaction was stirred for 15 h. Purification by preparative TLC on silica (pentane:diethyl ether, 3:1) afforded the title compound **27e** (46.6 mg, 0.126 mmol, 60% yield) as a colorless oil.

^{1}H NMR (500 MHz, $CDCl_3$) δ 7.34 – 7.29 (m, 2H), 7.26-7.22 (m, 2H), 7.20 (tt, *J* = 7.3, 1.3 Hz, 1H), 6.61 (s, 1H), 4.17 – 4.08 (m, 2H), 3.75 (s, 3H), 3.62 (s, 3H), 3.27 (dt, J = 15.9, 1.6 Hz, 1H), 3.09 – 3.02 (m, 2H), 2.60 (ddd, J = 13.5, 8.3, 1.9 Hz, 1H), 2.38 (t, J = 2.4 Hz, 1H), 2.04 (dd, J = 13.5, 9.2 Hz, 1H), 1.29 (s, 3H), 1.23 (s, 3H). **^{13}C NMR** (126 MHz, $CDCl_3$) δ 172.1, 141.1, 138.2, 128.8, 128.3, 126.9, 126.5, 81.5, 79.2, 73.3, 59.5, 53.0, 52.9, 51.8, 50.2, 40.2, 35.2, 23.7, 22.5. **HRMS** (ESI+) calcd for $[C_{22}H_{26}NaO_5]^+$ 393.1672 *m/z*; found $[M + Na]^+$ 393.1672 *m/z*.

Dimethyl (*E*)-3-benzylidene-4-(2-(benzyloxy)propan-2-yl)cyclopentane-1,1-dicar-boxylate (27f)

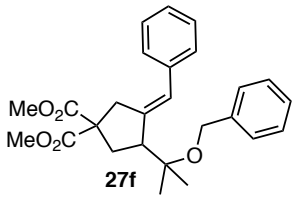

27f

Product **27f** was synthesized following the general procedure using enyne **26a** (50 mg, 0.210 mmol) and 10 equivalents of the benzyl alcohol whereby the reaction was stirred for 15 h. Purification by preparative TLC on silica (pentane:diethyl ether, 4:1) afforded the title compound **27f** (45.2 mg, 0.107 mmol, 51% yield) as a colorless oil.

^{1}H NMR (500 MHz, $CDCl_3$) δ 7.38 – 7.30 (m, 6H), 7.28 – 7.24 (m, 1H), 7.24 – 7.18 (m, 3H), 6.64 (s, 1H), 4.55 – 4.47 (m, 2H), 3.72 (s, 3H), 3.63 (s, 3H), 3.31 (dt, *J* = 15.9, 1.7 Hz, 1H), 3.15 (tt, *J* = 8.9, 2.3 Hz, 1H), 3.09 (dt, *J* = 15.9, 2.9 Hz, 1H), 2.64 (ddd, *J* = 13.5, 8.4, 1.9 Hz, 1H), 2.13 (dd, *J* = 13.4, 9.3 Hz, 1H), 1.35 (s, 3H), 1.29 (s, 3H). **^{13}C NMR** (126 MHz, $CDCl_3$) δ 172.1, 141.6, 139.7, 138.3, 128.7, 128.4, 128.3, 127.4, 127.3, 126.7, 126.4, 78.2, 63.7, 59.6, 52.89, 52.87, 52.1, 40.2, 35.2, 23.8, 22.6. **HRMS** (ESI+) calcd for $[C_{26}H_{30}NaO_5]^+$ 445.1985 *m/z*; found $[M + Na]^+$ 445.1984 *m/z*.

Dimethyl (*E*)-3-(2-(allyloxy)propan-2-yl)-4-benzylidenecyclopentane-1,1-dicarbo-xylate (27g)

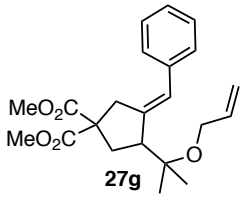

27g

Product **27g** was synthesized following the general procedure using enyne **26a** (50 mg, 0.210 mmol) and 10 equivalents of the allyl alcohol whereby the reaction was stirred for 15 h. Purification by preparative TLC on silica (pentane:diethyl ether, 4:1) afforded the title compound **27g** (27.3 mg, 0.073 mmol, 35% yield) as a colorless oil.

^{1}H NMR (500 MHz, $CDCl_3$) δ 7.34 – 7.29 (m, 2H), 7.24-7.24 (m, 2H), 7.19 (tt, *J* = 7.3, 1.3 Hz, 1H), 6.59 (s, 1H), 5.97 – 5.89 (m, 1H), 5.30 (dq, *J* = 17.2, 1.8 Hz, 1H), 5.13 (dq, *J* = 10.4, 1.6 Hz, 1H), 3.96 (qdt, *J* = 12.4, 5.2, 1.6 Hz, 2H), 3.74 (s, 3H), 3.62 (s, 3H), 3.28 (dt, *J* = 16.1, 1.5 Hz, 1H), 3.10 – 3.02 (m, 2H), 2.58 (ddd, *J* = 13.6, 8.2, 1.9 Hz, 1H), 2.05 (dd, *J* = 13.4, 9.3 Hz, 1H), 1.26 (s, 3H), 1.21 (s, 3H). **^{13}C NMR** (126 MHz, $CDCl_3$) δ 172.13, 172.12, 141.6, 138.3, 136.0, 128.8, 128.3, 126.7, 126.4, 115.7, 77.8, 62.6, 59.6, 52.90, 52.85, 51.7, 40.2, 35.2, 23.7, 22.6. **HRMS** (ESI+) calcd for $[C_{22}H_{28}NaO_5]^+$ 395.1829 *m/z*; found $[M + Na]^+$ 395.1822 *m/z*.

Dimethyl (*E*)-3-benzylidene-4-(2-hydroxypropan-2-yl)cyclopentane-1,1-dicarboxy-late (27h)

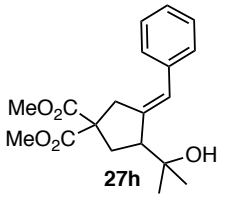

27h

Product **27h** was synthesized following general the procedure using enyne **26a** (50 mg, 0.210 mmol) and 10 equivalents of the water whereby the reaction was stirred for 3 h. Purification by preparative TLC on neutral alumina (pentane/diethyl ether 1:1) afforded the title compound **27h** (46.7 mg, 0.141 mmol, 67% yield) as a light-yellow oil.

^{1}H NMR (500 MHz, $CDCl_3$) δ 7.35 – 7.30 (m, 2H), 7.26 – 7.19 (m, 3H), 6.60 (s, 1H), 3.75 (s, 3H), 3.61 (s, 3H), 3.30 (dt, J = 15.7, 1.6 Hz, 1H), 3.03 (dt, J = 15.8, 2.8 Hz, 1H), 2.88 (tt, J = 8.6,

2.1 Hz, 1H), 2.65 (ddd, J = 13.6, 8.6, 1.8 Hz, 1H), 2.03 (dd, J = 13.6, 8.5 Hz, 1H), 1.28 (s, 3H), 1.24 (s, 3H). **^{13}C NMR** (126 MHz, $CDCl_3$) δ 172.2, 172.0, 141.9, 137.8, 128.8, 128.3, 127.2, 126.7, 73.4, 59.9, 54.8, 53.0, 52.9, 40.1, 35.2, 28.4, 26.1. **HRMS** (ESI+) calcd for $[C_{19}H_{24}NaO_5]^+$ 355.1516 *m/z*; found $[M + Na]^+$ 355.1514 *m/z*.

Dimethyl (*E*)-3-(4-fluorobenzylidene)-4-(2-methoxypropan-2-yl)cyclopentane-1,1-dicarboxylate (27k)

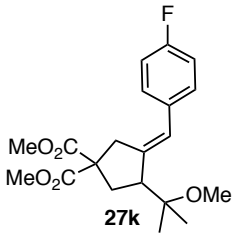

27k

Product **27k** was synthesized following the general procedure using enyne **26a** (30 mg, 0.126 mmol) whereby the reaction was stirred for 15 h. Purification by flash column chromatography (gradient starting with cyclohexane to cyclohexane/EtOAc 4:1) followed by preparative TLC on neutral alumina (pentane/diethyl ether 7:3) afforded the title compound **27k** (32.6 mg, 0.089 mmol, 71% yield) as a yellowish oil.

^{1}H NMR (400 MHz, $CDCl_3$) δ 7.22 – 7.16 (m, 2H), 7.04 – 6.96 (m, 2H), 6.49 (s, 1H), 3.74 (s, 3H), 3.63 (s, 3H), 3.22 (s, 3H), 3.20 (d, *J* = 17.0, Hz, 2H), 3.06 – 2.97 (m, 2H), 2.56 (ddd, *J* = 13.5, 8.3, 1.8 Hz, 1H), 2.04 (dd, *J* = 13.5, 9.1 Hz, 1H), 1.21 (s, 3H), 1.16 (s, 3H). **^{13}C NMR** (101 MHz, $CDCl_3$) δ 172.12, 172.07, 162.7, 160.31, 141.5 (d, *J* = 1.5), 134.4 (d, *J* = 3.4), 130.2 (d, *J* = 7.8), 125.4, 115.1, 115.0, 77.5, 59.6, 52.92, 52.89, 51.3, 49. 2, 40.0, 35.2, 23.1, 22.0. **^{19}F{^{1}H} NMR** (376 MHz, $CDCl_3$) δ -116.06. **HRMS** (ESI+) calcd for $[C_{20}H_{25}FNaO_5]^+$ 387.1578 *m/z*; found $[M + Na]^+$ 387.1577 *m/z*.

Dimethyl (*E*)-3-(4-chlorobenzylidene)-4-(2-methoxypropan-2-yl)cyclopentane-1,1-dicarboxylate (27l)

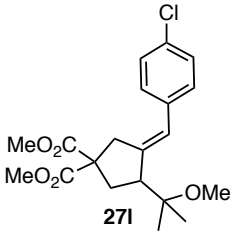

27l

Product **27l** was synthesized following general the procedure using enyne **26a** (50 mg, 0.210 mmol) whereby the reaction was stirred for 15 h. Purification by flash column chromatography (gradient starting with cyclohexane to cyclohexane/EtOAc 4:1) followed by preparative TLC on neutral alumina (pentane/diethyl ether 7:3) afforded the title compound **27l** (47.1 mg, 0.124 mmol, 59% yield) as a yellowish oil.

^{1}H NMR (500 MHz, $CDCl_3$) δ 7.30 – 7.26 (m, 2H), 7.18 – 7.14 (m, 2H), 6.49 (s, 1H), 3.75 (s, 3H), 3.63 (s, 3H), 3.22 (s, 3H), 3.20 (dt, *J* = 16.0, 1.7 Hz, 1H), 3.05 – 2.98 (m, 2H), 2.56 (ddd, *J* = 13.4, 8.1, 1.7 Hz, 1H), 2.04 (dd, *J* = 13.4, 9.1 Hz, 1H), 1.20 (s, 3H), 1.16 (s, 3H). **^{13}C NMR** (126 MHz, $CDCl_3$) δ 172.1, 172.0, 142.6, 136.7, 132.1, 130.0, 128.4, 125.3, 77.5, 59.6, 53.0, 52.9, 51.4, 49.2, 40.1, 35.2, 23.2, 22.0. **HRMS** (ESI+) calcd for $[C_{20}H_{25}{}^{35}ClNaO_5]^+$ 403.1283 *m/z*; found $[M + Na]^+$ 403.1287 *m/z*.

Dimethyl (*E*)-3-(4-bromobenzylidene)-4-(2-methoxypropan-2-yl)cyclopentane-1,1-dicarboxylate (27m)

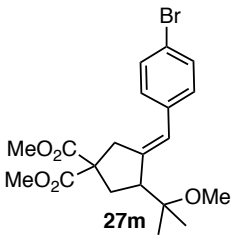

27m

Product **27m** was synthesized following the general procedure using enyne **26a** (30 mg, 0.126 mmol) whereby the reaction was stirred for 15 h. Purification by flash column chromatography (gradient starting with cyclohexane to cyclohexane/EtOAc 4:1) followed by preparative TLC on neutral alumina (pentane/diethyl ether 7:3) afforded the title compound **27m** (33.6 mg, 0.079 mmol, 63% yield) as a yellowish oil.

^{1}H NMR (500 MHz, $CDCl_3$) δ 7.45 – 7.40 (m, 2H), 7.12 – 7.08 (m, 2H), 6.47 (s, 1H), 3.75 (s, 3H), 3.63 (s, 3H), 3.22 (s, 3H), 3.19 (d, *J* = 15.8 Hz, 4H), 3.05 – 2.97 (m, 2H), 2.56 (ddd, *J* = 13.4, 8.0, 1.7 Hz, 1H), 2.04 (dd, *J* = 13.5, 9.0 Hz, 1H), 1.20 (s, 3H), 1.16 (s, 3H). **^{13}C NMR** (126 MHz, $CDCl_3$) δ 172.1, 172.0, 142.8, 137.1, 131.4, 130.3, 125.4, 120.3, 77.5, 59.5, 52.94, 52.92, 51.4, 49.2, 40.1, 35.2, 23.2, 22.0. **HRMS** (ESI+) calcd for $[C_{20}H_{25}{}^{79}BrNaO_5]^+$ 447.0778 *m/z*; found $[M + Na]^+$ 447.0771 *m/z*.

Dimethyl (*E*)-3-(4-iodobenzylidene)-4-(2-methoxypropan-2-yl)cyclopentane-1,1-dicarboxylate (27n)

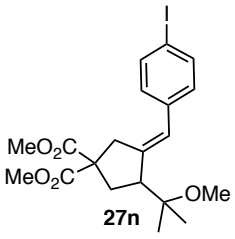

27n

Product **27n** was synthesized following the general procedure using enyne **26a** (60 mg, 0.252 mmol) whereby the reaction was stirred for 15 h. Purification by flash column chromatography (gradient starting with cyclohexane to cyclohexane/EtOAc 4:1) followed by preparative TLC on neutral alumina (pentane/diethyl ether 7:3) afforded the title compound **27n** (45.2 mg, 0.096 mmol, 38% yield) as a colorless oil.

^{1}H NMR (500 MHz, CDCl3) δ 7.65 – 7.61 (m, 2H), 6.99 – 6.95 (m, 2H), 6.45 (s, 1H), 3.74 (s, 3H), 3.63 (s, 3H), 3.22 (s, 3H), 3.19 (dt, *J* = 15.8, 1.7 Hz, 1H), 3.05 – 2.97 (m, 2H), 2.55 (ddd, *J* = 13.4, 8.1, 1.6 Hz, 1H), 2.03 (dd, *J* = 13.5, 9.1 Hz, 1H), 1.20 (s, 3H), 1.16 (s, 3H). **^{13}C NMR** (126 MHz, $CDCl_3$) δ 172.1, 172.0, 142.9, 137.7, 137.4, 130.6, 125.5, 91.7, 77.5, 59.6, 53.0, 52.9, 51.5, 49.2, 40.1, 35.2, 23.2, 22.0. **HRMS** (ESI+) calcd for $[C_{20}H_{25}INaO_5]^+$ 495.0639 *m/z*; found $[M + Na]^+$ 495.0631 *m/z*.

Dimethyl (*E*)-3-(2-methoxypropan-2-yl)-4-(4-(trifluoromethyl)benzylidene)cyclo-pentane-1,1-dicarboxylate (27o)

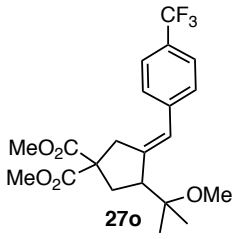

27o

Product **27o** was synthesized following the general procedure using enyne **26a** (50 mg, 0.210 mmol) whereby the reaction was stirred for 15 h. Purification by flash column chromatography (gradient starting with cyclohexane to cyclohexane/EtOAc 4:1) followed by preparative TLC on neutral alumina (pentane/diethyl ether 7:3) afforded the title compound **27o** (61.7 mg, 0.149 mmol, 71% yield) as a yellowish oil.

^{1}H NMR (400 MHz, $CDCl_3$) δ 7.56 (d, *J* = 8.1 Hz, 2H), 7.33 (d, *J* = 8.1 Hz, 2H), 6.58 (s, 1H), 3.75 (s, 3H), 3.63 (s, 3H), 3.23 (s, 3H), 3.22 (d, *J* = 15.9 Hz, 1H), 3.10 – 3.00 (m, 2H), 2.57 (ddd, *J* = 13.3, 8.1, 1.6 Hz, 1H), 2.06 (dd, *J* = 13.4, 9.2 Hz, 1H), 1.21 (s, 3H), 1.18 (s, 3H). **^{13}C NMR** (101 MHz, $CDCl_3$) δ 172.0, 171.9, 144.6, 141.7 (q, 1.3 Hz), 128.9, 128.3 (q, 32.4 Hz), 125.3, 125.2 (q, *J* = 3.8 Hz), 124.4 (q, *J* = 271.8 Hz), 77.4, 59.5, 52.98, 52.95, 51.5, 49.2, 40.2, 35.2, 23.2, 21.8. **^{19}F{^{1}H} NMR** (376 MHz, $CDCl_3$) δ -62.48. **HRMS** (ESI+) calcd for $[C_{21}H_{25}F_3NaO_5]^+$ 437.1546 *m/z*; found $[M + Na]^+$ 437.1553 *m/z*.

Dimethyl (*E*)-3-(4-cyanobenzylidene)-4-(2-methoxypropan-2-yl)cyclopentane-1,1-dicarboxylate (27p)

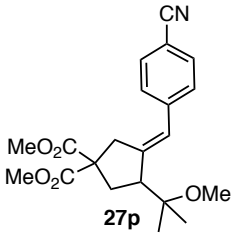

27p

Product **27p** was synthesized following the general procedure using enyne **26a** (30 mg, 0.126 mmol) whereby the reaction was stirred for 4 h. Purification by flash column chromatography (gradient starting with cyclohexane to cyclohexane/EtOAc 4:1) followed by preparative TLC on neutral alumina (pentane/diethyl ether 7:3) afforded the title compound **27p** (31.3 mg, 0.084 mmol, 67% yield) as a yellowish oil.

^{1}H NMR (500 MHz, $CDCl_3$) δ 7.60 (d, *J* = 8.4 Hz, 2H), 7.32 (d, *J* = 8.3 Hz, 2H), 6.58 (s, 1H), 3.75 (s, 3H), 3.63 (s, 3H), 3.22 (s, 3H), 3.21 (d, J = 15.4 Hz, 1H), 3.09 – 3.00 (m, 2H), 2.56 (ddd, *J* = 14.0, 8.3, 1.7, 1H), 2.05 (dd, *J* = 13.4, 9.4 Hz, 1H), 1.19 (s, 3H), 1.18 (s, 3H). **^{13}C NMR** (126 MHz, $CDCl_3$) δ 171.9, 171.8, 146.0, 142.8, 132.1, 129.2, 125.1, 119.3, 109.8, 77.5, 59.5, 53.04, 53.00, 51.7, 49.2, 40.3, 35.2, 23.3, 21.7. **HRMS** (ESI+) calcd for $[C_{21}H_{25}NNaO_5]^+$ 394.1625 *m/z*; found $[M + Na]^+$ 394.1629 *m/z* .

Dimethyl (*E*)-3-(4-(ethoxycarbonyl)benzylidene)-4-(2-methoxypropan-2-yl)cyclo-pentane-1,1-dicarboxylate (27q)

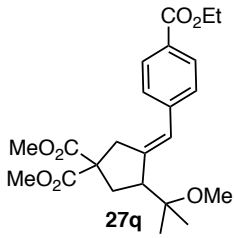

27q

Product **27q** was synthesized following the general procedure using enyne **26a** (50 mg, 0.210 mmol) whereby the reaction was stirred for 15 h. Purification by flash column chromatography (gradient starting with cyclohexane to cyclohexane/EtOAc 4:1) followed by preparative TLC on neutral alumina (pentane/diethyl ether 7:3) afforded the title compound **27q** (51.8 mg, 0.124 mmol, 59% yield) as a yellowish oil.

^{1}H NMR (400 MHz, $CDCl_3$) δ 8.00 – 7.96 (m, 2H), 7.31 – 7.26 (m, 2H), 6.58 (s, 1H), 4.37 (q, *J* = 7.1 Hz, 2H), 3.74 (s, 3H), 3.61 (s, 3H), 3.24 (dt, *J* = 16.0, 1.7 Hz, 1H), 3.23 (s, 3H), 3.11 – 3.00 (m, 2H), 2.57 (ddd, *J* = 13.4, 8.3, 1.7 Hz, 1H), 2.04 (dd, *J* = 13.4, 9.2 Hz, 1H), 1.39 (t, *J* = 7.1 Hz, 3H), 1.21 (s, 3H), 1.17 (s, 3H). **^{13}C NMR** (101 MHz, $CDCl_3$) δ 172.0, 171.9, 166.7, 144.5, 142.7, 129.6, 128.6, 128.3, 125.8, 77.5, 61.0, 59.5, 53.0, 52.9, 51.6, 49.2, 40.3, 35.1, 23.2, 21.9, 14.5. **HRMS** (ESI+) calcd for $[C_{23}H_{30}NaO_7]^+$ 441.1884 *m/z*; found $[M + Na]^+$ 441.1890 *m/z*.

Dimethyl (*E*)-3-(2-methoxypropan-2-yl)-4-(4-nitrobenzylidene)cyclopentane-1,1-dicarboxylate (27r)

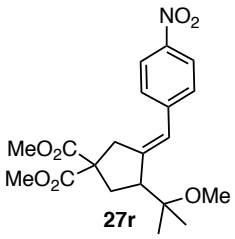

27r

Product **27r** was synthesized following the general procedure using enyne **26a** (50 mg, 0.210 mmol) whereby the reaction was stirred for 15 h. Purification by flash column chromatography (gradient starting with cyclohexane to cyclohexane/EtOAc 3:1) followed by preparative TLC on neutral alumina (pentane/diethyl ether 1:1) afforded the title compound **27r** (41.0 mg, 0.105 mmol, 50% yield) as a yellowish oil.

^{1}H NMR (500 MHz, $CDCl_3$) δ 8.20 – 8.16 (m, 2H), 7.39 – 7.35 (m, 2H), 6.64 (s, 1H), 3.76 (s, 3H), 3.64 (s, 3H), 3.23 (dt, *J* = 16.0, 1.7 Hz, 1H), 3.23 (s, 3H), 3.11 – 3.02 (m, 2H), 2.57 (ddd, *J* = 13.5, 8.3, 1.9 Hz, 1H), 2.07 (dd, *J* = 13.4, 9.2 Hz, 1H), 1.20 (s, 3H), 1.19 (s, 3H). **^{13}C NMR** (126 MHz, $CDCl_3$) δ 171.9, 171.7, 147.0, 146.1, 144.8, 129.2, 124.8, 123.7, 77.5, 59.5, 53.1, 53.0, 51.8, 49.2, 40.4, 35.2, 23.4, 21.7. **HRMS** (ESI+) calcd for $[C_{20}H_{25}NNaO_7]^+$ 414.1523 *m/z*; found $[M + Na]^+$ 414.1514 *m/z*.

Dimethyl (*E*)-3-(4-(tert-butyl)benzylidene)-4-(2-methoxypropan-2-yl)cyclopentane-1,1-dicarboxylate (27s)

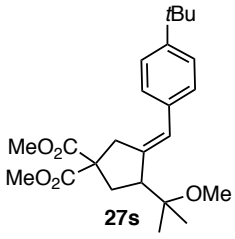

27s

Product **27s** was synthesized following the general procedure using enyne **26a** (60 mg, 0.252 mmol) whereby the reaction was stirred for 15 h. Purification by flash column chromatography (gradient starting with cyclohexane to cyclohexane/EtOAc 4:1) followed by preparative TLC on neutral alumina (pentane/diethyl ether 7:3) afforded the title compound **27s** (71.9 mg, 0.179 mmol, 71% yield) as a yellowish oil.

^{1}H NMR (400 MHz, $CDCl_3$) δ 7.37 – 7.32 (m, 2H), 7.22 – 7.17 (m, 2H), 6.51 (s, 1H), 3.75 (s, 3H), 3.63 (s, 3H), 3.29 (dt, *J* = 16.0, 1.6 Hz, 1H), 3.22 (s, 3H), 3.12 – 3.00 (m, 2H), 2.56 (ddd, *J* = 13.6, 8.4, 1.8 Hz, 1H), 2.05 (dd, *J* = 13.5, 9.0 Hz, 1H), 1.32 (s, 9H), 1.22 (s, 3H), 1.15 (s, 3H). **^{13}C NMR** (101 MHz, $CDCl_3$) δ 172.24, 172.21, 149.3, 140.9, 135.4, 128.5, 126.1, 125.2, 77.6, 59.7, 52.9, 51.5, 49.1, 40.2, 35.1, 34.6, 31.5, 23.1, 22.2. **HRMS** (ESI+) calcd for $[C_{24}H_{34}NaO_5]^+$ 425.2298 *m/z*; found $[M + Na]^+$ 425.2285 *m/z*.

Dimethyl (*E*)-3-([1,1'-biphenyl]-4-ylmethylene)-4-(2-methoxypropan-2-yl)cyclopen-tane-1,1-dicarboxylate (27t)

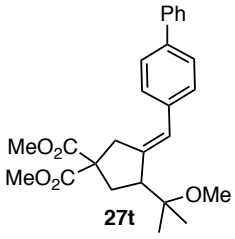

27t

Product **27t** was synthesized following the general procedure using enyne **26a** (60 mg, 0.252 mmol) whereby the reaction was stirred for 15 h. Purification by flash column chromatography (gradient starting with cyclohexane to cyclohexane/EtOAc 4:1) followed by preparative TLC on neutral alumina (pentane/diethyl ether 7:3) afforded the title compound **27t** (71.2 mg, 0.169 mmol, 67% yield) as a yellowish oil.

^{1}H NMR (500 MHz, $CDCl_3$) δ 7.62 – 7.59 (m, 2H), 7.58 – 7.55 (m, 2H), 7.46 – 7.42 (m, 2H), 7.36 – 7.31 (m, 3H), 6.58 (s, 1H), 3.76 (s, 3H), 3.64 (s, 3H), 3.33 (dt, *J* = 16.0, 1.7 Hz, 1H), 3.24 (s, 3H), 3.13 (dt, *J* = 16.0, 2.9 Hz, 1H), 3.06 (tt, *J* = 8.7, 2.2 Hz, 1H), 2.59 (ddd, *J* = 13.5, 8.4, 1.8 Hz, 1H), 2.07 (dd, *J* = 13.5, 9.0 Hz, 1H), 1.24 (s, 3H), 1.18 (s, 3H).**^{13}C NMR** (101 MHz, $CDCl_3$) δ 172.2, 172.1, 142.0, 141.0, 139.2, 137.3, 129.2, 128.9, 127.3, 127.1, 127.0, 126.0, 77.6, 59.7, 52.9, 51.6, 49.2, 40.3, 35.1, 23.1, 22.1. **HRMS** (ESI+) calcd for $[C_{26}H_{30}NaO_5]^+$ 445.1985 *m/z*; found $[M + Na]^+$ 445.1990 *m/z*.

Dimethyl (*E*)-3-(2-methoxypropan-2-yl)-4-(4-methylbenzylidene)cyclopentane-1,1-dicarboxylate (27u)

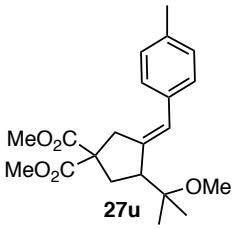

27u

Product **27u** was synthesized following the general procedure using enyne **26a** (30 mg, 0.126 mmol) whereby the reaction was stirred for 15 h. Purification by flash column chromatography (gradient starting with cyclohexane to cyclohexane/EtOAc 4:1) followed by preparative TLC on neutral alumina (pentane/diethyl ether 7:3) afforded the title compound **27u** (32.7 mg, 0.091 mmol, 72% yield) as a yellowish oil.

^{1}H NMR (500 MHz, $CDCl_3$) δ 7.16 7.10 (m, 4H), 6.49 (s, 1H), 3.74 (s, 3H), 3.62 (s, 3H), 3.25 (dt, *J* = 16.0, 1.4 Hz, 1H), 3.22 (s, 3H), 3.10 – 3.00 (m, 2H), 2.56 (ddd, *J* = 13.5, 8.4, 1.8 Hz, 1H), 2.34 (s, 3H), 2.04 (dd, *J* = 13.5, 8.9 Hz, 1H), 1.22 (s, 3H), 1.16 (s, 3H). **^{13}C NMR** (101 MHz, $CDCl_3$) δ 172.23, 172.21, 140.8, 136.1, 135.4, 129.0, 128.7, 126.3, 77.6, 59.7, 52.87, 52.86, 51.4, 49.2, 40.1, 35.1, 23.1, 22.2, 21.3. **HRMS** (ESI+) calcd for $[C_{21}H_{28}NaO_5]^+$ 383.1829 *m/z*; found $[M + Na]^+$ 383.1829 *m/z*.

Dimethyl (*E*)-3-(4-methoxybenzylidene)-4-(2-methoxypropan-2-yl)cyclopentane-1,1-dicarboxylate (27v)

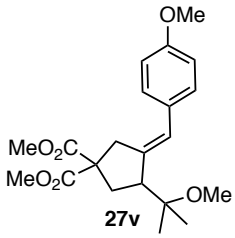

27v

Product **27v** was synthesized following the general procedure using enyne **26a** (60 mg, 0.252 mmol) whereby the reaction was stirred for 15 h. Purification by flash column chromatography (gradient starting with cyclohexane to cyclohexane/EtOAc 4:1) followed by preparative TLC on neutral alumina (pentane/diethyl ether 7:3)afforded the title compound **27v** (37.9 mg, 0.101 mmol, 40% yield) as a colorless oil.

^{1}H NMR (500 MHz, $CDCl_3$) δ 7.20 – 7.15 (m, 2H), 6.88 – 6.84 (m, 2H), 6.46 (s, 1H), 3.81 (s, 3H), 3.74 (s, 3H), 3.62 (s, 3H), 3.24 (dt, *J* = 16.0, 1.7 Hz, 1H), 3.22 (m, 3H), 3.08 – 2.98 (m, 2H), 2.56 (ddd, *J* = 13.5, 8.4, 1.9 Hz, 1H), 2.03 (dd, *J* = 13.4, 8.9 Hz, 1H), 1.22 (s, 3H), 1.15 (s, 3H). **^{13}C NMR** (126 MHz, $CDCl_3$) δ 172.24, 172.21, 158.2, 139.7, 131.0, 129.9, 125.9, 113.7, 77.6, 59.7, 55.4, 52.87, 52.85, 51.3, 49.2, 40.1, 35.1, 23.1, 22.2. **HRMS** (ESI+) calcd for $[C_{21}H_{28}NaO_6]^+$ 399.1778 *m/z*; found $[M + Na]^+$ 399.1771 *m/z*.

Dimethyl (*E*)-3-(2-methoxypropan-2-yl)-4-(3-methylbenzylidene)cyclopentane-1,1-dicarboxylate (27w)

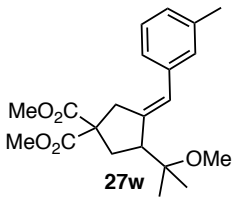

27w

Product **27w** was synthesized following the general procedure using enyne **26a** (30 mg, 0.126 mmol) whereby the reaction was stirred for 15 h. Purification by flash column chromatography (gradient starting with cyclohexane to cyclohexane/EtOAc 4:1) followed by preparative TLC on neutral alumina (pentane/diethyl ether 7:3) afforded the title compound **27w** (34.0 mg, 0.094 mmol, 75% yield) as a yellowish oil.

^{1}H NMR (500 MHz, $CDCl_3$) δ 7.17 – 7.10 (m, 4H), 6.53 (s, 1H), 3.71 (s, 3H), 3.64 (s, 3H), 3.24 (s, 3H), 3.07 – 2.99 (m, 2H), 2.88 (ddd, *J* = 15.7, 3.1, 2.3 Hz, 1H), 2.59 (ddd, *J* = 13.5, 8.5, 1.9 Hz, 1H), 2.23 (s, 3H), 2.05 (dd, *J* = 13.5, 9.0 Hz, 1H), 1.26 (s, 3H), 1.18 (s, 3H). **^{13}C NMR** (126 MHz, $CDCl_3$) δ 172.2, 172.1, 141.8, 137.7, 136.2, 129.8, 128.9, 126.8, 125.6, 125.5, 77.5, 59.3, 52.83, 52.76, 50.5, 49.2, 39.9, 35.3, 23.0, 22.2, 20.1. **HRMS** (ESI+) calcd for $[C_{21}H_{28}NaO_5]^+$ 383.1829 *m/z*; found $[M + Na]^+$ 383.1831 *m/z*.

Dimethyl (*E*)-3-(3-methoxybenzylidene)-4-(2-methoxypropan-2-yl)cyclopentane-1,1-dicarboxylate (27x)

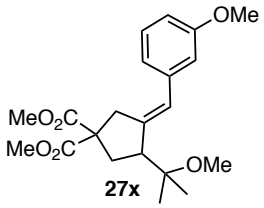

27x

Product **27x** was synthesized following the general procedure using enyne **26a** (30 mg, 0.126 mmol) whereby the reaction was stirred for 15 h. Purification by flash column chromatography (gradient starting with cyclohexane to cyclohexane/EtOAc 4:1) followed by preparative TLC on neutral alumina (pentane/diethyl ether 7:3) afforded the title compound **27x** (29.4 mg, 0.078 mmol, 62% yield) as a colorless oil.

^{1}H NMR (500 MHz, $CDCl_3$) δ 7.22 – 7.16 (m, 2H), 6.92 (td, *J* = 7.4, 0.8 Hz, 1H), 6.84 (d, *J* = 8.0 Hz, 1H), 6.59 (s, 1H), 3.80 (s, 3H), 3.73 (s, 3H), 3.61 (s, 3H), 3.22 (s, 3H), 3.12 (dt, *J* = 15.7, 1.6 Hz, 1H), 3.07 – 2.99 (m, 2H), 2.59 (ddd, *J* = 13.6, 8.4, 1.7 Hz, 1H), 2.10 (dd, *J* = 13.5, 8.6 Hz, 1H), 1.26 (s, 3H), 1.16 (s, 3H).**^{13}C NMR** (126 MHz, $CDCl_3$) δ 172.28, 172.27, 157.1, 141.6, 129.8, 127.9, 127.4, 121.7, 120.3, 110.6, 77.5, 59.6, 55.6, 52.82, 52.78, 51.2, 49.2, 40.2, 35.0, 22.9, 22.7. **HRMS** (ESI+) calcd for $[C_{21}H_{28}NaO_6]^+$ 399.1778 *m/z*; found $[M + Na]^+$ 399.1778 *m/z*.

Dimethyl (*E*)-3-(3-fluorobenzylidene)-4-(2-methoxypropan-2-yl)cyclopentane-1,1-dicarboxylate (27y)

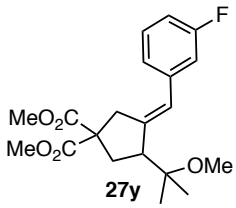

27y

Product **27y** was synthesized following the general procedure using enyne **26a** (30 mg, 0.126 mmol) whereby the reaction was stirred for 15 h. Purification by flash column chromatography (gradient starting with cyclohexane to cyclohexane/EtOAc 4:1) followed by preparative TLC on neutral alumina (pentane/diethyl ether 7:3) afforded the title compound **27y** (28.9 mg, 0.079 mmol, 63% yield) as a yellowish oil.

^{1}H NMR (400 MHz, $CDCl_3$) δ 7.26 (td, *J* = 8.0, 6.0 Hz, 1H), 7.00 (d, *J* = 7.8 Hz, 1H), 6.95 – 6.86 (m, 2H), 6.51 (s, 1H), 3.75 (s, 3H), 3.63 (s, 3H), 3.24 (dt, *J* = 16.0, 1.7 Hz, 1H) 3.22 (s, 3H), 3.07 – 2.98 (m, 2H), 2.56 (ddd, *J* = 13.4, 8.1, 1.7 Hz, 1H), 2.04 (dd, *J* = 13.5, 9.1 Hz, 1H), 1.21 (s, 3H), 1.16 (s, 3H). **^{13}C NMR** (101 MHz, $CDCl_3$) δ 172.1, 172.0, 162.9 (*J* = 245.1 Hz), 143.2, 140.5 (*J* = 7.7 Hz), 129.6 (*J* = 8.5 Hz), 125.5 (*J* = 2.2 Hz), 124.5 (*J* = 2.7 Hz), 115.3 (*J* = 21.3 Hz), 113.3 (*J* = 21.3 Hz), 77.5, 59.5, 53.0, 52.9, 51.4, 49.1, 40.2, 35.2, 23.2, 21.9. **^{19}F{^{1}H} NMR** (376 MHz, $CDCl_3$) δ -113.92. **HRMS** (ESI+) calcd for $[C_{20}H_{25}FNaO_5]^+$ 387.1578 *m/z*; found $[M + Na]^+$ 387.1582 *m/z*.

Dimethyl (*E*)-3-(3-bromobenzylidene)-4-(2-methoxypropan-2-yl)cyclopentane-1,1-dicarboxylate (27z)

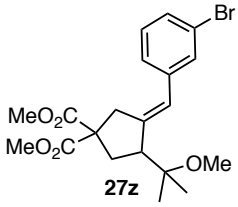

27z

Product **27z** was synthesized following the general procedure using enyne **26a** (30 mg, 0.126 mmol) whereby the reaction was stirred for 15 h. Purification by flash column chromatography (gradient starting with cyclohexane to cyclohexane/EtOAc 4:1) followed by preparative TLC on neutral alumina (pentane/diethyl ether 7:3) afforded the title compound **27z** (29.4 mg, 0.069 mmol, 55% yield) as a yellowish oil.

^{1}H NMR (400 MHz, $CDCl_3$) δ 7.36 (s, 1H), 7.32 (dt, *J* = 7.1, 2.0 Hz, 1H), 7.21 – 7.13 (m, 2H), 6.48 (s, 1H), 3.75 (s, 3H), 3.64 (s, 3H), 3.22 (s, 3H), 3.22 (dt, 15.9, 1.6 Hz, 1H), 3.07 – 2.97 (m, 2H), 2.56 (ddd, *J* = 13.3, 8.2, 1.7 Hz, 1H), 2.04 (dd, *J* = 13.4, 9.2 Hz, 1H), 1.20 (s, 3H), 1.16 (s, 3H). **^{13}C NMR** (101 MHz, $CDCl_3$) δ 172.02, 171.98, 143.5, 140.4, 131.5, 129.8, 129.4, 127.3, 125.2, 122.4, 77.5, 59.6, 53.0, 52.9, 51.4, 49.1, 40.1, 35.2, 23.2, 21.9. **HRMS** (ESI+) calcd for $[C_{20}H_{25}{}^{79}BrNaO_5]^+$ 447.0788 *m/z*; found $[M + Na]^+$ 447.0782 *m/z*.

Dimethyl (*E*)-3-(2-methoxypropan-2-yl)-4-(2-methylbenzylidene)cyclopentane-1,1-dicarboxylate (27aa)

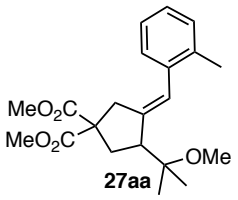

27aa

Product **27aa** was synthesized following the general procedure using enyne **26a** (30 mg, 0.126 mmol) whereby the reaction was stirred for 15 h. Purification by flash column chromatography (gradient starting with cyclohexane to cyclohexane/EtOAc 4:1) followed by preparative TLC on neutral alumina (pentane/diethyl ether 7:3) afforded the title compound **27aa** (30.8 mg, 0.086 mmol, 68% yield) as a yellowish oil.

^{1}H NMR (500 MHz, $CDCl_3$) δ 7.23 – 7.19 (m, 1H), 7.07 – 7.00 (m, 3H), 6.50 (s, 1H), 3.75 (s, 3H), 3.62 (s, 3H), 3.26 (dt, *J* = 16.0, 1.7 Hz, 1H), 3.22 (s, 3H), 3.08 (dt, *J* = 16.0, 2.9 Hz, 1H), 3.03 (tt, *J* = 8.6, 2.2 Hz, 1H), 2.57 (ddd, *J* = 13.5, 8.4, 1.8 Hz, 1H), 2.35 (s, 3H), 2.04 (dd, *J* = 13.5, 8.9 Hz, 1H), 1.23 (s, 3H), 1.16 (s, 3H). **^{13}C NMR** (126 MHz, $CDCl_3$) δ 172.2, 141.4, 138.2, 137.8, 129.5, 128.2, 127.2, 126.6, 125.8, 77.6, 59.7, 52.88, 52.86, 51.4, 49.2, 40.1, 35.1, 23.1, 22.2, 21.6. **HRMS** (ESI+) calcd for $[C_{21}H_{28}NaO_5]^+$ 383.1829 *m/z*; found $[M + Na]^+$ 383.1824 *m/z*.

Dimethyl (*E*)-3-(2-methoxybenzylidene)-4-(2-methoxypropan-2-yl)cyclopentane-1,1-dicarboxylate (27ab)

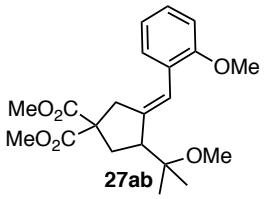

27ab

Product **27ab** was synthesized following the general procedure using enyne **26a** (30 mg, 0.126 mmol) whereby the reaction was stirred for 15 h. Purification by flash column chromatography (gradient starting with cyclohexane to cyclohexane/EtOAc 4:1) followed by preparative TLC on neutral alumina (pentane/diethyl ether 7:3) afforded the title compound **27ab** (32.2 mg, 0.086 mmol, 68% yield) as a colorless oil.

^{1}H NMR (500 MHz, $CDCl_3$) δ 7.23 (t, *J* = 7.8 Hz, 1H), 6.84 (d, *J* = 7.6 Hz, 1H), 6.78 – 6.74 (m, 2H), 6.51 (s, 1H), 3.81 (s, 3H), 3.74 (s, 3H), 3.63 (s, 3H), 3.27 (dt, *J* = 15.8, 1.7 Hz, 1H), 3.22 (s, 3H), 3.09 – 2.99 (m, 2H), 2.56 (ddd, *J* = 13.4, 8.3, 1.8 Hz, 1H), 2.04 (dd, *J* = 13.4, 9.1 Hz, 1H), 1.22 (s, 3H), 1.16 (s, 3H). **^{13}C NMR** (126 MHz, $CDCl_3$) δ 172.2, 172.1, 159.6, 142.1, 139.7, 129.2, 126.4, 121.4, 114.5, 111.9, 77.6, 59.6, 55.4, 52.90, 52.89, 51.4, 49.2, 40.2, 35.2, 23.1, 22.1. **HRMS** (ESI+) calcd for $[C_{21}H_{28}NaO_6]^+$ 399.1778 *m/z*; found $[M + Na]^+$ 399.1773 *m/z*.

Dimethyl (*E*)-3-(2-fluorobenzylidene)-4-(2-methoxypropan-2-yl)cyclopentane-1,1-dicarboxylate (27ac)

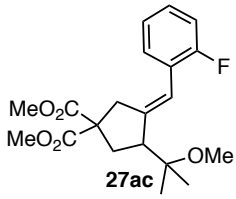

27ac

Product **27ac** was synthesized following the general procedure using enyne **26a** (30 mg, 0.126 mmol) whereby the reaction was stirred for 15 h. Purification by flash column chromatography (gradient starting with cyclohexane to cyclohexane/EtOAc 4:1) followed by preparative TLC on neutral alumina (pentane/diethyl ether 7:3) afforded the title compound **27ac** (30.3 mg, 0.083 mmol, 66% yield) as a yellowish oil.

^{1}H NMR (500 MHz, $CDCl_3$) δ 7.24 (td, *J* = 7.7, 1.8 Hz, 1H), 7.21 – 7.16 (m, 1H), 7.09 (td, *J* = 7.5, 1.1 Hz, 1H), 7.02 (ddd, *J* = 10.3, 8.1, 1.2 Hz, 1H), 6.53 (s, 1H), 3.73 (s, 3H), 3.64 (s, 3H), 3.23 (s, 3H), 3.09 (dt, *J* = 15.9, 2.0 Hz, 1H), 3.07 – 2.96 (m, 2H), 2.59 (ddd, *J* = 13.6, 8.4, 1.9 Hz, 1H), 2.08 (dd, *J* = 13.5, 9.0 Hz, 1H), 1.24 (s, 3H), 1.17 (s, 3H). **^{13}C NMR** (126 MHz, $CDCl_3$) δ 172.1, 172.0, 160.1 (d, *J* = 247.1 Hz), 144.2 (d, *J* = 1.1 Hz), 130.2 (d, *J* = 3.5 Hz), 128.3 (d, *J* = 8.4 Hz), 126.0 (d, *J* = 14.5 Hz), 123.7 (d, *J* = 3.5 Hz), 118.9 (d, *J* = 3.7 Hz), 115.4 (d, *J* = 22.3 Hz), 77.4, 59.4, 52.90, 52.87, 51.1, 49.2, 40.29 (d, *J* = 1.9 Hz), 35.2, 23.0, 22.2. **^{19}F{^{1}H} NMR** (376 MHz, $CDCl_3$) δ -115.70. **HRMS** (ESI+) calcd for $[C_{20}H_{25}FNaO_5]^+$ 387.1578 *m/z*; found $[M + Na]^+$ 387.1567 *m/z*.

Dimethyl (*E*)-3-(2-bromobenzylidene)-4-(2-methoxypropan-2-yl)cyclopentane-1,1-dicarboxylate (27ad)

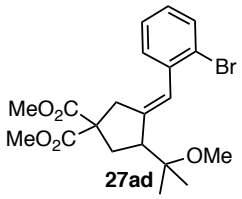

Product **27ad** was synthesized following the general procedure using enyne **26a** (30 mg, 0.126 mmol) whereby the reaction was stirred for 15 h. Purification by flash column chromatography (gradient starting with cyclohexane to cyclohexane/EtOAc 4:1) followed by preparative TLC on neutral alumina (pentane/diethyl ether 7:3) afforded the title compound **27ad** (33.6 mg, 0.079 mmol, 63% yield) as a yellowish oil.

^{1}H NMR (500 MHz, $CDCl_3$) δ 7.54 (dd, *J* = 7.8, 1.0 Hz, 1H), 7.28 – 7.23 (m, 2H), 7.09 – 7.05 (m, 1H), 6.56 (s, 1H), 3.72 (s, 3H), 3.67 (s, 3H), 3.24 (s, 3H), 3.08 – 3.01 (m, 2H), 2.88 (ddd, *J* = 15.7, 3.1, 2.2 Hz, 1H), 2.60 (ddd, *J* = 13.5, 8.4, 1.9 Hz, 1H), 2.07 (dd, *J* = 13.5, 9.2 Hz, 1H), 1.27 (s, 3H), 1.19 (s, 3H). **^{13}C NMR** (126 MHz, $CDCl_3$) δ 171.98, 171.97, 143.4, 138.5, 132.5, 130.4, 128.2, 127.2, 126.2, 124.1, 77.4, 59.3, 52.93, 52.88, 50.6, 49.3, 39.8, 35.3, 23.1, 22.3. **HRMS** (ESI+) calcd for $[C_{20}H_{25}{}^{79}BrNaO_5]^+$ 447.0788 *m/z*; found $[M + Na]^+$ 447.0781 *m/z*.

Dimethyl (*E*)-3-benzylidene-4-(2-methoxy-6-methylhept-5-en-2-yl)cyclopentane-1,1-dicarboxylate (27ag)

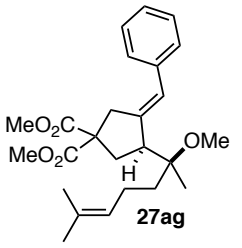

Product **27ag** was synthesized following the general procedure using enyne **26b** (50 mg, 0.163 mmol) whereby the reaction was stirred for 15 h. Purification by flash column chromatography (gradient starting with cyclohexane to cyclohexane/EtOAc 4:1) followed by preparative TLC on neutral alumina (pentane/diethyl ether 7:3) afforded the title compound **27ag** (44.6 mg, 0.108 mmol, 66% yield) as a yellowish oil.

^{1}H NMR (500 MHz, $CDCl_3$) δ 7.34 – 7.29 (m, 2H), 7.23 – 7.18 (m, 3H), 6.42 (s, 1H), 5.10 (ddq, *J* = 8.5, 5.7, 1.4 Hz, 1H), 3.74 (s, 3H), 3.60 (s, 3H), 3.23 (dt, *J* = 15.69, 1.7 Hz, 1H), 3.20 (s, 3H), 3.14 – 3.05 (m, 2H), 2.57 (ddd, *J* = 14.0, 8.6, 1.8 Hz, 1H), 2.15 (dd, *J* = 13.7, 8.3 Hz, 1H), 2.11 – 1.95 (m, 2H), 1.73 – 1.59 (m, 2H), 1.68 (d, *J* = 1.2 Hz, 3H), 1.62 (s, 3H), 1.12 (s, 3H). **^{13}C NMR** (126 MHz, $CDCl_3$) δ 172.3, 172.1, 141.9, 138.1, 131.7, 128.8, 128.3, 126.5, 126.5, 124.6, 79.1, 59.7, 52.89, 52.85, 49.9, 49.1, 40.3, 35.4, 34.2, 25.9, 22.2, 20.0, 17.8. **HRMS** (ESI+) calcd for $[C_{25}H_{34}NaO_5]^+$ 437.2298 *m/z*; found $[M + Na]^+$ 437.2288 *m/z*.

Dimethyl (*E*)-3-benzylidene-4-(methoxy(phenyl)methyl)cyclopentane-1,1-dicarbo-xylate (27ah)

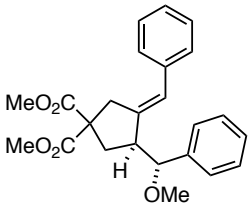

27ah

Product **27ah** was synthesized following the general procedure using enyne **26c** (50 mg, 0.175 mmol) whereby the reaction was stirred for 15 h. Purification by flash column chromatography (gradient starting with cyclohexane to cyclohexane/EtOAc 4:1) followed by preparative TLC on neutral alumina (pentane/diethyl ether 7:3) afforded the title compound **27ah** (47.5 mg, 0.120 mmol, 69% yield) as a yellowish oil.

^{1}H NMR (500 MHz, $CDCl_3$) δ 7.37 – 7.26 (m, 7H), 7.22 – 7.17 (m, 3H), 6.07 (s, 1H), 4.29 (d, *J* = 5.5 Hz, 1H), 3.76 (s, 3H), 3.62 (s, 3H), 3.24 (d, *J* =15.7 Hz, 1H), 3.23 (s, 3H), 3.19 (dt, *J* = 16.6, 2.7 Hz, 1H), 3. 12 – 3.09 (m, 1H), 2.41 (dd, *J* = 8.3, 1.7 Hz, 2H). **^{13}C NMR** (126 MHz, $CDCl_3$) δ 172.27, 172.25, 141.9, 140.7, 138.0, 128.6, 128.4, 128.3, 127.7, 127.3, 126.5, 124.5, 86.1, 59.7, 57.5, 52.90, 52.87, 51.8, 39.6, 34.1. **HRMS** (ESI+) calcd for $[C_{24}H_{26}NaO_5]^+$ 417.1672 *m/z*; found $[M + Na]^+$ 417.1675 *m/z*.

(*E*)-(3-benzylidene-4-(methoxy(phenyl)methyl)cyclopentane-1,1-diyl)bis(methylene) diacetate (27ai)

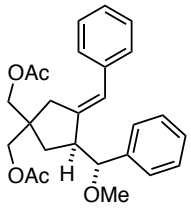

27ai

Product **27ai** was synthesized following the general procedure **B** using enyne **26d** (50 mg, 0.159 mmol) whereby the reaction was stirred for 15 h. Purification by flash column chromatography (gradient starting with cyclohexane to cyclohexane/EtOAc 4:1) followed by preparative TLC on neutral alumina (pentane/diethyl ether 7:3) afforded the title compound **27ai** (50.3 mg, 0.119 mmol, 75% yield) as a yellowish oil.

^{1}H NMR (500 MHz, $CDCl_3$) δ 7.38 – 7.26 (m, 7H), 7.22 – 7.16 (m, 3H), 6.20 (s, 1H), 4.31 (d, *J* = 5.1 Hz, 1H), 4.11 – 4.04 (m, 2H), 3.84 (d, *J* = 11.2 Hz, 1H), 3.76 (d, *J* = 11.2 Hz, 1H), 3.25 (s, 3H), 3.10 – 3.02 (m, 1H), 2.57 (dt, *J* = 16.1, 1.6 Hz, 1H), 2.37 (dt, *J* = 16.1, 2.8 Hz, 1H), 2.05 (s, 3H), 1.94 (s, 3H), 1.80 (dd, *J* = 13.6, 8.7 Hz, 1H), 1.67 (ddd, *J* = 13.6, 8.5, 1.5 Hz, 1H). **^{13}C NMR** (126 MHz, $CDCl_3$) δ 171.2, 171.1, 143.5, 140.7, 138.3, 128.5, 128.4, 128.3, 127.7, 127.4, 126.4, 124.9, 86.8, 68.1, 65.7, 57.5, 50.9, 45.3, 38.3, 31.5, 21.0, 20.9. **HRMS** (ESI+) calcd for $[C_{26}H_{30}NaO_5]^+$ 445.1985 *m/z*; found $[M + Na]^+$ 445.1983 *m/z*.

(*E*)-(3-(3-bromobenzylidene)-4-(methoxy(phenyl)methyl)cyclopentane-1,1-disulfonyl)dibenzene (27aj)

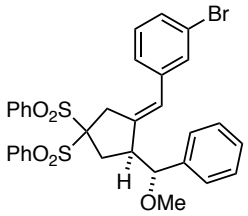

27aj

Product **27aj** was synthesized following the general procedure using enyne **26e** (50 mg, 0.111 mmol) whereby the reaction was stirred for 15 h. Purification by flash column chromatography (gradient starting with cyclohexane to cyclohexane/EtOAc 2:1) followed by preparative TLC on neutral alumina (pentane/diethyl ether 7:3) afforded the title compound **27aj** (55.8 mg, 0.088 mmol, 79% yield) as a white-off amorphous solid.

^{1}H NMR (500 MHz, $CDCl_3$) δ 8.12 – 8.07 (m, 2H), 7.72 (tt, *J* = 7.5, 1.2 Hz, 1H), 7.69 – 7.65 (m, 2H), 7.63 – 7.58 (m, 2H), 7.53 (tt, *J* = 7.5, 1.2 Hz, 1H), 7.39 – 7.32 (m, 3H), 7.30 – 7.15 (m, 8H), 6.97 (dt, *J* = 7.7, 1.3 Hz, 1H), 5.84 (s, 1H), 4.26 (d, *J* = 6.4 Hz, 1H), 3.62 (dt, *J* = 17.7, 2.7 Hz, 1H), 3.25 (s, 3H), 3.22 – 3.16 (m, 1H), 3.10 (dt, *J* = 17.6, 1.6 Hz, 1H), 2.95 (dd, *J* = 15.4, 7.2 Hz, 1H), 2.54 (ddd, *J* = 15.4, 8.5, 1.5 Hz, 1H). **^{13}C NMR** (126 MHz, $CDCl_3$) δ 141.2, 139.8, 139.4, 137.2, 135.3, 134.7, 134.6, 131.4, 131.3, 131.0, 129.99, 129.95, 128.8, 128.6, 128.2, 127.2, 127.0, 124.4, 122.5, 93.1, 85.8, 57.5, 52.6, 36.2, 31.8. **HRMS** (ESI+) calcd for $[C_{32}H_{29}{}^{79}BrNaO_5S_2]^+$ 659.0532 *m/z*; found $[M + Na]^+$ 659.0549 *m/z*.

(*E*)-(3-Benzylidene-4-(2-methoxypropan-2-yl)cyclopentane-1,1-diyl)dibenzene-sulfur(IV) oxide (1/2) (27ak)

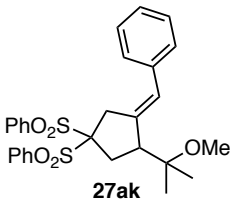

27ak

Product **27ak** was synthesized following the general procedure using enyne **26f** (50 mg, 0.124 mmol) whereby the reaction was stirred for 15 h. Purification by flash column chromatography (gradient starting with cyclohexane to cyclohexane/EtOAc 2:1) followed by preparative TLC on neutral alumina (pentane/diethyl ether 1:1) afforded the title compound **27ak** (47.5 mg, 0.093 mmol, 75% yield) as a white-off amorphous solid.

^{1}H NMR (500 MHz, $CDCl_3$) δ 8.14 – 8.10 (m, 2H), 7.72 (tt, *J* = 7.5, 1.2 Hz, 1H), 7.64 – 7.59 (m, 4H), 7.45 (tt, *J* = 7.5, 1.2 Hz, 1H), 7.37 – 7.32 (m, 2H), 7.27 (tt, *J* = 7.4, 1.3 Hz, 1H), 7.18 – 7.14 (m, 2H), 7.11 – 7.06 (m, 2H), 6.51 (s, 1H), 3.67 (ddd, *J* = 17.3, 3.4, 2.2 Hz, 1H), 3.24 – 3.18 (m, 4H), 3.07 (dt, *J* = 17.2, 1.5 Hz, 1H), 2.74 (dd, *J* = 15.4, 7.5 Hz, 1H), 2.63 (ddd, *J* = 15.5, 9.0, 1.7 Hz, 1H), 1.29 (s, 3H), 1.18 (s, 3H). **^{13}C NMR** (126 MHz, $CDCl_3$) δ 139.9, 137.6, 137.4, 134.9, 134.6, 134.4, 131.3, 131.0, 128.80, 128.77, 128.5, 128.3, 127.3, 127.1, 93.4, 77.5, 52.7, 49.5, 36.8, 31.8, 23.0, 22.4. **HRMS** (ESI+) calcd for $[C_{28}H_{30}NaO_5S_2]^+$ 533.1427 *m/z*; found $[M + Na]^+$ 533.1413 *m/z*.

(*Z*)-3-Benzylidene-4-(2-methoxypropan-2-yl)-1-tosylpyrrolidine (27al)

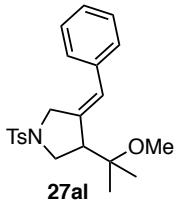

27al

Product **27al** was synthesized following the general procedure using enyne **26g** (50 mg, 0.180 mmol) whereby the reaction was stirred for 15 h. Purification by flash column chromatography (gradient starting with cyclohexane to cyclohexane/EtOAc 4:1) followed by preparative TLC on neutral alumina (pentane/diethyl ether 8:2) afforded the title compound **27al** (50.0 mg, 0.130 mmol, 72% yield) as a yellowish oil.

^{1}H NMR (400 MHz, CD_2Cl_2) δ 7.70 – 7.65 (m, 2H), 7.39 – 7.30 (m, 4H), 7.25 (tt, *J* = 7.4, 1.3 Hz, 1H), 7.17 – 7.12 (m, 2H), 6.43 (s, 1H), 4.10 (ddd, *J* = 14.3, 2.6, 1.6 Hz, 1H), 4.02 (dd, *J* = 14.2, 2.1 Hz, 1H), 3.48 (dd, *J* = 10.1, 3.6 Hz, 1H), 3.22 (dd, *J* = 10.1, 8.0 Hz, 1H), 3.11 (s, 3H), 2.94 – 2.89 (m, 1H), 2.41 (s, 3H), 1.17 (s, 3H), 1.05 (s, 3H). **^{13}C NMR** (101 MHz, CD_2Cl_2) δ 144.3, 138.2, 137.4, 133.7, 130.2, 129.0, 128.9, 128.2, 127.7, 127.2, 77.2, 51.8, 49.5, 48.5, 22.7, 22.3, 21.8. **HRMS** (ESI+) calcd for $[C_{22}H_{27}NNaO_3S]^+$ 408.1604 *m/z*; found $[M + Na]^+$ 408.1604 *m/z*.

(*Z*)-1-benzylidene-2-(2-methoxypropan-2-yl)-2,3-dihydro-1H-indene (27am)

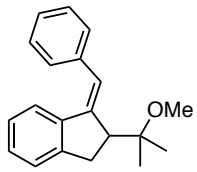

27am

Product **27am** was synthesized following the general procedure using enyne **26h** (50 mg, 0.294 mmol) whereby the reaction was stirred for 15 h. Purification by flash column chromatography (gradient starting with cyclohexane to cyclohexane/EtOAc 8:1) followed by preparative TLC on neutral alumina (pentane/diethyl ether 9:1) afforded the title compound **27am** (49.8 mg, 0.179 mmol, 61% yield) as a yellowish oil.

^{1}H NMR (500 MHz, $CDCl_3$) δ 7.38 – 7.32 (m, 4H), 7.29 – 7.25 (m, 1H), 7.21 (dt, *J* = 7.7, 0.8 Hz, 1H), 7.11 (td, *J* = 7.4, 1.1 Hz, 1H), 7.05 (d, *J* = 7.9 Hz, 1H), 6.88 (t, *J* = 7.6 Hz, 1H), 6.74 (s, 1H), 3.29 (s, 3H), 3.25 (ddd, *J* = 8.1, 2.8, 1.6 Hz, 1H), 3.09 (dd, *J* = 16.6, 8.1 Hz, 1H), 3.01 (dd, *J* = 16.6, 2.7 Hz, 1H), 1.31 (s, 3H), 0.91 (s, 3H). **^{13}C NMR** (126 MHz, $CDCl_3$) δ 147.4, 143.9, 140.4, 138.6, 128.7, 128.6, 128.2, 126.9, 125.7, 125.5, 124.9, 124.4, 77.7, 52.2, 49.2, 33.0, 22.6, 22.4. **HRMS** (ESI+) calcd for $[C_{20}H_{22}NaO]^+$ 301.1563 *m/z*; found $[M + Na]^+$ 301.1552 *m/z*.

Experimental mechanistic studies

Control experiment in the dark

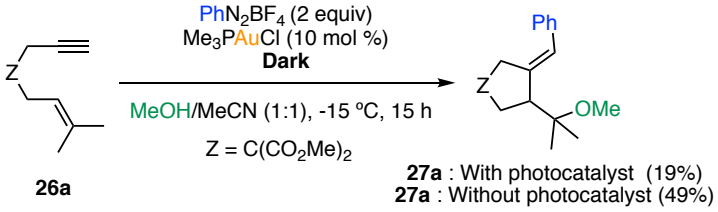

In the dark room (only red light), a reaction was set up following the general procedure both in the presence and in the absence of photocatalyst. After 15 h NMR yields were calculated showing the formation of **27a** in 19% and 49%. These results highlight the importance of a radical propagation mechanism in the absence of photocatalytic cycle.

Control experiment in the absence of aryldiazonium salts and photocatalyst

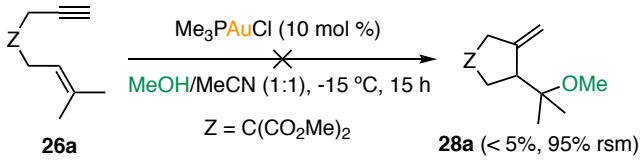

In the absence of diazonium salt and photocatalyst, **28a** could not be obtained starting from **26a**. This can be rationalized due to the lack of coordination vacant in gold(I) catalyst which hampers the coordination/activation of the alkyne. Since product **28a** is observed as a byproduct in the reaction, this experiment suggests that it might be formed upon protodeauration of alkenylgold(III) intermediate competing with reductive elimination to yield **27a**.

Control experiment in the absence of gold catalyst

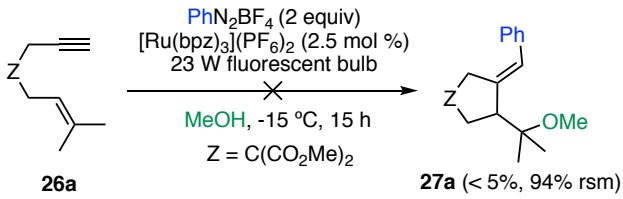

In the absence of gold catalyst, the reaction is shut down.

Control experiment on the oxidative addition of diazonium salt 30w to Me_3PAuCl:

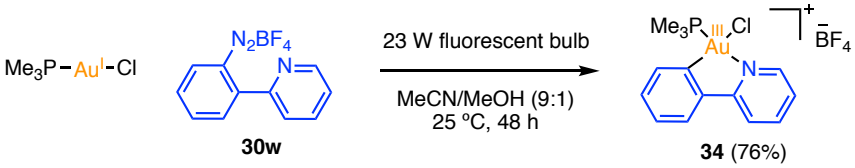

Under argon atmosphere, Me_3PAuCl (30 mg, 0.097 mmol) and 2-(pyridin-2-yl)benzenediazonium tetrafluoroborate (26.2 mg, 0.097 mmol, 1 equiv) were dissolved in a mixture of acetonitrile (0.9 ml) and MeOH (0.1 mL). The reaction was stirred for 48 h under the irradiation of a 23 W fluorescent desk lamp. Upon addition of diethyl ether, a white precipitate

was formed. Direct filtration allowed the isolation of pure **34** (40.5 mg, 0.74 mmol, 76%) as a white crystalline solid.

M.p. (pentane): 175-177 ºC. **^{1}H NMR** (400 MHz, Acetone-d_6) δ 9.58 – 9.54 (m, 1H), 8.49 – 8.42 (m, 2H), 8.19 – 8.14 (m, 1H), 7.96 (ddd, J = 7.2, 5.7, 1.3 Hz, 1H), 7.88 (tdd, J = 5.9, 3.0, 2.0 Hz, 1H), 7.64 – 7.53 (m, 2H), 2.46 (d, J = 13.6 Hz, 9H). **^{13}C NMR** (101 MHz, acetone-d_6) δ 164.1, 152.4, 148.7, 145.4, 145.0, 134.1 (d, J = 3.9 Hz), 133.0 (d, J = 6.4 Hz), 130.5, 128.3, 126.2 (d, J = 4.0 Hz), 122.8 (d, J = 2.7 Hz), 15.2 (d, J = 43.8 Hz). **^{31}P{^{1}H} NMR** (162 MHz, acetone-d_6) δ 21.7. **HRMS** (ESI+) calcd for $[C_{14}H_{17}AuClNP]^+$ *m/z* 462.0447; found $[M]^+$ *m/z* 462.0433.

Studies on the alternative mechanism for the formation of 27a

Dimethyl (Z)-3-benzylidene-4-(2-methoxypropan-2-yl)cyclopentane-1,1-dicarboxy-late (35)

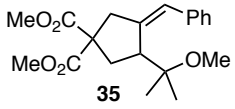

35

Enyne **26k** (50 mg, 0,159 mmol) and [JohnphosAuNCMe](SbF$_6$) (12.3 mg, 0.016 mmol, 10 mol %) were dissolved in MeOH (2 mL) and the reaction was stirred for 2 h. Direct evaporation of the reaction crude followed by purification on preparative TLC (pentane/diethyl ether, 7:3) afforded **35** (17 mg, 0.049 mmol, 31% yield) as a white solid.

M.p. (pentane): 86-89 ºC. **^{1}H NMR** (500 MHz, $CDCl_3$) δ 7.30 – 7.25 (m, 2H), 7.22 (d, J = 6.9 Hz, 2H), 7.16 (tt, J = 7.3, 1.5 Hz, 1H), 6.47 (s, 1H), 3.75 (s, 3H), 3.73 (s, 3H), 3.48 (dd, J = 8.6, 5.5 Hz, 1H), 3.28 (ddd, J = 14.3, 2.7, 1.5 Hz, 1H), 3.01 (s, 3H), 2.74 (d, J = 14.3 Hz, 1H), 2.65 (ddd, J = 13.9, 8.9, 1.5 Hz, 1H), 2.32 (dd, J = 13.9, 5.3 Hz, 1H), 0.89 (s, 6H). **^{13}C NMR** (126 MHz, $CDCl_3$) δ 172.8, 172.2, 143.4, 139.0, 128.45, 128.43, 126.5, 125.8, 78.1, 58.7, 52.9, 52.8, 49.1, 46.9, 45.0, 34.8, 23.6, 22.8. **HRMS** (ESI+) calcd for $[C_{20}H_{26}NaO_5]^+$ 369.1672 m/z; found [M + Na]+ 369.1672 m/z.

Control experiment on the isomerization of alkene 35

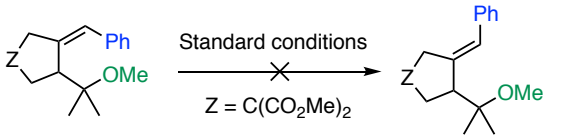

35 **27a** (0%, 100% rsm)

Product **35** (30 mg, 0.087 mmol), phenyldiazonium tetrafluoroborate (33.2 mg, 0.173 mmol, 2.0 equiv), [Ru(bpz)$_3$](PF$_6$)$_2$ (1.9 mg, 2.17 µmol, 2.5 mol%) and Me$_3$PAuCl (2,67, 8.66 µmol, 10 mol%) were placed in a vial equipped with a stir bar. To the vial kept in the dark was added the degassed solvent (MeOH/MeCN, 1:1) previously cooled at –15 ºC (0.04 M). The vial was evacuated and refilled with nitrogen three times. The mixture was placed at -15 ºC and stirred under a desk lamp with a 23 W fluorescent light bulb. After 15 h the starting material was fully recovered showing the non-feasibility of the isomerization, its remarkable stability under the reaction conditions and discarding the alternative proposed mechanism.

Assignment of the alkene configuration of 27a and 35 by NMR studies

^{1}H NMR for compound **27a**

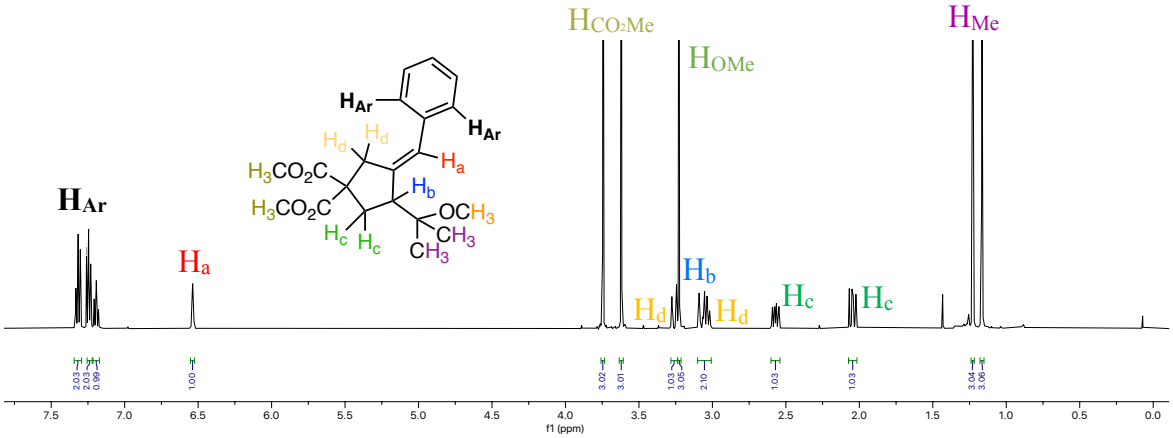

Goesy (nOe) Irradiation on vinylic proton H_a (6.54 ppm)

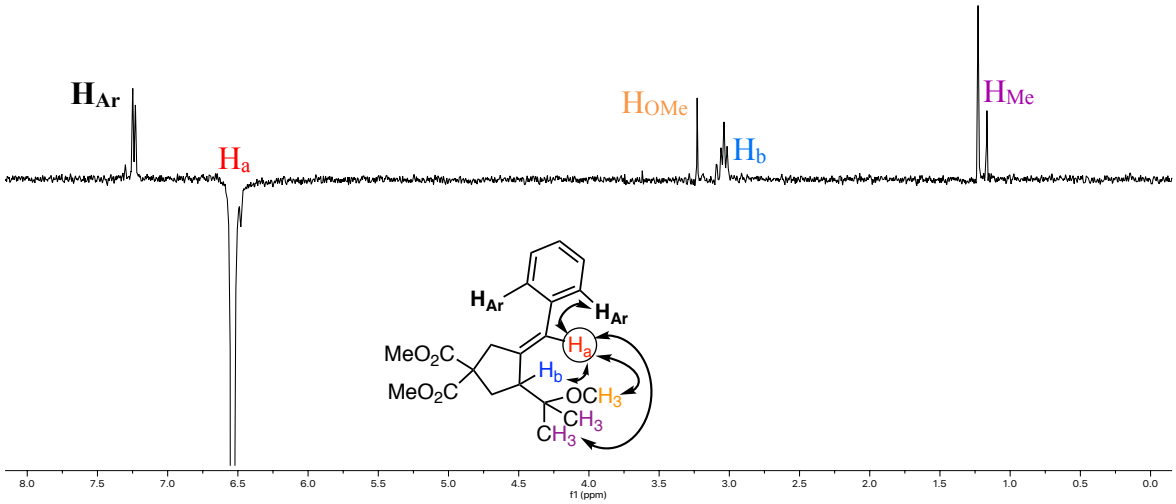

Goesy (nOe) Irradiation on aromatic $\mathbf{H_{Ar}}$ (7.24 ppm)

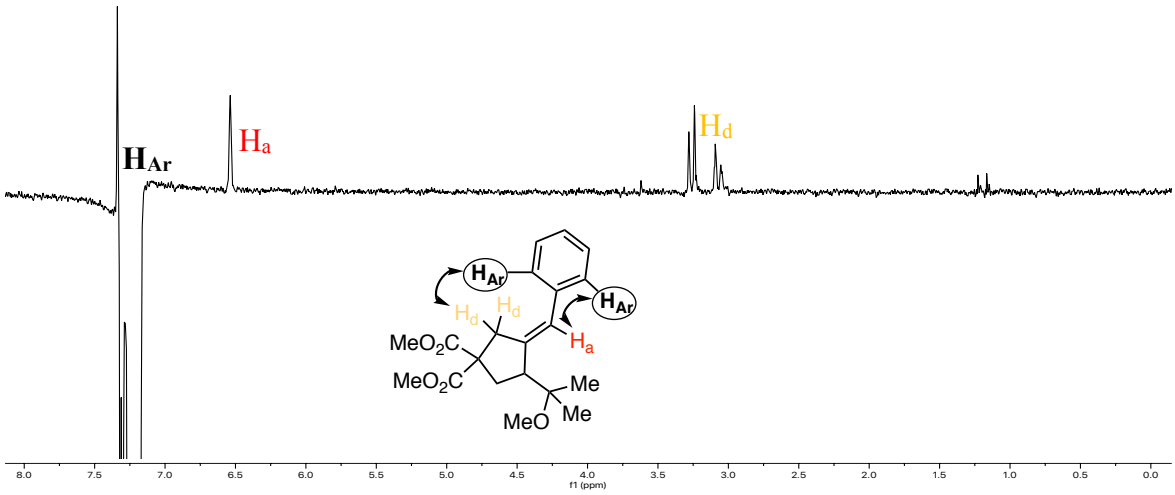

^{1}H NMR for compound **35**

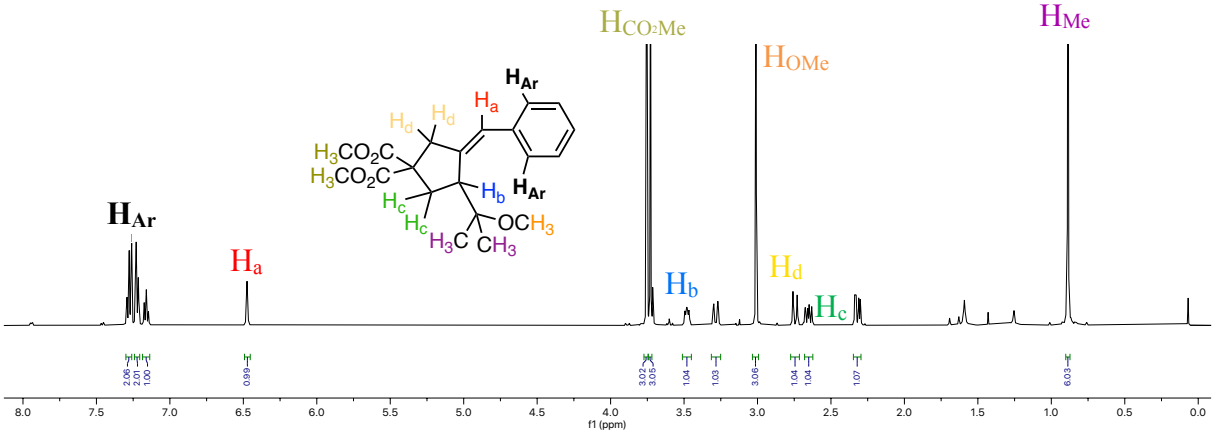

Goesy (nOe) Irradiation on vinylic proton H_a (6.47 ppm)

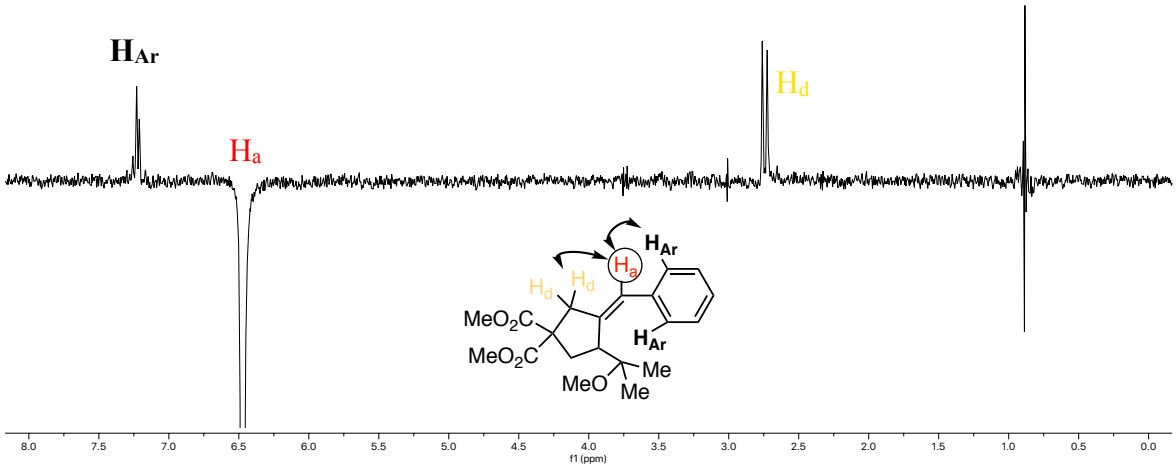

Goesy (nOe) Irradiation on aromatic proton $\mathbf{H_{Ar}}$ (7.22 ppm)

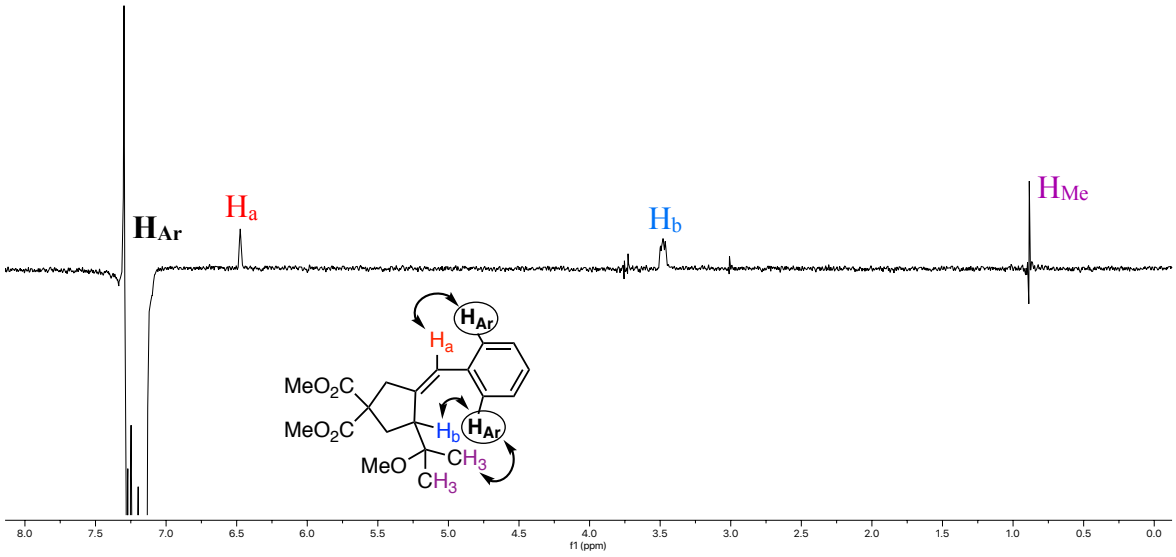

Chapter III:

Rhodium-Catalyzed ortho-Alkynylation of Nitroarenes

In collaboration with Dr. Eric Tan, Dr. Cristina García-Morales and Dr. Marc Montesinos-Magraner

Introduction

C–H Functionalization

"*The ideal synthesis creates a complex target… from available small molecules so functionalized as to allow constructions linking them together directly, in a sequence only of successive construction reactions involving no intermediary refunctionalizations, and leading directly to the structure of the target, not only its skeleton but also its correctly placed functionality.*"[1]

- Prof. James B. Hendrickson, 1975 -

Saving resources, energy and time are crucial aspects governing the evolution of modern synthetic chemistry, especially in multi-step and big-scale syntheses. The most efficient chemical transformation would involve the reaction between two or more organic fragments to generate a larger molecule containing all the atoms present in the initial materials in quantitative yield (Scheme 1). Ideally, the transformation would take place instantly, in the absence of solvent and under ambient conditions furnishing the pure product ready to engage in further reactions.

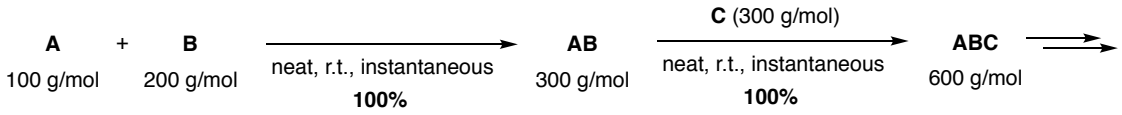

Scheme 1. Ideal chemical transformations.

Although such an ideal reaction rarely exists, the optimization of chemical processes in order to approach this ideality by minimizing the generation of waste (substrate excesses, undesired side-products, reagents, catalysts, solvents, energy, time, etc…) is key to develop a sustainable chemistry. Concepts such as atom-,[2] step-[3] or redox-economy[4] have been coined to appoint the efficiency of chemical synthesis and have gained importance over the past decades.

The coupling of two compounds often requires prefunctionalization steps, which results in a loss in terms of step- and atom-economy (Scheme 2a). Alternatively, the possibility to introduce new functionality *via* C–H bond transformation is a highly attractive strategy in covalent synthesis (Scheme 2b). Using this approach, the generation of waste is minimized and the range of available

1 Hendrickson, J. B. *J. Am. Chem. Soc.* **1975**, *97*, 5784–5800.

2 Trost, B. M. *Science* **1991**, *254*, 1471–1477. (b) Trost, B. M. *Angew. Chem. Int. Ed. Engl*. **1995**, *34*, 259–281. (c) Trost, B. M. *Acc. Chem. Res.* **2002**, 35, 695–705.

3 (a) Wender, P. A.; Croatt, M. P.; Witulski, B. *Tetrahedron* **2006**, *62*, 7505–7511. (b) Wender, P. A.; Verma, V. A.; Paxton, T. J.; Pillow, T. H. *Acc. Chem. Res.* **2008**, 41, 40–49. (c) Wender, P. A.; Miller, B. L. *Nature* **2009**, 460, 197–201.

4 (a) Richter, J. M.; Ishihara, Y.; Masuda, T.; Whitefield, B. W.; Llamas, T.; Pohjakallio, A.; Baran, P. S. *J. Am. Chem. Soc.* **2008**, *130*, 17938–17954. (b) Burns, N. Z.; Baran, P. S.; Hoffmann, R. W. *Angew. Chem. Int. Ed.* **2009**, *48*, 2854–28.

substrates broadens, including hydrocarbons, complex organic compounds or even synthetic and biological polymers.

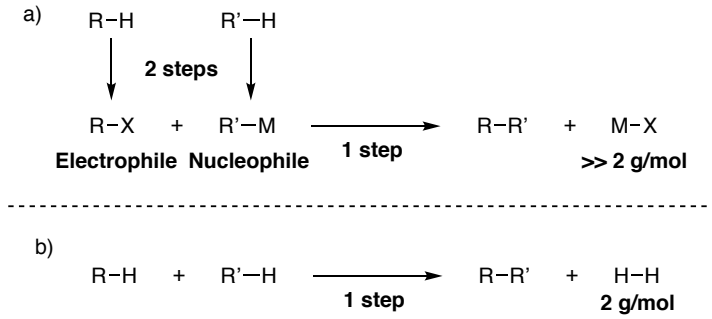

Scheme 2. a) Traditional coupling strategy. b) Coupling *via* C–H functionalization.

The selective functionalization of C–H bonds has been long considered the *Holy Grail* of synthetic chemistry. However, there are two important issues inherent to this strategy. The first concerns the low reactivity displayed by the robust C–H bonds. The kinetic inertness of these bonds, which is related to their apolar nature, can be illustrated by the values of the corresponding bond dissociation energies (BDE). As depicted in Figure 1, the BDE decreases along the series C(sp)–H > $C(sp)^2$–H > $C(sp)^3$–H and from primary > secondary > tertiary > allylic $C(sp)^3$–H bonds. This behavior is in line with the notion that the BDE is inversely proportional to the stability of the radicals obtained from homolytic dissociation of the bond. On the other hand, the tendency of C–H bond to cleave heterolytically (deprotonation) is proportional to the stability of the resulting conjugated base and it can be quantified by the measurement of the pK_a (Figure 1). The trend observed in this case is opposite to the one obtained for the homolytic cleavage, with exception of allylic C–H bonds.[5]

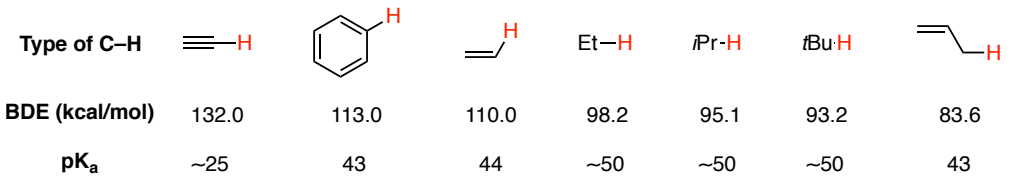

Figure 1. BDE and pK_a values for different representative types of C–H bonds.

These data confirm the difficulty associated with C–H bond cleavage. For a perspective, hydroiodic acid featuring a considerably weaker H–I bond, presents a BDE of 71.3 kcal/mol and a negative pK_a value.[6]

The second challenge inherent to direct C–H functionalization consists in solving selectivity issues. On one side, a highly reactive system has to be used in order to activate the kinetically stable C–H bonds. This can cause chemoselectivity problems if other functionalities

5 Roudesly, F.; Oble, J.; Poli, G. *J. Mol. Catal. A Chem.* **2017**, *426*, 275–296.

6 Blanksby, S. J.; Ellison, G. B. *Acc. Chem. Res.* **2003**, *36*, 255–263.

within the substrate react faster than the targeted C–H bond. On the other side, even with fully controlled chemoselectivity, moderately simple organic molecules incorporate several types of C–H bonds that might display similar chemical behavior, giving rise to low regio- and stereoselectivities (Figure 2).[5]

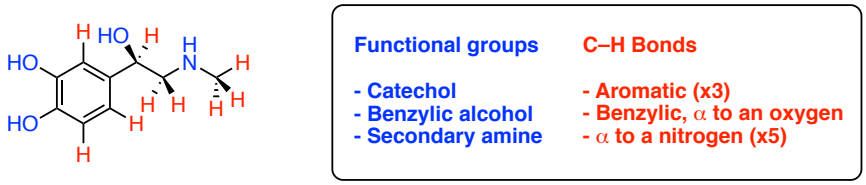

Figure 2. Adrenaline. Functional groups (blue) and potentially funtionalizable C–H bonds (red).

Despite these imposing challenges, significant advances have been reported in the field of direct C–H activation. In the next section, the pioneering works that led to the establishment of the field will be covered.

History

In the early 1880s, A. W. Hoffman synthesized a number of N-haloamines during his attempts to elucidate the structure of piperidine. The German chemist investigated their reactivity under acidic and basic conditions and in 1883 reported that upon treatment with sulfuric acid followed by basic work-up, bromopiperidine **1** formed δ-coneceine **2** (Scheme 3a).[7] This emblematic reaction stands as one of the first examples of C–H functionalization. Ulterior studies by Löffler and Freytag expanded this scope to other types of secondary amines and demonstrated the synthetic utility of the process by applying it in the concise synthesis of nicotine **4** from haloamine **3** (Scheme 3b).[8]

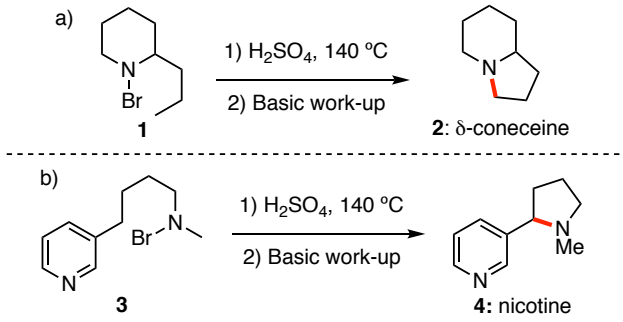

Scheme 3. a) Earliest example of alkyl C–H bond functionalization. b) Application of the strategy to the synthesis of nicotine.

7 (a) Hoffman, A. W. *Ber. Dtsch. Chem. Ges.* **1883**, *16*, 558–560. (b) Hoffman, A. W. *Ber. Dtsch. Chem. Ges.* **1885**, *18*, 5–23. (c) Hoffman, A. W. *Ber. Dtsch. Chem. Ges.* **1885**, *18*, 109–131. (d) Lellmann, E. *Ber. Dtsch. Chem. Ges.* **1890**, *23*, 2141–2142.

8 Löffler, K.; Freytag, C. *Ber. Dtsch. Chem. Ges.* **1909**, *42*, 3427–3431.

The mechanism of the so-called Hoffman-Löffler-Freytag reaction[9] was later studied first by Wawzonek and co-workers[10] and then by Corey.[11] Initially, under strong acidic media, haloamine **5** forms the corresponding ammonium salt **6**. Then, the homolytic cleavage of the N–Halogen bond is promoted by either heat, UV irradiation or hydrogen peroxide leading to a N-centered radical **7** that rapidly abstracts a hydrogen from a spatially close carbon forming the C-centered radical species **8**. Halogenation of this intermediate by reaction with **6** gives rise to intermediate **9** while propagating the radical chain mechanism. The final product **10** is formed upon cyclization of **9** during the basic work-up (Scheme 4).

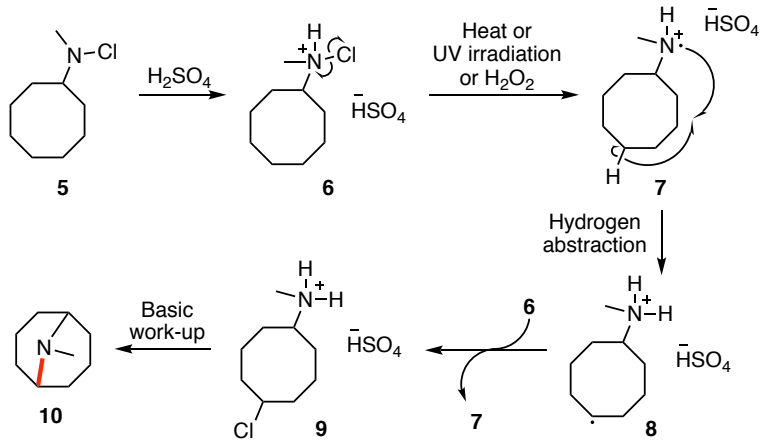

Scheme 4. Proposed mechanism for the Hoffman-Löffler-Freytag reaction.

In this reaction, the issue concerning the low reactivity of C–H bonds was addressed by the generation of a highly reactive N-centered radical and the selectivity observed arose from the structural proximity between the high energy radical generated and the C–H group to be functionalized during the intramolecular process.

The first example of metal-promoted C–H activation was reported by Volhard and Liebigs in 1892, and concerned the reaction between mercury(II) chloride and thiophene to give chloromercurytiophene (Scheme 5a).[12] Shortly after, Dimroth found that various arylmercury acetates could be synthesized from benzene derivatives and mercury(II) acetate (Scheme 5b).[13]

---

9 (a) Wolff, M. E. *Chem. Rev.* **1963**, *63*, 55–64. (b) Stella, L. *Angew. Chem. Int. Ed.* **1983**, *22*, 337–350. (c) Stateman, L. M.; Nakafuku, K. M.; Nagib, D. A. *Synthesis* **2018**, *50*, 1569–1586. (d) Kumar, G.; Pradhan, S. Chatterjee, I. *Chem. Asian J.* **2020**, *15*, 651–672.

10 (a) Wawzonek, S.; Thelen, P. J. *J. Am. Chem. Soc.* **1950**, *72*, 2118–2120. (b) Wawzonek, S.; Thelen, P. J. *J. Am. Chem. Soc.* **1951**, *73*, 2806–2808. (c) Wawzonek, S.; Culberston, T. P. *J. Am. Chem. Soc.* **1959**, *81*, 3367–3369.

11 Corey, E. J.; Hertler, W. R. *J. Am. Chem. Soc.* **1960**, *82*, 1657–1668.

12 Volhard, J.; Liebigs, J. *Ann. Chem.* **1892**, *267*, 172–185.

13 (a) Dimroth, O. *Ber. Dtsch. Chem. Ges.* **1898**, *31*, 2154–2156. (b) Dimroth, O. *Ber. Dtsch. Chem. Ges.* **1899**, *32*, 758. (c) Dimroth, O. *Ber. Dtsch. Chem. Ges.* **1902**, *35*, 2032–2045. (d) Dimroth, O. *Ber. Dtsch. Chem. Ges.* **1902**, *35*, 2853–2873.

Following these results, Kharasch and Isbell reported the first C–H auration of aromatic systems in 1931 (Scheme 5c).[14]

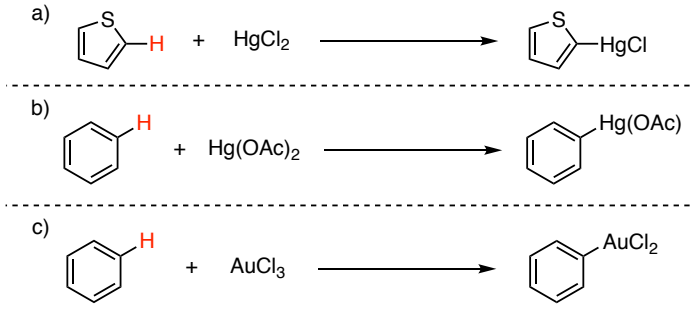

Scheme 5. Pioneering examples of electrophilic C–H mercuration (a and b) and auration (c).

In 1894, Fenton reported the first reported metal-catalyzed C–H functionalization. This work covers the oxidation of tartaric acid by hydrogen peroxide in the presence of a ferrous salt.[15] The highly reactive hydroxyl radicals generated during the reaction are powerful non-selective oxidants capable of oxidizing a wide variety of C–H bonds indiscriminately, which is one of the reasons why this system has been used to destroy hazardous organic pollutants from water.[16] For instance, hydroxyl radicals undergo rapid addition to arenes to form the corresponding phenols.[17]

Overview of Metal-Promoted Mechanisms for the Activation of C–H Bonds

From a mechanistic perspective, the activation of a C–H bond by a metallic complex can occur *via* two different pathways. Outer sphere mechanisms involve the interaction of the reactive C–H bond with a ligand from the transition metal complex. This is the case for C–H oxidation by metal-oxo species *via* the so-called rebound mechanism (Scheme 6a). This category also includes the metal-carbenes/nitrenes insertion into C–H bonds (Scheme 6b).[18]

14 Kharasch, M. S.; Isbell, H. S. *J. Am. Chem. Soc.* **1931**, *53*, 3053–3059.

15 (a) Fenton, H. J. H. *J. Chem. Soc., Trans.* **1894**, *65*, 899–911. For recent advances, see: (b) Walling, C. *Acc. Chem. Res.* **1975,** *8*, 125–131 (c) Neyens, E.; Baeyens, *J. Hazard. Mater.* **2003**, *98*, 33–50.

16 Huang, C. P.; Dong, C.; Tang, Z. *Waste Mgmt.* **1993**, *13*, 361–377.

17 Merz, J. H.; Waters, W. A. *J. Chem. Soc.* **1949**, 2427–2433.

18 (a) Smolinsky, G., Feuer, B. I. *J. Am. Chem. Soc.* **1964**, *86*, 3085–3088. (b) Demonceau, A.; Noels, A. F.; Hubert, A. J.; Teyessié, P. *Chem. Commun.* **1981**, 688–689. (c) Doyle, M. P.; Westrum, L. J.; Wolthius, W. N. E.; See, M. M.; Boone, W. P.; Bagheri, V.; Pearson, M. M. *J. Am. Chem. Soc.* **1993**, *115*, 958–964. (d) Doyle, M. P.; Duffy, R.; Ratnikov, M.; Zhou, L. *Chem. Rev.* **2010**, *110*, 704–724.

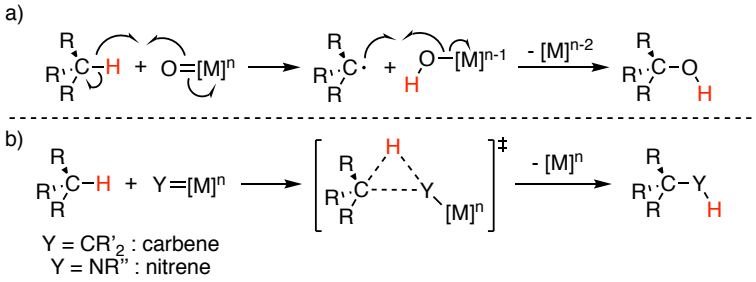

Scheme 6. a) Rebound mechanism for the oxidation of alkanes by metal-oxo complexes. b) Insertion of metal-carbenes/nitrenes into C–H bonds.

In contrast, in inner sphere mechanisms the initial interaction takes place between the reactive C–H bond and the metal center, giving rise to an organometallic complex. There are two main components contributing to this interaction: the charge transfer from the filled σ (C–H) bonding orbital to an empty metal-based *d* orbital from the metal (forward CT) and the back-donation from an occupied *d* orbital of the metal to the σ* (C–H) antibonding orbital (reverse CT). The weight of each component is dependent on the metal center, the steric and electronic properties of the metal environment and the substrate involved in the C–H activation process.[5]

The three main different proposed mechanisms for inner sphere C–H activation processes are discussed below.

1) Oxidative Addition

This pathway operates when highly nucleophilic metals are used to promote the C–H activation. In this extreme mechanistic scenario, the back-donation from the metal to the σ* (C–H) antibonding orbital is so important that the metal gets oxidized and the C–H bond is cleaved. As a result, two new M–C and M–H bonds are formed (Scheme 7).[19]

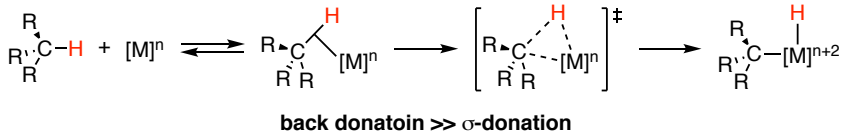

Scheme 7. C–H activation *via* oxidative addition.

In particular, oxidative addition mechanism is representative of electron-rich, d^8 low-valent, second- and third-row transition metal complexes, for which the enthalpy balance between the C–H bond break and the M–C and M–H bond formation to give the oxidized d^6 configuration, is not energetically so costly. The presence of electron-donor ligands such as NHC carbenes or phosphines, favors this nucleophilic mechanism.

19 Souillart, L.; Cramer, N. *Chem. Rev.* **2015**, *115*, 9410–9464.

2) Electrophilic Activation

On the other side of the spectrum, the coordination of C–H bond to electrophilic metals (forward CT >> reverse CT) results in a weakened C–H bond that can be heterolytically cleaved in the presence of a base. Most commonly, the deprotonation takes place intramolecularly and is assisted by a heteroatom basic ligand (halides, alkoxides…) or a bridging ligand (carboxylate, carbonate…) (Scheme 8). This mechanism, known as concerted metallation-deprotonation,[20] ambiphilic ligand-metal activation[21] or internal electrophilic substitution,[22] is often observed with electrophilic Pd(II), Pt(II), Rh(III), Ir(III) and Ru(II) complexes and it is favored by the use of electron-withdrawing ligands. Unlike the previous case, no change in the oxidation state of the metal occurs during the reaction.

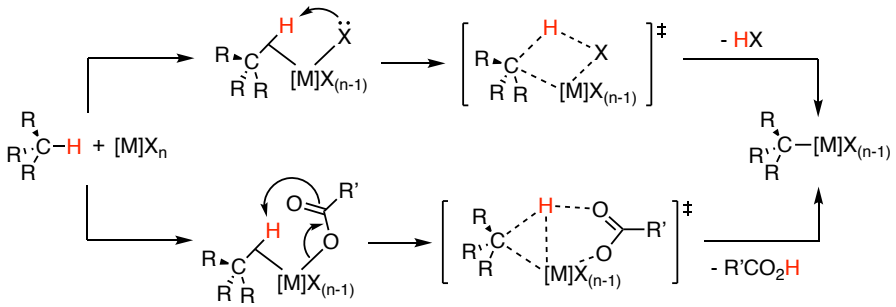

Scheme 8. C–H activation *via* ambiphilic concerted mechanisms.

3) σ-Bond Metathesis

The third type of mechanism involves the reaction of a metal–ligand bond with the C–H bond through the formation of a four-centers four-electrons transition state (Scheme 9).[23] This transformation is particular to metal compounds with a d^0 electron configuration, and observation of σ-bond metathesis is typified at early transition metal and lanthanide metallocene compounds in high oxidation states. However, metal fragments featuring d^4 to d^8 configurations can undergo σ-bond metathesis transformation as well.[24]

20 Gorelsky, S. I.; Lapointe, D.; Fagnoum K. *J. Am. Chem. Soc.* **2008**, *130*, 10848–10849.

21 Besora, M.; Braga, A. A. C.; Sameera, W. M. C.; Urbano, J.; Fructos, M. R.; Pérez, P. J.; Maseras, F. J. *J. Organomet. Chem.* **2015**, *784*, 2–12.

22 Oxgaard, J.; Tenn III, W. J.; Nielsen, R.J.; Periana, R. A.; Goddard III, W. A. *Organimetallics* **2007**, *26*, 1565–1567.

23 (a) Thompson, M. E.; Baxter, S. M.; Bulls, A. R.; Burger, B. J.; Nolan, M. C.; Santarsiero, B. D.; Schaefer, W. P.; Bercaw. J. E. *J. Am. Chem. Soc.* **1987**, *109*, 203–219. (b) Waterman, R. *Organometallics* **2013**, *32*, 7249–7263.

24 Perutz, R. N.; Sabo-Etienne, S. *Angew. Chem. Int. Ed.* **2007**, *46*, 2578–2592.

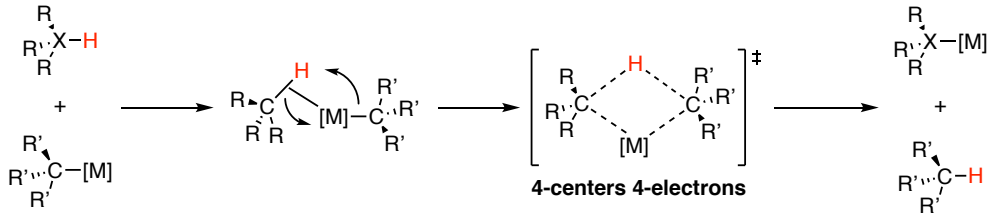

Scheme 9. C–H activation *via* σ-bond metathesis.

Electrophilic C(sp²)–H Alkynylation Reactions

The literature concerning the field of metal-promoted C–H activation is vast and has been reviewed in several occasions.[25,26] Often, regioselectivity is achieved by the use of directing groups that coordinate to the metal and favors the activation of one C–H bond over the others by steric reasons.[27] This introduction will focus on the relevant advances in electrophilic C(sp²)–H alkynylation reactions.

In 2002, Yamaguchi et al. reported the first metal-catalyzed electrophilic *ortho*-alkynylation of phenols.[28] Gallium trichloride proved to be the most efficient catalyst for the transformation and the addition of a lithium phenolate was key to regenerate intermediate **11** and achieve catalytic turnover. The reaction proceeds *via* carbometallation and subsequent insertion of chloroalkyne **12**. ß-Elimination furnishes the final product and regenerates the catalyst (Scheme 10). A similar methodology was used by the same group to develop the *ortho*-alkynylation of N-benzyl anilines.[29]

25 (a) Shilov, A. E.; Shul'pin, G. B. *Chem. Rev.* **1997**, *97*, 2879–2932. (b) Gensch, T.; Hopkinson, M. N.; Glorius, F.; Wencel-Delord, J. *Chem. Soc. Rev.* **2016**, *45*, 2900–2936.

26 For recent advances and future perspectives in the field, see: Crabtree, R. H.; Lei, A. *Chem. Rev.* **2017**, *117*, 8481–8142 and references therein.

27 (a) Engle, K. M.; Mei, T.-S.; Wasa, M.; Yu, J.-Q. *Acc. Chem. Res.* **2012**, *45*, 788–802. (b) Chen, Z.; Wang, B.; Zhang, J.; Yu, W.; Liu, Z.; Zhang, Y. *Org. Chem. Front.* **2015**, *2*, 1107–1295. (c) Sambiagio, C.; Schönbauer, D.; Blieck, R.; Dao-Huy, T.; Pototsching, G.; Schaaf, P.; Wiesinger, T.; Farooq Zia, M.; Wencel-Delord, J.; Besset, T.; Maes, B. U. W.; Schnürch *Chem. Soc. Rev.* **2018**, *47*, 6603–6743.

28 Kobayashi, K.; Arisawa, M.; Yamaguchi, M. *J. Am. Chem. Soc.* **2002**, *124*, 8528–8529.

29 Amemiya, R.; Fujii, A.; Yamaguchi, M. *Tetrahedron Lett.* **2004**, *45*, 4333–4335.

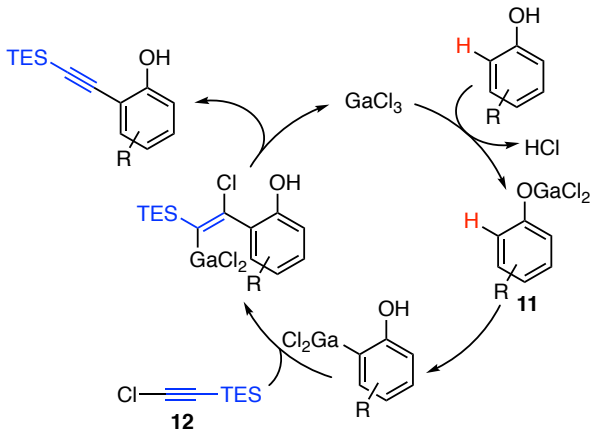

Scheme 10. Reported mechanism for the gallium(III)-catalyzed *ortho*-alkynylation of phenols.

Shortly after, the group of Gevorgyan reported the alkynylation of N-fused heterocycles mediated by a palladium catalyst using bromoalkynes as electrophiles.[30] In this case, oxidative addition of the C(sp)–Br bond is proposed to occur first followed by electrophilic aromatic substitution to generate cationic intermediate **13**. A sequence of rearomatization and reductive elimination closes the catalytic cycle affording the alkynylated product (Scheme 11).

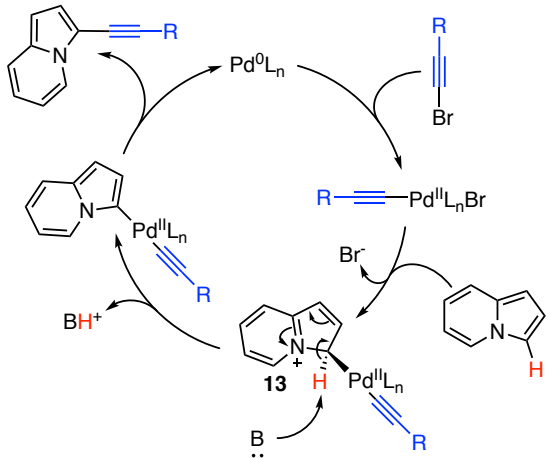

Scheme 11. Proposed mechanism for the palladium(II)-catalyzed alkynylation of indolizine.

Following this pioneering work, palladium catalysts have been extensively employed for the electrophilic alkynylation of C(sp^2)–H[31] and C(sp^3)–H bonds[32] using a variety of directing groups. Two main mechanisms have been proposed for this kind of transformations. When small

30 Seregin, I. V.; Ryabova, V.; Govergyan, V. *J. Am. Chem. Soc.* **2007**, *129*, 7742–7743.

31 For selected examples, see: (a) Tobisu, M.; Ano, Y.; Chatani, N. *Org. Lett.* **2009**, *11*, 3250–3252. (b) Ano, Y.; Tobisu, M.; Chatani, N. *Org. Lett.* **2012**, *14*, 354–357. (c) Zhao, Y.; He, G.; Nack, W. A.; Chen, G. *Org. Lett.* **2012**, *14*, 2948–2951. (d) Guan, M.; Chen, C.; Zhang, J.; Zeng, R.; Zhao, Y. *Chem. Commun.* **2015**, *51*, 12103–12106. (e) Schreib, B. S.; Fadel, M.; Carreira, E. M. *Angew. Chem. Int. Ed.* **2020**, *59*, 7818–7822.

32 For selected examples, see: (a) Ano, Y.; Tobisu, M.; Chatani, N. *J. Am. Chem. Soc.* **2011**, *133*, 12984–12986. (b) Liu, T.; Qiao, J. X.; Poss, M. A.; Yu, J.-Q. *Angew. Chem. Int. Ed.* **2017**, *56*, 10924–10927.

H/D kinetic isotopic effects (KIE) were measured (1–1.4), the reaction was proposed to proceed *via* a S_EAr pathway similar to the one depicted in Scheme 11. However, larger KIE values (>2) suggested that a different mechanism such as concerted protonation-demetallation, was likely to be in operation. In this scenario, the rate-limiting directed C–H activation occurs in first place followed by alkyne insertion and ß-heteroatom elimination (Scheme 12).[31a-b] The electrophilic C–H activation is assisted by the addition of a bridging carboxylate ligand.

Another conclusion that can be drawn from these studies is that the scope of alkynylating reagents is basically limited to the use of (TIPS)acetylenebromide.[31a-d, 32a] However, the groups of Yu and Carreira independently found that other sterically hindered bromoalkyne can be used as alkyne sources in different alkynylation reactions.[31e,32b]

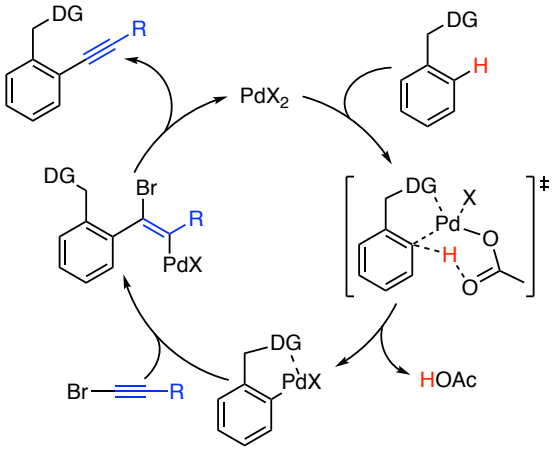

Scheme 12. Palladium(II)-catalyzed carboxylate-assisted C–H functionalization *via* concerted metallation-deprotonation. X = Halogen or acetate.

It is worth highlighting the study reported by van Gemmeren and co-workers on the palladium-catalyzed nondirected C_{aryl}–H alkynylation of arenes.[33] The use of $Pd(OAc)_2$ in combination with the amino acid derivative Ac–Phe-OH in the presence of pyrazine and Ag_2O resulted in a highly reactive system displaying an elevated sensitivity to steric effects. Under the optimized conditions, the alkynylation took place in the less sterically hindered position with remarkable regioselectivity.

Nickel catalysis has been also applied in C–H alkynylation reactions. The first example was reported by Miura et al. where a variety of azoles could be functionalized using bromoalkynes as coupling partners in the presence of a base.[34] In this case, the C–H bond is activated by deprotonation and the nickel catalyst promotes the coupling. However, nickel complexes have proved to activate of C–H bonds in the presence of a variety of directing groups through similar

33 Mondal, A.; Chen, H.; Flämig, L.; Wedi, P.; van Gemmeren, M. *J. Am. Chem. Soc.* **2019**, *141*, 18662–18667.

34 Matsuyama, N.; Hirano, K.; Satoh, T.; Miura, M. *Org. Lett.* **2009**, *11*, 4156–4159.

mechanisms to the ones described for the analogous palladium-catalyzed processes.[35] Interestingly, nickel(IV) species like **14** have been invoked as intermediates in mechanism involving a C–H activation *via* CMD followed by OA of the bromoalkyne and RE (Scheme13).[35b,d]

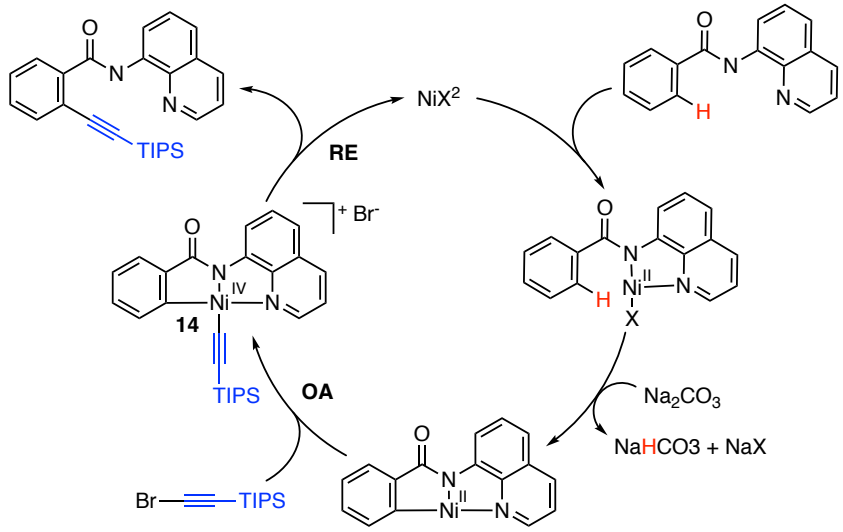

Scheme 13. Mechanism for the nickel-catalyzed electrophilic C–H alkynylation involving nickel(IV) intermediates like **14**.

Although other transition metals such as Ir,[36] Cu,[37]Au,[38] Ru[39] and Co[40] have been used to promote this type of C–H alkynylation reactions, Rh(III) catalysts have found a broader applicability in this field.

35 (a) Liu, Y.-J.; Liu, Y.-H.; Yan, S.-Y.; Shi, B.-F. *Chem. Commun.* **2015**, *51*, 6388–5391. (b) Yi, J.; Yang, L.; Xia, C.; Li, F. *J. Org. Chem.* **2015**, *80*, 6213–6221. (c) Liu, Y.-J.; Liu, Y.-H.; Yan, S.-Y.; Shi, B.-F. *Chem. Commun.* **2015**, *51*, 11650–11653. (d) Landge, V. G.; Shewale, C. H.; Jaiswal, G.; Sahoo, M. K.; Midya, S. P.; Balaraman, E. *Catal. Sci. Technol.* **2016**, *6*, 1946–1951. (e) Ruan, Z.; Lackner, S.; Ackermann, L. *ACS Catal.* **2016**, *6*, 4690–4693.

36 For selected examples, see: (a) Xie, F.; Qi, Z.; Yu, S.; Li, X. *J. Am. Chem. Soc.* **2014**, *136*, 4780–4787. (b) Wu, Y.; Yang, Y.; Zhou, B.; Li, Y. *J. Org. Chem.* **2015**, *80*, 1946–1951. (b) Chen, C.; Liu, P.; Tang, J.; Deng, G.; Zeng, X. *Org. Lett.* **2017**, *19*, 2474–2477. (c) Tan, E.; Zanini, M.; Echavarren, A. M. *Angew. Chem. Int. Ed.* **2020**, *59*, 10470–10473.

37 For selected examples, see: (a) Besselièvre, F.; Piguel, S. *Angew. Chem. Int. Ed.* **2009**, *48*, 9553–9556. (b) Kawano, T.; Matsuyama, N.; Hirano, K.; Satoh, T.; Miura, M. *J. Org. Chem.* **2010**, *75*, 1764–1766. See also: (c) Berciano, B. P.; Lebrequier, S.; Besselièvre, F.; Piguel, S. *Org. Lett.* **2010**, *12*, 4038–4041.

38 For selected examples, see: chapter II, references 24, 25 and 26. See also: Székely, A.; Péter, A.; Aradi, K.; Tolnai, G. L.; Novák, Z. *Org. Lett.* **2017**, *19*, 954−957.

39 For selected examples, see: (a) Ano, Y.; Tobisu, M.; Chatani, N. *Synlett* **2012**, *23*, 2763–2767. (b) Tan, E.; Konovalov, A. I.; Fernández, G. A.; Dorel, R.; Echavarren, A. M. *Org. Lett.* **2017**, *19*, 5561–5564. (c) Mei, R.; Zhang, S.-K.; Ackermann, L. *Org. Lett.* **2017**, *19*, 3171–3174.

40 (a) Zhang, Z.-Z.; Liu, B.; Wang, C.-Y.; Shi, B.-F. *Org. Lett.* **2015**, *17*, 4094−4097. (b) Landge, V. G.; Midya, S. P.; Rana, J.; Shinde, D. R.; Balaraman, E.; *Org. Lett.* **2016**, *18,* 5252–5255.

The rhodium(III)-catalyzed C–H activation for the construction of new C–C bonds was discovered more than 25 years ago.[41] The review by Colby, Bergman and Ellman summarizes the major advances in rhodium(III)-catalyzed alkylation and alkenylation of C–H bonds.[42] However, it was not until 2014 that the group of Loh reported the first example of amide-directed alkynylation of non-activated arenes using TIPS-EBX **15** (Scheme 14a).[43] Interestingly, while Wilkinson's catalyst had been used in most of the reactivity developed in rhodium(III)-catalyzed C–H activation reactions,[42] [(Cp*RhCl$_2$)$_2$] in the presence of NaOAc was found to perform better in this reaction. A KIE higher than 6 strongly suggests that the cleavage of the C–H bond takes place during the rate-limiting step of the catalytic cycle. On the bases of experimental evidences and previous reports,[44] the authors proposed a mechanism where the C–H activation occurs in first place *via* a concerted metallation-deprotonation pathway, followed by alkyne insertion and extrusion of 2-iodobenzoic acid.[45] These conditions were also applied to the alkynylation of acryl amides by the same group (Scheme 14b).[46]

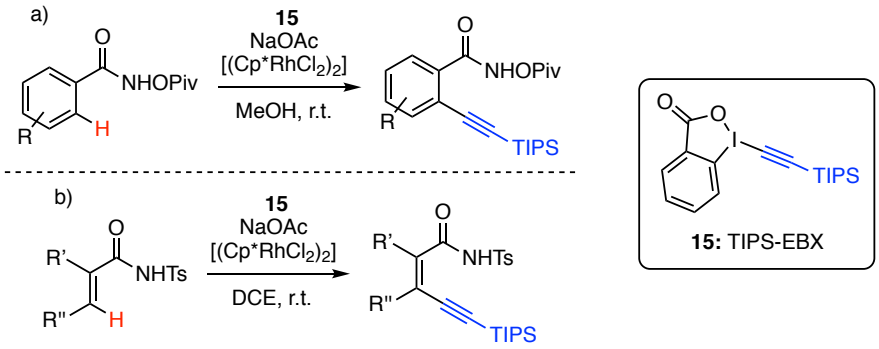

Scheme 14. Amide-directed rhodium(III)-catalyzed C–H alkynylation of: a) arenes; b) alkenes.

In parallel to the work of Loh, the group of Li also developed a version of the C–H alkynylation of arenes under chelation assistance.[36a] In this case, the rhodium(III) and iridium(III) catalysts used ([(Cp*MCl$_2$)$_2$]) displayed complementary reactivity leading to a broad reaction scope. Different N-based directing groups could be employed. Although different R-EBX alkynylating reagents could be used (R = silyl group or *t*Bu), when Ph-EBX was used, enol ester **16** was isolated as major product. In-depth experimental mechanistic investigations led to the

41 Lim, Y.-G.; Kim, Y. H.; Kang, J.-B. J. Chem. Soc., Chem. Commun. **1994**, 2267–2268.

42 Colby, D. A.; Bergman, R. B.; Ellman, J. A. *Chem. Rev.* **2010**, *110*, 624–655.

43 Feng, C.; Loh, T.-P. *Angew. Chem. Int. Ed.* **2014**, *53*, 2722–2726.

44 (a) Schipper, D. J.; Hutchinson, M.; Fagnou, K. *J. Am. Chem. Soc.* **2010**, *132*, 6910–6911. (b) Stuart, D. R.; Alsabeh, P.; Kuhn, M.; Fagnou, K. *J. Am. Chem. Soc.* **2010**, *132*, 18326–18339. (c) Patureau, F. W.; Besset, T.; Kuhl, N.; Glorius, F. *J. Am. Chem. Soc.* **2011**, *133*, 2154–2156.

45 The proposed mechanism includes a silyl migration step. This mechanism is not shown here due to the inconsistency of the ^{13}C-labeled experiments that supported this step.

46 (a) Feng, C.; Feng, D.; Luo, Y.; Loh, T.-P. *Chem. Commun.* **2014**, *50*, 9865–9868. (b) Feng, C.; Feng, D.; Loh, T.-P. *Org. Lett.* **2014**, *16*, 5956–5959.

identification of several plausible reaction intermediates and the proposal of different mechanisms. Thus, complex **17**, generated upon C–H activation of 2-phenylpyridine, reacts with the alkyne source *via* oxidative addition, giving rise to rhodium(V) intermediate **18**. Next, C(sp^2)–C(sp) reductive elimination affording η^2-complex **19** which undergoes product dissociation when sterically stabilized alkynes (R = silyl group or *t*Bu) are used. In contrast, phenyl-terminated alkynes react preferentially through alkyne insertion and protodemetallation delivering stilbene derivative **16**. Compound **18** can also undergo I–X reductive elimination yielding intermediate **20**. Importantly, no product from the RE was observed when independently synthesized **20** was stirred in CD_2Cl_2 24 h suggesting that this pathway might be less probable. The possible conversion of **17** into **20** through a redox neutral process could not be excluded (Scheme 15).

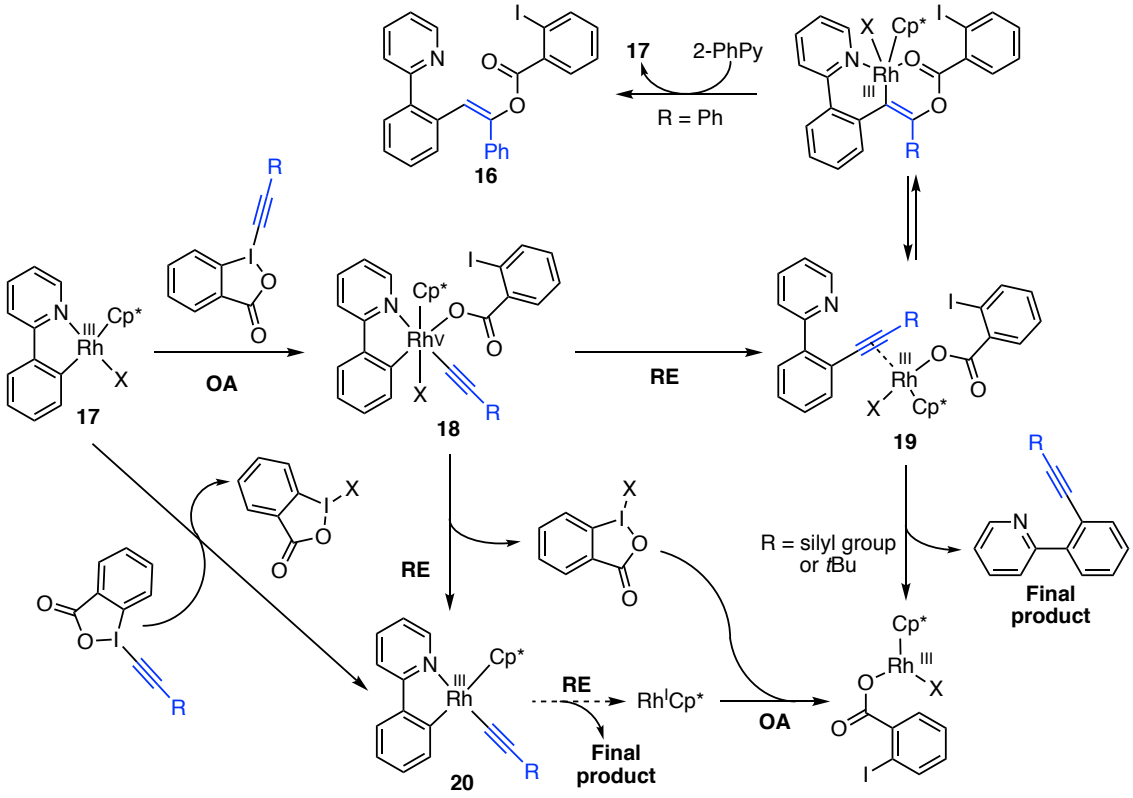

Scheme 15. Possible mechanism for the rhodium-catalyzed C–H alkynylation of arenes.

The above-presented proposals involve the presence of metal-alkynyl species due to the observation that intermediate **20** could act as catalyst for the reaction.[36a] The authors also contemplated the possibility of alternative mechanism with no intermediacy of such species. This pathway would involve the regioselective insertion of the alkyne into the Rh–C bond followed by the extrusion of 2-iodobenzoic acid. Upon 1,2-aryl migration and α-elimination the resulting rhodium(III) vinylidene **21** affords the alkynylated product (Scheme 16). However, this pathway was considered less probable because the indole product coming from the favorable intramolecular nucleophilic attack of the nitrogen onto the vinylidene in **21** could not be observed.

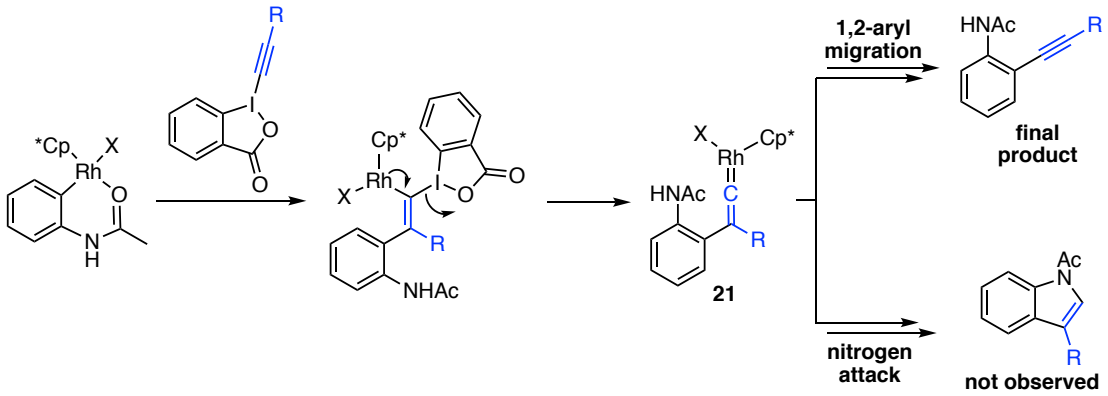

Scheme 16. Alternative mechanism for the rhodium-catalyzed C–H alkynylation of arenes.

The directed rhodium(III)-catalyzed electrophilic C–H alkynylation using silyl-EBX as alkynylating reagents has been applied to a variety of substrates employing different directing groups.[47] More recently, our group reported the C–H alkynylation of arenes in the presence of bromoalkynes directed by weakly coordinating groups such as esters, ketones, ethers, carbamates, sulfoxides, sulfones and thioethers.[48] The mechanism for the alkynylation of methyl benzoate **22** was investigated experimentally. Hence, no deuterium/proton exchange was observed when methyl benzoate-d_5 was submitted to the reaction conditions adding a proton source in the absence of bromoalkyne, which highlights the irreversibility of the C–H activation. Consisting with related reports, the KIE measured for the reaction (3.1) indicates that the C−H cleavage event occurs during the rate-determining step. A Hammett study was also conducted showing that electron-rich arenes react faster than the corresponding electron-poor substrates suggesting the formation of a slight positive charge in the aryl moiety within the highest energy transition state. In-detail computational investigations supported these experimental conclusions. According to the theoretical studies, after coordination of the rhodium(III) center to the directing group, a concerted but asynchronous ambiphilic activation of the C–H bond takes place where both, the electrophilic metal and an intramolecular basic ligand are key for the heterolytic scission of the C−H bond and formation of the C−Rh bond.[49] The resulting organometallic complex **23** undergoes regioselective alkyne insertion leading to vinylrhodium(III) intermediate **24**. Interestingly, the regioselectivity observed is the opposite found when EBX alkynylating reagents were used, which might be rationalized by the change in steric and electronic properties of these alkynylating reagents (Scheme 17). Finally, silver-assisted bromide elimination leads to the

47 For selected examples, see: (a) Zhang, X.; Qi, Z.; Gao, J.; Li, X. *Org. Biomol. Chem.* **2014**, *12*, 9329–9332. (b) Yang, X.-F.; Hu, X.-H.; Feng, C.; Loh, T.-P. *Chem. Commun.* **2015**, *51*, 2532–2535. (c) Kang, D.; Hong, S. *Org. Lett.* **2015**, *17*, 1938–1941. (d) Wang, S.-B.; Gu, Q.; You, S.-L. *J. Org. Chem.* **2017**, *82*, 11829–11835.

48 Tan, E.; Quinonero, O.; de Orbe, M. E.; Echavarren, A. M. *ACS Catal.* **2018**, *8*, 2166–2172.

49 Walsh, A. P.; Jones, W. D. *Organometallics* **2015**, *34*, 3400–3407.

formation of the desired product (Scheme 18). Alternative pathways involving the intermediacy of rhodium(V) species have been proven to be less favored.

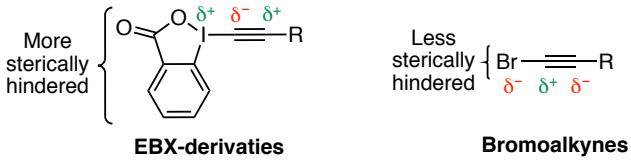

Scheme 17. Stereoelectronic differences between EBX-derivatives and bromoalkynes.

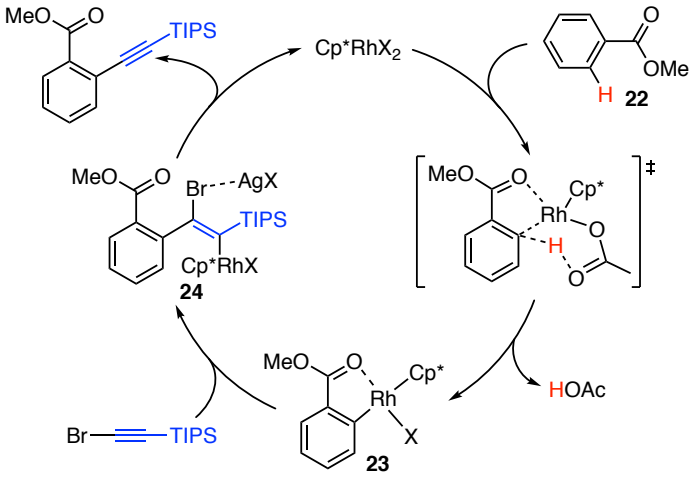

Scheme 18. Proposed mechanism for the rhodium(III)-catalyzed *ortho*-alkynylation of **22**.

A similar system resulted successful in the *ortho*-alkynylation of N-methylsulfoximines.[50]

Functionalization of Nitroarenes

Nitrobenzenes are among the most important bulk chemicals, used in a range of applications such as dyes, organic materials, solvents and perfumes.[51] With a price comparable to benzene, nitrobenzene serves as precursor to a wide variety of the functionalized aromatic building blocks. Nitrobenzenes can be functionalized at the *ipso*-position by reduction to an aniline and formation of the diazonium salt, allowing access to versatile aryl halides (Sandmeyer reaction).[52] More recently, the functionalization of nitrobenzenes gained momentum with the discovery that these substrates can be used as coupling partners in transition metal catalysis.[53] Nitrobenzenes are usually functionalized at the *meta*-position *via* electrophilic aromatic substitution, although functionalization at the *ortho*- and *para*-positions is also possible *via* the

50 Wang, T.; Wang, Y.-N.; Wang, R.; Wang, X.-S. *Chem. Asian J.* **2018**, *13*, 2449–2452.

51 (a) Nitro Compounds, Aromatic. Ullmann's Encyclopedia of Industrial Chemistry (6th ed.). Weinheim: Wiley-VCH, G. Booth, 2000; (b) Ono, N. *The Nitro Group in Organic Synthesis*; Wiley-VCH, 2001.

52 Smith, M. B.; March, J. *March's Advanced Organic Chemistry*, 5thEd; John Wiley & Sons, Inc.: New York, 2001.

53 For a recent review, see: Muto, K.; Okita, T.; Yamaguchi, J. *ACS Catal*. **2020**, *10*, 9856–9871.

so-called vicarious nucleophilic substitution,[51,54] where an α-halo-carbanion generated from a compound with an active methylene adds to the *ortho*- and/or *para*-position. However, this method is mainly limited to alkylation-type functionalization and often requires electronically activated nitrobenzenes to achieve synthetically useful yields and good selectivity (Figure 3).

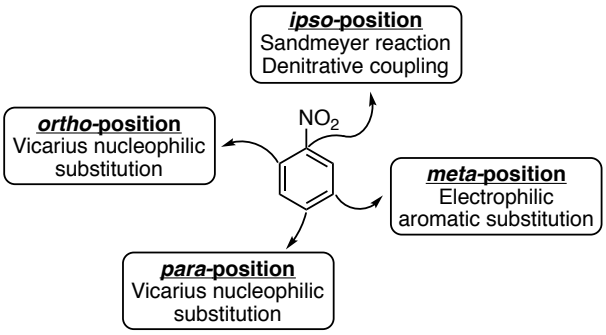

Figure 3. Different strategies for the functionalization of nitrobenzene.

Despite the ability of the ubiquitous nitro group to coordinate to metals,[55] its use as directing group in catalysis is rare and limited to direct arylation.[56] Expanding this reactivity to other types of derivatization reactions could lead to a general method for the selective *ortho*-functionalization of nitrobenzenes, an important and yet underdeveloped transformation. In this context, the *ortho*-alkynylation of nitrobenzenes stands as a suitable reaction, since the resulting *ortho*-alkynylnitroarene products can be used as precursors to generate valuable products such as indoles and other heterocyclic compounds.[57]

54 (a) Makosza, M.; Winiarski, J. *Acc. Chem. Res.* **1987**, *20*, 282–289. (b) Błaziak, K.; Danikiewicz, W.; Mąkosza, M. *J. Am. Chem. Soc.* **2016,** *138*, 7276–7281. (c) Czaban-Jóźwiak, J.; Loska, R.; Mąkosza, M. *J. Org. Chem.* **2016,** *81*, 11751–11757. (d) Brześkiewicz, J.; Loska, R.; Mąkosza, M. *J. Org. Chem.* **2018**, *83,* 8499–8508. (e) Khutorianskyi, V. V.; Klepetárová, B.; Beier, P. *Org. Lett.* **2019**, *21*, 5443–5446.

55 (a) Zhang, X.; Kanzelberger, M.; Emge, T. J.; Goldman, A. S. *J. Am. Chem. Soc.* **2004**, *126*, 13192–13193. (b) Puri, M.; Gatard, S.; Smith, D. A.; Ozerov, O. V. *Organometallics* **2011**, *30*, 2472–2482.

56 (a) Caron, L.; Campeau, L.-C.; Fagnou, K. *Org. Lett.* **2008**, *10*, 4533–4536. (b) Yi, A.; Aschenaki, Y.; Daley, R.; Davick, S.; Schnaith, A.; Wander, R.; Kalyani, D. *J. Org. Chem.* **2017**, *82*, 6946–6957.

57 For representative examples of *o*-alkynylnitroarenes as synthons, see: (a) Jadhav, A. M.; Bhunia, S.; Liao, H.-Y.; Liu, R.-S. *J. Am. Chem. Soc.* **2011**, *133*, 1769–1771. (b) Marien, N.; Brigou, B.; Pinter, B.; De Proft, F.; Verniest, G. *Org. Lett.* **2015**, *17*, 270–273. (c) Maier, M. S.; Huell, K.; Reynders, M.; Matsuura, B. S.; Leippe, P.; Ko, T.; Schaeffer, L.; Trauner, D. *J. Am. Chem. Soc.* **2019**, *141*, 17295–17304. Chen, H.; Cai, G.; Guo, A.; Zhao, Z.; Kuang, J.; Zheng, L.; Zhao, L.; Chen, J.; Guo, Y.; Liu, Y. *Macromolecules* **2019**, *52*, 6149–6159.

Objectives

Following our previous work on rhodium(III)-catalyzed C–H alkynylation reactions, we aimed to expand this reactivity to the use of the nitro group as regiodirecting element (Scheme 19).

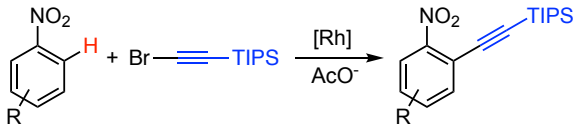

Scheme 19. Rhodium(III)-catalyzed *ortho*-alkynylation of nitroarenes.

To achieve this goal, the scope of nitroarenes and alkynylating reagents were studied using the optimal reaction conditions. Experimental and theoretical investigations were performed in order to gain more insights on the reaction mechanism.

Finally, the use of the *ortho*-alkynylated nitroarenes as precursors to synthesize valuable compounds was studied and the versatility of this C–H activation method was tested in *ortho*-functionalization reactions other than alkynylation.

Results and Discussion

Optimization

As a starting point, nitroarene **25a** was submitted to the reaction conditions described for the related rhodium(III)-catalyzed alkynylations recently reported.[48] The absence of reactivity at 50 ºC suggested that, compared to other aromatic moieties, more electron-deficient nitroarenes could require harsher conditions to undergo the C–H activation process. Gratifyingly, when the reaction was run at 80 ºC **25a** could be isolated in 35% yield and a further increase of the temperature to 110 ºC led to the quantitative formation the alkynylated product (Scheme 20).[58]

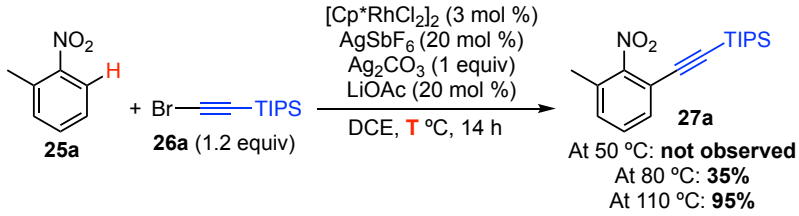

Scheme 20. Optimization of the rhodium(III)-catalyzed *ortho*-alkynylation of nitrobenzene **25a**.

Some control experiments were run in order to validate the efficiency of the optimal reaction conditions (Table 1).[58] No presence of **27a** could be detected in the absence of any additive confirming the essential role of all the components in the reaction (Table 1, entries 1-4). Other catalysts frequently used in C–H functionalization proved to be inactive in this transformation (Table 1, entry 5). The use of different silver salts (Table 1, entry 6), solvents (Table 1, entry 7), or carboxylate salts (Table 1, entry 8) led also to unsuccessful reactions.

Table 1. Control experiments on the rhodium(III)-catalyzed *ortho*-alkynylation of nitrobenzene.

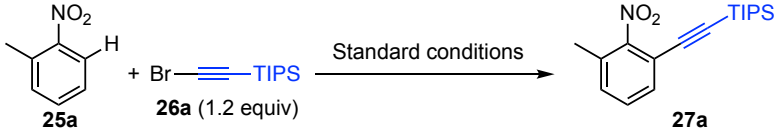

Entry	Deviation from Optimized Conditions	Yield 27a(%)
1	Without $[Cp^*RhCl_2]$	-
2	Without $AgSbF_6$	-
3	Without Ag_2CO_3	-
4	Without LiOAc	-
5	$[MnBr(CO)_5]$, $[Cp^*Co(CO)I_2]$, $[Pd(OAc)_2]$, $[Cp^*IrCl_2]$ or $[RuCl_2(p\text{-cymene})]_2$ instead of $[Cp^*RhCl_2]_2$	-
6	$AgNO_3$ or Ag_2O instead of Ag_2CO_3	-
7	THF or *tert*-amyl alcohol instead of DCE	-
8	NaOPiv instead of LiOAc	-

58 Tan, E. ICIQ PhD Thesis **2019**, unpublished results.

Reaction Scope

With the optimal reaction conditions in hand, the scope of nitroaromatic substrates was studied in collaboration with Dr. Eric Tan and Dr. Marc Montesinos-Magraner. As depicted in Scheme 21, a broad family of nitro-(hetero)arenes featuring different stereoelectronic properties could be used in the reaction, delivering the corresponding *ortho*-alkynylated products in moderate to excellent yields (95-32%). For substrates bearing no substituents in any of the *ortho* positions, dialkynylation products could be observed (mono- vs dialkynylation selectivity is shown in parentheses).

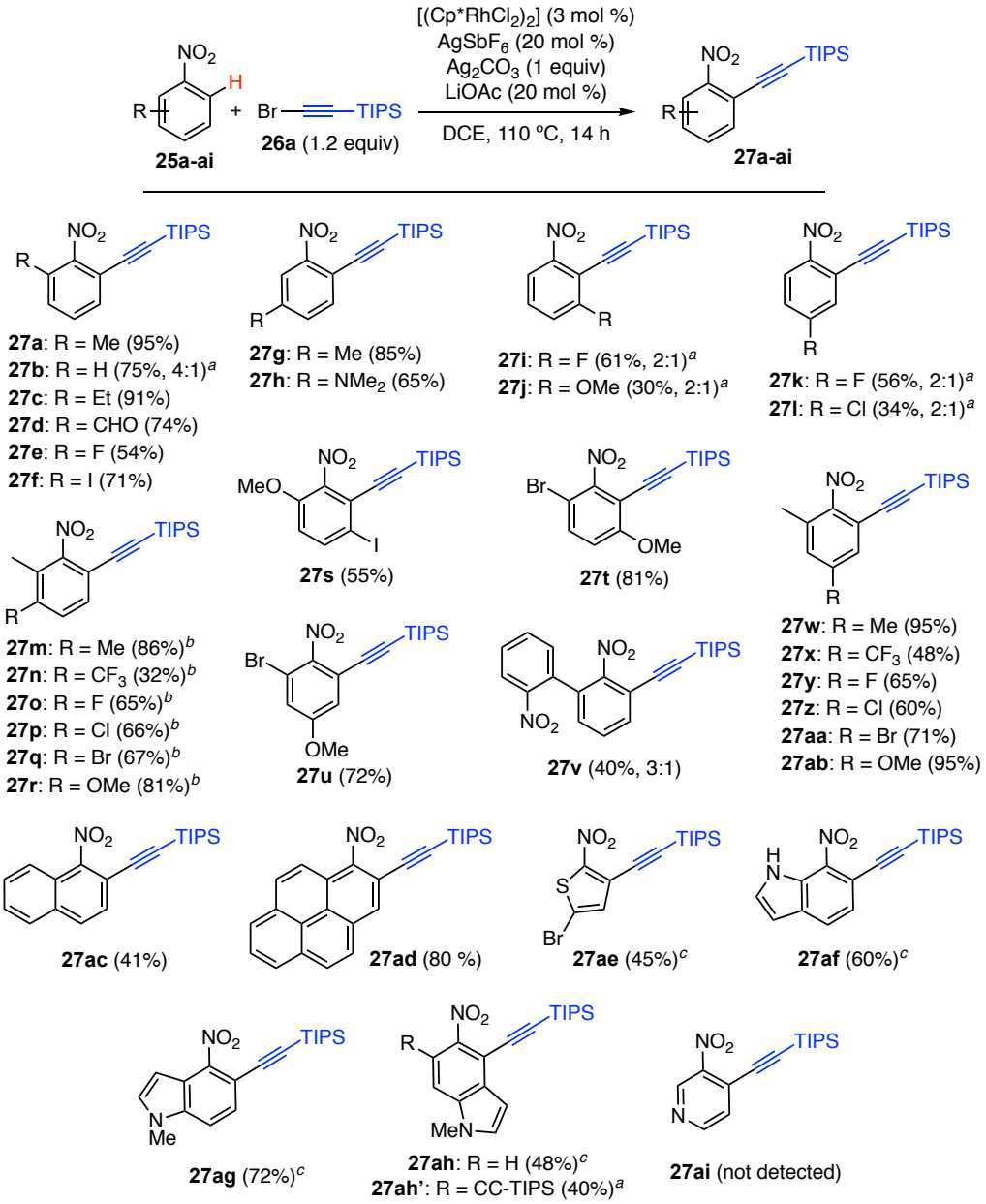

Scheme 21. Scope of nitroarenes substrates. [a] With 2 equiv. of bromo-alkyne. [b] At 100 °C. [c] With 2 equivalents of nitro-heteroarene.

Although different electron-donating and electron-withdrawing substituents were well-tolerated in the *ortho*, *meta* and *para* positions with respect to the nitro group, the reaction was not compatible with the presence of more coordinating directing groups such as amides or 2-pyridines. To evaluate the reactivity of the nitroarene compared to other weakly coordinating directing groups, different competition experiments were carried out (scheme 22). Thus, when nitrobenzene was submitted to the standard reaction conditions in the presence of an equimolar amount of a benzyl ether, a phenyl ketone, an aryl ester or an aryl sulfoxide, the alkynylation occurred almost exclusively in the competing aromatic group and only small amounts of nitroalkynylated product could be detected in some cases. These results highlight the lower reactivity of nitroarenes in this transformation with respect to other directed groups and evidence the incompatibility of such functionalities in the reaction.

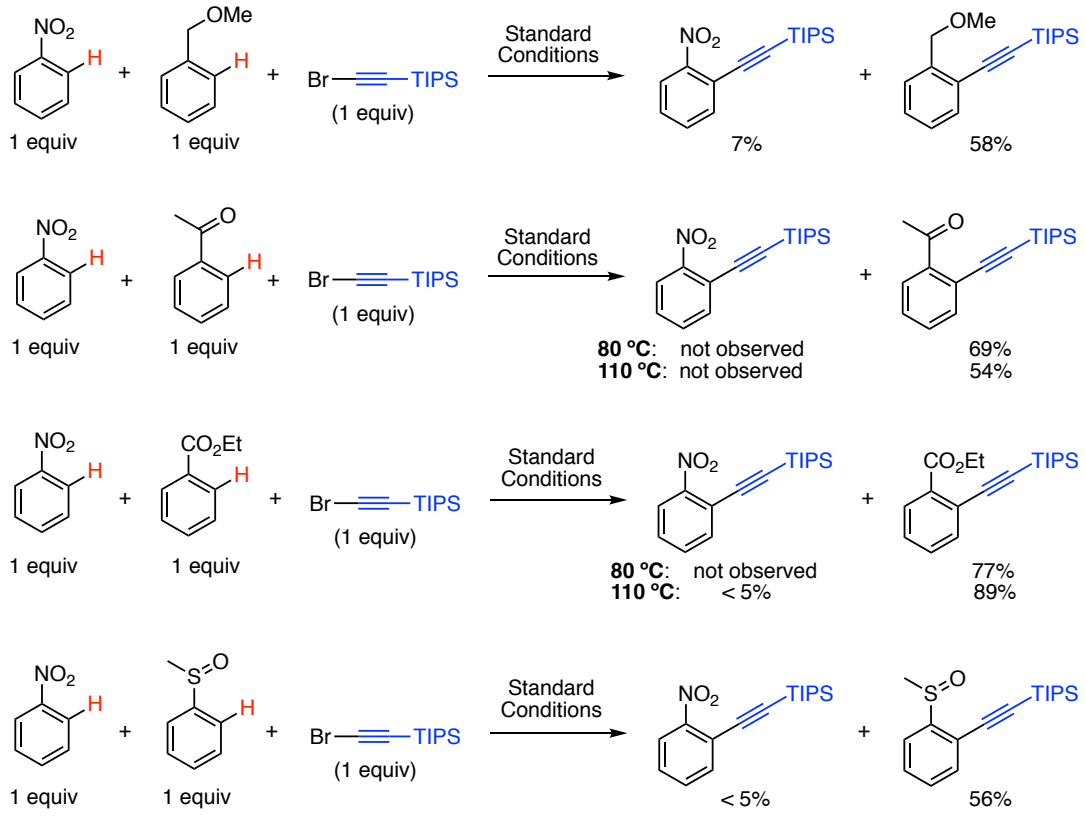

Scheme 22. Competition experiments between weakly coordinating groups in the directed rhodium(III)-catalyzed *ortho*-alkynylation of C(sp^2)–H bonds. Yields determined by NMR.

Under the same conditions, the alkynylation of nitrendipine, a commercialized antihypertensive agent, occurred with concomitant oxidation of the 1,4-dihydropyridine ring leading to alkynylated product **28** in 40% yield (Scheme 23).[58]

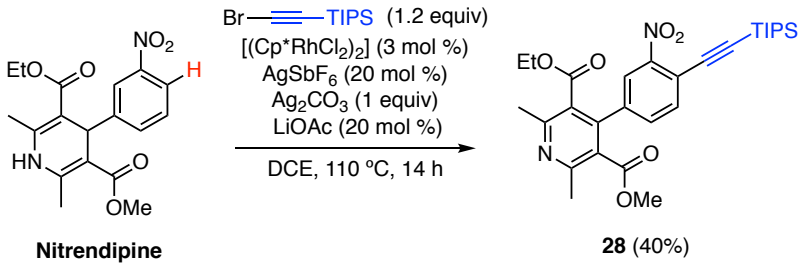

Scheme 23. Alkynylation of nitrendipine under the optimal reaction conditions.

Next, we explored the possibility of extending the methodology for the alkynylation of nitroalkenes and nitroalkanes (Scheme 24). The reaction yield dropped significantly when ß-nitrostyrenes were used as substrates. Products **27aj** and **27ak** form the alkynylation of ß-nitrostyrene **25aj** and 4-MeO-ß-nitrostyrene **25ak** could be detected in 7% and 20% NMR yield respectively, while 4-CF_3-ß-nitrostyrene remained untouched after 18 h under the standard conditions (**27al**). These results illustrate the preference of the system to activate electron-rich substrates, a trend that could also be observed in the alkynylation of the heteroaromatic nitroarenes (see scheme 22, compounds **27ae-ai**). However, other electron-activated alkenes did not deliver the corresponding alkynylated products (**27am-27aq**). Similarly, the alkynylation of nitroalkanes resulted unsuccessful using both [(Cp*$RhCl_2$)$_2$] or [(Cp*$IrCl_2$)$_2$] as catalyst and products **27ar-at** could not be detected.

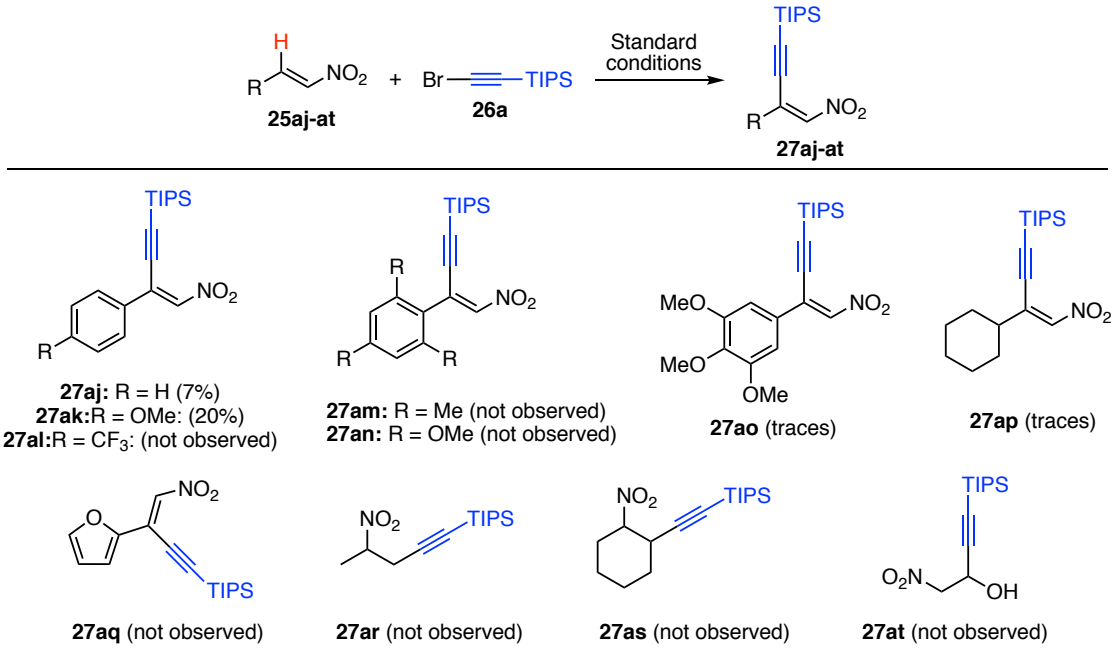

Scheme 24. Attempts on the Rh(III)/Ir(III)-catalyzed alkynylation of nitroalkenes and nitroalkanes.

In most cases, no side-products coming from the ß-nitrostyrene derivative could be detected and the starting material was recovered untouched. This observation encouraged us to attempt the most promising reaction under harsher conditions (Table 2). Unfortunately, when 4-MeO-ß-nitrostyrene **25ak** was submitted to the standard conditions at higher temperatures and longer

reaction times, **27ak** was obtained in similar or lower yields of (Table 2, entries 1-4). In light of these results, we hypothesized that higher temperatures could be leading to a faster degradation of the catalytic system, limiting the turnover number. Consequently, the reaction was also run under milder conditions using microwave irradiation. However, no improvement in the formation of **27ak** was achieved regardless of the reaction temperature and the alkynylated product could only be detected in trace amounts (Table 2, entries 5-7).

Table 2. Efforts towards the alkynylation of 4-MeO-ß-nitrostyrene **25ak**.

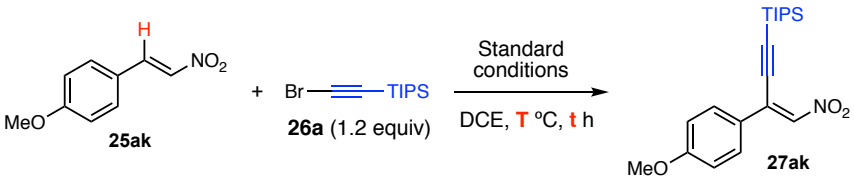

Entry	Temperature (°C)	Time (h)	Yield 27ak (%)[a]
1	130	16	17
2	130	72	19
3	150	16	9
4	150	72	5
5	MW 80	3	traces
6	MW 100	3	traces
7	MW 110	3	traces

[a] Yields determined by NMR using bromomesitylene as internal standard

Next, the scope of alkynylating reagents was investigated in collaboration with Dr. Marc Montesinos-Magraner. Different TIPS-protected haloalkynes were tried in first place (Table 3). Switching bromide (Table 3, entry 1) for chloride (**26b**) did not affect the reaction outcome (Table 3, entry 2). In contrast, using iodo-alkyne **26c** led to the formation of **27ak** in low yield (Table 3, entry 3). GC-MS analysis revealed that the haloalkyne was being consumed through a dimerization process. The use of lower temperatures reduced the formation of the dimer but did not have a positive impact on the formation of **27ak** (Table 3, entries 4-5). Terminal alkyne **26d** was also tested (Table 3, entry 6). In this case, only the diyne and the starting nitroarene **25ak** were detected.

Table 3. Screening of TIPS-protected alkynylating reagents.

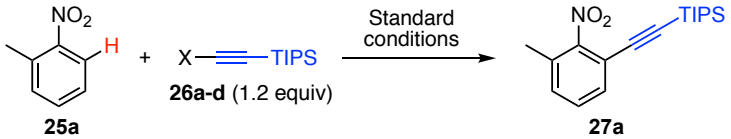

Entry	Alkyne	X	Temperature (°C)	Yield 27a (%)[a]
1	**26a**	Br	110	95
2	**26b**	Cl	110	96
3	**26c**	I	110	10
4	**26c**	I	80	13
5	**26c**	I	40	0
6	**26d**	H	110	-

[a] Yields determined by NMR using tetrachloroethane as internal standard

Finally, a screening of bromoalkynes bearing carbon-based groups was performed. To this end, highly reactive nitroarene **25r** was selected as model substrate. Arylalkynes proved to be unreactive and products **27au-aw** with different electronic properties could not be obtained. As stated in the introduction, in recent publications on palladium-catalyzed C–H alkynylation, other sterically hindered bromoalkyne were able to engage in C–H alkynylation reactions.[31e,32b] In our system, the described sterically congested bromoalkynes could not be used as alkynylating reagents (**27ax-az**). Various silyl-protected bromoalkynes were also tried in the reaction. In this case, relatively bulky groups such as -TES (triethylsilyl), -T*n*HexS (tri(*n-hexylsilyl*)), -TBDPS (*tert*-butyldiphenylsilyl) and -TPS (triphenylsilyl) could be used as alkynylating reagents and delivered products **27ba-bd** in moderate to good yields (32-74%), while less sterically hindered -TMS (trimethylsilyl) or -TBS (*tert*-butyldimethylsilyl) resulted unreactive (**27be-bf**) (Scheme 25).

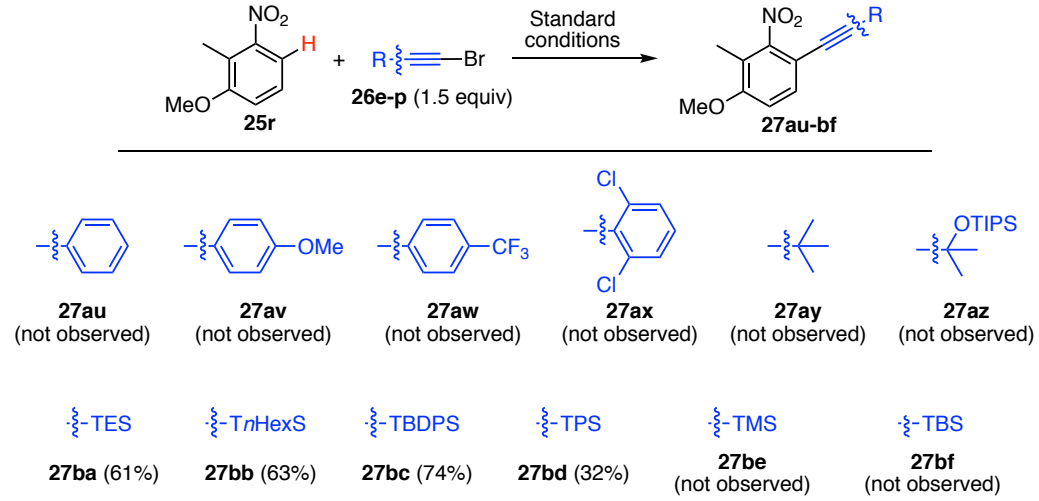

Scheme 25. Scope of bromoalkynes. Isolated yields given in parenthesis.

During the screening of silyl-protected bromoalkynes we observed that, at the end of the reaction, the excess of alkynylating reagent could only be detected when sterically hindered bromoalkynes (TIPS or TBDPS) were used. This indicated that less bulky bromoalkynes were being consumed in side-reactions that competed with the alkynylation of the nitroarene. Careful GC-MS analysis of the reaction crude where the TES-protected bromoalkyne **26k** was used, showed that both, chloroalkyne **12** and diyne **29** were being produced in variable amounts under the optimized conditions. Moreover, fluorosilane **30** could also be identified by GC-MS and ^{19}F NMR experiments (Scheme 26).

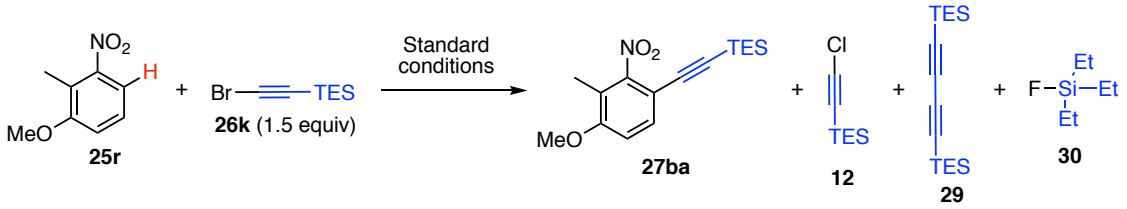

Scheme 26. Observed by-products formed during the alkynylation of **27r** using bromoalkyne **26k**.

Control experiments were run to clarify which additive was responsible for the formation each side-product (Scheme 27). No conversion was observed while heating the bromoalkyne in DCE at 120 ºC. The synthesis of the fluorosilane **30** was promoted by the presence of $AgSbF_6$ while the halogen scrambling and the dimerization reactions needed to produce **12** and **29** respectively, were catalyzed by the rhodium catalyst.

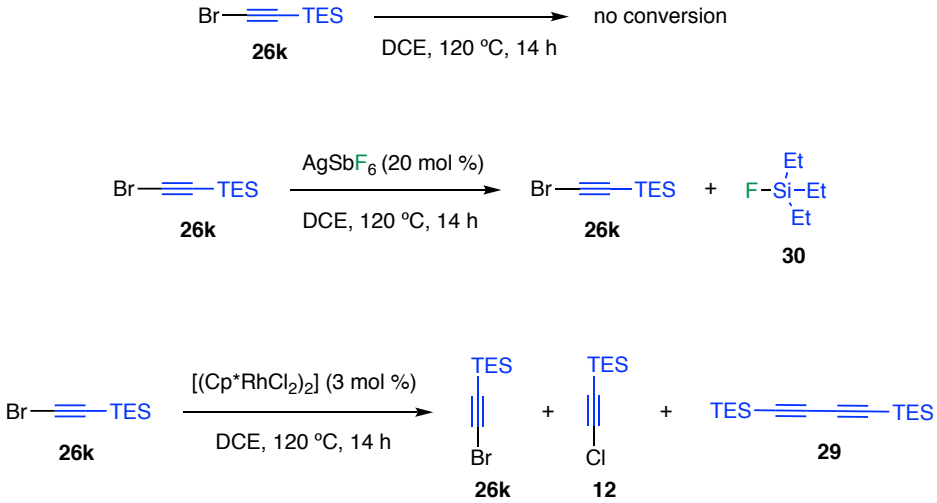

Scheme 27. Control experiments on the formation of by-products from bromoalkyne **26k**.

From these experimental results we concluded that, in the reaction mixture there are several competing pathways consuming the silyl-protected bromoalkyne, and the use of less accessible, sterically hindered silyl groups favors the desired alkynylation of the nitroarene over the others.

Synthetic Application

After the study of the reaction scope we wondered if the *ortho* selectivity achieved in the alkynylation could be extended to other functionalization reactions by trapping the $C(sp^2)$–Rh bond formed upon C–H activation with different electrophiles. Thus, when nitroarene **25w** was submitted to the optimized reaction conditions in the presence of NIS (N-iodosuccinimide), iodinated compound **31** was isolated in 60% yield (Scheme 28a). Interestingly, an overall regioselective *ortho*-arylation of nitrobenzene could be performed by a sequential Rh-catalyzed *ortho*-iodination/Pd-catalyzed Suzuki-Miyaura coupling leading to biaryl **32** in 50% yield (Scheme 28b).

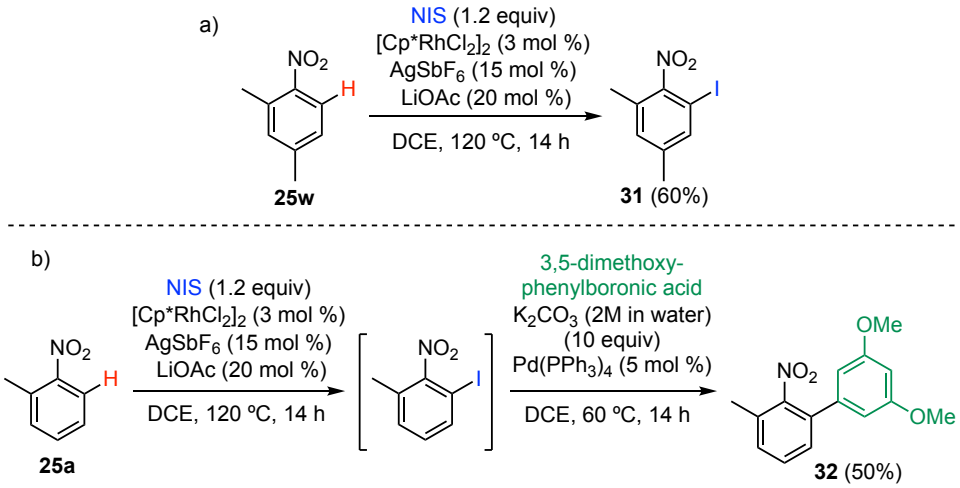

Scheme 28. a) Rhodium-catalyzed *ortho*–iodination of **25w**. b) One-pot *ortho*-arylation of **25a**.

Unfortunately, other commonly used electrophiles employed in rhodium-catalyzed C–H activation methodologies including ethyl acrylate, tropylium tetrafluoroborate, allylmethylcarbonate, diphenyldisulfide and allyltrimethylsinane did not deliver the corresponding *ortho*-functionalized compounds.

We also envisioned that the *ortho*-alkynylated nitroarene products could be easily converted in highly valuable indole derivatives through a nitro reduction/5-*endo*-dig cyclization sequence. Indeed, when nitroarene **27b** was treated with metallic iron in acidic medium, aniline **33** could be isolated in 90% yield. Subsequent cyclization catalyzed by [(JohnPhos)Au(NCMe)]SbF_6 readily produces indole **34** in 90% yield (Scheme 29).

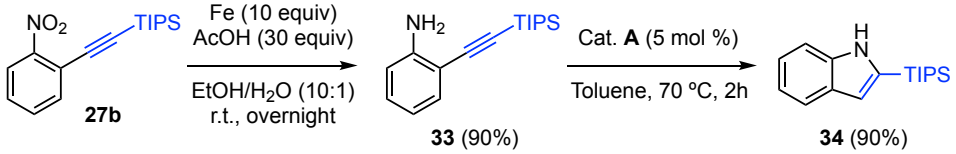

Scheme 29. Two-steps synthesis of indole derivative **34** from alkynylnitroarene **27b**.

We found that indole **34** could be synthetized in one-pot by treatment of **27b** with [$Ni(acac)_2$] using polymethylhydrosiloxane (PMHS) as reducing agent in ethereal solvents (Scheme 30). Among the different Ni-, Co-, Mn- and Fe-based systems tried, these were the only conditions that afforded the desired indole. Despite the modest yield, all the attempts to improve the reaction were unsuccessful. The major side-product observed during the reaction was the overreduced alkylaniline **35**.

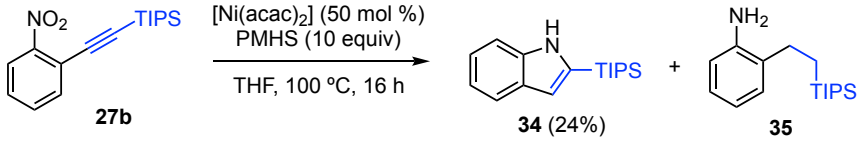

Scheme 30. One-pot procedure for synthesis of indole derivative **34** from nitroarene **27b**.

Finally, preliminary results show that the TIPS-protected nitroaryl-alkynes obtained as products in our methodology are suitable substrates for denitrative cross-coupling reactions.[53] Although this reactivity is now under development, the first attempts using [Pd(acac)$_2$] as catalyst, BrettPhos as ligand and K_3PO_4 as base display good reactivity towards the denitrative arylation and amination reactions (Scheme 31). This approach would pave the way for the efficient synthesis of *ortho*-substituted arylalkynes.

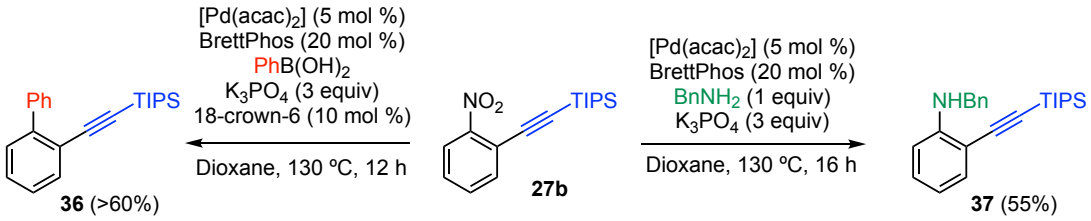

Scheme 31. Palladium-catalyzed denitrative arylation (left) and amination (right) of alkynylnitroarene **27b.**

Mechanistic Investigations

The mechanism of the reaction was investigated encompassing experimental and computational approaches.[59] In first place, the full mechanistic picture was studied using DFT calculations and **25a** as model substrate. According to our studies, after several dissociative ligand exchange events, intermediate **II** undergoes a turnover limiting C–H bond cleavage ($\Delta G^{\ddagger}$ = 25.1 kcal/mol, energy span) which proceeds through a concerted six-membered cyclic transition state with intramolecular acetate-assistance (Figure 4). The C–H cleavage transition state (**TS$_{II\text{-}III}$**) features a slightly elongated C1–H1 (1.277 Å) bond, whereas C1–Rh (2.248 Å) and H1–O1 (1.359 Å) bond distances are considerably contracted compared to the previous intermediate **II** (Table in Figure 3). This indicates that the bond forming and bond breaking events taking place between **II** and **III** are considerably asynchronous. These conclusions were supported by Natural Bond Orbital (NBO) analysis of **TS$_{II\text{-}III}$** (see experimental part). Two main electronic interactions not present in intermediate **II** related to the C–H bond cleavage event were observed. First, a lone pair on O1 delocalized over H1 (η_{O1}, 86.3% O1 and 7.2% H1) which highlights the role of the acetate in the abstraction of H1 during **TS$_{II\text{-}III}$**. Second, a natural localized molecular orbital (NLMO) analysis associated to σ-C1–H1 bond shows that is delocalized over Rh ($\Omega_{C1\text{-}H1}$, 65.4% C, 20.6% H and 8.6% Rh) indicating the formation of the C1–Rh bond during **TS$_{II\text{-}III}$**.

59 All calculations here presented were performed by Dr. Cristina García-Morales.

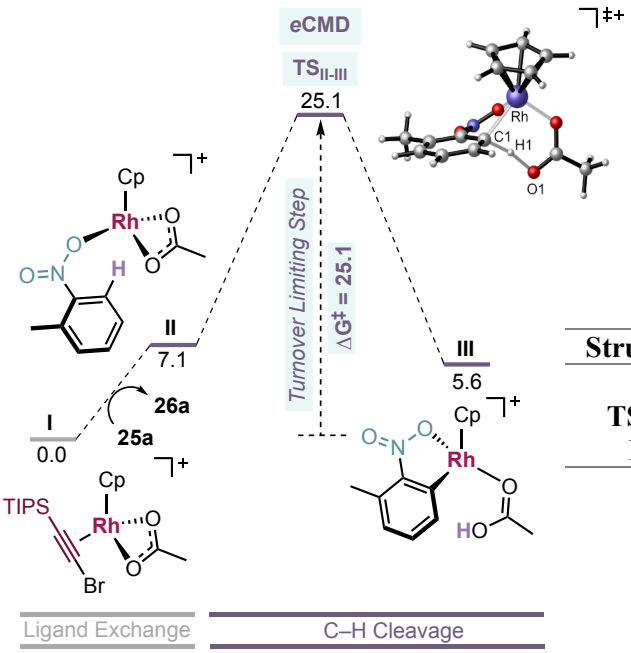

Structure	C1–H1	C1–Rh	O1–H1
II	1.084	3.350	2.339
TS$_{II-III}$	1.277	2.248	1.35
III	2.787	2.011	0.974

Distances given in Å.

Figure 4. Energy profile for the nitro-directed acetate-assisted C–H rhodation. Free energies in kcal/mol at 25 ºC. Relevant bond-distances in structures **II**, **TS$_{II-III}$** and **III** given in the table.

The mechanism follows with the dissociative substitution of acetic acid by bromoalkyne **26a**, giving rise to (η^2-alkyne)Rh intermediate **IV**, which undergoes alkyne insertion through a low energy transition state (**TS$_{IV-V}$**, $\Delta G^{\ddagger}$ =16.1 kcal/mol). The final step consists in an almost barrierless AgOAc-assisted β-debromination ($\Delta G^{\ddagger}$ = 5.8 kcal/mol) to form *ortho*-alkynylated nitrobenzene **27a** in an overall exergonic reaction (ΔG = -40.4 kcal/mol) (Figure 5).

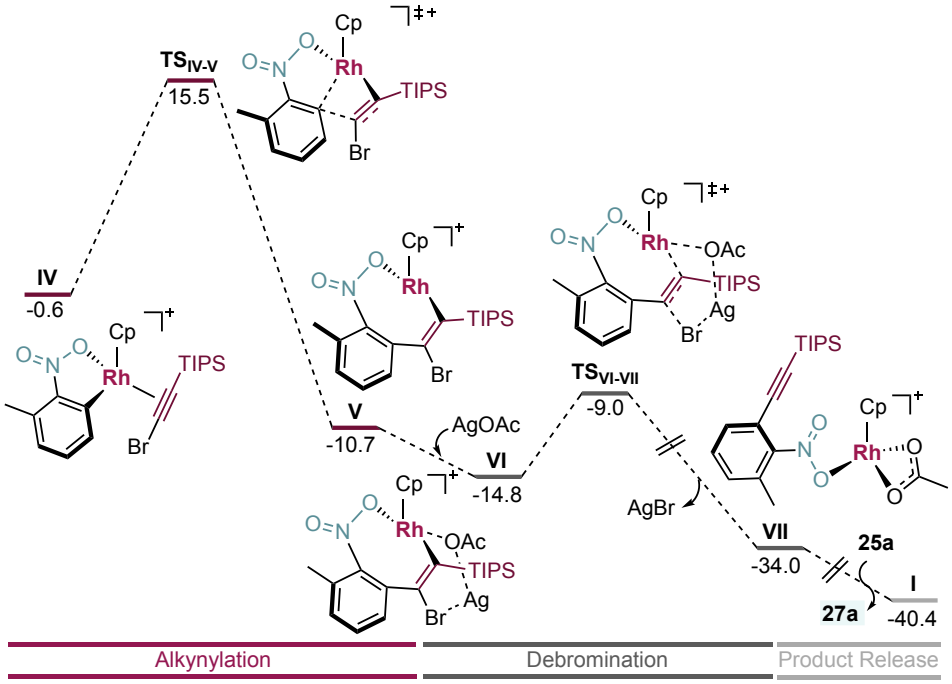

Figure 5. Final steps of the mechanism for the rhodium-catalyzed *ortho*-alkynylation of **25a**. Free energies in kcal/mol at 25 ºC.

To gain evidence of the reaction mechanism, the kinetic isotope effect (KIE) was calculated by measuring and comparing the initial rates for the alkynylation of nitrobenzene (**25b**) and perdeuterated nitrobenzene (**25b-*d*$_5$**) under the optimized conditions. The significant difference observed between both reaction rates (KIE_{exp} = 4.0), supports the computational finding that the C–H bond cleavage corresponds to the rate-limiting step of the catalytic cycle (Scheme 32a). Moreover, a theoretical KIE based on the free energy difference between [Cp*RhAlkyneOAc] (**I**) and the corresponding **TS$_{II-III}$** for the reaction of both, **25b** and **25b-*d*$_5$** at 110 °C was calculated. The result obtained (KIE_{DFT} = 4.2) accurately reproduces the experimental results (Scheme 32b).

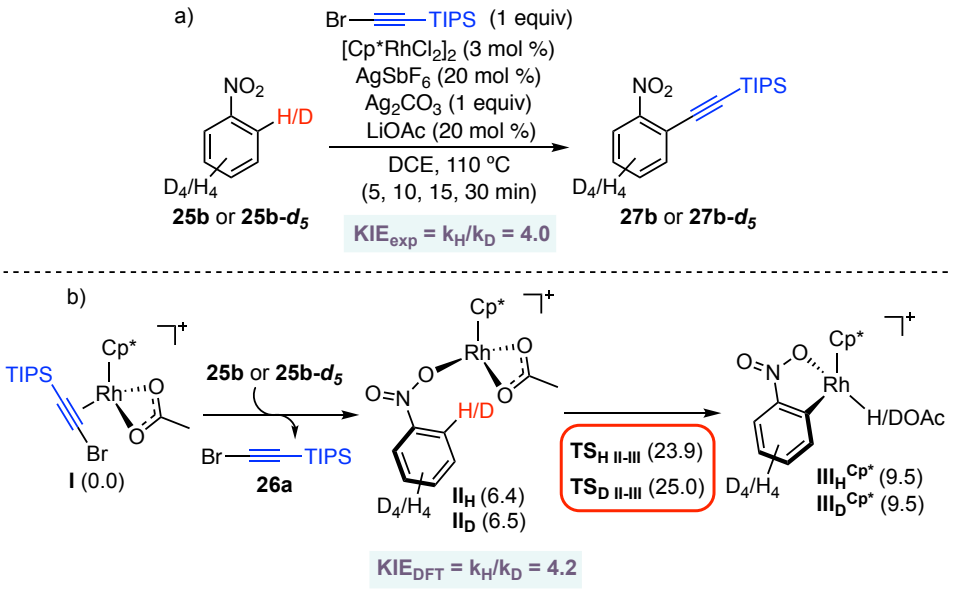

Scheme 32. a) Experimental KIE calculated at 110 °C using initial rates. b) Computed KIE at 110 °C using $\Delta G^{\ddagger}$ between **I** and **TS$_{H/D\ II-III}$**. Free energies in kcal/mol at 25 °C.

Through the investigation of the scope, we observed that the alkynylation worked more efficiently when electron-rich systems were used. To determine whether or not a positive charge was building up *ortho* to the nitro group during the highest energy transition state (**TS$_{II-III}$**), we performed initial rates measurements of *meta*-substituted 2-methylnitrobenzenes **25m,o-r** (Figure 6a). A Hammett correlation was found (R^2 = 0.95 using σ_p) with a negative ρ value (ρ = -3.6), suggesting a decrease of electron density at the aryl ring in the C–H activation step. A computational Hammett correlation could also be found between the free energy difference [Cp*RhAlkyneOAc] (**I**) and the corresponding **TS$_{II-III}$** and the σ_p parameter for a series of *meta*-substituted nitrobenzenes (ρ = -2.7, R^2 = 0.81) (Figure 6b). The computed negative ρ value is in agreement with the experimental results. To further understand the charge distribution in the transition state of the turnover limiting step, we assessed the charge accumulation ($\Delta\delta^+$) over the *meta*-substituted nitrobenzene fragment in the concerted transition states by NBO analysis. We observed a slight positive charge built up on the substituted nitrobenzenes ($\Delta\delta^+$ = 0.06-0.14),

which agrees with the trends observed by Hammett analysis. In fact, a straight regression line was obtained by plotting $\Delta\delta^{+}$ *vs* σ_p parameters ($R^2 = 0.89$) (Figure 6c).

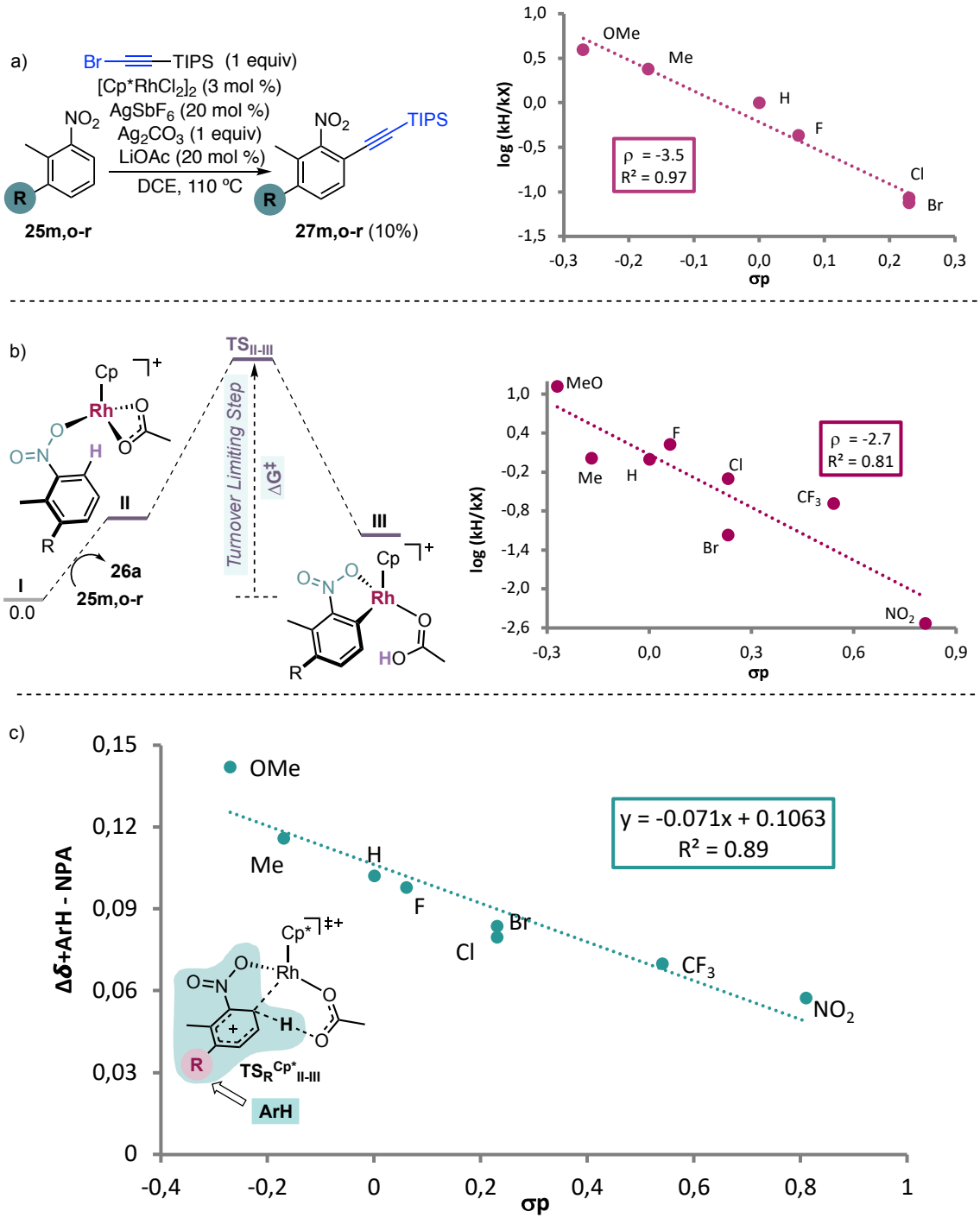

Figure 6. Hammett correlations: a) Experimental; using initial rates. b) Calculated; using $\Delta G^{\ddagger}$ between **I** and $\mathbf{TS_{R\ II\text{-}III}}$. c) Calculated; using charge accumulation in the ArH fragment.

Both the Hammett and NBO analysis suggest that the Rh-catalyzed C–H activation corresponds to an electrophilic concerted metalation deprotonation process, in which both an electrophilic metal and a basic ligand cooperate in the cleavage of the C–H bond.[49]

Conclusions

The development of the rhodium-catalyzed alkynylation of nitro(hetero)arenes has been accomplished. The reaction tolerates a wide variety of functional groups yielding mono- and dialkynylated products that can be used as precursors for the synthesis of indoles or further functionalized by denitrative cross-coupling reactions (Scheme 34). The selective C–H activation has also been extended to the *ortho*-iodination and the one-pot *ortho*-iodination/arylation of nitroarenes.

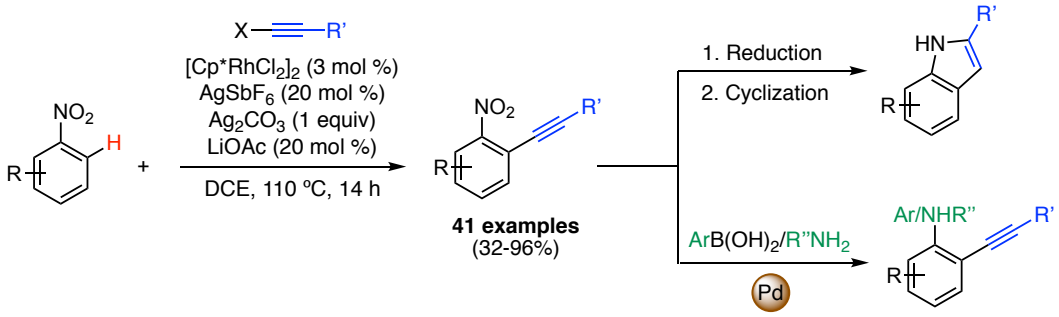

Scheme 33. Rhodium-catalyzed synthesis of *ortho*-alkynylnitroarenes and further derivatization.

Experimental and computational studies suggest that the turnover limiting C–H bond cleavage takes place through a concerted electrophilic concerted metalation deprotonation process. Hammett correlations and theoretical charge distribution analysis revealed the generation of a partial positive charge in the aromatic unit during the highest energy transition state, which is evidenced by the better performance of electron-rich substrates under the optimized conditions. Subsequent alkyne insertion and silver-assisted bromide elimination close the catalytic cycle delivering the desired products.

Experimental Part

General Information

Unless otherwise stated, all the reactions were performed under an inert atmosphere of argon. All solvents and other chemicals were used as received. Alkyne **26a**,[60a] **26b**,[60b] **26c**,[60c] **26d**,[60d] were prepared according to previous reports. Their spectral data are consistent with the previously reported. All the reactions were run in dry solvents (passed through an activated alumina column on a PureSolv™ solvent purification system). Reactions were followed using a GC-MS apparatus, by TLC (thin layer chromatography) or by NMR analysis. Analytical thin layer chromatography was carried out using TLC aluminum sheets coated with 0.2 mm of silica gel (Merck 60 F254) using UV light as the visualizing agent and an acidic solution of vanillin in ethanol or basic solution of $KMnO_4$ in water as stain. Chromatographic purifications were carried out using flash grade silica gel (PanReac Silica Gel 60, 40-63 μm) or automated flash column chromatographer CombiFlash Companion. Preparative thin layer chromatography was performed on TLC plates (Analtec Silica Gel GF UV254, 20×20 cm, 1000 μm). Melting points were determined using a Mettler Toledo MP70 melting point apparatus. NMR spectra were recorded at 298 K on BrukerAvance Ultrashield NMR spectrometers (300 MHz, 400 MHz, 500 MHz and 500 MHz with CryoProbe). Chemical shifts (δ) are reported in parts per million (ppm) and referenced to residual solvent (For ^{1}H NMR: $CDCl_3$ at 7.26 ppm, CD_2Cl_2 at 5.31 ppm, C_6D_6 at 7.16 ppm, CD_3OD at 3.31 ppm, for $^{13}C\{^1H\}$ NMR: $CDCl_3$ at 77.16 ppm, CD_2Cl_2 at 54.00 ppm, C_6D_6 at 128.06 ppm, CD_3OD at 49.00 ppm). The following abbreviations were used to explain multiplicities: s = singlet, d = doublet, t = triplet, q = quartet, p = pentet, m = multiplet, br s = broad singlet. Coupling constants (*J*) are reported in Hertz (Hz). Mass spectra were recorded on MicroTOF Focus or Maxis Impact spectrometers (both from Bruker Daltonics. X-ray diffraction data were collected at 100 K on a Rigaku MicroMax-007HF, Mo *Kα* rotating anode, equipped with a Pilatus 200 K detector or on a Bruker APEX DUO, Mo *Kα* Microfocus source E025 IuS anode, equipped with an APEX DUO detector using omega scans.

60 (a) Campbell, C. D.; Greenaway, R. L.; Holton, O. T.; Walker, P. R.; Chapman, H. A.; Russell, C. A.; Carr, G.; Thomson, A. E.; Anderson, E. A. *Chem. Eur. J.* **2015**, *21*, 12627–12639. (b) Wada, T.; Iwasaki, M.; Kondoh, A.; Yorimitsu, H.; Oshima, K. *Chem. Eur. J.* **2010**, *16*, 10671 – 10674. (c) Brand, J. P.; Waser, J. *Angew. Chem. Int. Ed.* **2010**, *49*, 7304 - 7307. (d) Nie, X.; Wang, G. *J. Org. Chem.* **2006**, *71*, 4734-4741.

Scope of the Rhodium-Catalyzed *Ortho-C–H* Alkynylation of nitroarenes

General procedure for the Rh-catalyzed ortho-C–H alkynylation of nitrobenzenes

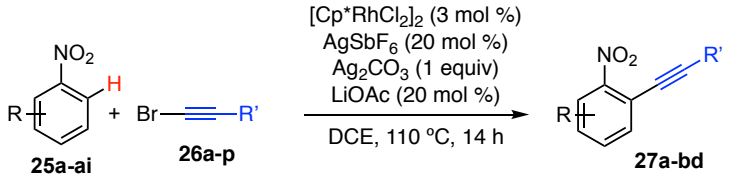

$[Cp^*RhCl_2]_2$ (3 mol%), Ag_2CO_3 (1 equiv), LiOAc (20 mol%), $AgSbF_6$ (20 mol%) were weighted in a vial inside a glovebox and dichloroethane (0.15 M) is added. Corresponding nitrobenzene **25a-ah** (0.2 mmol) and bromoalkyne (**26a-p**) (1.2 equiv) are then added and the vial is sealed. The reaction mixture is stirred at 110 °C for 14 h outside the glovebox. After cooling to room temperature, the reaction mixture is filtrated through celite and purified by column chromatography, with a gradient from cyclohexane 100% to 1/1 cyclohexane/ethyl acetate to yield corresponding products **27a-bd**.

Triisopropyl((3-methyl-2-nitrophenyl)ethynyl)silane (27a)

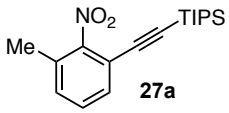

Compound **27a** was synthesized according to the general procedure and it was obtained as a colorless liquid in 95% yield.

^{1}H NMR (300 MHz, $CDCl_3$) δ 7.43 (dt, J = 7.7, 1.0 Hz, 1H), 7.32 (t, J = 7.7 Hz, 1H), 7.24 (ddd, J = 7.7, 1.5, 1.0 Hz, 1H), 2.34 (s, 3H), 1.13 (s, 21H). **^{13}C NMR** (75 MHz, $CDCl_3$) δ 153.3, 131.1, 131.0, 129.7 (2C), 116.5, 99.5, 98.6, 18.5, 17.3, 11.2. **HRMS** (APCI+) *m/z* calc. for $C_{18}H_{28}NO_2Si$ $[M+H]^+$: 318.1884. Found: 318.1884.

Triisopropyl((2-nitrophenyl)ethynyl)silane (27b)

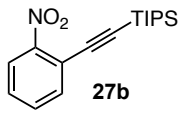

Compound **27b** was synthesized according to the general procedure using 2 equiv of 1-bromo-2-(triisopropylsilyl)acetylene (**26a**) and it was obtained as a white solid in 75% yield.

Mp 55 °C. **^{1}H NMR** (300 MHz, $CDCl_3$) δ 8.03 (dd, J = 8.2, 0.9 Hz, 1H), 7.69 (dd, J = 7.7, 1.3 Hz, 1H), 7.57 (td, J = 7.7, 1.3 Hz, 1H), 7.49 – 7.42 (m, 1H), 1.17 (s, 21H). **^{13}C NMR** (75 MHz, $CDCl_3$) δ 150.0, 135.4, 132.6, 128.6, 124.4, 118.7, 101.1, 100.8, 18.6, 11.2. **HRMS** (ESI+) *m/z* calc. for $C_{17}H_{25}NNaO_2Si$ $[M+Na]^+$: 326.1547. Found: 326.1536.

((2-Nitro-1,3-phenylene)bis(ethyne-2,1-diyl))bis(triisopropylsilane) (27b‘)

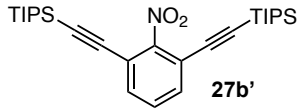

Compound **27b’** was synthesized according to the general procedure using 2 equiv of 1-bromo-2-(triisopropylsilyl)acetylene (**26a**) and it was obtained as a purple solid in 15% yield.

Mp 75 °C. **^{1}H NMR** (300 MHz, $CDCl_3$) δ 7.52 (d, J = 8.2 Hz, 2H), 7.37 (dd, J = 8.2, 7.1 Hz, 1H), 1.12 (s, 42H). **^{13}C NMR** (75 MHz, $CDCl_3$) δ 154.8, 132.9, 129.6, 116.8, 99.9, 98.5, 18.5, 11.1. **HRMS** (ESI+) *m/z* calc. for $C_{28}H_{45}NNaO_2Si_2$ $[M+Na]^+$: 506.2881. Found: 506.2861.

((3-Ethyl-2-nitrophenyl)ethynyl)triisopropylsilane (27c)

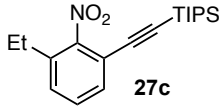

Compound **27c** was synthesized according to the general procedure and it was obtained as a yellow liquid in 91% yield.

^{1}H NMR (300 MHz, $CDCl_3$) δ 7.41 (dd, *J* = 7.6, 1.7 Hz, 1H), 7.34 (t, *J* = 7.6 Hz, 1H), 7.27 (dd, *J* = 7.6, 1.7 Hz, 1H), 2.61 (q, *J* = 7.6 Hz, 2H), 1.23 (t, *J* = 7.6 Hz, 3H), 1.11 (s, 21H). **^{13}C NMR** (75 MHz, $CDCl_3$) δ 153.0, 135.4, 130.9, 129.8, 129.6, 116.3, 99.4, 98.4, 24.4, 18.5, 14.8, 11.1. **HRMS** (APCI+) *m/z* calc. for $C_{19}H_{30}NO_2Si$ $[M+H]^+$: 332.2040. Found: 332.2027.

2-Nitro-3-((triisopropylsilyl)ethynyl)benzaldehyde (27d)

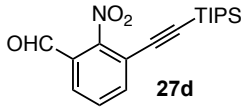

Compound **27d** was synthesized according to the general procedure and it was obtained as an orange solid in 74% yield.

Mp 50 °C. **^{1}H NMR** (300 MHz, $CDCl_3$) δ 10.49 (s, 1H), 7.81 (m, 2H), 7.60 (t, *J* = 8.0 Hz, 1H), 1.13 (m, 21H). **^{13}C NMR** (75 MHz, $CDCl_3$) δ 188.3, 148.1, 137.7, 132.8, 132.1, 125.7, 123.4, 101.7, 100.4, 18.6, 11.2. **HRMS** (ESI+) *m/z* calc. for $C_{18}H_{25}NNaO_3Si$ $[M+Na]^+$: 354.1496. Found: 354.1496.

((3-Fluoro-2-nitrophenyl)ethynyl)triisopropylsilane (27e)

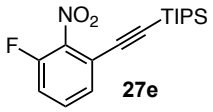

Compound **27e** was synthesized according to the general procedure and it was obtained as a colorless liquid in 54% yield.

^{1}H NMR (300 MHz, $CDCl_3$) δ 7.49 – 7.36 (m, 2H), 7.22 (ddd, *J* = 9.6, 7.9, 1.8 Hz, 1H), 1.13 (s, 21H). **^{13}C NMR** (101 MHz, $CDCl_3$) δ 153.5 (d, *J* = 258.3 Hz), 131.6 (d, *J* = 8.6 Hz), 129.1 (d, *J* = 3.7 Hz), 119.0, 117.1, 116.9, 101.4, 98.1 (d, *J* = 3.7 Hz), 18.48, 11.12. **^{19}F{^{1}H} NMR** (376 MHz, $CDCl_3$) δ -122.44. **HRMS** (APCI+) *m/z* calc. for $C_{17}H_{25}FNO_2Si$ $[M+H]^+$: 322.1633. Found: 322.1632.

((3-Iodo-2-nitrophenyl)ethynyl)triisopropylsilane (27f)

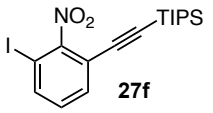

Compound **27f** was synthesized according to the general procedure and it was obtained as a colorless liquid in 71% yield.

^{1}H NMR (300 MHz, $CDCl_3$) δ 7.81 (dd, *J* = 7.9, 1.2 Hz, 1H), 7.53 (dd, *J* = 7.9, 1.2 Hz, 1H), 7.12 (t, *J* = 7.9 Hz, 1H), 1.10 (m, 21H). **^{13}C NMR** (75 MHz, $CDCl_3$) δ 157.2, 139.6, 132.6, 130.5, 117.3, 100.7, 98.3, 84.4, 18.5, 11.1. **HRMS** (APCI+) *m/z* calc. for $C_{17}H_{25}INO_2Si$ $[M+H]^+$: 430.0694. Found: 430.0702.

Triisopropyl((4-methyl-2-nitrophenyl)ethynyl)silane (27g)

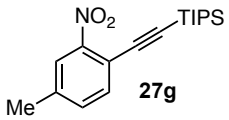

Compound **27g** was synthesized according to the general procedure and it was obtained as a red solid in 85% yield.

Mp 55 °C. **^{1}H NMR** (300 MHz, $CDCl_3$) δ 7.82 (dd, *J* = 1.8, 0.9 Hz, 1H), 7.55 (d, *J* = 7.9 Hz, 1H), 7.35 (ddd, *J* = 7.9, 1.8, 0.9 Hz, 1H), 2.44 (s, 3H), 1.16 (s, 21H). **^{13}C**

NMR (75 MHz, $CDCl_3$) δ 149.8, 139.6, 135.1, 133.3, 124.7, 115.7, 101.2, 99.4, 21.2, 18.5, 11.2. **HRMS** (APCI+) *m/z* calc. for $C_{18}H_{28}NO_2Si$ $[M+H]^+$: 318.1884. Found: 318.1882.

***N*,*N*-Dimethyl-3-nitro-4-((triisopropylsilyl)ethynyl)aniline (27h)**

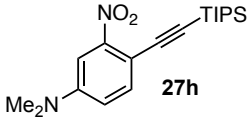

Compound **27h** was synthesized according to the general procedure and it was obtained as a red solid in 65% yield.

Mp 105 °C. **^{1}H NMR** (300 MHz, $CDCl_3$) δ 7.46 (d, *J* = 8.8 Hz, 1H), 7.21 (d, *J* = 2.7 Hz, 1H), 6.78 (dd, *J* = 8.8, 2.7 Hz, 1H), 3.04 (s, 6H), 1.15 (s, 21H). **^{13}C NMR** (75 MHz, $CDCl_3$) δ 151.2, 149.7, 135.9, 115.3, 106.5, 104.8, 102.3, 95.7, 40.1, 18.6, 11.3. **HRMS** (ESI+) *m/z* calc. for $C_{19}H_{31}N_2O_2Si$ $[M+H]^+$: 347.2149. Found: 347.2146.

((2-Fluoro-6-nitrophenyl)ethynyl)triisopropylsilane (27i)

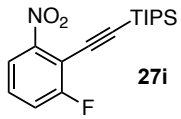

Compound **27i** was synthesized according to the general procedure using 2 equiv of 1-bromo-2-(triisopropylsilyl)acetylene (**26a**) and it was obtained as a red solid in 60% yield.

Mp 70 °C. **^{1}H NMR** (300 MHz, $CDCl_3$) δ 7.83 (dt, *J* = 7.7, 1.4 Hz, 1H), 7.46 – 7.32 (m, 2H), 1.15 (m, 21H). **^{13}C NMR** (101 MHz, $CDCl_3$) δ 163.9 (d, *J* = 255.7 Hz), 150.8, 128.8 (d, *J* = 8.8 Hz), 120.0 (d, *J* = 4.9 Hz), 119.8 (d, *J* = 20.5 Hz), 108.6 (d, *J* = 20.5 Hz), 107.8 (d, *J* = 4.9 Hz), 93.2, 18.5, 11.2. **^{19}F NMR** (376 MHz, $CDCl_3$) δ -104.62 (dd, *J* = 8.0, 5.5 Hz). **HRMS** (APCI+) *m/z* calc. for $C_{17}H_{25}FNO_2Si$ $[M+H]^+$: 322.1633. Found: 322.1644.

((4-Fluoro-2-nitro-1,3-phenylene)bis(ethyne-2,1-diyl))bis(triisopropylsilane) (27i')

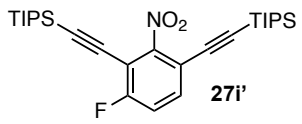

Compound **27i'** was synthesized according to the general procedure using 2 equiv of 1-bromo-2-(triisopropylsilyl)acetylene (**26a**) and it was obtained as a white solid in 30% yield.

Mp 70 °C. **^{1}H NMR** (300 MHz, $CDCl_3$) δ 7.48 (dd, *J* = 8.5, 5.2 Hz, 1H), 7.16 (t, *J* = 8.5 Hz, 1H), 1.10 (m, 42H). **^{13}C NMR** (101 MHz, $CDCl_3$) δ 162.1 (d, *J* = 259.4 Hz), 155.3, 133.7 (d, *J* = 8.6 Hz), 117.3 (d, *J* = 22.0 Hz), 112.9 (d, *J* = 4.4 Hz), 107.0 (d, *J* = 22.0 Hz), 106.2 (d, *J* = 3.6 Hz), 99.6 (d, *J* = 1.8 Hz), 97.6 (d, *J* = 1.6 Hz), 91.6, 18.5, 18.4, 11.1, 11.1. **^{19}F NMR** (376 MHz, $CDCl_3$) δ -103.51 (dd, *J* = 8.0, 5.2 Hz). **HRMS** (APCI+) *m/z* calc. for $C_{28}H_{45}FNO_2Si_2$ $[M+H]^+$: 502.2967. Found: 502.2969.

Triisopropyl((2-methoxy-6-nitrophenyl)ethynyl)silane (27j)

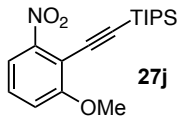

Compound **27j** was synthesized according to the general procedure using 2 equiv of 1-bromo-2-(triisopropylsilyl)acetylene (**26a**) and it was obtained as a brown solid in 30% yield.

Mp 75 °C. **^{1}H NMR** (300 MHz, $CDCl_3$) δ 7.52 (dd, *J* = 8.3, 1.0 Hz, 1H), 7.35 (t, *J* = 8.3 Hz, 1H), 7.09 (dd, *J* = 8.3, 1.0 Hz, 1H), 3.92 (s, 3H), 1.15 (s, 21H). **^{13}C NMR** (75 MHz, $CDCl_3$) δ 162.1,

152.2, 128.7, 115.9, 114.6, 108.4, 105.9, 96.1, 56.6, 18.6, 11.3. **HRMS** (APCI+) *m/z* calc. for $C_{18}H_{28}NO_3Si$ $[M+H]^+$: 334.1833. Found: 334.1828.

((4-Methoxy-2-nitro-1,3-phenylene)bis(ethyne-2,1-diyl))bis(triisopropylsilane) (27j').

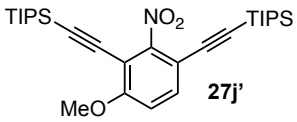

Compound **27j'** was synthesized according to the general procedure using 2 equiv of 1-bromo-2-(triisopropylsilyl)acetylene (**26a**) and it was obtained as a brown solid in 15% yield.

Mp 85 °C. **^{1}H NMR** (300 MHz, $CDCl_3$) δ 7.46 (d, *J* = 8.8 Hz, 1H), 6.90 (d, *J* = 8.8 Hz, 1H), 3.93 (s, 3H), 1.12 (s, 21H), 1.11 (s, 21H). **^{13}C NMR** (75 MHz, $CDCl_3$) δ 160.7, 156.0, 133.6, 111.9, 108.4, 106.8, 104.1, 98.6, 97.0, 94.5, 58.5, 18.5, 11.1. The signals at 18.5 and 11.1 ppm correspond to the 18 C for both TIPS groups. **HRMS** (APCI+) *m/z* calc. for $C_{29}H_{48}NO_3Si_2$ $[M+H]^+$: 514.3167. Found: 514.3169.

((5-Fluoro-2-nitrophenyl)ethynyl)triisopropylsilane (27k)

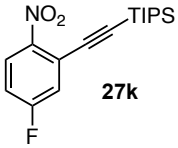

Compound **27k** was synthesized according to the general procedure using 2 equiv of 1-bromo-2-(triisopropylsilyl)acetylene (**26a**) and it was obtained as a red liquid in 56% yield.

^{1}H NMR (300 MHz, $CDCl_3$) δ 8.09 (dd, *J* = 9.1, 5.1 Hz, 1H), 7.33 (dd, *J* = 8.5, 2.8 Hz, 1H), 7.13 (ddd, *J* = 9.1, 7.2, 2.8 Hz, 1H), 1.14 (m, 21H). **^{13}C NMR** (101 MHz, $CDCl_3$) δ 164.2 (d, *J* = 257.2 Hz), 146.2, 127.2 (d, *J* = 10.2 Hz), 122.0 (d, *J* = 24.5 Hz), 121.5 (d, *J* = 11.0 Hz), 116.0 (d, *J* = 23.4 Hz), 103.0, 100.1 (d, *J* = 2.1 Hz), 18.6, 11.2. **^{19}F NMR** (376 MHz, $CDCl_3$) δ -104.60 (td, *J* = 7.9, 5.1 Hz). **HRMS** (APCI+) *m/z* calc. for $C_{17}H_{25}FNO_2Si$ $[M+H]^+$: 322.1633. Found: 322.1641.

((5-Fluoro-2-nitro-1,3-phenylene)bis(ethyne-2,1-diyl))bis(triisopropylsilane) (27k')

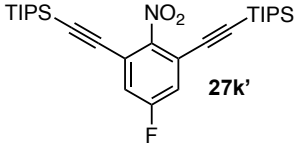

Compound **27k'** was synthesized according to the general procedure using 2 equiv of 1-bromo-2-(triisopropylsilyl)acetylene (**26a**) and it was obtained as a yellow liquid in 30% yield.

^{1}H NMR (400 MHz, $CDCl_3$) δ 7.19 (s, 2H), 1.10 (m, 42H). **^{13}C NMR** (75 MHz, $CDCl_3$) δ 161.5 (d, *J* = 253.4 Hz), 154.0, 119.9 (d, *J* = 24.7 Hz), 119.0 (d, *J* = 11.5 Hz), 101.6, 97.7, 18.5, 11.1. **^{19}F NMR** (376 MHz, $CDCl_3$) δ -108.68 (t, *J* = 8.1 Hz). **HRMS** (APCI+) *m/z* calc. for $C_{28}H_{45}FNO_2Si_2$ $[M+H]^+$: 502.2967. Found: 502.2965.

((5-Chloro-2-nitrophenyl)ethynyl)triisopropylsilane (27l)

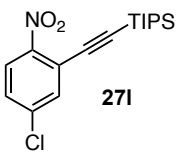

Compound **27l** was synthesized according to the general procedure using 2 equiv of 1-bromo-2-(triisopropylsilyl)acetylene (**26a**) and it was obtained as a white solid in 34% yield.

Mp 60 °C. **^{1}H NMR** (300 MHz, $CDCl_3$) δ 8.00 (d, *J* = 8.8 Hz, 1H), 7.62 (d, *J* = 2.3 Hz, 1H), 7.40 (dd, *J* = 8.8, 2.3 Hz, 1H), 1.14 (s, 21H). **^{13}C NMR** (75 MHz, $CDCl_3$) δ 155.1, 139.2, 135.0, 128.8,

125.9, 120.4, 103.0, 99.9, 18.6, 11.2. **HRMS** (APCI+) *m/z* calc. for $C_{17}H_{25}ClNO_2Si$ $[M+H]^+$: 338.1338. Found: 338.1340.

((5-Chloro-2-nitro-1,3-phenylene)bis(ethyne-2,1-diyl))bis(triisopropylsilane) (27l')

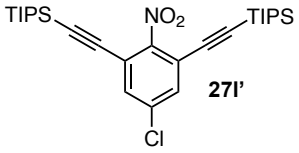

27l'

Compound **27l'** was synthesized according to the general procedure using 2 equiv of 1-bromo-2-(triisopropylsilyl)acetylene (**26a**) and it was obtained as a yellow liquid in 18% yield.

^{1}H NMR (300 MHz, $CDCl_3$) δ 7.47 (s, 2H), 1.10 (m, 42H). **^{13}C NMR** (75 MHz, $CDCl_3$) δ 153.1, 135.6, 132.5, 118.3, 101.7, 97.4, 18.5, 11.1. **HRMS** (APCI+) *m/z* calc. for $C_{28}H_{45}ClNO_2Si_2$ $[M+H]^+$: 518.2672. Found: 518.2673.

((3,4-Dimethyl-2-nitrophenyl)ethynyl)triisopropylsilane (27m)

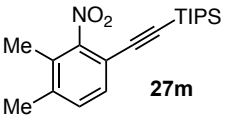

27m

Compound **27m** was synthesized according to the general procedure and it was obtained as a white solid in 86% yield.

Mp 89 °C. **^{1}H NMR** (500 MHz, $CDCl_3$) δ 7.30 (d, *J* = 7.9 Hz, 1H), 7.18 (d, *J* = 7.9 Hz, 1H), 2.32 (s, 3H), 2.18 (s, 3H), 1.10 (s, 21H). **^{13}C NMR** (101 MHz, $CDCl_3$) δ 154.2, 139.3, 131.0, 130.4, 128.0, 113.9, 99.8, 97.6, 20.4, 18.7, 14.4, 11.3. **HRMS** (APCI+) calcd for $[C_{19}H_{30}NO_2Si]^+$ 332.2040 *m/z*; found $[M + H]^+$ 332.2042 *m/z*.

Triisopropyl((3-methyl-2-nitro-4-(trifluoromethyl)phenyl)ethynyl)silane (27n)

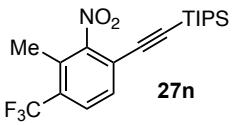

27n

Compound **27n** was synthesized according to the general procedure and it was obtained as a white solid in 32% yield.

Mp 83 °C. **^{1}H NMR** (500 MHz, $CDCl_3$) δ 7.68 (d, *J* = 8.2 Hz, 1H), 7.51 (d, *J* = 8.2 Hz, 1H), 2.39 (d, *J* = 1.6 Hz, 3H), 1.14 – 1.08 (m, 21H). **^{13}C NMR** (126 MHz, $CDCl_3$) δ 155.0, 130.8, 130.1 (q, *J* = 31.3 Hz), 128.8 (q, *J* = 1.4 Hz), 127.1 (q, *J* = 5.7 Hz), 123.2 (q, *J* = 274.13 Hz), 120.1, 102.44, 98.2, 18.6, 13.8 (q, *J* = 2.4 Hz), 11.26. **^{19}F{^{1}H} NMR** (471 MHz, $CDCl_3$) δ -61.39. **HRMS** (APCI+) calcd for $[C_{19}H_{27}F_3NO_2Si]^+$ 386.1758 *m/z*; found $[M + H]^+$ 386.1753 *m/z*.

((4-Fluoro-3-methyl-2-nitrophenyl)ethynyl)triisopropylsilane (27o)

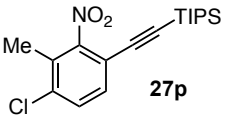

27p

Compound **27o** was synthesized according to the general procedure and it was obtained as a white solid in 65% yield.

Mp 44 °C. **^{1}H NMR** (500 MHz, $CDCl_3$) δ 7.41 (dd, *J* = 8.6, 5.3 Hz, 1H), 7.11 (t, *J* = 8.7 Hz, 1H), 2.23 (d, *J* = 2.1 Hz, 3H), 1.10 (s, 21H). **^{13}C NMR** (126 MHz, $CDCl_3$) δ 160.5 (d, *J* = 252.4 Hz), 154.4, 132.2 (d, *J* = 8.74 Hz), 118.7 (d, *J* = 22.4 Hz), 117.1 (d, *J* = 23.6 Hz), 112.8 (d, *J* = 4.3 Hz), 98.64 (d, *J* = 1.6 Hz), 98.59 (d, *J* = 1.9 Hz), 18.7, 11.3, 10.0 (d, *J* = 4.1 Hz). **^{19}F{^{1}H} NMR** (471 MHz, $CDCl_3$) δ -110.21. **HRMS** (APCI+) calcd for $[C_{18}H_{27}FNO_2Si]^+$ 336.1790 *m/z*; found $[M + H]^+$ 336.1775 *m/z*.

((4-Chloro-3-methyl-2-nitrophenyl)ethynyl)triisopropylsilane (27p)

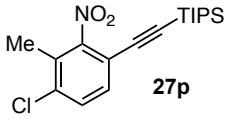

27p

Compound **27p** was synthesized according to the general procedure and it was obtained as a white solid in 65% yield.

Mp 70 °C. **^{1}H NMR** (500 MHz, $CDCl_3$) δ 7.41 (d, *J* = 8.4 Hz, 1H), 7.35 (d, *J* = 8.4 Hz, 1H), 2.32 (s, 3H), 1.10 (d, *J* = 3.5 Hz, 21H). **^{13}C NMR** (126 MHz, $CDCl_3$) δ 154.4, 135.8, 131.4, 130.6, 128.5, 115.1, 100.0, 98.6, 18.6, 15.3, 11.3. **HRMS** (APCI+) calcd for $[C_{18}H_{27}{}^{35}ClNO_2Si]^+$ 352.1494 *m/z*; found $[M + H]^+$ 352.1491 *m/z*.

((4-Bromo-3-methyl-2-nitrophenyl)ethynyl)triisopropylsilane (27q)

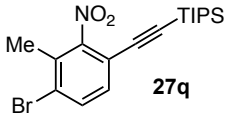

27q

Compound **27q** was synthesized according to the general procedure and it was obtained as a white solid in 67% yield.

Mp 83 °C. **^{1}H NMR** (500 MHz, $CDCl_3$) δ 7.60 (d, *J* = 8.3 Hz, 1H), 7.27 (d, *J* = 8.4 Hz, 1H), 2.35 (s, 3H), 1.10 (d, *J* = 3.6 Hz, 21H). **^{13}C NMR** (126 MHz, $CDCl_3$) δ 154.1, 133.9, 131.5, 130.0, 126.0, 115.7, 100.2, 98.7, 18.6, 18.3, 11.3. **HRMS** (APCI+) calcd for $[C_{18}H_{27}{}^{79}BrNO_2Si]^+$ 396.0989 *m/z*; found $[M + H]^+$ 396.0983 *m/z*.

Triisopropyl((4-methoxy-3-methyl-2-nitrophenyl)ethynyl)silane (27r)

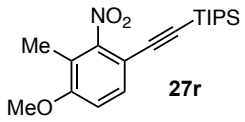

27r

Compound **27r** was synthesized according to the general procedure and it was obtained as a white solid in 86% yield.

Mp 99 °C. **^{1}H NMR** (500 MHz, $CDCl_3$) δ 7.38 (d, *J* = 8.6 Hz, 1H), 6.84 (d, *J* = 8.6 Hz, 1H), 3.88 (s, 3H), 2.13 (s, 3H), 1.10 (s, 21H). **^{13}C NMR** (126 MHz, $CDCl_3$) δ 158.2, 154.5, 131.8, 119.2, 111.1, 108.2, 99.7, 96.2, 56.3, 18.68, 11.4, 10.9. **HRMS** (APCI+) calcd for $[C_{19}H_{30}NO_3Si]^+$ 348.1989 *m/z*; found $[M + H]^+$ 348.1993 *m/z*.

((6-Iodo-3-methoxy-2-nitrophenyl)ethynyl)triisopropylsilane (27s)

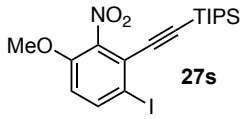

27s

Compound **27s** was synthesized according to the general procedure and it was obtained as a white solid in 55% yield.

Mp 60 °C. **^{1}H NMR** (300 MHz, $CDCl_3$) δ 7.82 (d, *J* = 8.9 Hz, 1H), 6.75 (d, *J* = 8.9 Hz, 1H), 3.87 (s, 3H), 1.13 (m, 21H). **^{13}C NMR** (75 MHz, $CDCl_3$) δ 150.4, 143.7, 140.2, 123.4, 114.1, 104.6, 100.5, 89.1, 56.7, 18.6, 11.2. **HRMS** (APCI+) *m/z* calc. for $C_{18}H_{27}INO_3Si$ $[M+H]^+$: 460.0799. Found: 460.0809.

((3-Bromo-6-methoxy-2-nitrophenyl)ethynyl)triisopropylsilane (27t)

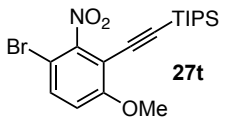

27t

Compound **27t** was synthesized according to the general procedure and it was obtained as a red solid in 81% yield.

Mp 79 °C. **^{1}H NMR** (300 MHz, $CDCl_3$) δ 7.49 (d, *J* = 9.0 Hz, 1H), 6.86 (d, *J* = 9.0 Hz, 1H), 3.91 (s, 3H), 1.12 (s, 21H). **^{13}C NMR** (75 MHz, $CDCl_3$) δ 160.3, 153.9, 133.3, 113.2, 108.3, 105.1, 102.1, 94.3, 56.7, 18.4, 11.1. **HRMS** (APCI+) *m/z* calc. for $C_{18}H_{27}BrNO_3Si$ $[M+H]^+$: 412.0938. Found: 412.0946.

((3-Bromo-5-methoxy-2-nitrophenyl)ethynyl)triisopropylsilane (27u)

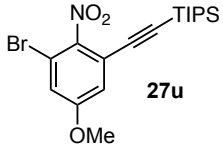

27u

Compound **27u** was synthesized according to the general procedure and it was obtained as a yellow solid in 72% yield.

Mp 85 °C. **^{1}H NMR** (300 MHz, $CDCl_3$) δ 7.50 (d, *J* = 9.0 Hz, 1H), 6.87 (d, *J* = 9.0 Hz, 1H), 3.92 (s, 3H), 1.12 (s, 21H). **^{13}C NMR** (75 MHz, $CDCl_3$) δ 160.4, 133.3, 113.2, 108.4, 106.3, 105.1, 102.2, 94.3, 56.7, 18.5, 11.1. **HRMS** (ESI+) *m/z* calc. for $C_{18}H_{26}BrNNaO_3Si$ $[M+H]^+$: 434.0758. Found: 434.0756.

((2,2'-Dinitro-[1,1'-biphenyl]-3-yl)ethynyl)triisopropylsilane (27v)

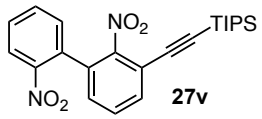

27v

Compound **27v** was synthesized according to the general procedure using 2 equiv of 1-bromo-2-(triisopropylsilyl)acetylene (**26a**) and it was obtained as a red solid in 40% yield.

Mp 100 °C. **^{1}H NMR** (300 MHz, $CDCl_3$) δ 8.14 (dd, *J* = 7.9, 1.7 Hz, 1H), 7.69 – 7.57 (m, 3H), 7.49 (t, *J* = 7.9 Hz, 1H), 7.33 (dd, *J* = 7.2, 1.9 Hz, 1H), 7.26 (dd, *J* = 7.9, 1.4 Hz, 1H), 1.11 (m, 21H). **^{13}C NMR** (75 MHz, $CDCl_3$) δ 150.9, 148.0, 133.4, 133.1, 131.6, 131.5, 130.7, 130.0, 130.0, 129.6, 125.0, 117.3, 100.1, 99.0, 18.5, 11.1. **HRMS** (APCI+) *m/z* calc. for $C_{23}H_{29}N_2O_4Si$ $[M+H]^+$: 425.1891. Found: 425.1881.

2,2'-Dinitro-[1,1'-biphenyl]-3,3'-diyl)bis(ethyne-2,1-diylbis(triisopropylsilane) (27v')

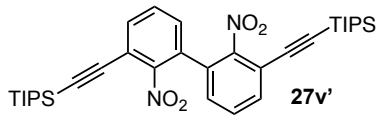

27v'

Compound **27v'** was synthesized according to the general procedure using 2 equiv of 1-Bromo-2-(triisopropylsilyl)acetylene (**26a**) and it was obtained as a yellow solid in 15% yield.

Mp 150 °C. **^{1}H NMR** (300 MHz, $CDCl_3$) δ 7.66 (dd, *J* = 7.8, 1.4 Hz, 2H), 7.46 (t, *J* = 7.8 Hz, 2H), 7.30 (dd, *J* = 7.8, 1.4 Hz, 2H), 1.13 (d, *J* = 2.7 Hz, 42H). **^{13}C NMR** (75 MHz, $CDCl_3$) δ 151.9, 134.1, 130.0, 129.9, 128.5, 117.6, 100.6, 98.7, 18.5, 11.1. **HRMS** (APCI+) *m/z* calc. for $C_{34}H_{49}N_2O_4Si_2$ $[M+H]^+$: 605.3225. Found: 605.3244.

((3,5-Dimethyl-2-nitrophenyl)ethynyl)triisopropylsilane (27w)

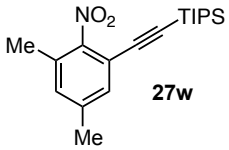

27w

Compound **27w** was synthesized according to the general procedure and it was obtained as a white solid in 95% yield.

Mp 55 °C. **^{1}H NMR** (400 MHz, $CDCl_3$) = 7.23 (s, 1H), 7.04 (s, 1H), 2.34 (s, 3H), 2.30 (s, 3H), 1.13 (s, 21H). **^{13}C NMR** (101 MHz, $CDCl_3$) δ 151.1, 140.2, 131.8, 131.4, 129.8, 116.4, 99.8, 97.9, 20.9, 18.5, 17.4, 11.2. **HRMS** (APCI+) *m/z* calc. for $C_{19}H_{30}NO_2Si$ $[M+H]^+$: 332.2040. Found: 332.2038.

Triisopropyl((3-methyl-2-nitro-5-(trifluoromethyl)phenyl)ethynyl)silane (27x)

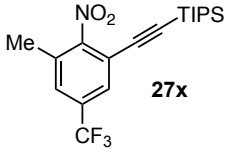

27x

Compound **27x** was synthesized according to the general procedure and it was obtained as a yellow liquid in 48% yield.

^{1}H NMR (500 MHz, $CDCl_3$) δ 7.68 – 7.64 (m, 1H), 7.50 (dd, *J* = 1.9, 1.0 Hz, 1H), 2.39 (s, 3H), 1.13 – 1.09 (m, 21H). **^{13}C NMR** (126 MHz, $CDCl_3$) δ 154.9, 132.1 (q, *J* = 33.5 Hz), 130.9 (q, *J* = 2.5 Hz), 128.0 (q, *J* = 3.7 Hz), 127.8 (q, *J* = 3.7 Hz), 122.7 (q, *J* = 273.2 Hz), 117.5, 101.4, 97.9 (q, *J* = 2.5 Hz), 18.5, 17.3, 11.1. **^{19}F{^{1}H} NMR** (376 MHz, $CDCl_3$) δ -63.29. **HRMS** (APCI+) *m/z* calc. for $C_{19}H_{27}F_3NO_2Si$ $[M+H]^+$: 386.1758. Found: 386.1763.

((5-Fluoro-3-methyl-2-nitrophenyl)ethynyl)triisopropylsilane (27y)

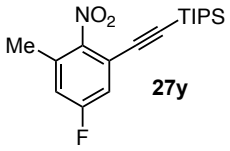

27y

Compound **27y** was synthesized according to the general procedure and it was obtained as a yellow liquid in 65% yield.

^{1}H NMR (400 MHz, $CDCl_3$) δ 7.10 (ddd, *J* = 8.3, 2.7, 0.6 Hz, 1H), 6.97 – 6.92 (m, 1H), 2.34 (d, *J* = 0.7 Hz, 3H), 1.10 (m, 21H). **^{13}C NMR** (101 MHz, $CDCl_3$) δ 161.8 (d, *J* = 252.3 Hz), 149.7, 133.0 (d, *J* = 9.4 Hz), 118.9 (d, *J* = 10.8 Hz), 118.1 (d, *J* = 23.2 Hz), 117.8 (d, *J* = 24.8 Hz), 100.4, 98.4 (d, *J* = 2.8 Hz), 18.5, 17.8 (d, *J* = 1.4 Hz), 11.1. **^{19}F NMR** (376 MHz, $CDCl_3$) δ -109.29 (t, *J* = 8.4 Hz). **HRMS** (APCI+) *m/z* calc. for $C_{18}H_{27}FNO_2Si$ $[M+H]^+$: 336.1790. Found: 336.1804.

((5-Chloro-3-methyl-2-nitrophenyl)ethynyl)triisopropylsilane (27z)

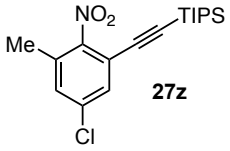

27z

Compound **27z** was synthesized according to the general procedure and it was obtained as a yellow liquid in 66% yield.

^{1}H NMR (400 MHz, $CDCl_3$) δ 7.39 (dd, *J* = 2.2, 0.7 Hz, 1H), 7.23 (dq, *J* = 2.3, 0.8 Hz, 1H), 2.31 (d, *J* = 0.7 Hz, 3H), 1.10 (m, 21H). **^{13}C NMR** (126 MHz, $CDCl_3$) δ 151.6, 135.6, 131.7, 131.0, 130.7, 118.2, 100.6, 98.2, 18.5, 17.4, 11.1. **HRMS** (APCI+) *m/z* calc. for $C_{18}H_{27}ClNO_2Si$ $[M+H]^+$: 352.1494. Found: 352.1501.

((5-Bromo-3-methyl-2-nitrophenyl)ethynyl)triisopropylsilane (27aa)

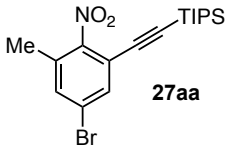

27aa

Compound **27aa** was synthesized according to the general procedure and it was obtained as a yellow liquid in 67% yield.

^{1}H NMR (400 MHz, $CDCl_3$) δ 7.55 (dd, *J* = 2.1, 0.7 Hz, 1H), 7.39 (dq, *J* = 1.5, 0.7 Hz, 1H), 2.31 (d, *J* = 0.7 Hz, 3H), 1.12 – 1.09 (m, 21H). **^{13}C NMR** (101 MHz, $CDCl_3$) δ 152.1, 133.9, 133.6, 131.8, 123.5, 118.3, 100.7, 98.1, 18.5, 17.3, 11.1. **HRMS** (APCI+) *m/z* calc. for $C_{18}H_{27}BrNO_2Si$ $[M+H]^+$: 396.0989. Found: 396.0990.

Triisopropyl((5-methoxy-3-methyl-2-nitrophenyl)ethynyl)silane (27ab)

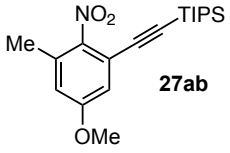

27ab

Compound **3ab** was synthesized according to the general procedure and it was obtained as a yellow liquid in 81% yield.

^{1}H NMR (500 MHz, $CDCl_3$) δ 6.86 (d, *J* = 2.7 Hz, 1H), 6.71 (dd, *J* = 2.7, 0.8 Hz, 1H), 3.82 (s, 3H), 2.31 (s, 3H), 1.11 (m, 21H). **^{13}C NMR** (126 MHz, $CDCl_3$) δ 159.8, 146.9, 132.4, 118.4, 116.8, 115.6, 99.9, 98.4, 55.7, 18.5, 18.2, 11.1. **HRMS** (APCI+) *m/z* calc. for $C_{19}H_{30}NO_3Si$ $[M+H]^+$: 348.1989. Found: 348.1999.

Triisopropyl((1-nitronaphthalen-2-yl)ethynyl)silane (27ac)

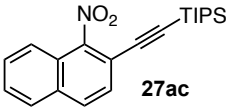

27ac

Compound **27ac** was synthesized according to the general procedure and it was obtained as a red solid in 41% yield.

Mp 67 °C. **^{1}H NMR** (300 MHz, $CDCl_3$) δ 7.92 – 7.85 (m, 2H), 7.75 (dt, *J* = 8.6, 1.1 Hz, 1H), 7.67 – 7.53 (m, 3H), 1.14 (m, 21H). **^{13}C NMR** (75 MHz, $CDCl_3$) δ 150.8, 133.1, 130.2, 129.0, 128.3, 128.1, 128.0, 124.1, 121.7, 114.0, 100.8, 99.8, 18.6, 11.2. **HRMS** (ESI+) *m/z* calc. for $C_{18}H_{26}BrNNaO_3Si$ $[M+Na]^+$: 354.1884. Found: 354.1887.

Triisopropyl((1-nitropyren-2-yl)ethynyl)silane (27ad)

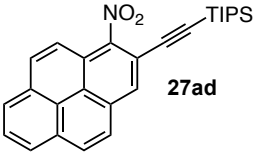

27ad

Compound **27ad** was synthesized according to the general procedure and it was obtained as a brown solid in 80% yield.

Mp 120 °C. **^{1}H NMR** (300 MHz, $CDCl_3$) δ 8.30 – 8.07 (m, 6H), 7.98 (m, 2H), 1.22 (s, 21H). **^{13}C NMR** (75 MHz, $CDCl_3$) δ 149.9, 146.5, 131.6, 130.7, 130.1, 129.8, 128.2, 127.3, 127.1, 126.7, 125.9, 123.6, 123.2, 122.4, 119.9, 113.7, 100.4, 99.1, 18.6, 11.3. **HRMS** (APCI+) *m/z* calc. for $C_{27}H_{30}NO_2Si$ $[M+H]^+$: 428.2040. Found: 428.2033.

((5-bromo-2-nitrothiophen-3-yl)ethynyl)triisopropylsilane (27ae)

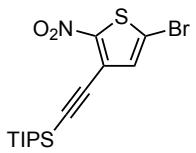

Compound **27ae** was synthesized according to the general procedure using 2 equiv. of heteroarene **25ae** and it was obtained as an orange solid in 45% yield.

^{1}H NMR (500 MHz, $CDCl_3$) δ 6.97 (s, 1H), 1.60 (hept, *J* = 7.5 Hz, 3H), 1.12 (d, *J* = 7.5 Hz, 18H). **^{13}C NMR** (126 MHz, $CDCl_3$) δ 165.3, 161.2, 150.3, 133.25, 126.9, 124.3, 18.8, 12.5. **HRMS** (ESI) m/z calc. for $C_{15}H_{22}BrNNaO_2SSi$ $[M+Na]^+$: 410.0216. Found: 410.0211.

7-nitro-6-((triisopropylsilyl)ethynyl)-1*H*-indole (27af)

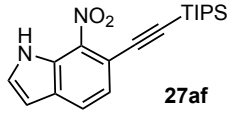

27af

Compound **27af** was synthesized according to the general procedure using 2 equiv. of heteroarene **25af** and it was obtained as an orange solid in 60% yield.

^{1}H NMR (500 MHz, $CDCl_3$) δ 10.01 (s, 1H), 7.82 (dd, *J* = 8.1, 0.7 Hz, 1H), 7.49 – 7.35 (m, 2H), 6.67 (d, *J* = 1.0 Hz, 1H), 1.20-1.17 (m, 21H). **^{13}C NMR** (126 MHz, $CDCl_3$) δ 133.9, 131.1, 129.6,

127.65, 127.1, 126.8, 114.7, 104.1, 103.95, 100.45, 18.7, 11.4. **HRMS** (ESI) m/z calc. for $C_{19}H_{26}N_2NaO_2Si$ $[M+Na]^+$: 365.1656. Found: 365.1656.

1-methyl-4-nitro-5-((triisopropylsilyl)ethynyl)-1*H*-indole (27ag)

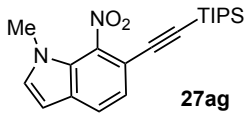

27ag

Compound **27ag** was synthesized according to the general procedure using 2 equiv. of heteroarene **25ag** and it was obtained as an orange solid in 72% yield.

^{1}H NMR (300 MHz, $CDCl_3$) δ 7.49-7.43 (m, 2H), 7.26 (d, *J* = 3.2 Hz, 1H), 6.96 (d, *J* = 3.1 Hz, 1H), 3.87 (s, 1H), 1.22-1.12 (m, 21H). **^{13}C NMR** (126 MHz, $CDCl_3$) δ 142.7, 137.7, 133.0, 127.5, 122.6, 113.6, 111.1, 103.1, 101.5, 97.55, 33.3, 18.7, 11.4. **HRMS** (ESI) m/z calc. for $C_{20}H_{28}N_2NaO_2Si$ $[M+Na]^+$: 379.1812. Found: 379.1815.

1-methyl-5-nitro-4-((triisopropylsilyl)ethynyl)-1*H*-indole (27ah)

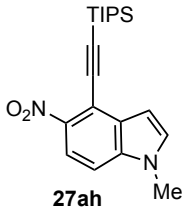

27ah

Compound **27ah** was synthesized according to the general procedure using 2 equiv. of heteroarene **25ah** and it was obtained as an orange solid in 48% yield. **^{1}H NMR** (500 MHz, $CDCl_3$) δ 8.02 (d, *J* = 9.0 Hz, 1H), 7.28 (dd, *J* = 9.0, 0.8 Hz, 1H), 7.21 (d, *J* = 3.2 Hz, 1H), 6.83 (dd, *J* = 3.2, 0.8 Hz, 1H), 3.85 (s, 3H), 1.38 – 0.73 (m, 21H). **^{13}C NMR** (126 MHz, $CDCl_3$) δ 143.0, 137.8, 132.1, 131.5, 118.6, 112.45, 109.0, 103.95, 103.5, 100.5, 33.3, 18.7, 11.4. **HRMS** (ESI) m/z calc. for $C_{20}H_{28}N_2N_aO_2Si$ $[M+Na]^+$: 379.1812. Found: 379.1802.

1-methyl-5-nitro-4,6-bis((triisopropylsilyl)ethynyl)-1*H*-indole (27ah')

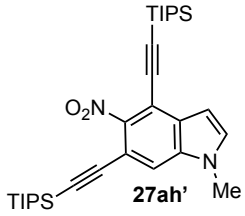

27ah'

Compound **27ah'** was synthesized according to the general procedure using 2 equiv. of 1-bromo-2-(triisopropylsilyl)acetylene (**26a**) and it was obtained as a brown solid in 40% yield.

^{1}H NMR (500 MHz, $CDCl_3$) δ 7.42 (d, *J* = 0.9 Hz, 1H), 7.23 (d, *J* = 3.1 Hz, 1H), 6.67 (dd, *J* = 3.1, 0.9 Hz, 1H), 3.82 (s, 3H), 1.17-1.11 (m, 42H). .**^{13}C NMR** (126 MHz, $CDCl_3$) δ 148.7, 135.3, 133.2, 129.75, 114.1, 109.9, 109.4, 103.1, 101.5, 100.9, 98.1, 95.93, 33.3, 18.62, 18.60, 11.3, 11.2. **HRMS** (ESI) m/z calc. for $C_{31}H_{48}N_2NaO_2Si_2$ $[M+Na]^+$: 559.3147. Found: 559.3126.

Triethyl((4-methoxy-3-methyl-2-nitrophenyl)ethynyl)silane (27ba)

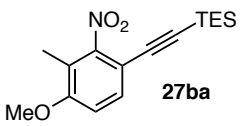

27ba

Product **3aj** was synthesized following general procedure starting from 1-methoxy-2-methyl-3-nitrobenzene (30.0 mg, 0.179 mmol) and using 1.5 equiv of bromoalkyne **26k**. Purification by flash chromatography on silica (pentane:diethyl ether, 98:2) afforded the title compound **3aj** (33.6 mg, 0.110 mmol, 61% yield) as a light yellow oil.

^{1}H NMR (500 MHz, $CDCl_3$) δ 7.38 (dd, *J* = 8.6, 0.4 Hz, 1H), 6.84 (d, *J* = 8.6 Hz, 1H), 3.88 (s, 3H), 2.13 (s, 3H), 1.02 (t, *J* = 7.9 Hz, 9H), 0.64 (q, *J* = 7.9 Hz, 6H). **^{13}C NMR** (126 MHz, $CDCl_3$) δ 158.2, 154.5, 131.8, 119.3, 111.2, 108.1, 99.2, 97.2, 56.3, 10.9, 7.5, 4.4. **HRMS** (ESI+) calcd for $[C_{16}H_{23}NO_3Si]^+$ 328.1339 *m/z*; found $[M + H]^+$ 328.1345 *m/z*.

Tri(*n*-hexyl)((4-methoxy-3-methyl-2-nitrophenyl)ethynyl)silane (27bb)

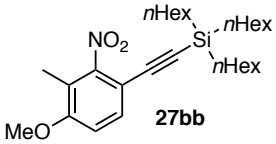

27bb

Product **27bb** was synthesized following general procedure starting from 1-methoxy-2-methyl-3-nitrobenzene (30.0 mg, 0.179 mmol) and using 1.5 equiv of bromoalkyne **26l**. Purification by flash chromatography on silica (pentane:diethyl ether, 98:2) afforded the title compound **27bb** (53.1 mg, 0.112 mmol, 63% yield) a light yellow oil.

^{1}H NMR (500 MHz, $CDCl_3$) δ 7.36 (d, *J* = 8.5 Hz, 1H), 6.84 (d, *J* = 8.6 Hz, 1H), 3.87 (s, 3H), 2.13 (s, 3H), 1.42 – 1.23 (m, 24H), 0.91 – 0.85 (m, 9H), 0.66 – 0.60 (m, 6H). **^{13}C NMR** (126 MHz, $CDCl_3$) δ 158.2, 154.5, 131.7, 119.3, 111.1, 108.2, 99.1, 98.0, 56.3, 33.3, 31.7, 23.9, 22.8, 14.3, 13.3, 10.9. **HRMS** (ESI+) calcd for $[C_{28}H_{48}NO_3Si]^+$ 474.3398 *m/z*; found $[M + H]^+$ 474.3390 *m/z*.

***Tert*-butyl((4-methoxy-3-methyl-2-nitrophenyl)ethynyl)diphenylsilane (27bc)**

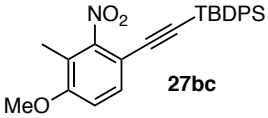

27bc

Product **27bc** was synthesized following general procedure starting from 1-methoxy-2-methyl-3-nitrobenzene (30.0 mg, 0.179 mmol) and using 1.5 equiv of bromoalkyne **26m**. Purification by flash chromatography on silica (pentane:diethyl ether, 95:5) afforded the title compound **27bc** (57.2 mg, 0.133 mmol, 74% yield) as a light yellow solid.

M.p. (pentane) = 108–110 ºC. **^{1}H NMR** (500 MHz, $CDCl_3$) δ 7.84 – 7.79 (m, 4H), 7.50 (d, *J* = 8.6 Hz, 1H), 7.43 – 7.37 (m, 6H), 6.89 (d, *J* = 8.6 Hz, 1H), 3.90 (s, 3H), 2.18 (s, 3H), 1.12 (s, 9H). **^{13}C NMR** (126 MHz, $CDCl_3$) ^{13}C NMR (126 MHz, $CDCl_3$) δ 158.6, 154.4, 135.8, 133.0, 132.1, 129.7, 127.9, 119.5, 111.3, 107.8, 101.8, 94.9, 56.4, 27.1, 18.9, 11.0. **HRMS** (ESI+) calcd for $[C_{26}H_{28}NO_3Si]^+$ 430.1833 *m/z*; found $[M + H]^+$ 430.1827 *m/z*.

Triphenyl((4-methoxy-3-methyl-2-nitrophenyl)ethynyl)silane (27bd)

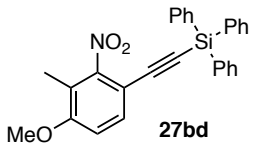

27bd

Product **27bd** was synthesized following general procedure starting from 1-methoxy-2-methyl-3-nitrobenzene (30.0 mg, 0.179 mmol) and using 1.5 equiv of bromoalkyne **26n**. Purification by flash chromatography on silica (pentane:diethyl ether, 95:5) afforded the title compound **27bd** (26.1 mg, 0.058 mmol, 32% yield) as a light yellow solid.

M.p. (pentane) = 161–164 ºC. **^{1}H NMR** (500 MHz, $CDCl_3$) δ 7.71 – 7.64 (m, 6H), 7.49 (d, *J* = 8.6 Hz, 1H), 7.46 – 7.37 (m, 9H), 6.87 (s, 1H), 3.89 (s, 3H), 2.17 (s, 3H). **^{13}C NMR** (126 MHz,

$CDCl_3$) δ 158.8, 154.4, 135.8, 133.2, 132.2, 130.2, 128.2, 128.1, 119.7, 111.3, 107.6, 102.4, 94.5, 56.4, 11.0. **HRMS** (ESI+) calcd for $[C_{28}H_{24}NO_3Si]^+$ 450.1520 *m/z*; found $[M + H]^+$ 450.1509 *m/z*.

3-Ethyl 5-methyl 2,6-dimethyl-4-(3-nitro-4-((triisopropylsilyl)ethynyl)phenyl)-pyridine-3,5-dicarboxylate (28)

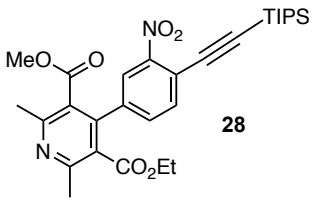

28

Compound **28** was synthesized according to the general procedure starting from commercial nitrendipene and it was obtained as a purple liquid in 40% yield.

^{1}H NMR (300 MHz, $CDCl_3$) δ 7.97 (d, *J* = 1.8 Hz, 1H), 7.69 (d, *J* = 8.0 Hz, 1H), 7.46 (dd, *J* = 8.0, 1.8 Hz, 1H), 4.14 (q, *J* = 7.1 Hz, 2H), 3.67 (s, 3H), 2.64 (s, 3H), 2.63 (s, 3H), 1.17 (s, 21H), 1.10 (t, *J* = 7.1, 3H). **^{13}C NMR** (75 MHz, $CDCl_3$) δ 179.1, 167.6, 167.1, 156.2, 149.6, 143.2, 137.0, 135.3, 132.2, 126.6, 126.3, 124.2, 118.8, 102.8, 100.5, 61.9, 52.6, 23.0, 18.6, 18.3, 13.8, 11.2. **HRMS** (ESI+) *m/z* calc. for $C_{29}H_{39}N_2O_6Si$ $[M+H]^+$: 539.2572. Found: 539.2572.

Synthetic Application

*Rhodium-Catalyzed C–H Iodination of Nitrobenzene **25w***

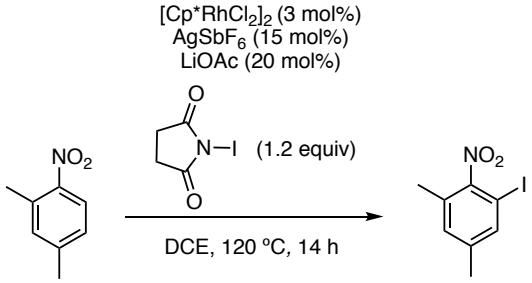

25w **31**

1-iodo-3,5-dimethyl-2-nitrobenzene (31)

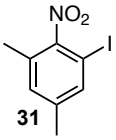

31

$[Cp^*RhCl_2]_2$ (3 mol%), LiOAc (0.2 equiv), $AgSbF_6$ (0.15 equiv) were weighted in a vial inside a glovebox and dichloroethane (0.2M) is added. **25w** (0.2 mmol) and N-iodosuccinimide (1.2 equiv) are then added and the vial is sealed. The reaction mixture is stirred at 120 °C for 14 h. After cooling to the room temperature, the reaction mixture is filtrated through celite and purified by column chromatography, with a gradient from cyclohexane 100% to 9/1 cyclohexane/ethyl acetate to yield 1-iodo-3,5-dimethyl-2-nitrobenzene **31** in 60% yield as a yellow liquid.

^{1}H NMR (300 MHz, $CDCl_3$) δ 7.55 (s, 1H), 7.07 (s, 1H), 2.31 (s, 3H), 2.33 (s, 3H).

The ^{1}H NMR data is consistent with the one previously reported.[61]

61 Sapountzis, I.; Dube, H.; Lewis, R.; Gommermann, N.; Knochel, P. *J. Org. Chem.* **2005**, *70*, 2445-2454.

*One-pot ortho-arylation of nitrobenzene **25a***

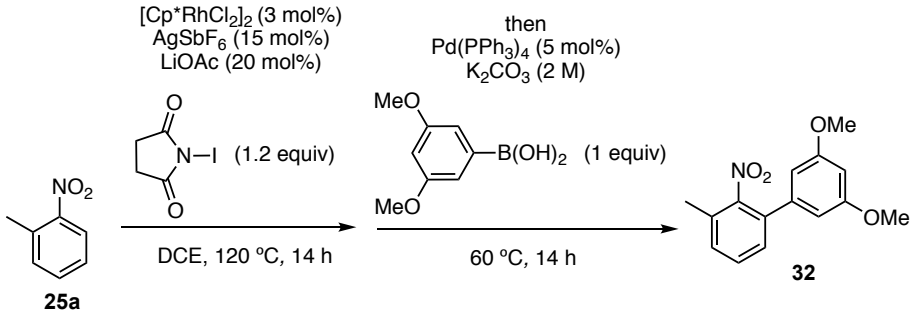

3',5'-dimethoxy-3-methyl-2-nitro-1,1'-biphenyl (32)

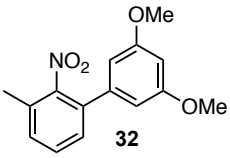

$[Cp^*RhCl_2]_2$ (3 mol %), LiOAc (0.2 equiv), $AgSbF_6$ (0.15 equiv) were weighted in a vial inside a glovebox and dichloroethane (0.2M) is added. **25a** (0.2 mmol) and N-iodosuccinimide (1.2 equiv) are then added and the vial is sealed. The reaction mixture is stirred at 120 °C for 14 h. After cooling to the room temperature, the vial is opened and $Pd(PPh_3)_4$ (5 mol%), K_2CO_3 (1 mL, 2M in water) and 3',5'-dimethoxy-3-methyl-2-nitro-1,1'-biphenyl (1 equiv) are then added. The reaction is stirred at 60 °C for 14 hours. After cooling to the room temperature, the reaction is diluted with water, extracted with DCM, dried over $MgSO_4$. The crude is then purified by column chromatography, with a gradient from cyclohexane 100% to 1/1 cyclohexane/ethyl acetate to yield **32** in 50% yield as a yellow solid.

Mp 90 °C. **^{1}H NMR** (300 MHz, $CDCl_3$) δ 7.64 – 7.61 (m, 1H), 7.40 (ddt, J = 7.8, 1.4, 0.7 Hz, 1H), 7.32 (d, J = 7.8 Hz, 1H), 6.49 – 6.46 (m, 1H), 6.43 (m, 2H), 3.79 (d, J = 0.6 Hz, 6H), 2.46 (d, J = 0.7 Hz, 3H). **^{13}C NMR** (75 MHz, $CDCl_3$) δ 160.8, 139.3, 138.8, 133.3, 132.9, 131.5, 126.9, 124.2, 106.2, 100.0, 55.4, 20.9. **HRMS** (APCI+) *m/z* calc. for $C_{15}H_{16}NO_4$ $[M+H]^+$: 274.1074. Found: 274.1083.

Synthesis of 2-(triisopropylsilyl)-1H-indole (X) from Xb.

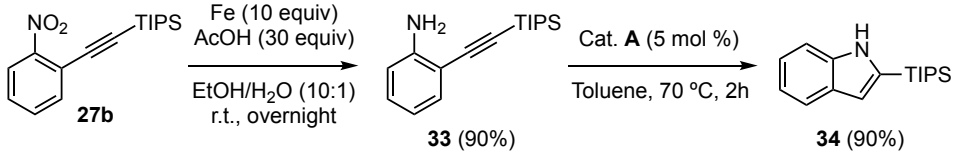

2-((triisopropylsilyl)ethynyl)aniline (33)

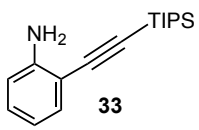

To a solution of **27b** in a mixture of EtOH/H_2O (10:1, 0.05 M) AcOH (30 equiv) is added, followed by Fe (10 equiv). The suspension is stirred at room temperature overnight.The reaction mixture is filtered through a pad of Celite®, washing with EtOAc. The mixture is then poured into a separating flask, and washed with aq. sat. $NaHCO_3$, H_2O and brine. The organic layer is dried over $MgSO_4$. The crude mater is purified by flash column chromatography using 5% DCM in cyclohexane as eluent, affording compound **33** a yellow oil in 90% yield.

^{1}H NMR (400 MHz, $CDCl_3$) δ 7.36 – 7.31 (m, 1H), 7.13 (ddd, *J* = 8.2, 7.3, 1.6 Hz, 1H), 6.74 – 6.61 (m, 2H), 4.27 (s, 2H), 1.19 – 1.14 (m, 21H). **^{13}C NMR** (101 MHz, $CDCl_3$) δ 148.4, 132.6, 129.8, 117.8, 114.3, 108.4, 103.9, 96.0, 18.9, 11.4. **HRMS** (ESI+) *m/z* calc. for $C_{17}H_{28}NSi$ $[M+H]^+$: 274.1986. Found: 274.1984. The spectroscopic data agrees with previously reported values.[62]

2-(triisopropylsilyl)-1*H*-indole (34)

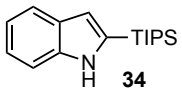

34

Compound **33** and [(Johnphos)Au(NCCH$_3$)]SbF$_6$ (5 mol%) were dissolved in toluene (0.1 M) and the solution was stirred at 70 ºC for 2 h. Then, the solvent was removed by rotatory evaporation, and the crude mixture was purified by flash column chromatography using 5% DCM in cyclohexane as eluent, affording compound **34** in 90% yield. **^{1}H NMR** (400 MHz, $CDCl_3$) δ 8.09 (s, 1H), 7.65 (dd, *J* = 7.8, 1.1 Hz, 1H), 7.42 (dd, *J* = 8.1, 1.0 Hz, 1H), 7.19 (ddd, *J* = 8.1, 7.0, 1.2 Hz, 1H), 7.10 (ddd, *J* = 8.0, 7.0, 1.0 Hz, 1H), 6.78 (dd, *J* = 2.1, 1.0 Hz, 1H), 1.39 (d, *J* = 7.2 Hz, 3H), 1.15 (d, *J* = 7.4 Hz, 18H). **^{13}C NMR** (101 MHz, $CDCl_3$) δ 138.7, 133.8, 128.7, 122.2, 120.6, 119.6, 113.7, 110.8, 18.8, 11.4. **HRMS** (ESI-) *m/z* calc. for $C_{17}H_{26}NSi$ $[M-H]^-$: 272.1840. Found: 272.1835.

Experimental Mechanistic Investigations

Kinetic Isotope Effect (Parallel experiments, initial rates measurements).

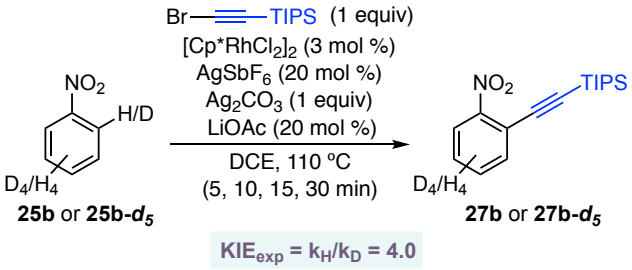

The kinetic isotope effect (KIE) was determined by measuring the initial rates of the reactions with hydrogenated and deuterated substrates. 5 Reactions with hydrogenated substrates and 5 reactions with deuterated substrates were stopped at 5, 10, 15, 20, and 30 minutes, using the following procedure:

$[Cp^*RhCl_2]_2$ (3 mol %), Ag_2CO_3 (1 equiv), LiOAc (0.2 equiv), $AgSbF_6$ (0.2 equiv) were weighted in a vial inside a glovebox and dichloroethane (0.15M) is added. Nitrobenzene (0.2 mmol) and 1-bromo-2-(triisopropylsilyl)acetylene (**26a**, 1 equiv) are then added and the vial is sealed. The reaction mixture is stirred at 110 °C outside the glovebox for the indicated time. After cooling to the room temperature, the reaction mixture is filtrated through celite and

62 Le, C. M.; Hou, X.; Sperger, T.; Schoenebeck, F.; Lautens, M. *Angew. Chem. Int. Ed.* **2015**, *54*, 15897–15900.

bromomesitylene is added. The yield of the mono-alkynylated product was determined by ^{1}H NMR analysis of the crude using bromomesitylene as internal standard (Table S1).

Table S1. Time and yields for the Rh-catalyzed ortho-alkynylation of **3b** and **3b-*d*$_5$**.

Time (min)	NMR yield 27b (%)	NMR yield 27b-*d*$_5$ (%)
5	1.4	0.22
10	3.2	0.55
15	5.2	0.7
20	6.6	1.2
30	9.5	2.3

For **27b**: y = 1.95x - 0.7 ; R^2 = 0.99; For **27b-*d*$_5$**: y = 0.48x - 0.4. R^2 = 0.89

KIE = $k_{27b}/k_{27b\text{-}d5}$ = 1.95/0.48 = 4

Hammett Plot Study

A Hammett plot study was carried out by measuring the initial rate of the *ortho*-alkynylation of six differently *meta*-substituted nitrobenzenes. Ten identical reactions were run in parallel for each derivative. These reactions were stopped at different times in the first 10-15% of conversion. Reproducibility issues were prevented by using AgOAc instead of Ag_2CO_3-LiOAc system.

Representing yield *vs* reaction time, a straight line was obtained for each derivative. The slope value (k_R) of these straight lines corresponds to the initial reaction rate and can be conveniently used for the Hammett plot analysis (Table S2 and Figure S1).

Table S2. Hammett plot data.

Substituent (R)	k_R	k_R/k_H	Log (k_R/k_H)	σ_p	σ_p^+
Br	0.06	0.0714	-1.13	0.23	0.15
Cl	0.07	0.0833	-1.07	0.23	0.11
F	0.36	0.4286	-0.37	0.06	-0.07
H	0.84 (k_H)	1.0000	0.00	0.00	0.00
Me	2.02	2.4048	0.38	-0.17	-0.31
OMe	4.80	5.7143	0.60	-0.26	-0.78

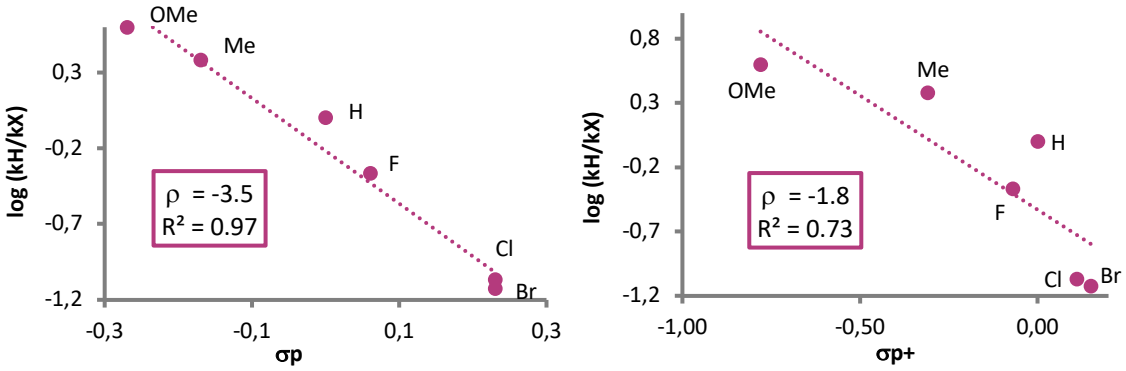

Figure S1. Hammett Plot using σ_P values (left) and σ_P^+ values (right).

The negative value of the slope illustrates the formation of a partial positive charge in the TS of higher energy. We observe that the correlation with σ_P values fits better the experimental results ($R^2 = 0.97$), which points in the direction of a relatively low stabilization by resonance of this partial positive charge.

NBO Analysis – NLMOs

Table S3. Natural localized molecular orbitals (NLMOs) associated to the lone pair over O1 and C1–H1 bond. Contribution of main atoms in percent and NBOs donor-acceptor related to the analyzed NLMO.

Interaction	Analysis	II (X = Rh)	TS_{II-III} (X = H1)
σ_{O1-X} bond (X = Rh or H1)	NLMO	$2p_y(O1)$	$2p_y(O1)$
	O1	83.9%	86.3%
	H1	0.02%	7.23%
	Rh	7.34%	1.1%
	NBO donor	n_{O1}	n_{O1}
	NBO acceptor	Ω^*_{Rh-C17} (47.46 kcal/mol)	Ω^*_{C1-H1} (108.32 kcal/mol)
σ_{C1-H1} bond	NLMO	Ω_{C1-H1}	Ω_{C1-H1}
	C1	64.2%	65.4%
	H1	34.7%	20.6%
	Rh	0.1%	8.6%
	NBO donor	Ω_{C1-H1}	Ω_{C1-H1}
	NBO acceptor	Ω^*_{Rh-C17} (0.12 kcal/mol)	$3Cn_{Rh-C15-C21}$ (19.65 kcal/mol)

NBO types: n_A = nonbonded lone pair (1 center. valence), n_A* = unfilled nonbonded (1 center, valence), Ω_{A-B} = bond (2 centers, valence), Ω^*_{A-B} = antibond (2 centers, valence), 3Cn = 3 filled centers bond.

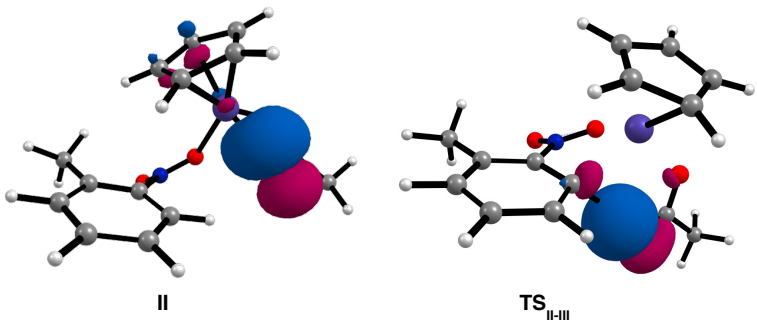

Figure S2. NLMOs plot associated to the lone pair over O1 of **II** (left) and **TS_{II-III}** (right).

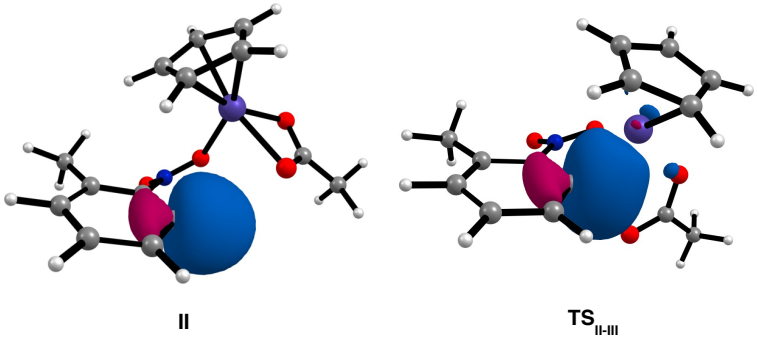

Figure S3. NLMOs plots associated to the activated C1–H1 bond of **II** (left) and **TS$_{II-III}$** (right).

General Conclusions

In the first chapter of this Doctoral Thesis, we summarized our contribution to the field of asymmetric gold(I) catalysis with an application in total synthesis by developing a robust methodology for the enantioselective cyclization of 1,6-enynes that was successfully employed in the first total synthesis of carexane I, P and O. Experimental and theoretical investigations suggest that the excellent enantioselectivities arise from non-covalent interactions between the substrate and the well-defined mononuclear gold(I) complex.

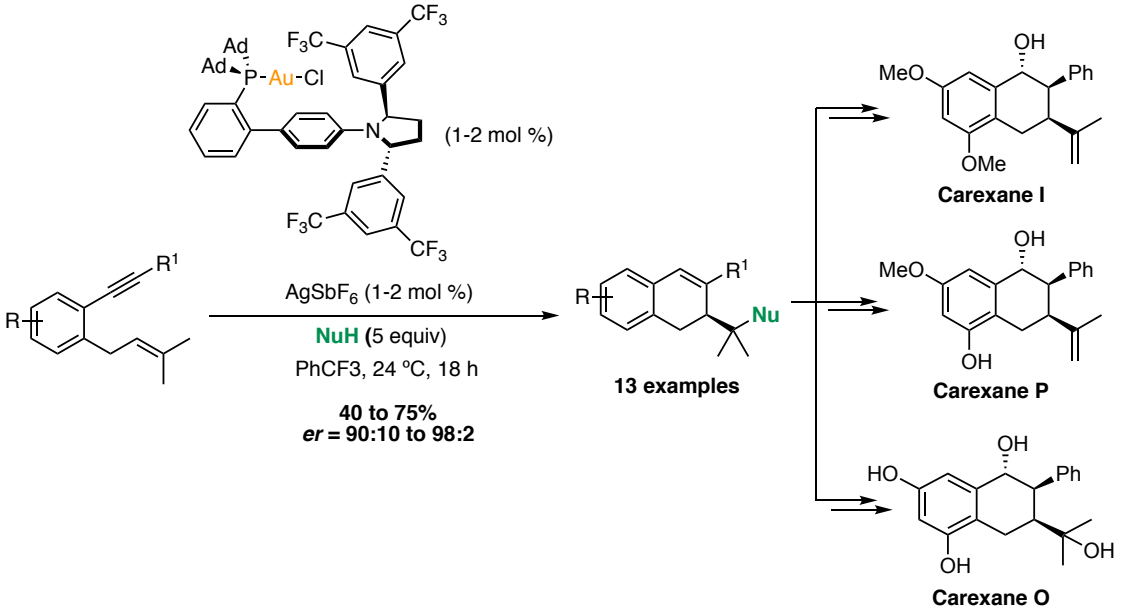

The second chapter of the Doctoral Thesis covers our work on the development of the photoredox-assisted gold(I)/gold(III)-catalyzed arylative alkoxycyclization of 1,6-enynes in the presence of aryldiazonium salts and an external alcohol. Experimental results suggest that the gold(I) catalyst can be oxidized to the corresponding gold(III) species in the presence of photochemically generated aryl radicals. Enyne cyclization is then promoted by the gold(III) center generating an alkenylgold(III) intermediate that undergoes RE affording the arylated compounds. The reaction tolerated a wide variety of functional groups delivering the exocyclic alkenes in moderate to good yields with the complementary configuration to the one previously reported in other gold(I)-catalyzed transformations.

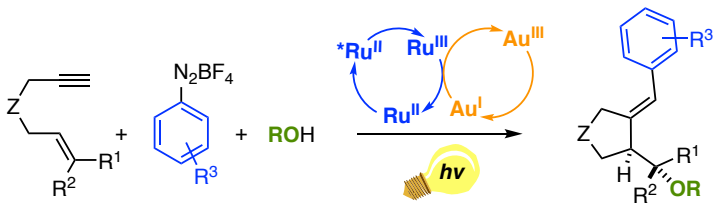

The last chapter summarizes our experimental efforts towards the possibility of using the nitro moiety as directing group in the rhodium(III)-catalyzed C–H alkynylation of arenes. Although high temperatures were needed, the reaction worked efficiently yielding differently

substituted mono- and dialkynylated products that could be used as precursors for the synthesis of indoles or could be further functionalized by denitrative cross-coupling reactions. The selective C–H activation was extended to the *ortho*-iodination and the one-pot *ortho*-iodination/arylation of nitroarenes. Experimental and computational studies suggest that the turnover limiting C–H bond cleavage takes place through a concerted electrophilic concerted metalation deprotonation process.

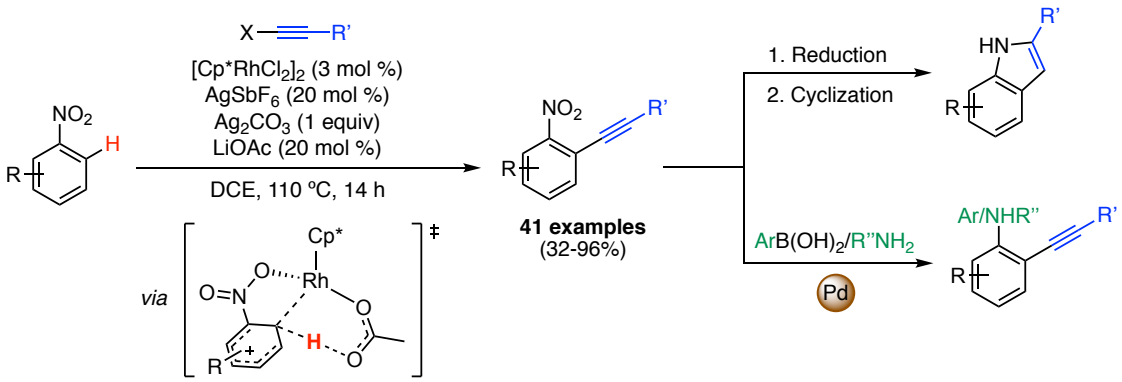

UNIVERSITAT ROVIRA I VIRGILI
From Gold-Catalyzed Asymmetric or Photoredox-Assisted Cyclizations to Rhodium-Catalyzed C–H Alkynylations
Joan Guillem Mayans Peñarrubia

UNIVERSITAT ROVIRA I VIRGILI
From Gold-Catalyzed Asymmetric or Photoredox-Assisted Cyclizations to Rhodium-Catalyzed C–H Alkynylations
Joan Guillem Mayans Peñarrubia

UNIVERSITAT ROVIRA I VIRGILI
From Gold-Catalyzed Asymmetric or Photoredox-Assisted Cyclizations to Rhodium-Catalyzed C–H Alkynylations
Joan Guillem Mayans Peñarrubia

UNIVERSITAT
ROVIRA i VIRGILI